

**QUANTUM CHEMISTRY OF ION-  
MOLECULE INTERACTIONS IN GROUND  
AND LOW-LYING EXCITED STATE**

**THESIS SUBMITTED FOR THE DEGREE OF  
DOCTOR OF PHILOSOPHY  
IN SCIENCE (CHEMISTRY)  
OF THE  
VIDYASAGAR UNIVERSITY**

**BISWARUP MANDAL**  
**Department of Chemistry and Chemical Technology**  
**Vidyasagar University**  
**Midnapore – 721102**  
**February-2017**



*Dedicated  
To  
My Parents*







**VIDYASAGAR UNIVERSITY**  
MIDNAPORE, WEST BENGAL 721102  
DEPARTMENT OF CHEMISTRY AND CHEMICAL TECHNOLOGY

---

This is to certify that the Thesis entitled '**Quantum chemistry of ion-molecule interactions in ground and low-lying excited state**' is the result of work done by Mr. Biswarup Mandal M.Sc., himself under my direct guidance and supervision and that he has fulfilled all the conditions necessary for the Ph.D. examination of the Vidyasagar University. This work has never been submitted in full or part, for the award of any degree by the candidate or by any other person.

Mr. Biswarup Mandal has delivered one Pre-registration seminar on Dec. 2008, he completed the course work conducted by Vidyasagar University according to Ph.D. regulation. He has delivered one Pre-submission seminar on 05-07-2016. Both the lectures were highly appreciated by the audience.

PROF. BHUDEB RANJAN DE  
SUPERVISOR



## **DECLARATION**

I here by declare that the matter embodied in the thesis entitled “**Quantum chemistry of ion-molecule interactions in ground and low-lying excited state**” in the result of investigations carried out by me under the supervision of Prof. Bhudeb Ranjan De, Department of Chemistry and Chemical Technology, Vidyasagar University, Paschim Medinipur, India.

I also affirm that this work is original and has not been submitted elsewhere for the award of degree, diploma, membership etc.

Vidyasagar University,  
Paschim Medinipur, West Bengal,  
INDIA.

BISWARUP MANDAL



## **ACKNOWLEDGEMENT**

This is great pleasure to express my deep gratitude to my revered teacher Prof. Bhudeb Ranjan De, Vidyasagar University, for affectionate guidance and constant encouragement, received during the entire tenure of this work.

I gratefully acknowledge the financial support of CSIR, New Delhi.

I wish to record the constant help and cooperation that I received from my research colleagues Dr. Umasankar Senapati, Dr. Debducti De.

Finally, with great pleasure, I wish to express my deep indebtedness to all the respected teachers, Prof. S. S. Islam, Prof. B. G. Bag, Dr. S. Dalai, Prof. A. Misra, Prof. Amiya Panda, Dr. S. Roy, Dr. S. Manna and Dr. M. Islam for their valuable suggestions and also to the Vidyasagar University for permitting me to do research work in the laboratory of the Department of Chemistry.

Theoretical Laboratory,  
Department of Chemistry and Chemical Technology,  
Vidyasagar University, Midnapore, 721102, India.

BISWARUP MANDAL



# CONTENTS

<b>Chapter</b>	<b>Page No.</b>
<b>Chapter 1: General introduction and objectives</b>	<b>1-24</b>
Abstract	1
1.1 General introduction and objectives	2-13
1.2 References	14-24
<b>Chapter 2: Brief outline of the theory of AM1 method and DFT method</b>	<b>25-42</b>
Abstract	25
2.1 LCAO-MO approach	26-27
2.2 Roothaan's-RHF theory for closed-shell systems	27-29
2.3 Roothaan's-RHF theory for open shell systems	29-31
2.4 The Pople-Nesbet UHF theory for open-shell systems	31-32
2.5 Excited state calculations	33-34
2.6 Density functional theory (DFT)	34-36
2.7 Calculation of molecular properties	36-39
A: Molecular geometry	36
B: Charge density, Cation affinities, Hardness and Transition energy	36-39
2.8 Polarizable Continuum Model (PCM)	40
2.9 References	41-42
<b>Chapter 3: The comparative proton affinities of a series of conjugated <math>\alpha,\beta</math>-unsaturated carbonyl compounds [Acrolien (ACL), 4-hydroxy-2-nonenal (HNE), Methyl vinyl ketone (MVK), Acrylamide (ACR), Methyl acrylate (MA), Ethylmethacrylate (EMA) in ground state. A DFT based computational study in both gas and aqueous phases.</b>	<b>43-59</b>
Abstract	43
3.1 Introduction	44-46
3.2 Computational details	46-47
3.3 Results and discussion	47-51
3.4 Conclusion	51
3.1.1 to 3.1.7 Tables	52-54
3.2.1 Figure	46
3.2.2 Figure	48
3.2.3 Figure	55-57
3.5 References	58-59

<b>Chapter 4: Ground state lithium cation affinities (LCA) and associate parameters of a series of <math>\alpha</math>, <math>\beta</math>-unsaturated carbonyl compounds of type-2-alkene chemical class (ACL, HNE, MVK, ACR, MA and EMA): A Comparative DFT based computational study in both gas and aqueous phases.</b>	<b>60-79</b>
Abstract	60
4.1 Introduction	61-64
4.2 Computational details	64-65
4.3 Results and discussion	65-70
4.4 Conclusion	70
4.1.1 to 4.1.8 Tables	71-74
4.2.1 Figure	64
4.2.2 Figure	65
4.2.3 Figure	75-76
4.5 References	77-79
<b>Chapter 5: Ground state sodium cation affinities (SCA) and associate parameters of a series of <math>\alpha,\beta</math>-unsaturated carbonyl compounds of type-2-alkene chemical class (ACL, HNE, MVK, ACR, MA and EMA ): A Comparative DFT based computational study in both gas and solvent phases.</b>	<b>80-106</b>
Abstract	80
5.1 Introduction	81-83
5.2 Computational details	84
5.3 Results and discussion	85-91
5.4 Conclusion	92
5.1.1 to 5.1.9 Tables	93-99
5.2.1 Figure	83
5.2.2 Figure	85
5.2.3 Figure	100-103
5.5 References	104-106
<b>Chapter 6: The proton affinities of a series of <math>\beta</math>-substituted Acrylamide in the ground state: A DFT based computational study.</b>	<b>107-120</b>
Abstract	107
6.1 Introduction	108
6.2 Computational details	109
6.3 Results and discussion	109-112
6.4 Conclusion	112
6.1.1 to 6.1.4 Tables	113-114
6.2.1 Figures	109
6.2.2 to 6.2.4 Figure	115-116
6.2.5 Figure	117-118
6.5 References	119-120



<b>Chapter 7: The comparative study of basicities, Li<sup>+</sup> and Na<sup>+</sup> affinities of a series of heterocyclic molecules (Pyrrole, Furan, Thiophene and Pyridine) in the ground state. A DFT Study.</b>	<b>121-144</b>
Abstract	121
7.1 Introduction	122-124
7.2 Computational details	124-125
7.3 Results and discussion	125-132
7.4 Conclusion	132
7.1.1 to 7.1.8 Tables	133-138
7.2.1 Figure	125
7.2.2 Figure	139-140
7.2.3 to 7.2.4 Figures	141
7.5 References	142-144
<b>Chapter 8: The ground state Cu<sup>2+</sup> ion affinities of Glycine, Alanine and Cysteine in gas and aqueous phase: A DFT based computational study.</b>	<b>145-162</b>
Abstract	145
8.1 Introduction	146-147
8.2 Computational details	147-148
8.3 Results and discussion	148-152
8.4 Conclusion	153
8.1.1 to 8.1.7 Tables	154-157
8.2.1 Figures	158-160
8.5 References	161-162
<b>Chapter 9: Proton affinities of a series of <math>\alpha,\beta</math> unsaturated carbonyl compounds of type-2- alkene (ACL, HNE, MVK, ACR, MA, EMA ), in the gas and aqueous phase in their low-lying excited triplet state. A DFT/ PCM-SCRF approach.</b>	<b>163-182</b>
Abstract	163
9.1 Introduction	164-166
9.2 Computational details	166-167
9.3 Results and discussion	167-171
9.4 Conclusion	171-172
9.1.1 to 9.1.9 Tables	173-177
9.2.1 Figure	166
9.2.2 Figure	167
9.2.3 Figure	178
9.2.4 Figure	179
9.5 References	180-182

**Chapter 10: Low-lying excited state lithium cation affinities (LCA) and associate parameters of a series of  $\alpha,\beta$ -unsaturated carbonyl compounds of type-2-alkene chemical class (ACL, HNE, MVK, ACR, MA and EMA ) : A Comparative DFT based computational study in both gas and solvent phases. 183-200**

Abstract	183
10.1 Introduction	184-186
10.2 Computational details	186-187
10.3 Results and discussion	187-191
10.4 Conclusion	191
10.1.1 to 10.1.7 Tables	192-196
10.2.1 Figure	186
10.2.2 Figure	187
10.2.3 to 10.2.4 Figure	197-198
10.5 References	199-200

**Chapter 11: The proton affinities of a series of heterocyclic compounds pyrrole, furan, thiophene and pyridine in their low-lying excited triplet state: A DFT based comparative study. 201-220**

Abstract	201
11.1 Introduction	202-203
11.2 Computational details	204
11.3 Results and discussion	204-209
11.4 Conclusion	210
11.1.1 to 11.1.7 Tables	211-215
11.2.1 Figure	204
11.2.2 Figure	216
11.2.3 Figure	217
11.5 References	218-220

**Chapter 12: The lithium affinities of a series of heterocyclic compounds pyrrole, furan, thiophene and pyridine in their low-lying excited triplet state: A DFT based comparative study. 221-239**

Abstract	221
12.1 Introduction	222-223
12.2 Computational details	223-224
12.3 Results and discussion	224-230
12.4 Conclusion	230
12.1.1 to 12.1.9 Tables	231-234
12.2.1 Figure	224
12.2.2 to 12.2.4 Figure	235-236
12.5 References	237-239

# **CHAPTER 1**

## **General Introduction and Objectives**



**Abstract:** This Chapter contains

- Brief introduction
- Literature survey (though not sufficiently exhaustive)
- Objectives of the present thesis

## 1.1 General introduction and objectives

Gas phase ion chemistry is a field of science encompassed within both chemistry and physics. It is the science that studies ions and molecules in the gas phase, most often enabled by some form of mass spectrometry. The knowledge of reaction mechanism is most essential to understand or describe the macroscopic chemical changes of matter on molecular basis in the area of chemistry and biology. Reaction mechanism of organic chemistry has been studied for long time in detail both theoretically and experimentally to develop the advanced correlation between structure and reactivity. In the last few years (> 20), gas phase ionic chemistry captured major area in the field of chemical research. Gas phase reaction of ions with molecules has been an ever increasing interest in the field of both theoretical and experimental research. Normally chemists (all over the World) were well concerned with the importance of ion-molecule reactions in the gas phase. First at all, Radiation chemistry was made some essential steps for developing these types of reactions and were due to Lind.<sup>1</sup> Ion-molecule reaction plays an important role in plasma Chemistry. These reactions are the main sources of ion and particle in the space. Ion-molecular reactions were able to interpret radio-lytic systems after it was demonstrated with mass spectrometer in 1950s.<sup>2</sup> In recent years, the study of the ion- molecule reactions in gas phase has lead to precise determination of intrinsic acid- base properties. Chemical reactivity of organic molecules can be determined fairly in gaseous environment.<sup>3</sup> Reaction of a cation with polar molecule is treated as acid-base reaction where cations act as acid and molecule as base. Acid – base properties of chemical compounds and also the definition of acid and bases were developed over 300 years ago.<sup>4-7</sup> In 1923, Bronsted<sup>8,9</sup> and Lowry<sup>10,11</sup> gave the first idea about proton transfer reaction of a conjugate acid – base pair (Base + Proton  $\leftrightarrow$  Acid). Cation–dipole interactions occupy a major area of theoretical research and

became useful in various field of Chemistry.<sup>12-16</sup> It plays important role in atmospheric Chemistry, molecular biology and also in the field of mass spectrometry. Both mass spectrometry and gas phase ion Chemistry have made essential contribution to the area of experimental and theoretical research not only by providing various analytical tools but also allowing the ion–molecule reactions in the gas phase excluding solvent effects. Scientists from experimental<sup>12,17-38</sup> and theoretical<sup>39-80</sup> field focused attention on cation–dipole interactions considering their unquestionable importance in various field of Chemistry. In particular, application of Ion Cyclotron Resonance (ICR)<sup>81</sup> and High Pressure Mass Spectrometry (HPMS)<sup>12b</sup> have provided good results of kinetics and thermo chemical properties of Physical Organic Chemistry. On the contrary, the mechanistic impacts become less important, especially overview of the scarce and largely indirect results on basic features of organic reactions occurred in gas phase. So the experimental structural, stereochemical and thermo chemical results are still insufficient and further exploration in need. Stability of the complexes in ion-molecule (closed shell) reaction depends on interaction enthalpies. Higher enthalpy change ( $-\Delta H$ ) leads to higher stability of the complex.<sup>15a, 80a, 82</sup>

Besides ion-molecule (polar) interactions, the cation– $\pi$  interactions also play an important role in nature, particularly in molecular recognition and enzyme catalysis. These interactions are treated as non-covalent molecular interaction between electron rich  $\pi$  systems (benzene, acetylene) and adjacent metal cation  $\text{Li}^+$  and  $\text{Na}^+$ . Complex formed in this type of interactions<sup>33a,83-86</sup> are stable as the complexes formed in interaction of cation with traditional ligand like amines, water and others. The most studied cation- $\pi$  interactions involve binding between an aromatic  $\pi$  system and an alkali metal or nitrogenous cation.<sup>87</sup> It is obvious from literature,<sup>88-92</sup> benzene has been selected more as base compared to many other ion-  $\pi$  systems<sup>93,94</sup> to study  $\pi$  –

## Chapter 1

cation interactions in gas as well as in solvent phase. Because of the simplest aromatic structure, six  $C^{\delta-}-H^{\delta+}$  bond dipole of benzene produce a negative electrostatic zone on the face of  $\pi$  system and insist cation attacked to the surface.

In recent years, proton transfer reactions are of considerable importance in Chemistry. Before introducing proton transfer reactions in gas phase, reactions have been studied extensively in solution phase. It is a fundamental reaction studied in both gas and solvent.<sup>95</sup> Proton transfer reaction is very simple where proton ( $H^+$ ) binds with molecule and proton affinity evaluated from energy difference between protonated complex and unprotonated base. Formally, the relationship between the enthalpy of formation of  $BH^+$  and its neutral counterpart, B, is defined in terms of a quantity called the proton affinity (PA). This is the negative of the enthalpy change of the hypothetical protonation reaction. A large number of theoretical studies have been reported in the literature.<sup>12a, 96</sup> Expectedly, studies of the gas phase basicity and accompanying proton affinity of the molecules covering a large area of experimental and theoretical research in Chemistry because of their important role in bio-molecular process. Computational method has advantage of calculating proton affinity of molecule. It provides absolute rather than relative proton affinity results.<sup>96,97-99</sup> Semiempirical method<sup>100,101</sup> has been used widely to obtain proton affinity of the molecules. There are many instances of proton attack on carbonyl oxygen in the primary step of a carbonyl system.<sup>102-105</sup> De et al.<sup>106,107</sup> reported ground state basicities of a series of aliphatic and aromatic conjugated carbonyl systems. Some different types of basicity and proton affinities have been reported experimentally by Arnet et al.<sup>108</sup> and drawn a comparison of H-bond affinity and proton affinity. Quantitative proton affinities along with hydrogen affinity and ionization potential of a series of alkylamines and their related alicyclic, saturated heterocyclic compounds have been investigated using ICR technique and also



studied with *abinitio* CNDO/2 method successfully by Donald H. Aue<sup>109</sup> in 1976. Drummond and MacMohan<sup>110</sup> calculated the proton affinity value for acetones and fluorinated formaldehydes spectrometrically (ICR). Proton affinity of those compounds has also been studied by semiempirical molecular orbital (MO) method and verifies the authenticity of MNDO approach. Proton affinity results obtained from MNDO calculation method<sup>111</sup> have been in good agreement with experimental results.

Besides basicities, proton affinities, necessity of alkali metal cation ( $\text{Li}^+$ ,  $\text{Na}^+$ ,  $\text{K}^+$  etc.) affinity calculation of the molecule / compound has been largely increased to understand the nature of acid-base reactions in gas phase and also the variation of thermo chemical properties in different solvents. Metal ions play important role in biochemical process.<sup>112</sup> Almost 30% of enzyme-catalyzed reactions in living systems are effected by modified electron flow of enzyme or substrate in presence of metal ions. Metal ions are generally positively charged, they can form bond with other atoms by sharing electron pair. Like hydrogen ion, metal ions are also treated as Lewis acids in acid- base reactions. In a acid-base reaction, metal ion bonded with ligand atom (O, N, S, etc.). Generally ligands are electron rich, they donate electron to the metal and formed non-covalent bond. Ions having more than one positive charge ( $\text{Cu}^{+2}$ ,  $\text{Ni}^{+2}$ ,  $\text{Zn}^{+2}$  etc.) can bonded with more than one ligand around them at a time. Ion-molecular reactions have been carried out for a long time not only to determine interaction energies but also to obtain detailed information of ionic structures. Uses of several experimental techniques like Collision Induced Dissociation (CID) or collisionally activated dissociation provides primary structures during collisional activation, ion-molecule reactions provide ions secondary structures and key information that helps to determine the ionic structures in gas phase under thermal equilibrium condition.

## Chapter 1

Since alkali metal ions like  $\text{Li}^+$ ,  $\text{Na}^+$ ,  $\text{K}^+$ , take part in many important biological processes,<sup>113,114</sup> estimation of exact interaction energy can help us to know the proper function of biological fragments in living systems. Investigation of thermodynamic<sup>34a</sup> (enthalpies, Free energies) of the reactions are useful to determine the cation affinity or basicity order of the bases in absence of solvent. It was seen that, gas phase basicity, proton affinity calculation is very tough to determine under experimental<sup>115</sup> condition. Then application of quantum methods is started for calculating energetic properties of gas phase reactions. Gas phase basicity, proton affinity values of small molecule have been successfully calculated by *abinitio* method but it is proved unable to provide reliable values for comparatively large molecule. Ozment et al.<sup>116</sup> also reported that semiempirical methods such as AM1, MNDO, and PM3 are not so reliable in calculations of proton affinity. Then density functional theory (DFT) has been drawn much attention as successful tool of quantum Chemistry for more than fifteen years. The electronic structures, stability and bonding (Hydrogen, alkali halides-halide ions) of the complexes have been studied<sup>79,80a</sup> theoretically. Comparative *abinitio* study<sup>117</sup> of cation ( $\text{H}^+$ ,  $\text{Li}^+$ ,  $\text{Na}^+$ ) – dipole interactions of hydrogen and alkali halides have already been performed to quantify the cation affinities and special attention has been given to the nature of bonding of the complexes. In 1982, Smith et al.<sup>44</sup> performed a computational investigation on proton, lithium and sodium complexes of several 1<sup>st</sup> row and 2<sup>nd</sup> row bases and made a comprehensive discussion on interaction energies, geometrical structures of the optimized complexes.

Interaction of organic compounds or biological molecules with alkali cations has drawn much attention in the gas phase reactions.<sup>113,114</sup> These interactions are equally important for chemical and biological process conducting in solution.<sup>118</sup> For example, ion salvation,<sup>118a</sup> catalysis,<sup>118b</sup> affinity of active compounds toward cations and

antimicrobials activity.<sup>118c</sup> Alkali metal cations are first metal cations studied in gas phase due to their Lewis acid properties and also their easy production under vacuum. To evaluate the most accurate results of affinity of the bases toward alkali cations, most of the studied were performed experimentally like HPMS,<sup>12b,119</sup> CID,<sup>120</sup> ion cyclotron resonance (ICR)<sup>81,121,122</sup> and latest Fourier transform–ion cyclotron resonance (FT- ICR).<sup>123</sup> Affinities for various charged species (except H<sup>+</sup>), specifically affinities for alkali metal cations have been studied by Cook's kinetic method.<sup>124</sup> For proton transfer reactions, application of methods are restricted to pure, stable and volatile compounds, the problem may be strict when the methods applied in alkali metal cation transfer reactions, particularly during the exploratory study of Na<sup>+</sup> affinity determinations.<sup>125</sup>

A large number of computational calculations have been performed to investigate the interaction energies and geometrical parameters in different carbonyl base – alkali metal reactions. Burk et al<sup>126</sup> performed a comparative studies of alkali metal cation basicities of some Lewis bases using different computational methods (DFT B3LYP/6-311+G\*\*, G2, G2 (MP2), G3, and CBS-QB3). Computational calculations were performed by Bark et al.<sup>127</sup> to evaluate proton and lithium cation affinity (LCA), lithium cation basicity (LCB) of some  $\beta$  di-carbonyl compounds (acetylacetone, hexafluoroacetylacetone, diacetamide, and hexafluorodiacetamide) , the results obtained from this calculations are in good agreement with experimental values. G2 and G2(MP2) calculations of LCBs for 37 compounds and density functional theory (B3LYP/6-311+G\*\*) calculations of LCBs of 63 compounds were reported by Burk et al.<sup>128</sup>

Sodium occurs in all known biological systems, generally functioning as electrolytes inside and outside cells.<sup>129</sup> Sodium cation interactions with various organic molecules

## Chapter 1

/compounds have also covered major area in both theoretical and experimental research. Hoyau et al. studied Sodium cation interactions<sup>130</sup> with 40 different bases in the year 1999. Both experimental (FT-ICR) and computational methods (MP2 (full) /6-31G\*) were applied for evaluating sodium cation affinity (SCA) values of 50 molecules by McMahon and Ohanessian.<sup>131</sup> DFT B3LYP/6-311+G(3df,2p) calculations were performed by Lau et al.<sup>132</sup> to calculate the potassium cation basicity of large number of bases (136 number). The ground state sodium cation affinity of a series of substituted acetophenones was reported earlier by Senapati et al.<sup>133</sup> in the year 2010.

Sodium cation affinity of a number of amino acids / peptides has been measured both computationally and experimentally. In 2003 Kish et al. investigated the SCA's of amino acids in Laboratory by collision activated dissociation method and established the results as the ladder of sodium affinities via Cooks's kinetic method.<sup>134</sup> Obtained SCA values was verified theoretically using MP2(full)/6-31G\* method of calculation. Recently Sodium cation affinities of di-, tri- and tetra peptides was calculated using MP2(full) / 6-311+G\* method by Wang et al.<sup>135</sup> Results obtained in this investigation are found very close to the experimental values. In 2008, The Na<sup>+</sup> ion affinities of asparagine, glutamine, histidine and arginine were also studied theoretically.<sup>136</sup> Metal binding properties of L- glutamic acid and L- aspartic acid were examined experimentally<sup>137</sup> by S. S. A. Sajadi in 2010. Both single charged (Na<sup>+</sup>, Li<sup>+</sup>) and double charged (Mg<sup>+2</sup>, Mn<sup>+2</sup>, Cu<sup>+2</sup> and Zn<sup>+2</sup>) cations were used in this experiment.

Copper ion (Cu<sup>+</sup>, Cu<sup>+2</sup>) plays an important role in oxidation, dioxygen transport and electron transfers are of some biological process.<sup>138-143</sup> This is important to know, the binding energies and coordination mode of copper ion in metal protein, not only to understand the structures and biological functions but also need to interpret the experimental results. Numerous numbers of computational and experimental researches

on amino acids – metal cation interactions have been conducted successfully. In 1996, *abinitio* calculations of  $\alpha$ -amino acids were carried out for evaluating absolute affinities for  $\text{Cu}^+$  ion in gas phase by Ohanessian and Hoyau.<sup>144</sup> Nino Russo et al.<sup>145</sup> reported the  $\text{Cu}^+$  and  $\text{Cu}^{+2}$  affinity results of  $\alpha$ -alanine by DFT/ 6-311++ G\*\* calculation method . From this study it was found that stability order of metalated complex and coordination sites are different, depending upon the nature of the cation. Alkali metal cation- amino acid complexes have also been studied theoretically.<sup>146,147</sup> In 2008, alkali metal interactions of Serine (Ser) and Threonine (Thr) have been performed<sup>148</sup> by threshold collision-induced dissociation and also by Quantum chemical calculations at three different levels, B3LYP, B3P86, and MP2(full), using the 6-311+G(2d,2p) basis set and it was seen that, theoretical results show good agreement with experimental results.

Aromatic compounds are important in industry and play key roles in the biochemistry of all living things.<sup>149</sup> The  $\pi$ - conjugated polymers with electronic and optical functionalities have been attracting much attention. Especially,  $\pi$ -conjugated compounds of six, five, four membered aromatic units such as benzene, pyridine, thiophene, pyrrole and furan have been attracting strong interest.<sup>150</sup> Plenty of research journals have been published in this field. Structural, electronic properties of fury pyridine molecules have been studied computationally at B3LYP/ 6-311++G (2d,p) level.<sup>151</sup> Wu et al.<sup>152</sup> reported on the nature of interactions of pyridine, furan and thiophene with  $\text{LiNH}_2$  with various DFT including B3LYP, MO6, MO6-2X methods. DFT study of five- and six-membered compounds present in hydrotreatment process was performed by Valencia et al.<sup>153</sup> In 2012, they observed geometrical modifications, proton affinities and explained stabilization energies of the complexes.

The heterocyclic molecules (pyrrole, furan, thiophene and pyridine) have lately attracted attention due to their “shifted pKa values” upon complexation to metal ions,

## Chapter 1

because it can rationalize the existence of nucleobases of different protonation state at physiological  $P^H$ .

Several conjugated  $\alpha$ ,  $\beta$ -unsaturated carbonyl compounds of type-2 alkene series are treated as environmental pollutants; they can produce toxicity via a common molecular mechanism. Ambient mixture of these pollutants is injurious to human health.<sup>154</sup> So their interactions with ions need special attention.

From the above literature survey (though not sufficiently exhaustive), it was found that, a large number of theoretical studies have been performed taking different carbonyl compounds, heterocyclic compounds, amino acids. But no such systematic theoretical and comparative studies have been performed to quantify the cation affinities ( $H^+$ ,  $Li^+$ ,  $Na^+$ ) and basicities for several conjugated  $\alpha$ ,  $\beta$ -unsaturated carbonyl compounds (acrolein, 4-hydroxy 2-nonenol, methyl vinyl ketone, Acrylamide, methyl acrylate and ethyl methacrylate).

So far, detailed comprehensive and comparative study of gas phase proton affinity, gas phase basicity, alkali metal cation ( $Li^+$ ,  $Na^+$ ) affinity and basicity of N or O or S heterocyclic compound (pyrrole, furan, thiophene and pyridine) are rather scarce.

We have searched (though not sufficiently exhaustive) the literature (before this work has been undertaken), no detailed, systematic and comparative computational studies on  $Cu^{2+}$  interaction with glycine, alanine and cysteine in both gas and aqueous phase have been performed.

Therefore the present research work will concentrate to quantify proton, lithium and sodium cation affinities and basicities of the above mentioned carbonyl compounds with the help of most reliable DFT / B3LYP computational method at hybrid triple zeta 6-311G (d,p) basis set in gas phase and also in solvent phases in ground state (Chapter 3, Chapter 4, Chapter 5) and some of them in low-lying excited triplet state (Chapter 9,

Chapter 10). The semiempirical quantum chemical AM1 method have been also employed (In chapter 3) to calculate the gas phase proton affinities of the  $\alpha,\beta$ -unsaturated carbonyl compounds (mentioned before). The results obtained in AM1 method were too inferior to the DFT proton affinities which are estimated considerably less. Therefore, AM1 method is not applied in further investigations.

In present work, we have reported the gas phase proton affinities and some associates thermochemical properties of Acrylamide and its  $\beta$ -substituted counterparts (Including electron releasing and electron withdrawing group) in Chapter 6.

This work will give attention to estimate important geometrical and thermodynamic properties such as proton affinity, gas phase basicity, lithium and sodium cation affinity and basicity of pyrrole, furan, thiophene and pyridine in ground state (Chapter 7) and low-lying excited state also (Chapter 11, Chapter 12).

Work will also focus on  $\text{Cu}^{+2}$  interactions of three important amino acids in the ground state to find out the nature of interactions, affinities toward  $\text{Cu}^{+2}$  ions and also the electronic and molecular structures of complexes in gas and aqueous phase (Chapter 8).

In order to understand the structural behavior and electronic properties in solvents, the work has been carried out using SCRF-PCM<sup>155</sup> (Polarizable Continuum Model) optimization process at the same level of theory.

Parallel to gas phase experimental studies on ion-molecule interactions, advance computational investigation (with Gaussian '03', Gaussian '09' program package) can provide very good results in this field of research. This thesis is an assemblage of our theoretical works to search out new information about structural and energetic properties of cations ( $\text{H}^+$ ,  $\text{Li}^+$ ,  $\text{Na}^+$ ,  $\text{Cu}^{2+}$ ) interactions with some organic aliphatic and aromatic compounds.

## Chapter 1

The thesis consists of following chapters.

- Chapter I:** General introduction and objectives (the present chapter).
- Chapter 2:** Brief outline of the theory of AM1 and DFT method.
- Chapter 3:** The comparative proton affinities of a series of conjugated  $\alpha,\beta$ -unsaturated carbonyl compounds [Acrolien (ACL), 4-hydroxy-2-nonenal (HNE), Methyl vinyl ketone (MVK), Acrylamide (ACR), Methyl acrylate (MA), Ethyl methacrylate (EMA) in ground state. A DFT based computational study in both gas and aqueous phases.
- Chapter 4:** Ground state lithium cation affinities (LCA) and associate parameters of a series of  $\alpha,\beta$ -unsaturated carbonyl compounds of type-2-alkene chemical class (ACL, HNE, MVK, ACR, MA and EMA ): A Comparative DFT based computational study in both gas and aqueous phases.
- Chapter 5:** Ground state sodium cation affinities (SCA) and associate parameters of a series of  $\alpha,\beta$ -unsaturated carbonyl compounds of type-2-alkene chemical class (ACL, HNE, MVK, ACR, MA and EMA ): A Comparative DFT based computational study in both gas and solvent phases.
- Chapter 6:** The proton affinities of a series of  $\beta$ -substituted Acrylamide in the ground state: A DFT based computational study.
- Chapter 7:** The comparative study of basicities,  $\text{Li}^+$  and  $\text{Na}^+$  affinities of a series of heterocyclic molecules (Pyrrole, Furan, Thiophene and Pyridine) in the ground state. A DFT Study.
- Chapter 8:** The ground state  $\text{Cu}^{2+}$  ion affinities of Glycine, Alanine and Cysteine in gas and aqueous phase: A DFT based computational study.



- Chapter 9:** Proton affinities of a series of  $\alpha,\beta$  unsaturated carbonyl compounds of type-2-alkene (ACL, HNE, MVK, ACR, MA, EMA), in the gas and aqueous phase in their low-lying excited triplet state. A DFT/PCM-SCRF approach.
- Chapter 10:** Low-lying excited state lithium cation affinities (LCA) and associate parameters of a series of  $\alpha,\beta$ -unsaturated carbonyl compounds of type-2-alkene chemical class (ACL, HNE, MVK, ACR, MA and EMA): A Comparative DFT based computational study in both gas and solvent phases.
- Chapter 11:** The proton affinities of a series of heterocyclic compounds pyrrole, furan, thiophene and pyridine in their low-lying excited triplet state: A DFT based comparative study.
- Chapter 12:** The lithium affinities of a series of heterocyclic compounds pyrrole, furan, thiophene and pyridine in their low-lying excited triplet state: A DFT based comparative study.

## 1.2 References

- (1) Lind, S. G. *The Chemical Effects of  $\alpha$  particles and Electrons* Chemical Catalog Co. 1928.
- (2) Ferguson, E. E. *Ion-molecule reactions. Annual Review of Physical Chemistry*, **1975**, 26, 17–38.
- (3) De Hoffmann, E.; Charrette, J.; Stroobant, V. *Mass Spectrometry Principles and Applications*; John Wiley & Sons: Chichester, 1999.
- (4) King, E. J. *Acid-Base Equilibria*, Pergamon Press, Oxford, 1965.
- (5) Finston, H. L.; Rychtman, A. C. *A New View of Current Acid-Base Theories*, Wiley, New York, 1982. Haney, M. A.; Franklin, J. L. *J. Phys. Chem.* **1969**, 73, 4328.
- (6) Bell, R. P. *The Proton in Chemistry*, 2nd ed., Cornell University Press, Ithaca, New York, 1973.
- (7) Gillespie, R. J. *Proton Acids, Lewis Acids, Hard Acids, Soft Acids and Superacids*, in: Caldin, E.; Gold, V. (Eds.), *Proton-Transfer Reactions*, Chapman and Hall, London, 1975, ch. 1.
- (8) Brønsted, J. N. *Rec. Trav. Chim. Pays-Bas*, **1923**, 42, 718–728.
- (9) Brønsted, J. N. *Chem. Rev.* **1928**, 5, 231–338.
- (10) Lowry, T. M. *Chem. Ind. (London)*, **1923**, 42, 43–47.
- (11) Lowry, T. M. *Chem. Ind. (London)*, **1923**, 42, 1048–1052.
- (12) (a) Beauchamp, J. L. *Annu. Rev. Phys. Chem.* **1971**, 22, 527. (b) Kebarle, P. *Annu. Rev. Phys. Chem.* **1977**, 28, 445. (c) *Gas Phase Ion Chemistry*; Bowers, M. T., Ed.; Academic Press: New York, 1979; Vols. 1 and 2; 1984; Vol. 3. (d) Walder, R., Franklin, J. L. *Int. J. Mass. Spectrom. Ion. Phys.* **1980**, 36, 85. (e) Ng, C. Y. *Adv. Chem. Phys.* **1983**, 52, 263.

- (13) Martin, T. P. *Phys. Rep.* **1983**, *95*, 167.
- (14) Turner, N. H.; Dunlap, B. I.; Colton, R. J. *Anal. Chem.* **1984**, *56*, 373R.
- (15) (a) Castleman, A. W., Jr.; Keesee, R. G. *Chem. Rev.* **1986**, *86*, 589. (b) Sauer, J.; Hobza, P.; Zahradnik, R. *J. Phys. Chem.* **1980**, *84*, 3318.
- (16) (a) Keesee, R. G.; Castleman, Jr., A. W. *J. Phys. Chem. Ref. Data* **1985**, *15*, 1011. (b) Mark, T. D.; Castleman, A. W., Jr. *Adv. At. Mol. Phys.* **1985**, *20*, 66.
- (17) Haney, M. A.; Franklin, J. L. *J. Phys. Chem.* **1969**, *73*, 4328
- (18) Wolf, J. F.; Staley, R. H.; Koppel, I.; Taagepera, M.; McIver, R. T.; Beauchamp, J. L.; Taff, R. W. *J. Am. Chem. Soc.* **1977**, *99*, 5417.
- (19) Tiedeman, P. W.; Anderson, S. L.; Seyer, S. T.; Hirooke, T.; Ng, C. Y.; Mahan, B. H.; Lee, Y. T. *J. Chem. Phys.* **1979**, *71*, 605.
- (20) Schafer, E.; Saykally, R. J. *J. Chem. Phys.* **1984**, *80*, 2973; **1984**, *81*, 4189.
- (21) Chupka, W. A. *J. Chem. Phys.* **1959**, *30*, 458.
- (22) Berkowitz, J.; Tasman, H. A.; Chupka, W. A. *J. Chem. Phys.* **1962**, *36*, 2170.
- (23) Buck, R. P.; Hass, J. R. *Anal. Chem.* **1973**, *45*, 2208.
- (24) Mohazzabi, P.; Searcy, A. W. *J. Chem. Phys.* **1974**, *61*, 4358.
- (25) Reck, G. P.; Mathur, B. P.; Rothe, E. W. *J. Chem. Phys.* **1977**, *66*, 3847.
- (26) Honda, F.; Lancaster, G. M.; Fukuda, Y.; Rabalais, W. *J. Chem. Phys.* **1978**, *69*, 4931.
- (27) Pflam, P.; Pfarr, P.; Sattler, K.; Recknagel, E. *Surf. Sci.* **1985**, *156*, 165.
- (28) Kappes, M. M.; Radi, P.; Schar, M.; Schumacher, E. *Chem. Phys. Lett.* **1985**, *113*, 243.
- (29) Huber, K. P.; Herzberg, G. *Constants of Diatomic Molecules*; Van Nostrand Reinhold: 1979.
- (30) Bartmess, J. E., McIver, Jr., R. T. In *Gas Phase Ion Chemistry*; Bowers, M. T., Ed.; Academic Press: New York, 1979; Vol. 2, p 87.

## Chapter 1

- (31) JANAF Thermochemical Tables: *J. Phys. Chem. Ref. Data* **1985**, *14*, Suppl. 1.
- (32) Klimenko, N. M. *Chemical Bonding and Molecular Structure* (in Russian); Nauka: Moscow, 1984; p 36.
- (33) (a) Woodin, R. L.; Beauchamp, J. L. *J. Am. Chem. Soc.* **1978**, *100*, 501. (b) Woodin, R. L.; Beauchamp, J. L. *Chem. Phys.* **1979**, *41*, 1.
- (34) (a) Dzidic, I.; Kebarle, P. *J. Phys. Chem.* **1970**, *74*, 1466. (b) Searless, S. K.; Kebarle, P. *Can. J. Chem. Phys.* **1969**, *47*, 2619. (c) Davidson, W. R.; Kebarle, P. *J. Am. Chem. Soc.* **1976**, *98*, 6125, 6133.
- (35) Taft, R. W. Private Communication, cited in the following: Lias, S. G.; Shold, D. M.; Ausloos, P. *J. Am. Chem. Soc.* **1980**, *102*, 2540.
- (36) Emsley, J. *Chem. Soc. Rev.* **1980**, *9*, 91.
- (37) Larson, J. W.; McMahon, T. B. *Inorg. Chem.* **1984**, *23*, 2029.
- (38) Botschwina, P. *Ion and Cluster-Ion Spectroscopy and Structure*; Elsevier: Amsterdam, 1989.
- (39) Schuster, P. In *Electron-Solvent and Anion Solvent Interactions*; Kevan, L., Webster, B. C., Eds.; Elsevier: Amsterdam, 1976.
- (40) (a) Morokuma, K. *J. Chem. Phys.* **1971**, *55*, 1236. (b) Kitaura, K.; Morokuma, K. *Int. J. Quantum Chem.* **1976**, *10*, 325. (c) Umeyama, H.; Morokuma, K. *J. Am. Chem. Soc.* **1976**, *98*, 4400. (d) Morokuma, K. *Acc. Chem. Res.* **1977**, *10*, 294. (e) Morokuma, K.; Kitaura, K. In *Molecular Interactions*; Ratajczak, H., Orville-Thomas, W. J., Eds.; Wiley: New York, 1980; Vol. 1, p 21.
- (41) (a) Berthod, H.; Pullman, A. *Chem. Phys. Lett.* **1980**, *70*, 434. (b) Berthod, H.; Pullman, A. *Isr. J. Chem.* **1980**, *19*, 299. (c) Kollman, P. *Chem. Phys. Lett.* **1978**, *55*, 555. (d) Pullman, A.; Brochen, P. *Chem. Phys. Lett.* **1975**, *34*, 7. (e) Kollman, P.; Rothenberg, S. *J. Am. Chem. Soc.* **1977**, *99*, 1333.

- (42) Jeziorski, B.; Kotos, W. In *Molecular Interactions*; Ratajczak, H., Orville-Thomas, W. J., Eds.; Wiley: Chichester, 1982; Vol. 3.
- (43) Reed, A. E.; Curtiss, L. A.; Weinhold, F. *Chem. Rev.* **1988**, 88, 899.
- (44) Smith, S. F.; Chandrasekhar, J.; Jorgensen, W. L. *J. Phys. Chem.* **1982**, 86, 3308.
- (45) (a) Lin, S. M.; Wharton, J. G.; Grice, R. *Mol. Phys.* **1973**, 26, 317. (b) Rittner, E. S. *J. Chem. Phys.* **1951**, 19, 1030. (c) Brumer, P.; Karplus, M. *J. Chem. Phys.* **1976**, 64, 5165.
- (46) Del Bene, J. E.; Frisch, M. J.; Pople, J. A. *J. Phys. Chem.* **1985**, 89, 3669.
- (47) Swanton, D. J.; Bacskay, G. B.; Hugh, N. S. *Chem. Phys.* **1986**, 107, 25.
- (48) Tomoda, S. *J. Mol. Struct.* **1988**, 177, 199.
- (49) Stams, D. A.; Johri, K. K.; Morton, T. H. *J. Am. Chem. Soc.* **1988**, 110, 699.
- (50) Gill, P. M. W.; Radom, L. *J. Am. Chem. Soc.* **1988**, 110, 4931.
- (51) Del Bene, J. E.; Shavitt, I. *Int. J. Quantum Chem. Quantum Chem. Symp.* **1989**, 23, 445.
- (52) Del Bene, J. E.; Shavitt, I. *J. Phys. Chem.* **1990**, 94, 5514.
- (53) Curtiss, L. A.; Jones, C.; Trucks, G. W.; Raghavachari, K.; Pople, J. A. *J. Chem. Phys.* **1990**, 93, 2537.
- (54) Li, Y.; Wang, X.; Jensen, F.; Houk, K. N.; Olah, G. A. *J. Am. Chem. Soc.* **1990**, 112, 3922.
- (55) Kollman, P.; Rothenberg, S. *J. Am. Chem. Soc.* **1977**, 99, 1333.
- (56) Huber, H.; Latajka, Z. *J. Comput. Chem.* **1983**, 4, 252.
- (57) Del Bene, J. E.; Frisch, M. J.; Raghavachari, K.; Pople, J. A.; Schleyer, P. v. R. *J. Phys. Chem.* **1983**, 87, 73.
- (58) Latajka, Z.; Scheiner, S. *Chem. Phys. Lett.* **1984**, 105, 435.
- (59) Pross, A.; Radom, L. *J. Am. Chem. Soc.* **1981**, 103, 6049.

## Chapter 1

- (60) Shevardina, L. B.; Pinchuk, V. M. *J. Struct. Chem.* **1988**, 29, 523.
- (61) Tikilyainen, A. A.; Zyubin, A. S.; Charkin, O. P. Russ, *J. Inorg. Chem.* **1989**, 34, 613.
- (62) Yakobson, V. V.; Musaev, D. G.; Zyubin, A. S.; Mebel, A. M.; Charkin, O. P. *Sov. J. Coord. Chem.* **1989**, 15, 847.
- (63) Chronister, E. L.; Morton, T. H. *J. Am. Chem. Soc.* **1990**, 112, 133.
- (64) Rechsteiner, C. E.; Buck, R. P.; Pedersen, L. *J. Chem. Phys.* **1976**, 65, 1659.
- (65) Bounds, D. G.; Hinchliffe, A. *Mol. Phys.* **1979**, 38, 717.
- (66) Bounds, D. G.; Hinchliffe, A. *Mol. Phys.* **1980**, 40, 989.
- (67) Zakzhevskii, V. G.; Boldyrev, A. I.; Charkin, O. P. *Chem. Phys. Lett.* **1981**, 71, 193.
- (68) Zakzhevskii, V. G.; Boldyrev, A. I.; Charklin, O. P. *Chem. Phys. Lett.* **1981**, 81, 93.
- (69) Gutsev, G. L.; Boldyrev, A. I. *Chem. Phys. Lett.* **1982**, 92, 262.
- (70) Bounds, D. G. *Mol. Phys.* **1984**, 51, 1135.
- (71) Galli, G.; Andreoni, W.; Tosi, M. P. *Phys. Rev. A* **1986**, 34, 3580.
- (72) Sunil, K. K.; Jordan, K. D. *Chem. Phys. Lett.* **1988**, 143, 366.
- (73) Krasnov, K. S. *J. Struct. Chem.* **1983**, 24, 1.
- (74) Ozerova, V. M.; Solomonik, V. G.; Krasnov, K. S. *J. Struct. Chem.* **1983**, 24, 316.
- (75) Solomonik, V. G.; Sliznev, V. V.; Pogrebnaya, T. P. *J. Struct. Chem.* **1988**, 29, 675.
- (76) Mebel, A. M.; Klimenko, N. M.; Charkin, O. P. *J. Struct. Chem.* **1988**, 29, 357.
- (77) Klimenko, N. M.; Mebel, A. M.; Charkin, O. P. *J. Struct. Chem.* **1988**, 29, 364.
- (78) Jena, P.; Khanna, S. N.; Rao, B. K. *Chem. Phys. Lett.* **1990**, 171, 439.
- (79) Sannigrahi, A. B.; Kar, T.; Nandi, P. K. *Chem. Phys. Lett.* **1992**, 198, 67.

- (80) (a) Sannigrahi, A. B.; Nandi, P. K.; Kar, T. *J. Mol. Struct. (Theochem)* **1994**, *306*, 85. (b) Sannigrahi, A. B.; Nandi, P. K.; Schleyer, P. v. R. *Chem. Phys. Lett.* **1993**, *204*, 73.
- (81) Staley, R. H.; Beauchamp, J. L. *J. Am. Chem. Soc.* **1975**, *97*, 5920–5921.
- (82) Sannigrahi, A. B.; Nandi, P. K.; Schleyer, P. v. R. *J. Am. Chem. Soc.* **1994**, *116*, 7225.
- (83) Sunner, J.; Nishizawa, K.; Kebarle, P. *J. Phys. Chem.* **1981**, *85*, 1814.
- (84) Guo, B. C.; Purnell, J. W.; Castleman, A. W., Jr.; *Chem. Phys. Lett.* **1990**, *168*, 155.
- (85) Armentrout, P. B.; Rodgers, M. T. *J. Phys. Chem. A* **2000**, *104*, 2238.
- (86) Deakyne, C. A.; Meotner (Mautner), M. *J. Am. Chem. Soc.* **1985**, *107*, 469.
- (87) Tsuzuki, S.; Yoshida, M.; Uchimaru, T.; Mikami, M. *J. Phys. Chem. A* **2001**, *105*(4), 769–773.
- (88) Cabarcos, O. M.; Weinheimer, C. J.; Lisy, J. M. *J. Chem Phys.* **1998**, *108*, 5151-5154.
- (89) Cabarcos, O. M.; Weinheimer, C. J.; Lisy, J. M. *J. Chem Phys.* **1999**, *110*, 8429-8435.
- (90) Kim, D.; Hu, S.; Tarakeshwar, P.; Kim, K. S.; Lisy, J. M. *J. Phys. Chem. A* **2003**, *107*, 1228.
- (91) Deakyne, C. A.; Meotner, M. *J. Am. Chem. Soc.* **1985**, *107*, 474.
- (92) Meotner, M.; Deakyne, C. A. *J. Am. Chem. Soc.* **1985**, *107*, 469.
- (93) Ma, J. C.; Dougherty, D. A. *Chem. Rev.* **1997**, *97*, 1303.
- (94) Amicangelo, J. C.; Armentrout, P. B. *J. Phys. Chem. A* **2000**, *104*, 11420.
- (95) Bowers, M. T. *Gas-phase Ion Chemistry*, Academic Press: New York, **1973**, 2, 1-14.
- (96) Bagno, A.; Scorrano, G. *J. Phys. Chem.* **1996**, *100*, 1536.

## Chapter 1

- (97) Maksic, M. E.; Hodoscek, M.; Kovacek, D.; Maksic, Z. B.; Primorac, M. J. *Mol. Struct. (Theochem)* **1997**, 417, 131.
- (98) Mishchuk, Y. R.; Potyagaylo, A. L.; Hovorun, D. M. *J. Mol. Struct. (Theochem)* **2000**, 552, 283-289.
- (99) Deakyne, G. A. *Int. J. Mass Spectrom.* **2003**, 227, 601.
- (100) Htto, A. H.; Prescher, D.; Gey, E.; Schrader, S. J. *Fluorine Chem.* **1997**, 82, 55.
- (101) Capitani, J. F. *J. Mol. Struct. (Theochem)* **1995**, 332, 21.
- (102) Bhattacharya, S. P.; Rakshit, S. C.; Banerjee, M. *J. Mol. Struct. (Theochem)* **1983**, 94, 253.
- (103) Dekock, J. R. L.; Kohin, M. S. *J. Mol. Struct. (Theochem)* **1983**, 94, 343.
- (104) Strusz, O. P.; Kapny, E.; Kosmntza, C.; Robb, M. A.; Theodorakopoulos, G.; Cizmadia, I. G. *Theo. Chem. Acta.* **1978**, 48, 215.
- (105) Yamadagni, R.; Kebarle, P. J. *J. Am. Chem. Soc.* **1973**, 96, 3727.
- (106) Pandit, S.; De, D.; De, B. R. **2006**, *J. Mol. Structure (Theochem)*, 760, 245.
- (107) Senapati, U.; De, D.; De, B. R. **2008**, *Indian Journal of Chemistry*, 47A, 548-550.
- (108) Arnett, E. M.; Mitchell, E. J.; Murty, T. S. S. R. *J. Am. Chem. Soc.* **1974**, 96, 3875.
- (109) Donald H. Aue.; Hugh M. Webb.; Michael T. Bowers. Quantitative Proton Affinities, Ionization Potentials, and Hydrogen Affinities of Alkylamines, **1976**, *J. Am. Chem. Soc.* 98(2), 311-317.
- (110) Drummond, D. F.; McMahon, T. B. *J. Phys. Chem.* **1981**, 85, 3746.



- (111) (a) Dewar, M. J. S.; McKee, M. L. *J. Am. Chem. Soc.* **1977**, *99*, 5231. (b) Brint, P.; Healy, E. F.; Spalding, T. R.; Whelan, T. *J. Chem. Soc., Dalton Trans.* **1981**, 2515. (c) Eckert-Maksić, M.; Maksić, Z. B. *J. Chem. Soc., Perkin Trans.* **1981**, *2*, 1462. (d) Olivella, S.; Vilarrasa, J. *J. Heterocycl. Chem.* **1981**, *18*, 1189. (e) Chadha, R.; Ray, N. K. *Theor. Chim. Acta.* **1982**, *60*, 579.
- (112) Poonia, N. S.; Bajaj, A. V. *Chem. Rev.* **1979**, *79*, 389.
- (113) Segel, H. Metal ions in Biological systems, **1973-1981**, 1-20, Marcel Dekker, New York.
- (114) Frausta Dasilva, J. J. R.; Williams, R. J. P. The Biological Chemistry of elements, Oxford University press, 1991.
- (115) Dixon, D. A.; Lias, S. G. *Molecular Structure and Energetics*, **1987**, *2*, *Physical Measurements*, edited by Liebman, J. F.; Greenberg, A. (VCH, Deereld Beach, FL).
- (116) Ozment, J. L.; Schmiedekamp, A. M. *Int. J. Quantum Chem.* **1992**, *43*, 783.
- (117) Sannigrahi, A. B.; Nandi, P. K.; Schleyer, P. R. *J. Am. Chem. Soc.* **1994**, *116(16)*, 7225.
- (118) (a) Castelman, A. W.; Keesee, R. G. *Acc. Chem. Res.* **1986**, *19*, 413. (b) Gal, G-F.; Maria, P. C. *Prog. Phys. Org. Chem.* **1990**, *17*, 159. (c) Nagelkerke, R.; Pregel, M. J.; Dunn, E. J.; Thatcher, G. R. J.; Buncel, E. *Org. React. (Tartu)* **1995**, *24*, 449. (d) Cox, B. G.; Schneider, H. Coordination and Transport Properties of Macrocyclic Compounds in solution, *Elsevier*, New York, 1992.
- (119) a) Sunner, J.; Kebarle, P. *J. Am. Chem. Soc.* **1984**, *106*, 6135 and references therein. (b) Tissandier, M. D.; Cowen, K. A.; Feng, W. Y.; Gundlach, E.; Cohen, M. H.; Earhart, A. D.; Coe, J. V.; Tuttle, T. R., Jr. *J. Phys. Chem. A* **1998**, *102*, 7787.

## Chapter 1

- (120) (a) More, M. B.; Glendening, E. D.; Ray, D.; Feller, D.; Armentrout, P. B. *J. Phys. Chem.* **1996**, *100*, 1605. (b) Rodgers, M. T.; Armentrout, P. B. *J. Phys. Chem. A* **1997**, *101*, 1238. (c) Rodgers, M. T.; Armentrout, P. B. *J. Phys. Chem. A* **1997**, *101*, 2614
- (121) Wieting, R. D.; Staley, R. H.; Beauchamp, J. L. *J. Am. Chem. Soc.* **1975**, *97*, 924.
- (122) Taft, R. W.; Anvia, F.; Gal, J.-F.; Walsh, S.; Capon, M.; Holmes, M. C.; Hosn, K.; Oloumi, G.; Vasanwala, R.; Yazdani, S. *Pure Appl. Chem.* **1990**, *62*, 17.
- (123) (a) Anvia, F.; Walsh, S.; Capon, M.; Koppel, I. A.; Traft, R. W.; de paz, J. L. G.; Catalon, J. *J. Am. Chem. Soc.* **1990**, *112*, 5095. (b) Alcami, M.; Mo, O.; Yanez, M.; Anvia, F.; Traft, R. W. *J. Phys. Chem.* **1990**, *94*, 4796.
- (124) (a) McLuckey, S. A.; Cameron, D.; Cook, R. G. *J. Am. Chem. Soc.* **1981**, *103*, 1313. (b) Cook, R. G.; Patrick, J. S.; Kotiaho, T.; McLuckey, S. A. *Mass Spectrom. Rev.* **1994**, *13*, 287.
- (125) Maria, P. C.; Anvia, F.; Traft, R. W. Presented at Techiques et Mecanismes de Formation des Ions. Soc. Fr. Chim. Soc.; Fr. Spectrom. Masse. Paris, 22-24 November, **1992**.
- (126) Burk, P.; Sults, M.-L.; Jaana, T. T. *Proc. Estonian Acad. Sci. Chem.* **2007**, *56*, 3, 107.
- (127) Burk, P.; Taul, K.; Jaana, T. T. *Croat. Chem. Acta.* **2009**, *82(1)*, 71.
- (128) Burk, P.; Koppel, I. A.; Koppel, I.; Kurg, R.; Gal, J.-F.; Maria, P.-C.; Herreros, M.; Notario, R.; Abboud, J.-L. M.; Anvia, F.; Taft, R. W. *J. Phys. Chem. A* **2000**, *104*, 2824.
- (129) Winter, Mark. "Web Elements Periodic Table of the Elements | Sodium | biological information". *Web Elements*, Retrieved 13 January, 2012.

- (130) Hoyau, S.; Norrman, K.; McMahon, T. B.; Ohanessian, G. *J. Am. Chem. Soc.* **1999**, *121*, 8864.
- (131) McMahon, T. B.; Ohanessian, G. *Chem. Eur. J.* **2000**, *6*, 2931.
- (132) Lau, J. K.-C.; Wong, C. H. S.; Ng, P. S.; Siu, F. M.; Ma, N. L.; Tsang, C. W. *Chem. Eur. J.* **2003**, *9*, 3383 and references therein.
- (133) Senapati, U.; De, D.; De, B. R. *Mol. Simul.* **2010**, *36(6)*, 448.
- (134) Kish, M. M.; Ohanessian, G.; Wesdemiotis, C. *Int. J. Mass Spectrom.* **2003**, *227*, 509
- (135) Wang, P.; Wesdemiotis, C.; Kapota, C.; Ohanessian, G. *J. Am. Soc. Mass Spectrom.* **2007**, *18*, 541.
- (136) Wang, P.; Ohanessian, G.; Chrys Wesdemiotis, C. *Int. J. Mass Spectrom.* **2008**, *269*, 34.
- (137) Sajadi, S. S. A. *Natural Science* **2010**, *2(2)*, 85-90.
- (138) Karlin, K. D.; Tyeklar, Z. *Bioinorganic Chemistry of Copper*, Chapman and Hall, New York, 1993.
- (139) Karlin, K. D.; Zubieta, J. *Biological and Inorganic Copper Chemistry*, Vols. I and II, Adenine, Guilderland, NY, 1986.
- (140) Karlin, K. D.; Zubieta, J. (eds). *Copper Coordination Chemistry: Biological and Inorganic Perspectives*, Adenine: Guilderland, NY, 1986.
- (141) Lippard, S. J.; Berg, J. M. *Principles of Bioinorganic Chemistry*, University Science Books: Mill Valley, CA, 1994.
- (142) Lavanant, H.; Hoppiliard, Y. *J. Mass Spectrom.* **1997**, *32*, 1037.
- (143) Tao, W. A.; Zhang, D.; Wuang, F.; Thomas, P. D.; Cooks, R. G. *Anal. Chem.* **1999**, *71*, 4427.
- (144) Hoyau, S.; Ohanessian, G. *J. Am. Chem. Soc.* **1997**, *119*, 2016.
- (145) Marrini, T.; Russo, N.; Tascano, M. *J. Mass Spectrom.* **2002**, *37*, 786.

## Chapter 1

- (146) Hoyau, S.; Norrman, K.; McMahon, T. B.; Ohanessian, G. *J. Am. Chem. Soc.* **1999**, *121*, 8864.
- (147) Moision, R. M.; Armentrout, P. B. *J. Phys. Chem. A* **2002**, *106*, 10350.
- (148) Ye, S. J.; Clark, A. A.; Armentrout, P. B. *J. Phys. Chem. B* **2008**, *112*, 10291.
- (149) Denniston, K. J.; Topping, J.; Dwyer, T. M. *General Organic and Biochemistry*, 5th Edition, Towson University, 2007.
- (150) Prasad, P. N.; Williams, D. J. *Introduction to Nonlinear Optical Effects in Organic Molecules and Polymers*, Wiley, 1990.
- (151) Mehmet, B.; YÖRÜK, E. Physics Department Gazi University, Turkey, Proceedings of the 9th WSEAS International Conference on Applied Computer Science.
- (152) Junyong, W.; Yan, H.; Hao, C.; Zhong, A.; Weiliang, C. *Comp. Theor. Chem.* **2012**, *1000*, 52.
- (153) Valencia, D.; Klimova, T.; García-Cruz, I. *Fuel (Elsevier)* **2012**, *100*, 177.
- (154) LoPachin, R. M.; Terrence Gavin. “*Molecular Mechanism of Acrylamide Neuro Toxicity: Lesson Learned from Organic Chemistry*” **2012**, *12*, 120.
- (155) Mennucci, B.; Tomasi, J.; Cammi, R.; Cheeseman, J.R. *et al.*, Polarizable Continuum Model (PCM) Calculations of Solvent Effects on Optical Rotations of Chiral Molecules. *J. Phys. Chem.* **2002**. *106(25)*, 6102-6113.

## **CHAPTER 2**

**Brief outline of the theory of AM1 and DFT method**



## Abstract

Impressions of semiempirical AM1 and density functional theory (DFT) have been conferred. We have utilized this DFT method with its hybrid parameters B3LYP and 6-311G (d,p) basis sets in all calculations. DFT method has been used both for ground and low-lying excited triplet state properties. We have also employed the semiempirical AM1 method for the investigation of the ground state properties in some cases. Polarizable Continuum Model (PCM) has been employed for the optimization process in solvent phases at the same level of the theory. This chapter deals briefly with the AM1 and DFT theories and their parametrization scheme.

Most of the Computational Chemistry calculations based on the Quantum mechanics. Computational Chemistry is now used as a tool by researchers to investigate geometrical parameters and different thermodynamic properties of molecules. It can solve large number of Chemical problems applying both mathematical and theoretical principles.

In present time, advanced or modern Computer programs are utilized to execute quantum mechanical calculation on large number of molecules. Nowadays, Quantum Chemical calculations are drawn such a great importance in the field of theoretical research in organic, inorganic and physical chemistry.

Quantum Chemistry put forward an approach to comprehend and elucidate a large areas of Chemistry like spectroscopy, reactivity etc. Molecular materials can also be designed by calculating different molecular properties with the help of quantum Chemistry. In this chapter we have conversed the fundamental concepts and ideas in the rear of quantum Chemistry.

## 2.1 LCAO-MO Approach

The wave function of a molecular eigen state can be found out by the solution of the molecular Schrödinger equation

$$\hat{H}\psi_p(r, R) = E_p\psi_p(r, R) \quad (2.1)$$

where  $\hat{H}$  is non-relativistic quantum mechanical Hamiltonian operator of the system,  $\{E_p\}$  are the eigen values of the eigen states  $\{\psi_p\}$ . For a system containing “n” electrons and “N” nuclei the Hamiltonian operator in a.u. is

$$\hat{H} = -\frac{1}{2} \sum_{k=1}^N \frac{\nabla_k^2}{m_k} - \frac{1}{2} \sum_{\mu=1}^n \nabla_{\mu}^2 - \sum_{\mu} \sum_k \frac{Z_k}{r_{\mu k}} + \sum_{k,l} \frac{Z_k Z_l}{r_{kl}} + \sum_{\mu < \nu} \frac{1}{r_{\mu \nu}} \quad (2.2)$$



The first and second term represent respectively the operators for kinetic energy of the nuclei,  $m_k$  be the mass in a.u. of the  $k^{\text{th}}$  nucleus and electrons. The third term represents the operator for electron-nucleus attraction potential energy. The fourth term is the operator for internuclear repulsion energy. The last term represents the operator for inter-electronic coulomb repulsion energy. Solution of the equation (2.1) is very difficult due to the fact that several different types of motions like electronic motion, vibrational motions, rotational motions of the nuclei are coupled. However, equation (2.1) can be solved approximately by making certain assumptions and approximations. Born and Oppenheimer<sup>1</sup> (BO) suggested that massive nuclei move so slowly relative to the electronic motion that the electrons can be thought of as being in quasi stationary states during the course of the nuclear vibration and separation of electronic and nuclear motions is permitted. As per this BO approximation the molecular electronic wave functions  $\psi^*(r, R)$  are obtained by solving the equation

$$\hat{H}^* \psi_p^* = E_p^* \psi_p^* \quad (2.3)$$

where  $\hat{H}^*$  represents the electronic Hamiltonian operator and is

$$\hat{H}^* = -\frac{1}{2} \sum_{\mu=1}^n \nabla_{\mu}^2 - \sum_{\mu} \sum_k \frac{Z_k}{r_{\mu k}} + \sum_{\mu < \nu} \frac{1}{r_{\mu \nu}} \quad (2.4)$$

and  $E_p^*(R)$  depends parametrically on nuclear co-ordinates  $R$  and can be used to describe the potential surface on which the nuclei move. Equation (2.3) is solved by Roothaan's method.<sup>2</sup>

## 2.2 ROOTHAAN'S-RHF THEORY FOR CLOSED-SHELL SYSTEMS

According to this theory a closed-shell system of  $2n$  electrons is described by a single Slater determinant of  $n$  doubly occupied MO's. In the LCAO scheme an MO can be expressed in the matrix form,

Chapter 2

$$\Psi_p = \Phi C_p \quad (2.5)$$

where  $C_p$  is a column matrix of the coefficients and  $\Phi$  is a row matrix of  $m$  real AO's,  $\{\phi_i\}$ . The coefficient matrix  $C = [c_1, c_2, \dots, c_p, \dots]$  and the orbital energy matrix  $\varepsilon$ , are obtained by solving the matrix equation,

$$FC = SC\varepsilon \quad (2.6)$$

where  $F_{ij} = \langle \phi_i | \hat{F} | \phi_j \rangle = \langle \phi_i | \hat{h} + \sum_p^n (2\hat{J}_p - \hat{K}_p) | \phi_j \rangle$

$$= h_{ij} + \sum_{k,l=1}^m P_{kl} [\langle ij|kl \rangle - \frac{1}{2} \langle ik|jl \rangle] \quad (2.7)$$

$\varepsilon$  is the diagonal matrix of orbital energies and  $S_{ij} = \langle \phi_i | \phi_j \rangle$

In the equation (2.7)

$$P_{kl} = 2 \sum_{p=1}^n C_{kp} C_{lp} \quad (2.8)$$

$$\langle ij|kl \rangle = \left\langle \phi_i(1)\phi_j(1) \left| \frac{1}{r_{12}} \right| \phi_k(2)\phi_l(2) \right\rangle$$

In the AM1 method (Austin Model 1) only the valence electrons are treated explicitly, the inner shell being treated as a part of the rigid nonpolarisable core. The valence orbitals are specified by the atom centre. The matrix elements of the Fock operator are given by

$$F_{ii} = U_{ii} + \sum_k^A P_{kk} [\langle ii|kk \rangle - \frac{1}{2} \langle ik|ik \rangle] + \sum_{B \neq A} (P_{BB} - Z_B) g_{AB} \quad (2.9)$$

$$F_{ij} = \frac{3}{2} P_{ij} \langle ij|ij \rangle - \frac{1}{2} P_{ij} \langle ii|jj \rangle, \text{ both } \phi_i \text{ and } \phi_j \text{ on } A \quad (2.10)$$

$$F_{ij} = \beta_{AB} - \frac{1}{2} P_{ij} g_{AB}, \phi_i \text{ on } A \text{ and } \phi_j \text{ on } B \quad (2.11)$$

It may be noted that here all electron repulsion integrals involving orbitals on the same atom are evaluated in a manner different from that followed in the evaluation of similar integrals involving orbitals on different atoms.

## 2.3 ROOHTHAAN'S-RHF THEORY<sup>3</sup> FOR OPEN-SHELL SYSTEMS

According to this theory the doubly occupied closed-shell orbitals,  $\{\psi_c\}$ , and the partially occupied open-shell orbitals,  $\{\psi_o\}$ , of an open-shell system are obtained as solutions of two different eigen value equations. These are given by

$$\hat{F}_c \psi_c = \eta_c \psi_c \quad (2.12)$$

$$\hat{F}_o \psi_o = \eta_o \psi_o \quad (2.13)$$

where  $\eta$ 's are orbital energies and

$$\hat{F}_c = \hat{h} + 2\hat{J}_c - \hat{K}_c + 2\hat{J}_o - \hat{K}_o + 2\alpha\hat{L}_o - \beta\hat{M}_o \quad (2.14)$$

$$\hat{F}_o = \hat{h} + 2\hat{J}_c - \hat{K}_c + 2a\hat{J}_o - b\hat{K}_o + 2\alpha\hat{L}_c - \beta\hat{M}_c \quad (2.15)$$

In equations (2.14) and (2.15)

$$\alpha = \frac{1-a}{1-f} \quad \text{and} \quad \beta = \frac{1-b}{1-f}$$

where “ $a$ ” and “ $b$ ” are constants depending upon the specific case, “ $f$ ” is the fractional occupancy of the open-shell. We will use “ $p, q$ ” indices for closed-shell orbitals and “ $r, s$ ” for open-shell orbitals, and “ $t$ ” for orbitals of either set.

The various operators of equation (2.14) and (2.15) are defined as follows:

$$\hat{J}_c = \sum_p \hat{J}_p, \quad \hat{J}_o = f \sum_r \hat{J}_r, \quad \hat{J}_t = \hat{J}_c + \hat{J}_o \quad (2.16)$$

Chapter 2

$$\hat{K}_c = \sum_p \hat{K}_p, \hat{K}_o = f \sum_r \hat{K}_r, \hat{K}_t = \hat{K}_c + \hat{K}_o \quad (2.17)$$

$$\hat{L}_c = \sum_p \hat{L}_p, \hat{L}_o = f \sum_r \hat{L}_r, \hat{L}_t = \hat{L}_c + \hat{L}_o \quad (2.18)$$

$$\hat{M}_c = \sum_p \hat{M}_p, \hat{M}_o = f \sum_r \hat{M}_r, \hat{M}_t = \hat{M}_c + \hat{M}_o \quad (2.19)$$

The operators  $\hat{L}_t$  and  $\hat{M}_t$  act on an arbitrary orbital as follows:

$$\hat{L}_t \psi = \langle \psi_t | \hat{J}_o | \psi \rangle \psi_t + \langle \psi_t | \psi \rangle \hat{J}_o \psi_t \quad (2.20)$$

$$\hat{M}_t \psi = \langle \psi_t | \hat{K}_o | \psi \rangle \psi_t + \langle \psi_t | \psi \rangle \hat{K}_o \psi_t \quad (2.21)$$

This is known as the double Hamiltonian method. We have used the single Hamiltonian method of Roothaan in which both  $\psi_c$  and  $\psi_o$  are obtained as eigen functions of a single Fock operator. The corresponding eigen value equations are

$$\hat{F} \psi_c = \varepsilon_c \psi_c \quad (2.22)$$

$$\hat{F} \psi_o = \varepsilon_o \psi_o \quad (2.23)$$

$$\text{where } \varepsilon_c = \eta_c + \chi_o \quad (2.24)$$

$$\varepsilon_o = \eta_o + \chi_o \quad (2.25)$$

$$\hat{F} = \hat{h} + 2\hat{J}_t - \hat{K}_t + 2\alpha(\hat{L}_t - \hat{J}_o) + \beta(\hat{M}_o - \hat{K}_o) \quad (2.26)$$

$$\varepsilon_c = \eta_c + \xi_c \quad (2.27)$$

$$\varepsilon_o = \eta_o + \xi_o \quad (2.28)$$

The elements of  $\xi$  matrix are obtained by

$$\xi_{pq} = \langle \psi_p | 2\alpha\hat{J}_o - \beta\hat{K}_o | \psi_q \rangle \quad (2.29)$$

$$\xi_{rs} = f \langle \psi_r | 2\alpha\hat{J}_o - \beta\hat{K}_o | \psi_s \rangle \quad (2.30)$$

In the LCAO scheme, eigen values and eigen vectors are obtained as solutions of the matrix equation,

$$FC = SCE \quad (2.31)$$

where

$$\begin{aligned} F_{ij} &= h_{ij} + 2(\hat{J}_c + \hat{J}_o)_{ij} - (\hat{K}_c + \hat{K}_o)_{ij} - 2\alpha(\hat{J}_o)_{ij} + \beta(\hat{K}_o)_{ij} + 2\alpha(\hat{L}_t)_{ij} - \beta(\hat{M}_t)_{ij} \\ &= h_{ij} + 2\sum_{kl} (P_t)_{kl} \langle ij|kl \rangle - \sum_{kl} (P_t)_{kl} \langle ik|jl \rangle - \alpha \sum_{kl} (P_o)_{kl} \langle ij|kl \rangle \\ &\quad + 0.5\beta \sum_{kl} (P_o)_{kl} \langle ik|jl \rangle + 2\alpha S_{ij} [\sum_k \{(P_t)_{ik} (\hat{J}_o)_{kj} + (\hat{J}_o)_{ik} (P_t)_{kj}\}] \\ &\quad - \beta S_{ij} [\sum_k \{(P_t)_{ik} (\hat{K}_o)_{kj} + (\hat{K}_o)_{ik} (P_t)_{kj}\}] \end{aligned} \quad (2.32)$$

The various terms appearing in the right-hand side of equation (2.32) have the following definitions:

$$(P_c)_{ij} = 2\sum_p C_{pi} C_{pj}, \quad (P_o)_{ij} = 2f\sum_r C_{ri} C_{rj}$$

$$(\hat{J}_c)_{ij} = 0.5\sum_{kl} (P_c)_{kl} \langle ij|kl \rangle, \quad (\hat{J}_o)_{ij} = 0.5\sum_{kl} (P_o)_{kl} \langle ij|kl \rangle$$

$$(\hat{K}_c)_{ij} = 0.5\sum_{kl} (P_c)_{kl} \langle ik|jl \rangle, \quad (\hat{K}_o)_{ij} = 0.5\sum_{kl} (P_o)_{kl} \langle ik|jl \rangle$$

$$(P_t)_{ij} = 0.5[(P_c)_{ij} + (P_o)_{ij}]$$

within the framework of AM1 approximations,<sup>4</sup> equation (2.31) reduces to

$$FC = CE \quad (2.33)$$

and the matrix elements of the Fock operator takes the appropriate form having the suitable parametrization scheme.

## 2.4 The Pople-Nesbet UHF theory<sup>5</sup> for open-shell systems

In the RHF theory for open-shell systems described in the previous section the total wave function is expressed as a linear combination of Slater determinants to make it an eigen

## Chapter 2

function of the  $\hat{S}^2$  operator. According to the Pople-Nesbet UHF theory, the total wave function of a system of  $n$  electrons is described by a single Slater determinant of  $n_\alpha$  orbitals with  $\alpha$  spin and  $n_\beta$  orbitals with  $\beta$  spin, where  $n_\alpha + n_\beta = n$ . Such a wave function is, in general, not an eigen function of the  $\hat{S}^2$  operator. Application of the variational principle leads to two coupled Hartree-Fock equations, one for the orbitals with  $\alpha$  spin and the other for the orbitals with  $\beta$  spin. The pertinent equations in the matrix form are given by

$$F^\alpha C^\alpha = S C^\alpha E^\alpha \quad (2.34)$$

$$F^\beta C^\beta = S C^\beta E^\beta \quad (2.35)$$

where

$$F_{ij}^\alpha = h_{ij} + \sum_{kl} [P_{kl} \langle ij | kl \rangle - P_{kl}^\alpha \langle ik | jl \rangle] \quad (2.36)$$

$$F_{ij}^\beta = h_{ij} + \sum_{kl} [P_{kl} \langle ij | kl \rangle - P_{kl}^\beta \langle ik | jl \rangle] \quad (2.37)$$

with

$$P_{ij} = P_{ij}^\alpha + P_{ij}^\beta = \sum_p^{n_\alpha} C_{pi}^\alpha C_{pj}^\alpha + \sum_q^{n_\beta} C_{qi}^\beta C_{qj}^\beta \quad (2.38)$$

In the AM1 approximation equations (2.34) and (2.35) reduce respectively to

$$F^\alpha C^\alpha = C^\alpha E^\alpha \quad (2.39)$$

$$F^\beta C^\beta = C^\beta E^\beta \quad (2.40)$$

and the matrix elements of the Fock operator take the appropriate form with suitable parametrization schemes for both  $\alpha$  spin and  $\beta$  spin orbitals.

## 2.5 Excited state calculations

The basic features of the excited state calculations are as follows:

- (a) The canonical SCF MO's comprising the occupied and virtual orbital subspaces are generated by the Hartree-Fock method using the modified values of some of the parameters discussed later.
- (b) The virtual orbitals thus obtained are utilized to generate the excited state wavefunctions by single replacement of the occupied orbitals. Such an excitation scheme would give rise to only singlet and triplet states in the case of a closed-shell ground state. The wave functions of the excited states can be written as

$${}^1\Psi = \sum_{pr} {}^1C_{pr} {}^1\psi_{p \rightarrow r} \quad (2.41)$$

$${}^3\Psi = \sum_{pr} {}^3C_{pr} {}^3\psi_{p \rightarrow r} \quad (2.42)$$

where  ${}^{1,3}\psi_{p \rightarrow r}$  denote the wave functions of a singlet and triplet state obtained by exciting an electron from the occupied orbital  $\psi_p$  to the virtual orbital  $\psi_r$ . Each excitation of this type would give rise to three degenerate states corresponding to  $M_S = 1, 0$  and  $-1$  components of a triplet and a singlet ( $M_S = 0$ ). The wave functions of the states with  $M_S = 0$  can be written as

$${}^{1,3}\psi_{p \rightarrow r} = \frac{1}{2} \left( \left| \psi_1 \bar{\psi}_1 \psi_2 \bar{\psi}_2 \dots \psi_p \bar{\psi}_r \dots \right| \mp \left| \psi_1 \bar{\psi}_1 \psi_2 \bar{\psi}_2 \dots \bar{\psi}_p \psi_r \dots \right| \right) \quad (2.43)$$

The eigen values and eigen vectors of the excited states are obtained by solving the following CI matrix equations:

$${}^1H^1C = {}^1E^1C \quad (2.44)$$

$${}^3H^3C = {}^3E^3C \quad (2.45)$$

where  ${}_{1,3}H_{p \rightarrow r, q \rightarrow s} = \langle {}_{1,3}\psi_{p \rightarrow r} | \hat{H} | {}_{1,3}\psi_{q \rightarrow s} \rangle$ ,  $\hat{H}$  being the Hamiltonian operator of the system,  ${}_{1,3}C$  are the coefficient matrices in the CI expansion and  ${}_{1,3}E$  are diagonal matrices whose elements are excitation energies. The Hamiltonian matrix elements can be easily evaluated using the Slater-Condon rules given below:

$$H_{p \rightarrow r, q \rightarrow s} = \delta_{pq} \delta_{rs} (\varepsilon_r - \varepsilon_p) + [1 + (-1)^s][\langle pr | qs \rangle - \langle pq | rs \rangle] \quad (2.46)$$

where  $s = 0$  and  $1$  refer to a singlet and triplet state respectively,  $\varepsilon$ 's are orbital energies and  $\langle pq | rs \rangle$  etc., are electron repulsion integrals over MO's.

## 2.6 Density functional theory (DFT)

This is a quantum mechanical method which can be used to investigate the electronic structure of many body systems in particular, molecules and the condensed phase. In Computational Chemistry, DFT method treated as most popular and versatile.

This theory has recently become popular in quantum chemistry because present day approximate functionals provide a useful balance between accuracy and computational cost, allowing much larger systems to be treated than traditional ab initio methods, retaining much of their accuracy. This theory is the way of approaching any interacting problem, by mapping it exactly to a much easier-to-solve non-interacting problem.

For an  $N$ -electron system the density  $\rho(\vec{r})$  is defined as

$$\rho(\vec{r}) = N \int \Psi^*(q_1, q_2, \dots, q_{3N}) \Psi(q_1, q_2, \dots, q_{3N}) dq_1 \dots dq_{3N} \quad (2.47)$$

This method owes its origin to the Hohenberg-Kohn theorem<sup>6</sup> which demonstrated the existence of a unique functional which determines the ground state energy and density exactly. As per the work of Kohn and Sham<sup>7</sup> the electronic energy is partitioned by the approximate functionals as given below:



$$E = E^T + E^V + E^J + E^{XC} \quad (2.48)$$

where the terms have the usual meaning,  $E^{XC}$  is the exchange-correlation term and includes the remaining part of the electron-electron interactions, i.e., antisymmetry of the quantum mechanical wave function and dynamic correlation of the motions of the individual electrons. All these terms except nuclear-nuclear repulsion are functions of electron density ( $\rho$ ).

$E^{XC}$  is usually divided into separate parts, exchange and correlation parts corresponding to same spin and mixed spin interactions respectively.

$$E^{XC}(\rho) = E^X(\rho) + E^C(\rho) \quad (2.49)$$

where  $E^X(\rho)$  and  $E^C(\rho)$  are exchange functional and correlation functional respectively.

In actual practice self-consistent Kohn-Sham DFT calculations are performed in an iterative manner analogous to SCF computation of Hartree-Fock theory as pointed out by Kohn and Sham. Hartree-Fock theory also includes an exchange term as part of its formulation.

A very popular hybrid functionals has been introduced by Becke<sup>8</sup> which include a mixture of Hartree-Fock and DFT exchange along with DFT correlation as:

$$E_{hybrid}^{XC} = c_{HF} E_{HF}^X + c_{DFT} E_{DFT}^{XC} \quad (2.50)$$

where the  $c$ 's are constants. The B3LYP is:

$$E_{B3LYP}^{XC} = E_{LDA}^X + c_0(E_{HF}^X - E_{LDA}^X) + c_X \Delta E_{B88}^X + E_{VWN3}^C + c_C(E_{LYP}^C - E_{VWN3}^C) \quad (2.51)$$

Here,  $c_0$  allows any admixture of Hartree-Fock and LDA local exchange to be used.

Becke's gradient correlation to LDA exchange is also included, scaled by the parameter

$c_X$ . Similarly *VWN3* local correlation functional is also used, and it may be optionally corrected by LYP correlation correction via the parameter  $c_C$ . In B3LYP functional parameters were determined by fitting to the atomization energies, ionization potentials, proton affinities and first-row atomic energies in the G1 molecule set.

## 2.7 Calculation of molecular properties

### A: Molecular geometry

From knowledge of various parameters the relevant Fock matrices are constructed and the eigen value equations are solved iteratively. We thus get the orbital energies, the total electronic energy, the MO coefficients and consequently the charge density matrix. The electronic energy when added to the nuclear-nuclear repulsion energy calculated by the point charge approximation gives the total molecular energy at a particular geometry of the molecule. The equilibrium geometry of a molecule is then determined by the self-consistent variation of total energy with respect to all possible internal coordinates and finding the nuclear conformation corresponding to the absolute minimum in the total energy.

### B: Charge density, cation affinities, hardness, softness, electrophilicity index and transition energy

For closed-shell systems we have calculated the charge densities by the usual RHF method (for such systems electron spin density turns out to be zero by the RHF method) and for the open-shell systems these are calculated by the UHF method. We shall describe here only the UHF method for the calculation of the quantity, since the RHF method for closed-shell systems is a special case of the UHF method. We have used the Mulliken scheme. The Mulliken population analysis is the historically most important wave function based method<sup>9</sup>. Results of this analysis strongly depend on the used molecular

basis set<sup>10</sup>. Even with its known deficiency, Mulliken population analysis is still used widely due to its simplicity. Mulliken population analysis computes charges by dividing orbital overlap evenly between the two atoms involved. Since atomic charge is not a quantum mechanical observable, all methods for computing it are necessarily arbitrary. The charge distribution on atom can be analyzed with another population analysis method namely Natural Population Analysis (NPA). NPA is a more refined wave function based method. It solves most of the problems of Mulliken population analysis by constructing most appropriate sets (natural) of atomic basis functions<sup>11,12</sup>. The density matrix is evaluated as follows:

For open-shell systems the  $\alpha$  and  $\beta$  electrons are in different orbitals, resulting in two sets of MO expansion coefficients:

$$\phi_i^\alpha = \sum_{\mu} c_{\mu i}^\alpha \chi_{\mu} \quad (2.52)$$

$$\phi_i^\beta = \sum_{\mu} c_{\mu i}^\beta \chi_{\mu} \quad (2.53)$$

$$P_{\lambda\sigma}^\alpha = \sum_{i=1}^{occ} \alpha_i^* c_{\lambda i}^\alpha c_{\sigma i}^\alpha \quad (2.54)$$

$$P_{\lambda\sigma}^\beta = \sum_{i=1}^{occ} \beta_i^* c_{\lambda i}^\beta c_{\sigma i}^\beta \quad (2.55)$$

$$P_{AA} = \sum_{\lambda, \sigma} (P_{\lambda\sigma}^\alpha + P_{\lambda\sigma}^\beta) \quad (2.56)$$

Within the ZDO approximation, the diagonal elements of the  $P^\alpha$  and  $P^\beta$  matrices give the  $\alpha$ - and  $\beta$ - electron population. The elements of the  $P$  matrices are given by

$$P_{ij}^\alpha = \sum_{p=1}^{occ} C_{ip}^\alpha C_{jp}^\alpha$$

$$\text{and } P_{ij}^\beta = \sum_{p=1}^{occ} C_{ip}^\beta C_{jp}^\beta \quad (2.57)$$

## Chapter 2

The summation of electron populations over AO's centred on a given atom is the gross electron population,  $P_{AA}$  of atom A and summation of  $P_{AA}$  overall atoms is the number of valence electrons of the system. Thus

$$P_{AA} = \sum_i^A (P_{ii}^{\alpha} + P_{ii}^{\beta}) \quad (2.58)$$

We have calculated cation affinities ( $\Delta E$ ) of molecules at the equilibrium geometry of the ground and lowest excited triplet state. Cation affinity is defined as  $\Delta E = (E_{BM^+} - E_B - E_{M^+})$ , hartree. Where B is the molecule and M = H, Li, Na and Cu.  $BM^+$  is the  $H^+$ ,  $Li^+$  and  $Na^+$  complexes of the molecule B. The values of  $E_{M^+}$  are given in the respective section.  $E_{H^+} = 0$ .

In addition, the proton affinity (PA), gas-phase basicity (GB), of molecule (B) can be defined in terms of the gas phase reaction  $B + H^+ \leftrightarrow [BH^+]$ . The PA is the negative of the enthalpy change and GB is the negative of the free energy change associated with this reaction.

The Metal cation affinity (MCA) and basicity also can be defined in terms of the same type of reaction  $B + M^+ \leftrightarrow [B M^+]$  (M = Li, Na, Cu) where metal cation affinity is the negative of the enthalpy change and basicity is the negative of the free energy change associated with this reaction.

To obtain the energetic values [enthalpy (H) and free energy (G)], vibrational frequency calculations have been performed on the optimized structures of the molecules at the same level of theory. In this calculation, an optimized energy is used as input. Then the frequency calculation should be performed employing same theoretical model and the basis set as the one that was utilized to find the optimized geometry of the molecule.<sup>13,14</sup>

As the global parameter we have chosen the hardness,  $\eta$  and electronegativity ( $\chi$ ). If  $I$  be the ionization potential and  $A$  be the electron affinity then chemical hardness ( $\eta$ ) can be expressed in the Koopmans' framework<sup>15,16</sup> as:

$$\eta = (I - A)/2 = (\epsilon_{\text{LUMO}} - \epsilon_{\text{HOMO}})/2 \quad (2.59)$$

where  $I \approx -\epsilon_{\text{HOMO}}$  and  $A \approx -\epsilon_{\text{LUMO}}$

To account for the stability of a molecule and the direction of acid-base reactions Pearson<sup>17-19</sup> introduced 'softness' parameter in chemistry. The inverse of hardness<sup>20</sup> can be defined as softness (S).

$$S = \frac{1}{2\eta} \quad (2.60)$$

We have also calculated electrophilicity index ( $\omega$ ) which can be considered as a measure of electrophilicity of the ligand. Parr et al.<sup>21</sup> defined electrophilicity index ( $\omega$ ) as

$$\omega = \mu^2/2\eta \quad (2.61)$$

Where ' $\mu$ ' known as chemical potential. The electronic chemical potential ( $\mu$ ) defined by parr and pearson<sup>22</sup> as the characteristic of electronegativity of molecules can be obtained from HOMO- LUMO energies.  $\mu = (\epsilon_{\text{LUMO}} + \epsilon_{\text{HOMO}})/2$

We have also calculated the computed transition energies, hartree [ $1s_0 \rightarrow T_1$  (low-lying excited triplet state)] and shifts caused by  $\text{BM}^+$  complex formation.

Transition energy is defined as:

Transition energy of B = (Energy of B in the triplet state) – (Energy of B in the ground state) and Transition energy of  $\text{BM}^+$  = (Energy of  $\text{BM}^+$  in the triplet state) – (Energy of  $\text{BM}^+$  in the ground state)

Cation induced shift (CIS) is defined as:

$$\text{CIS} = (\text{Transition energy of } \text{BM}^+) - (\text{Transition energy of B})$$

## 2.8 Polarizable Continuum Model (PCM)

The default case in quantum chemical calculations is to perform the calculation in the gas phase. This means that the molecule is isolated in space and does not interact with its environment. Inclusion of solvent effects may change the equilibrium geometry and charge distribution. Since solvation preferentially stabilizes more polar systems, it may change the conformational preference of molecules. In order to account for solvent interactions, a solvent model can be used. The one used in our investigation of molecular properties in both ground state (Chapter 3, 4, 5, 8) and low-lying excited state (Chapter 9 and 10) is Polarizable Continuum Model (PCM).<sup>23</sup> One of the more modern methods to deal with implicit solvation is the Polarizable Continuum Model (PCM). This model is based upon the idea of generating multiple overlapping spheres for each of the atoms within the molecule inside of a dielectric continuum. This method treats the continuum as a polarizable dielectric and thus is sometimes referred to as dielectric PCM (DPCM). The PCM model calculates the free energy of solvation by attempting to sum over three different terms,

$$G_{\text{solvation}} = G_{\text{electrostatic}} + G_{\text{dispersion-repulsion}} + G_{\text{cavitation}}$$

Dielectric constant of the solvents are utilized to simulate the corresponding solvent environment.

## 2.9 References

- (1) Born, M.; Oppenheimer, J. R. *Ann. Phys.* **1927**, 87, 457.
- (2) Roothaan, C. C. J. *Rev. Mod. Phys.* **1951**, 23, 69.
- (3) Roothaan, C. C. J. *Rev. Mod. Phys.* **1960**, 32, 179.
- (4) Dewar, M. J. S.; Zoebisch, E. G.; Healy, E. F.; Stewart, J. J. P. *J. Am. Chem. Soc.* **1985**, 107, 3902.
- (5) Pople, J. A.; Nesbet, R. K. *J. Chem. Phys.* **1954**, 22, 571.
- (6) Hohenberg, P.; Kohn, W. *Phys. Rev. B* **1964**, 136, 864.
- (7) Kohn, W.; Sham, L. J. *Phys. Rev. A* **1965**, 140, 1133.
- (8) Becke, A. D. *J. Chem. Phys.* **1993**, 98, 5648.
- (9) Mulliken, R. S. *J. Chem. Phys.* **1955**, 23, 1833.
- (10) Jensen, F. *Introduction to Computational Chemistry*; Wiley: New York, 1999.
- (11) Reed, A. E.; Weinstock, R. B.; Weinhold, F. A. *J. Chem. Phys.* **1985**, 83, 735.
- (12) Reed, A. E.; Curtiss, L. A.; Weinhold, F. *Chem. Rev.* **1988**, 88, 899.
- (13) Foresman, J.B.; Frish, C. *Exploring Chemistry with Electronic Structure Methods*, 2<sup>nd</sup> Edition, Gaussian Inc., Pittsburgh, PA., 1996.
- (14) Chambers, C. C.; Thomson, D. L. *J. Phys. Chem.* **1995**, 99, 15881.
- (15) Parr, R. G.; Pearson, R. G. *J. Am. Chem. Soc.* **1983**, 105, 7512.
- (16) Pearson, R. G. *Chemical Hardness: Applications from Molecules to Solids* (Wiley-VCH, Weinheim), 1997.
- (17) Pearson, R. G. *Coord. Chem. Rev.* **1990**, 100, 403.
- (18) Pearson, R. G. *Hard and Soft Acids and Bases* (Dowden, Hutchinson and Ross: Stroudsburg, PA) 1973.
- (19) Hancock, R. D.; Martell, A. E. *J. Chem. Educ.* **1996**, 73, 654.
- (20) Yang, W.; Parr, R. G. *Proc. Natl. Acad. Sci. USA* **1985**, 82, 6723.

## Chapter 2

- (21) Parr, R. G.; szentpaly, L. v.; Liu, S. *J. Am. Chem. Soc.* **1999**, *121*, 1922.
- (22) Parr, R. G.; Pearson, R. G. *J. Am. Chem. Soc.* **1983**, *105*, 7512.
- (23) Mennucci, B.; Tomasi, J.; Cammi, R.; Cheeseman, J.R. *et al.*, Polarizable Continuum Model (PCM) Calculations of Solvent Effects on Optical Rotations of Chiral Molecules. *J. Phys. Chem.* **2002**, *106(25)*, 6102-6113.



## **CHAPTER 3**

The comparative proton affinities of a series of conjugated  $\alpha,\beta$ -unsaturated carbonyl compounds [ Acrolien (ACL), 4-hydroxy-2-nonenal (HNE), Methyl vinyl ketone (MVK), Acrylamide (ACR), Methyl acrylate (MA), Ethylmethacrylate (EMA) in ground state. A DFT based computational study in both gas and aqueous phases.



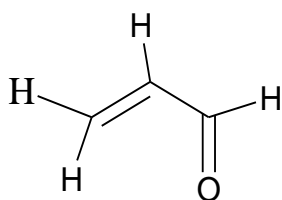
## Abstract

The proton affinities (PA) of a series of  $\alpha,\beta$ -unsaturated carbonyl compounds [acrolein (ACL), 4-hydroxy-2-nonenal (HNE), methyl vinyl ketone (MVK), acrylamide (ACR), methyl acrylate (MA) and ethyl methacrylate (EMA) and their O-protonated counterparts have been computed using density functional theory [Becke, Lee, Yang and Parr(B3LYP)] method using 6-311G(d,p)] basis sets with complete geometry optimizations in both gaseous and aqueous phase. The O-protonation in both phases is observed to be exothermic and the stereochemical disposition of proton is observed to be almost equal in each case. PA values are affected due to the presence of different length of alkyl chain and different substituent at carbonyl carbon. In gas phase PA of acrylamide is maximum whereas it is minimum in acrolein. In aqueous phase the PA of the carbonyl compounds decrease in the order as  $-\text{H} > -\text{NH}_2 > -\text{CH}_3 > -\text{OC}_2\text{H}_5 > -\text{OCH}_3$  substituent at carbonyl carbon. Atom electron density is recorded by natural population analysis (NPA) along with Mulliken net charge. A proper correlation of proton affinities with a number of computed system parameters like net charge on the carbonyl oxygen of unprotonated and protonated bases, charge on proton of protonated bases and also the computed hardness ( $\eta$ ) of the unprotonated bases in both phases have been explained thoroughly. The overall basicities are explicated considering the contribution from carbonyl group and distant atom.

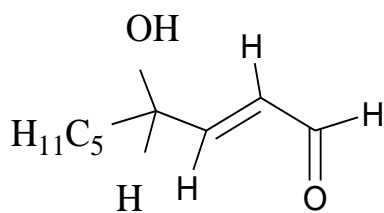
### 3.1 Introduction

The  $\alpha,\beta$ -unsaturated carbonyl compounds of type-2-alkene series [acrolein (ACL), 4-hydroxy-2-nonenal (HNE), methyl vinyl ketone (MVK), acrylamide (ACR), methyl acrylate (MA) and ethyl methacrylate (EMA)] are considered as soft electrophiles due to their corresponding pi-electron mobility. Members of this type-2-alkene series are treated as deadly environmental pollutants as they produce toxicity via common molecular mechanism.<sup>1</sup> Interaction of proton (Lewis acid) with carbonyl compounds (Base) is an important part of biological science and Chemistry. Proton affinity (PA) is the negative of the enthalpy change of proton-base interaction implying that higher the proton affinity, higher the basicity. Gas phase basicity and proton affinity are generally characterised by  $B[g] + H^+[g] \rightarrow BH^+[g]$  ... (1) and  $B^-[g] + H^+[g] = BH$ . Ground state basicities of carbonyl compounds are well recognised.<sup>2-4</sup> In recent study the binding nature of ion with ligand (donor site) has been a research direction of physical organic chemistry and computational chemistry.<sup>5</sup> There are many instances of proton attack on carbonyl oxygen in the primary step of a carbonyl system.<sup>6-9</sup> Experimental data of proton affinity are scarcely available<sup>10</sup> in ground state and it is not an easy task to determine experimental PA values in a protonation reaction.<sup>11</sup> Ground state gas phase basicities of a series of aliphatic and aromatic conjugated carbonyl systems have been reported.<sup>12,13</sup> There are no such comparative theoretical results on PA which have still been found for several conjugated  $\alpha,\beta$ -unsaturated carbonyl compounds of the type-2 alkene chemical class in both phase together. Therefore we are compelled to turn to theory to investigate some quantitative thought on proton affinity of a structurally related and biologically important carbonyl compounds in gas phase and in aqueous phase with the help of density functional theory B3LYP (DFT) method at the 6-311G(d,p) basis set level.<sup>14</sup> We examine here theoretically, the PA of various carbonyl compounds towards Lewis acid  $H^+$ , and draw the comparison to the equivalent reaction with proton in gas phase as well as in

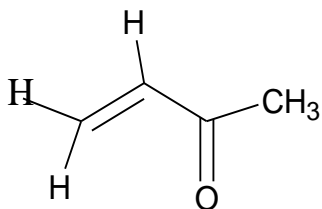
aqueous phase. We are especially interested on the effect of solvation, geometric features, conjugation and some other chemical properties. We investigated the PA of these studied carbonyl compounds using semiempirical quantum chemical AM1 method. Results obtained from this theoretical calculation are included for the sake of comparison. The BSSE corrections are not taken into account for this theoretical study. We have studied the interaction of  $H^+$  ion with different electron rich site present in the compound that is carbonyl oxygen- $H^+$  interaction, carbonyl  $\pi$ - $H^+$  interaction and also the other electronegative atom- $H^+$  interaction. We observed that carbonyl oxygen- $H^+$  interaction energy is much lower in the series and this gives the more stable complexes. Gas phase proton affinity determination reflect the thermodynamic and electronic properties of the compound avoiding more complicated solvent effect,<sup>15</sup> but in this study we search the solvation effect on different molecular properties in the ground state. Charge on proton ( $q_H^+$ ) in the protonated complexes in both gas and aqueous phases are noticed carefully and it is seen that migration of charge density to the added proton has taken place. Computed PA values indicate that both pre-protonation charge distribution local to chromophore and protonated complex relaxation charge density are involve to develop the overall basicity of the compounds. Since the selected carbonyl compounds are known as toxic pollutants, we have studied their comparative electrophilic nature by calculating some quantum mechanical parameters from their HOMO–LUMO energy gap. Compounds studied in this theoretical calculation are given below in figure 1 with their respective abbreviated names.



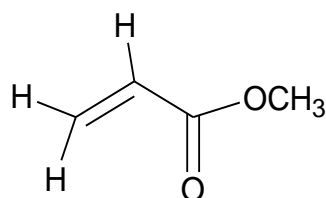
Acrolein (ACL)



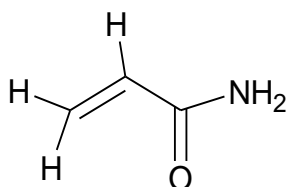
4-hydroxy -2- nonenal (HNE)



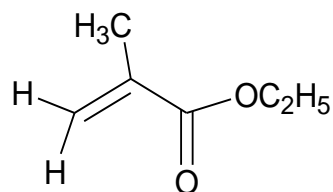
Methyl vinyl ketone (MVK)



Methyl acrylate (MA)



Acryl amide (ACR)



Ethyl methacrylate (EMA)

**Figure 3.2.1** Structures of the  $\alpha,\beta$ -unsaturated carbonyl compounds.

### 3.2 Computational details

These quantum mechanical studies have been carried out using Gaussian'09' software (Gauss-view).<sup>16</sup> The optimization has been done in B3LYP(DFT) method. The semiempirical AM1 quantum chemical method also has been used to calculate the gas phase proton affinity of the studied carbonyl compounds. Since the accuracy of the computed properties is sensitive to the quality of the basis set, we employ triplet split-valence basis set with polarisation function 6-311G (d,p). Water was selected as solvent from solvent list for structural optimization of the free bases and their O-H<sup>+</sup> complexes using polarisable continuum model (PCM)<sup>17</sup> at the same basis set. Mulliken population analysis<sup>18</sup> and NBO

analysis (NPA only) are used to determine natural charges on all atoms from the free bases and their protonated complexes. The unscaled vibrational frequency calculations have been performed at the same level of theory. Proton affinity (PA) at 298.15k is defined as the enthalpy change of the protonation reaction (1).  $PA = [(\Delta H_{BH^+}) - (\Delta H_B + \Delta H_H^+)]$ . H= Total enthalpy of the corresponding reaction.

### 3.3 Results and discussion

The  $\alpha,\beta$ -unsaturated carbonyl compounds (Given in **Figure 3.2.1**) and their  $O-H^+$  complexes have been computed in B3LYP(DFT) method at 6-311G(d,p) basis set level in both gaseous and aqueous phase. Reactions are observed to be exothermic, therefore thermodynamically favourable. The calculated proton affinity (PA) values in AM1 and DFT method of the free bases with their respective names and proper abbreviation are listed in **Table 3.1.1** and **Table 3.1.2** respectively. Generated atomic charge is not important in this quantum mechanical calculation. Mulliken net charge densities among the atoms have been observed. Charges among the atoms computes by separating orbital overlap equally between two shared atoms. **Table 3.1.3** reports the net charge on carbonyl oxygen ( $q_{O^-}$ ) of the compounds before protonation and of the protonated complexes and charge on proton ( $q_{H^+}$ ) in protonated complexes. According to the semiempirical (AM1) calculated results, PA value of ACL, HNE, MVK, ACR, MA and EMA have been estimated 183.48, 176.26, 176.89, 167.16, 176.17 and 173.0 kcal /mole respectively, which are considerably less relative to their estimated values reported in literature (**Table 3.1.1**). Therefore other quantum mechanical properties obtained by this method are not considered in this chapter. From **Table 3.1.2** we observed that, proton affinity is predicted to be highest in ACR ( $-218.56$  kcal/mole) in gas phase while ACL exhibits highest affinity ( $-284.01$  kcal/mole) towards proton in aqueous media. The different PA values of the  $\alpha,\beta$ -unsaturated carbonyl compounds indicate the non-unique effect of conjugated double bond and they are influenced by the different substituent

## Chapter 3

at carbonyl carbon. In gas phase, highest PA value in ACR is due to the presence of  $-\text{NH}_2$  group at the carbonyl carbon. Beside C-C double bond effect, lone-pair electron on nitrogen atom also move towards binding oxygen makes it more electron rich and enhanced the proton affinity values. Gas phase proton affinity increases in the order of  $\text{ACL} < \text{MVK} < \text{MA} \leq \text{EMA} < \text{HNE} < \text{ACR}$ , where in aqueous phase it follows the decreasing order  $\text{ACL} > \text{ACR} > \text{HNE} > \text{MVK} > \text{EMA} > \text{MA}$ . In presence of solvation effect this order appeared by almost reversed due to the electronic relaxation effect. ACL shows the highest affinity to proton. Because there is no possibility of hydrogen bond formation at any centre of the compound which can restrict the shifting of  $\pi$  electron at the binding site, so the resonance effect (+R) increases the electro negativity of binding oxygen and accelerate the proton-oxygen interaction. PA value of HNE ( $-259.78$  kcal/mole) appear less compared to ACL in aqueous phase because of the possibility of hydrogen bond formation with hydroxyl oxygen, but it provide higher PA value than MVK, MA and EMA, this is due to the positive inductive effect (+I) exhibited by the long alkyl chain attached to the carbonyl group shifting partial negative charge at oxygen binding site<sup>19</sup>. PA value varies due to the presence of different substituent at the carbonyl carbon and it also effected slightly by the substituent ( $-\text{H}$  or  $-\text{CH}_3$ ) present at the  $\alpha$ -carbon of the molecule.

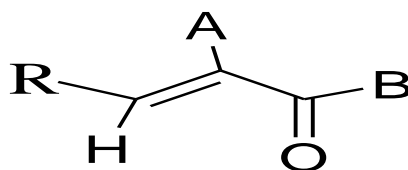


**Figure 3.2.2** Structures for conjugated  $\alpha,\beta$ -unsaturated carbonyl compounds of type-2-alkene chemical class. (R =  $-\text{H}$  or alkyl group, A =  $-\text{H}$  or  $-\text{CH}_3$  and B =  $-\text{H}$ ,  $-\text{CH}_3$ ,  $-\text{OCH}_3$ ,  $-\text{NH}_2$ ,  $-\text{OC}_2\text{H}_5$ ).

PA increases in gas phase following the order as B =  $-\text{H} < -\text{CH}_3 < -\text{OCH}_3 < -\text{OC}_2\text{H}_5 < -\text{NH}_2$ . Effect of B [ $-\text{CH}_3$ ,  $-\text{OCH}_3$  and  $-\text{OC}_2\text{H}_5$ ] on PA are more or less same for these three



unsaturated compounds. Positive inductive effect (+I) of methyl group at  $\alpha$  position increase PA little bit in ethyl methacrylate ( $A = -CH_3$ ) compared to methylacrylate ( $A = -H$ ). Lone-pair electron on nitrogen of amide group lost their mobility towards carbonyl oxygen due to the hydrogen bond formation ( $N \cdots H$ ) in water, which is one of the causes for decreasing PA of ACR compared to ACL. +I character of methyl group enhance the PA of MVK ( $-259.6$  kcal/mole). Effect of  $-OCH_3$  at B is less on PA compare to  $-OC_2H_5$ , because both substituent has negative inductive effect (-I) and resonance (+R) effect, but due to more resonance character ( $-OCH_3 < -OC_2H_5$ ) PA value of EMA ( $-258.15$  kcal/mole) is predicted little more compared to MA ( $-257.52$  kcal/mole) in aqueous phase. For  $\alpha, \beta$ -unsaturated carbonyl compounds PA increases in the order  $B = -OCH_3 < -OC_2H_5 < -CH_3 < -NH_2 < -H$  (in acrolein) in aqueous phase. From **Table 3.1.3** it is obvious that net charge on  $O^-$  atom is higher in free bases in each compound in comparison to their protonated complex indicate their high protonation tendency. Charge on proton of the protonated complexes reveals the fact of extensive charge transfer during protonation, proton added to the carbonyl oxygen form a strong covalent  $\sigma$  bond. Charge density on O-atom increased markedly in aqueous phase compare to gas phase indicating the higher charge separation in water. It is well supported by increased dipole moment in aqueous phase than that in the gas phase. Charge on proton and oxygen atom in the complexes clearly show that shifting of charge is not local, it come from all over the molecules. Computed net charge on oxygen atom in free bases and protonated complexes are within the range  $-0.2864$  e to  $-0.3594$  e and  $-0.1465$  e to  $-0.2505$  e in gas phase. It is  $-0.3701$ e to  $-0.4635$ e and  $-0.1742$  e to  $-0.2750$  e for free base and their  $O-H^+$  complexes in aqueous phase respectively. Charge on adjunct proton lies within  $0.2991$ e to  $0.3206$  e in gas phase, a little increases in aqueous phase (from  $0.323$ e to  $0.3437$ e).

Some selected optimized geometrical features like bond distance (C-O and O-H),  $\angle C-O-H^+$  bond angle surrounding carbonyl group of the computed compounds are reported in

**Table 3.1.4** and **3.1.5**. The  $r(\text{C}-\text{O})$  bond length effected with the protonation, it elongated in protonated complexes by 0.069Å to 0.092Å in gas phase and 0.067Å to 0.097Å in aqueous phase. In complexes,  $r(\text{O}-\text{H}^+)$  bond distance remain almost identical for all compounds both in gas and aqueous phases, it varies iota (0.0062Å in gas phase and 0.0087Å in aqueous phase). The  $\angle\text{C}-\text{O}-\text{H}^+$  bond angles in the optimized complexes lies within 111.59° to 117.57° and 111.397° to 113.97 in gas and aqueous phase respectively. The local stereochemical and other quantum mechanical parameters obtained from DFT[B3LYP] theoretical study at 6-311G(d,p) basis set level suggest to conclude that the PA of the selected carbonyl compounds can not be explained correctly by local carbonyl site properties only, it must need to consider the entire molecular contribution. We have also analysed some other global quantum mechanical parameters to observe the comparative electrophilic nature by calculating electrophilic index ( $\omega$ ), hardness ( $\eta$ ) and softness ( $\sigma$ ) from HOMO–LUMO energy gap of the free carbonyl compounds in both gas and aqueous phases. We observed from the data reported in **Table 3.1.6** and **Table 3.1.7** that, ACL ( $\omega = 0.1495$  and 0.1352 in gas and aqueous phase respectively) and HNE ( $\omega = 0.1461$  and 0.1496 in gas and aqueous phase respectively) are two most strong electrophile compared to rest four compounds and EMA ( $\omega = 0.1108$  and 0.1063 in gas and aqueous phase) shows the weakest electrophilic reactivity. Based on their corresponding quantum mechanical parameters, the selected carbonyl compounds follow the electrophilicity order as  $\text{HNE} \geq \text{ACL} \gg \text{MVK} \geq \text{MA} > \text{ACR} > \text{EMA}$  in aqueous, albeit controversial in gaseous phase where ACL exhibit highest electrophilicity compared to HNE. The global parameter hardness ( $\eta$ ) calculated from the  $E_{\text{LUMO}} - E_{\text{HOMO}}$  energy gap as  $\text{Hardness} (\eta) = [E_{\text{LUMO}} - E_{\text{HOMO}}]/2$ . It is the scale of ground state stability of the relative compounds. Calculated quantum mechanical data's are tabulated in **Table 3.1.6** and **3.1.7**. We have seen, the  $\eta$  values is predicted to be highest in EMA ( $\eta = 0.1137$  and 0.1172 in gas and aqueous phase) is the most stable among the six compounds.

### 3.4 Conclusion

Investigated PA values of six  $\alpha,\beta$ -unsaturated conjugated carbonyl compounds in both gas phase and aqueous phase using DFT(B3LYP) method employing triple valance basis set 6-311G(d,p) can't be explained exactly considering only electronic and stereochemical optimized parameter at or around the carbonyl moiety, proton affinities are strongly affected by the different substituents (B = -H, -CH<sub>3</sub>, -OCH<sub>3</sub>, -OC<sub>2</sub>H<sub>5</sub> and -NH<sub>2</sub>) attached to the carbonyl carbon. The PA values of the compounds obtained in AM1 method of calculation are too less relative to their results reported in literature, thus not reliable. DFT proton affinities are far superior to the AM1 PA results. Proton affinities of the bases markedly change due to solvation. Interaction enthalpies are more negative in water. +I effect of  $\alpha$ -methyl group, +R (resonance) and - I effect of the -OCH<sub>3</sub>, -OC<sub>2</sub>H<sub>5</sub> group are responsible for small increase of PA in EMA. So it can be concluded that PA of the  $\alpha,\beta$ -unsaturated carbonyl compounds are obtained considering the different electronic properties strongly. It has been found that selected carbonyl derivatives are harder in aqueous phase. The electro-chemical properties of the protonated complexes clear the fact that the interaction between binding oxygen site and proton is preferably an ion-induced dipole interaction and ion-dipole attraction as well rather than a covalent interaction. Overall protonation reactions are spontaneous.

**Table 3.1.1** Computed proton affinities (PA) of six  $\alpha,\beta$ -unsaturated carbonyl compounds for both gas phase at the equilibrium geometry of the ground state by AM1 method. All data of PAs are in hartree and kcal/mole unit.

Molecule	Gas phase PA	
	(in hartree)	(in kcal/mol)
Acrolein(ACL)	- 0.2924	-183.48 (-194.019)*
4-hydroxy-2-nonenal(HNE)	- 0.2809	-176.26 (----)
Methyl vinyl ketone (MVK)	- 0.2819	-176.89 (-200.478)*
Acrylamide (ACR)	- 0.2664	-167.16 (-208.30)*
Methyl acrylate (MA)	- 0.2807	-176.17 (-199.28)*
Ethyl methacrylate (EMA)	- 0.2757	-173.0 (-203.11)*

Experimental PA values of the respective compounds are noted in the parenthesis.

Ref: Grutzmacher *et al.* 1989.

**Table 3.1.2** Computed proton affinities (PA) of six  $\alpha,\beta$ -unsaturated carbonyl compounds for both gas and aqueous phase at the equilibrium geometry of the ground state. All data of PAs are in hartree and kcal/mole unit.

Molecule	Gas phase PA		Aqueous phase PA	
	( hartree)	( kcal/mol)	( hartree)	( kcal/mole)
ACL	- 0.3207	-201.24 (-194.019)*	- 0.4526	-284.01
HNE	- 0.3427	-215.04 (----)	- 0.414	-259.78
MVK	- 0.3336	-209.33 (-200.478)*	- 0.4137	-259.60
ACR	- 0.3483	-218.56 (-208.30)*	- 0.4269	-267.88
MA	- 0.3342	-209.71 (-199.28)*	- 0.4104	-257.52
EMA	- 0.3361	-210.90 (-203.11)*	- 0.4114	-258.15

\* Experimental PA values of the respective compounds are noted in the parenthesis.

Ref: Grutzmacher *et al.* 1989.

**Table 3.1.3** Computed Mulliken net charge on carbonyl oxygen atom ( $q_{O^-}$ ) of free base ( $B_1$ ) and O-protonated complexes ( $B_1H^+$ ) and net charge on proton ( $q_{H^+}$ ) of the O-protonated complexes at the equilibrium ground state and dipole moment( $p$ ) in debye of the free bases in both phases.

Molecule	Gas phase				Aqueous phase			
	$q_{O^-}$		$q_{H^+}$	$p$	$q_{O^-}$		$q_{H^+}$	$p$
	$B_1$	$B_1H^+$	$B_1H^+$		$B_1$	$B_1H^+$	$B_1H^+$	
ACL	-0.2864 (-0.5056)	-0.1465 (-0.5002)	0.3200 (0.5181)	3.15	-0.4675 (-0.5673)	-0.1742 (-0.5162)	0.3389 (0.5299)	4.04
HNE	-0.2944 (-0.5214)	-0.2101 (-0.5187)	0.3206 (0.5169)	2.12	-0.3490 (-0.5530)	-0.2090 (-0.5234)	0.3437 (0.5312)	2.83
MVK	-0.3022 (-0.5494)	-0.1995 (-0.5425)	0.3162 (0.517)	2.7	-0.3574 (-0.5979)	-0.2090 (-0.5538)	0.3354 (0.5298)	3.51
ACR	-0.3594 (-0.6048)	-0.2505 (-0.5837)	0.3171 (0.5152)	3.88	-0.4316 (-0.6714)	-0.2750 (-0.5979)	0.3307 (0.5230)	5.14
MA	-0.3157 (-0.5670)	-0.1889 (-0.5567)	0.2991 (0.5085)	4.32	-0.3778 (-0.6265)	-0.222 (-0.5757)	0.323 (0.5238)	5.56
EMA	-0.3553 (-0.5587)	-0.2192 (-0.5772)	0.3106 (0.5187)	1.78	-0.3701 (-0.6180)	-0.2374 (-0.5854)	0.3278 (0.5304)	5.51

\*Data written in parenthesis are obtained from NPA analysis.

**Table 3.1.4** Geometrical features of the free base and O-protonated base (length in Å and angle in degree) at the equilibrium ground state in gas phase.

Molecule	Free Base	O-Protonated complexes		
	$r(C-O)$	$r(C-O)$	$r(O-H^+)$	$\angle C-O-H^+$
ACL	1.208	1.277	0.9761	114.720
HNE	1.21	1.298	0.9771	113.560
MVK	1.213	1.291	0.9721	117.570
ACR	1.22	1.30	0.9686	113.275
MA	1.203	1.296	0.9684	113.577
EMA	1.208	1.298	0.9743	111.597

**Table 3.1.5** Geometrical features of the free base and O-protonated base (length in Å and angle in degree) at the equilibrium ground state in aqueous phase.

Molecule	Free Base	O-Protonated complexes		
	$r(C-O)$	$r(C-O)$	$r(O-H^+)$	$\angle C-O-H^+$
ACL	1.221	1.277	0.9762	113.970
HNE	1.21	1.288	0.9715	112.712
MVK	1.219	1.286	0.9728	113.1269
ACR	1.230	1.307	0.9687	112.432
MA	1.212	1.295	0.9694	113.4703
EMA	1.212	1.295	0.9749	111.397

### Chapter 3

**Table 3.1.6** Computed hardness, softness, chemical potential and electrophilic index of the free base (B<sub>1</sub>) in the gas phase ground state by DFT method. Hardness ( $\eta$ ) =  $[\epsilon_{\text{LUMO}} - \epsilon_{\text{HOMO}}]/2$ , Softness( $\sigma$ ) =  $1/\eta$ , Chemical potential ( $\mu$ ) =  $[\epsilon_{\text{LUMO}} + \epsilon_{\text{HOMO}}]/2$ , Electrophilic index( $\omega$ ) =  $\mu^2/2\eta$ .

Molecule	$\epsilon_{\text{HOMO}}$	$\epsilon_{\text{LUMO}}$	$\eta$	$\sigma$	$\mu$	$\omega$
ACL	-0.2649	-0.0735	0.0957	10.44	-0.1692	0.1495
HNE	-0.2603	-0.0717	0.0943	10.60	-0.166	0.1461
MVK	-0.2565	-0.0639	0.0963	10.38	-0.1602	0.1332
ACR	-0.2593	-0.0477	0.1058	9.45	-0.1535	0.1113
MA	-0.2781	-0.0614	0.1083	9.23	-0.1697	0.1329
EMA	-0.2725	-0.0451	0.1137	8.79	-0.1588	0.1108

**Table 3.1.7** Computed hardness (hartree), softness, chemical potential and electrophilic index of the free base (B<sub>1</sub>) in the aqueous phase ground state by DFT method.

{Hardness( $\eta$ ) =  $[\epsilon_{\text{LUMO}} - \epsilon_{\text{HOMO}}]/2$ , Softness( $\sigma$ ) =  $1/\eta$ , Chemical potential( $\mu$ ) =  $[\epsilon_{\text{LUMO}} + \epsilon_{\text{HOMO}}]/2$ , Electrophilic index( $\omega$ ) =  $\mu^2/2\eta$ .

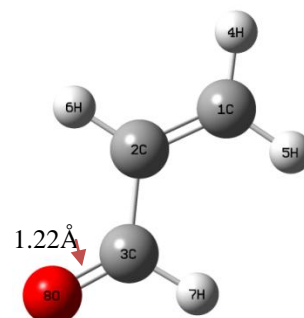
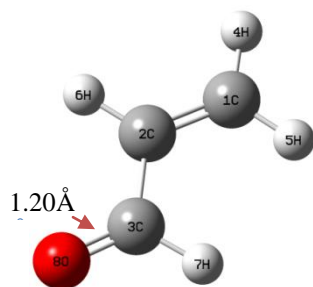
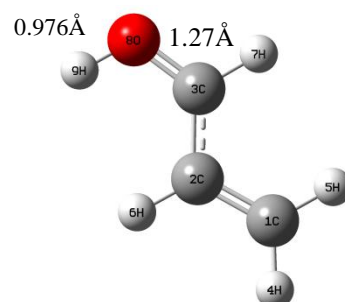
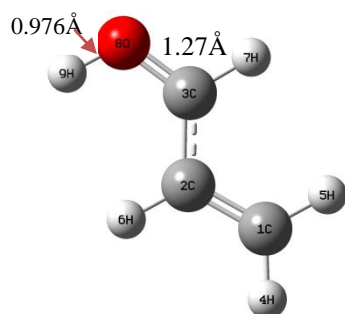
Molecule	$\epsilon_{\text{HOMO}}$	$\epsilon_{\text{LUMO}}$	$\eta$	$\sigma$	$\mu$	$\omega$
ACL	-0.26124	-0.06480	0.0982	10.18	-0.1630	0.1352
HNE	-0.26641	-0.07356	0.0964	10.37	-0.1699	0.1496
MVK	-0.26312	-0.06646	0.0983	10.16	-0.1647	0.1379
ACR	-0.26802	-0.04818	0.1099	9.09	-0.1581	0.1136
MA	-0.2887	-0.06312	0.1127	8.36	-0.1759	0.1371
EMA	-0.27515	-0.04065	0.1172	8.52	-0.1579	0.1063

$B_1$  and  $B_1H^+$ 

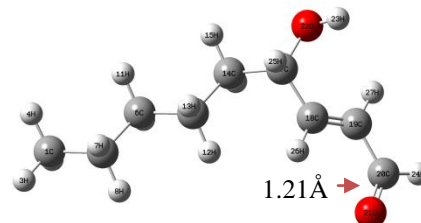
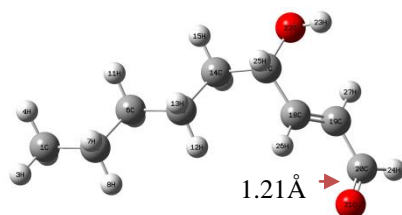
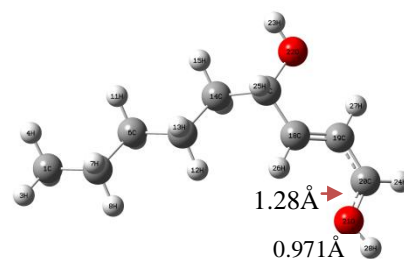
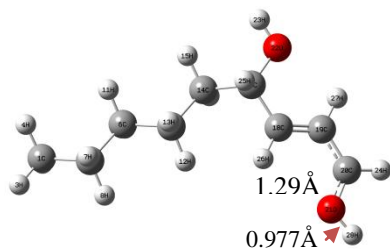
Gas phase

Aqueous phase

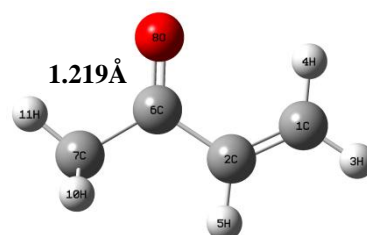
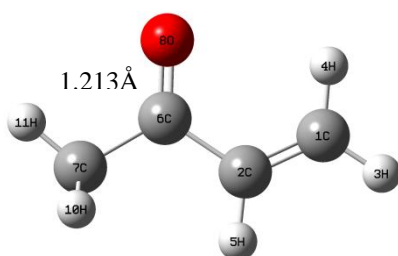
ACL

ACL ( $O-H^+$ )

HNE

HNE ( $O-H^+$ )

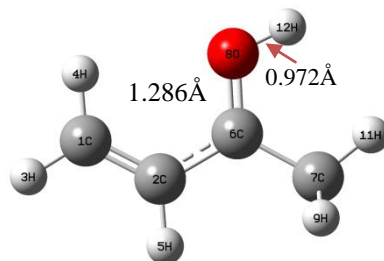
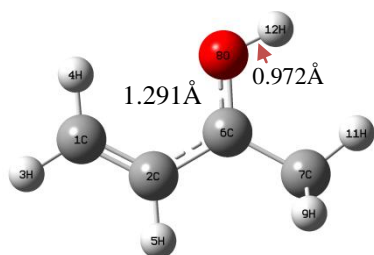
MVK



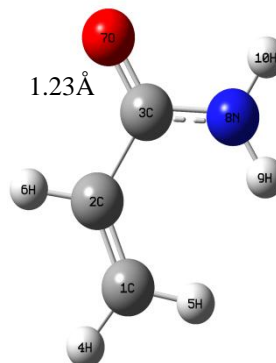
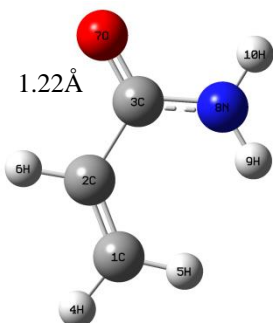
Gas phase

Aqueous phase

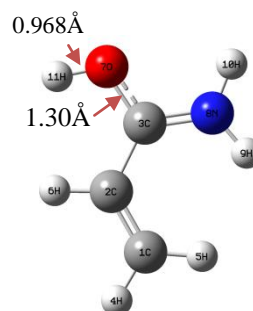
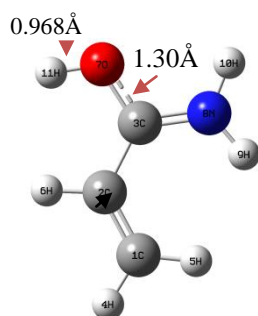
MVK (O-H<sup>+</sup>)



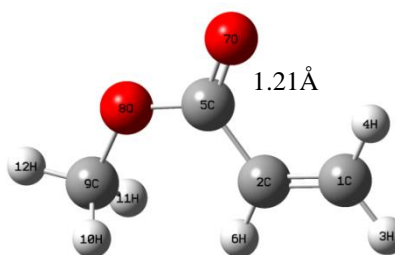
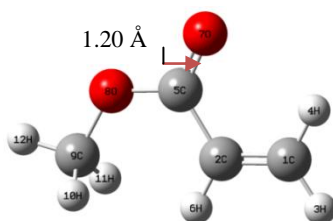
ACR



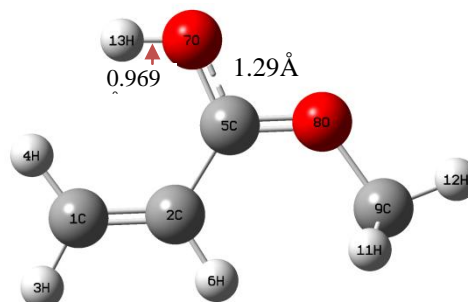
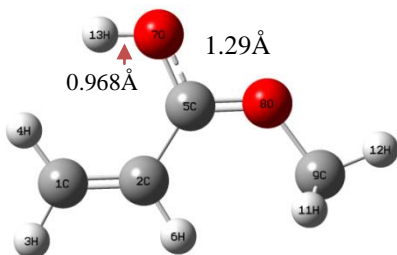
ACR (O-H<sup>+</sup>)



MA



MA(O-H<sup>+</sup>)





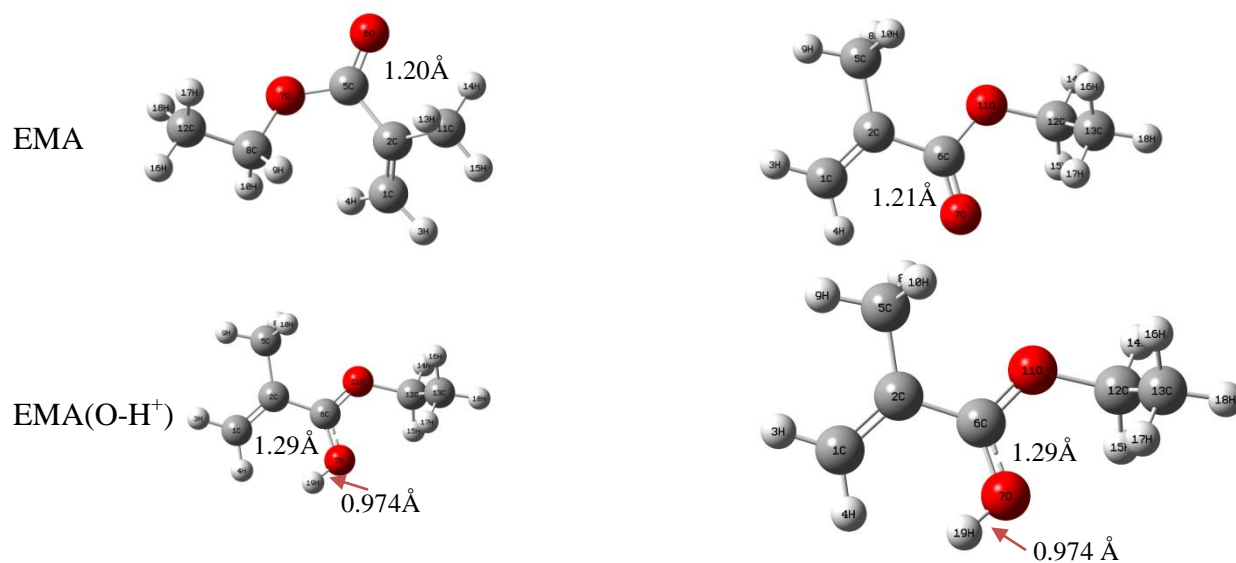


**Figure 3.2.3** Optimized structure of selected conjugated  $\alpha,\beta$ -unsaturated carbonyl compounds and their carbonyl oxygen- $H^+$  complexes in gas and aqueous phase.

### 3. 5 References

- (1) LoPachin, R. M.; Gavin, T. *Environmental Health Perspectives*. **2012**, *12*, 120.
- (2) Beauchamp, J. L. *Interaction between ions and molecules*, New York, Plenum, **1974**, 413,459,489.
- (3) Bhome, D. K.; Mackay, G. I.; Shiff, H. I.; Hemsworth, R. S. *J. Chem. Phys.* **1974**, *61*, 2175.
- (4) Brauman, J. I.; Blair, L. K. *J. Am. Chem. Soc.* **1970**, *92*, 5986.
- (5) Meyer, E. A.; Castellano, R. K.; Diederich, F. *Angew. Chem. Int. Ed.* **2003**, *42*, 1210-1250.
- (6) Bhattacharyya, S. P.; Rakshit, S. C.; Banerjee, M. *J. Mol. Struct. (Theochem)* **1983**, *91*, 253.
- (7) Dekock, J. R. L.; Kohin, M. S. *J. Mol. Struct. (Theochem)* **1983**, *94*, 343.
- (8) Strusz, O. P.; Kapny, E.; Kosmntza, C.; Robb, M. A.; Theodorakopoulos, G.; Cizmadia, I. G. *Theoretica Chim. Acta.* **1978**, *48*, 215.
- (9) Yamadagni, R.; Kebarle, P. J. *J. Am. Chem. Soc.* **1973**, *96*, 3727.
- (10) Burk, P.; Koppel, I. A.; Koppel, I.; Kurg, R.; Gal, J.-F.; Maria, P.-C.; Herreros, M.; Notario, R.; Abboud, J.-L. M.; Anvia, F.; Taft, R. W. *J. Phys. Chem. A* **2000**, *104*, 2824.
- (11) Dixon, D. A.; Lias, S. G. *Molecular Structure and Energetics*. **1987**, Vol. 2, *Physical Measurements*, edited by Liebman, J. F.; Greenberg, A. (VCH, Deereld Beach, FL).
- (12) Pandit, S.; De, D.; De, B. R. *J. Mol. Struct. (Theochem)* **2006**, *760*, 245.
- (13) Senapati, U.; De, D.; De, B. R. *Indian J. Chem.* **2008**, *47A*, 548-550.
- (14) Lee, C.; Yang, W.; Parr, R. G. *Phys. Rev.* **1988**, *B37*, 785.
- (15) Wolf, R.; Grutzmacher, H. F. *New J. Chem.* **1990**, *14*, 379-382.

- (16) Frisch, M. J.; Trucks, G. W.; Schlegel, H. B.; Scuseria, G. E.; Robb, M. A.; Cheeseman, J. R.; Scalmani, G.; Barone, V.; Mennucci, B.; Petersson, G.A.; et al. *Gaussian 09, Revision A.02*, Gaussian, Inc., Wallingford, CT, 2009.
- (17) Tomasi, J.; Mennucci, B.; Cancès, E. *J. Mol. Struct. (Theochem)* **1999**, *464(1-3)*, 211-226.
- (18) Mulliken, R. S. Electronic Population Analysis on LCAO–MO Molecular Wave Functions, *I. J. Chem. Phys.* **1955**, *23(10)*, 1833-1840.
- (19) Striegel, A. M.; Piotrowiak, A. P.; Stephen, M. B.; Cole, R. B. *J. Am. Soc. Mass Spectrom.* **1999**, *10*, 254-260.



## **CHAPTER 4**

**Ground state lithium cation affinities (LCA) and associate parameters of a series of  $\alpha,\beta$ -unsaturated carbonyl compounds of type-2-alkene chemical class (ACL, HNE, MVK, ACR, MA and EMA ): A Comparative DFT based computational study in both gas and aqueous phases.**



## Abstract

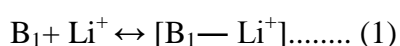
A DFT [B3LYP] /6-311G(d,p) calculations were performed to evaluate the lithium cation affinities (LCA) for a set of  $\alpha,\beta$ -unsaturated carbonyl derivatives of type-2-alkene chemical class (acrolein, 4-hydroxy-2-nonenal, methyl vinyl ketone, acrylamide, methyl acrylate and ethylmethacrylate). The interaction energies were calculated to quantify the affinity of the bases for the  $\text{Li}^+$  cation. LCA values are influenced by the electronic nature of the alkyl chain adjacent to the carbonyl carbon and also different substituent at functional carbon. Lithium cation basicity ( $\text{LCB} = -\Delta G_{\text{Li}^+}$ ), change of entropy ( $\Delta S$ ) during complexation in each compound has been analysed systematically. Acrylamide exhibit the highest LCA value in gas phase as well as in aqueous phase compared to others in the series. Complete geometry optimization both before and after  $\text{Li}^+$  complex formation were performed in both phases. Geometric and electronic parameters were correlated with the strength of the metal-ligand interactions. Net charges on the atoms of free bases and their O- $\text{Li}^+$  complexes are evaluated by natural population analysis (NPA) and Mulliken population analysis. The energetic, structural and electronic properties of the complexes indicate that the interaction between the  $\text{Li}^+$  ion and a carbonyl base is preferably an electrostatic interaction as well rather than a covalent interaction. The overall reactivity is explained by entire molecular contribution in addition to the contribution from the carbonyl group.

## 4.1 Introduction

Interaction of metal cation with carbonyl base has a great effect on living systems and is a subject of growing interest in biochemistry due to their pertinent functions in many biological processes.<sup>1,2</sup> Alkali metal ions were the first metal cations to be studied in the gas phase due to their strong Lewis acid properties and their easy production in vacuum. In comparison to transition metal ions, alkali metal cations are reacting more readily with ligands. They form adducts or clusters, that can be considered as ions 'solvated' by one or several ligands.<sup>3</sup>  $\text{Li}^+$  cation is inevitable for the human body, play an important role in many biological activities like synthesis of blood protein, maintenance of blood pressure.<sup>4,5</sup> In biological process  $\text{Li}^+$  ion interact with many biological molecules having different functional group. Lithium cation also prefers to interact with carbonyl oxygen atom of  $-\text{CHO}$ ,  $-\text{COOH}$ ,  $-\text{COMe}$ ,  $-\text{COOMe}$ ,  $-\text{COOEt}$  and nitrogen atom of amine, amide.<sup>6-11</sup> Two important Lewis acid proton ( $\text{H}^+$ ) and  $\text{Li}^+$  cation shows different nature during bond formation with the ligand molecule.<sup>12</sup> Proton formed a covalent  $\sigma$  bond with the ligand molecule to a great extent of charge transfer. Proton contains 0.4 or less unit of positive charge in the complex whereas alkali cation (sodium or lithium) retains with 0.8 to 0.9 units of positive charge in the same type of interactions.<sup>12</sup> Therefore the bond formed between lithium cation and ligand molecule is largely ionic. Due to hard acid character (according to Pearson's HSAB theory) of lithium cation it prefers to bind with oxygen donor ligand (hard base) and formed stable complex. Oxygen atom has small Vanderwaal raddi and is more polarisable compared to nitrogen and other electronegative species. This is one of the causes of  $\text{O-Li}^+$  strong interaction. In order to evaluate more accurate alkali metal cation affinity values, a number of experimental methods like high pressure mass spectrometry (HPMS),<sup>13-16</sup> Ion cyclotron resonance (ICR),<sup>17-21</sup> unimolecular dissociation–Cook's kinetic method,<sup>22,23</sup> energy resolved collision-induced dissociation (CID),<sup>24-26</sup> and photo dissociation and radiative association kinetics<sup>27,28</sup> have been



utilised extensively. Previous studies have developed intension to study this type of acid-base interactions theoretically. Some ground state  $\text{Li}^+$  affinities of substituted acetophenones were reported.<sup>29</sup> In the present chapter, selected conjugated  $\alpha,\beta$ -unsaturated carbonyl derivatives of type-2-alkene chemical class are biologically important, they produce toxicity via common molecular mechanism that could pose a significant risk to human health.<sup>30</sup> Proton affinities of the same compounds have already been reported in our previous chapter. The objectives of the present work to evaluate a bunch of reliable quantum mechanical data with a comparative discussion of lithium ion affinities (LCA) of this given class of unsaturated carbonyl derivatives considering their C–C double bond conjugation effect, Inductive effect (+I, –I) and resonance (+R, –R) character of different substituent attached to functional carbon and at ‘ $\alpha$ ’ carbon of the carbonyl derivatives. In this present work we calculate LCA, lithium cation basicities (LCB) and relative electronic, geometrical properties of six carbonyl compounds theoretically with the help of DFT [B3LYP] method using the most accurate atom-centred split valence with polarization functions 6-311 G (d,p) basis set level<sup>31,32</sup> in both gaseous and aqueous phase. Lithium cation basicity (LCB) is defined as negative value of the free energy change ( $-\Delta G^{298.15\text{k}}_{\text{Li}^+}$ ) of the following thermodynamic equilibrium.



Lithium cation affinity (LCA) is defined as the negative value of the enthalpy change ( $-\Delta H^{298.15\text{k}}_{\text{Li}^+}$ ) of the above equation. LCA values for the lithium ion- Lewis base complexes are also evaluated using the optimization energies of free bases and of their  $\text{Li}^+$  complexes with the help of following equation

$\text{LCA} = \Delta H^{298.15\text{K}} = \{E^{298.15\text{k}}(\text{B1M}) - [E^{298.15\text{k}}(\text{B1}) + E^{298.15}(\text{M})]\} + \Delta(\text{pV}) \dots (2)$ . Where  $E^{298.15\text{k}}(\text{B}_1)$ ,  $E^{298.15\text{k}}(\text{M})$  are energy of the free base and metal cation and  $E^{298.15}(\text{B1M})$  is the energy of the metal complex. We substitute  $\Delta(\text{pV}) = \text{RT}$  in our calculation. Detail analyses on Ligand- metal bond formation in each carbonyl base in gas phase has been carried out and the effect of solvent has been observed. In this paper we also report entropy change ( $\Delta S^{298.15\text{k}}$ ) of

## Chapter 4

the corresponding reactions. *Abinitio* hartree-fock calculations were also performed in the present work at the same basis set level. But results obtained from DFT calculation are much better compared to H-F calculation therefore H-F results are neglected. General atomic charges are not an important quantum mechanical parameter. Charges on atom obtained from Mulliken population analysis (MPA) vary with different basis set used, till it used widely. In this theoretical analysis we have analysed the charges on carbonyl oxygen and on  $\text{Li}^+$  cation obtained from natural population analysis (NPA) and Ligand to Metal Charge Transfer ( $q_{\text{CT}}$ ) in the complexes have been calculated in both gas and solvent phase. Distribution of charge density among the specific atoms in free bases and their lithium ion complexes has been analyzed to understand the overall modulation of LCA values.

Acrylamide has two donor sites (O and N), in order to examine the proper binding sites of Acrylamide for  $\text{Li}^+$  cation, we optimized the geometry where  $\text{Li}^+$  ion kept free (not directly bonded with any donor site in initial input), We observed O- $\text{Li}^+$  complex is formed with same optimization energy (-254.7450 hartree) and 1.71Å O- $\text{Li}^+$  bond distance, then we have not performed the same optimization process for the rest five compounds in this series. Solvation effects on lithium cation affinities have been noticed carefully in this theoretical study. Compounds studied in this theoretical calculation are listed bellow with their name and proper abbreviation.

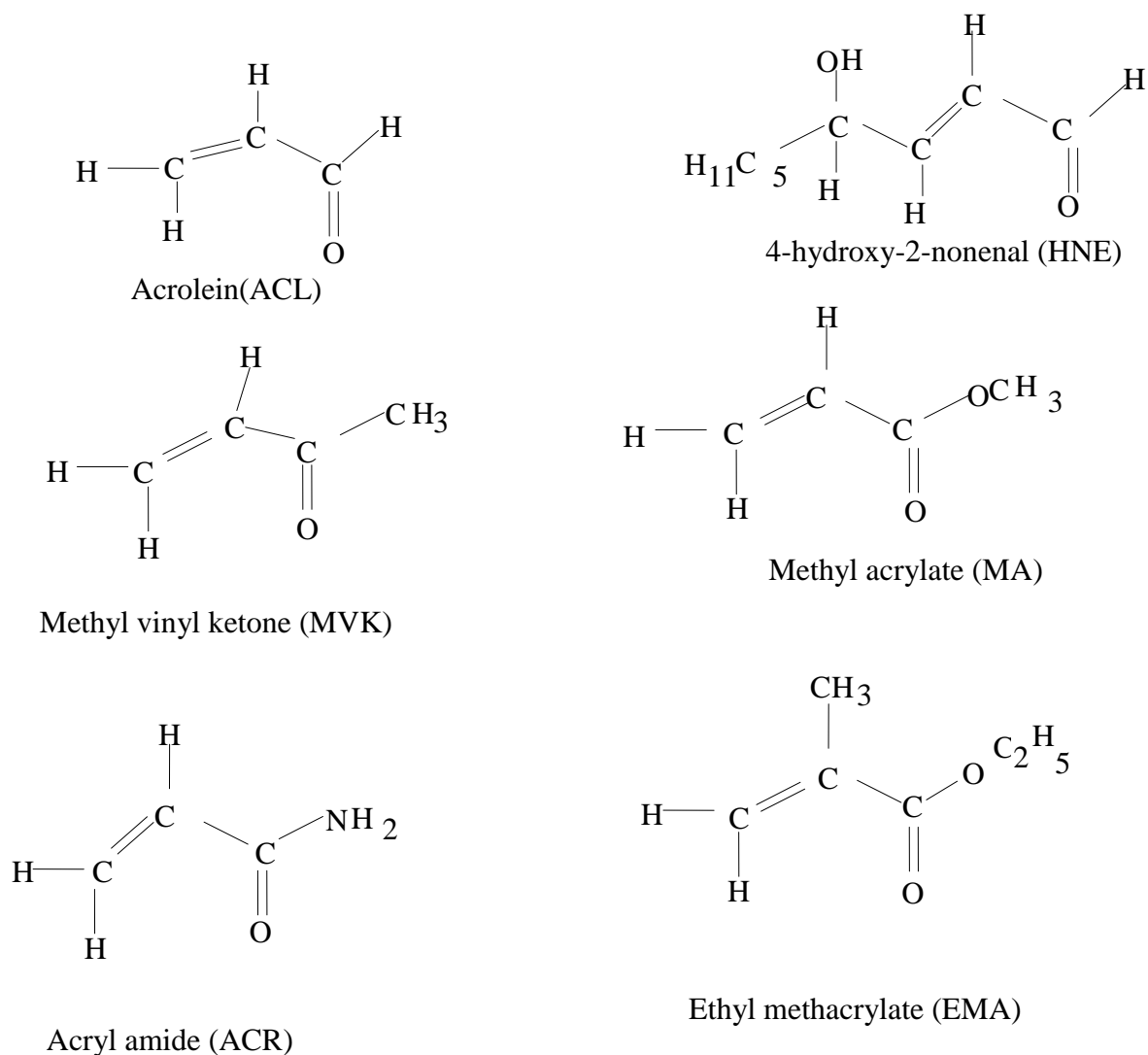


**Figure 4.2.1** Structures of several  $\alpha$ ,  $\beta$ -unsaturated carbonyl compounds.

## 4.2 Computational details

All calculations were performed using the Gaussian '09' program.<sup>33</sup> To evaluate the ability of a less time consuming method to produce the lithium cation affinity, we use DFT [B3LYP] hybrid method with high accuracy level of 6-311 G (d, p) basis set. In order to understand and to evaluate the electronic and structural behaviour in solvents, we carried out the SCRF-PCM<sup>34</sup> geometry optimization process at the same level of theory. Water was selected as solvent from solvent list. Dielectric constant 78.39 has been utilised to simulate the aqueous

environment. Mulliken population analysis<sup>35</sup> and NPA are applied to determine equivalent charges on all atoms from the free bases and their metal complexes. The magnitude of BSSE was evaluated at the B3LYP/ 6-311G (d,p) level for a small test set of molecules using counterpoise correction<sup>36</sup> and found to be small (0.5 kcal/mol or less) therefore BSSE corrections are not taken into account for present theoretical calculation. Gibbs free energies (G) and enthalpies (H) were evaluated using unscaled frequencies calculation at the same level of basis set.

### 4.3 Results and discussion

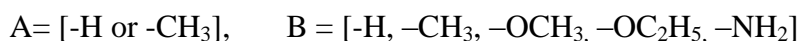
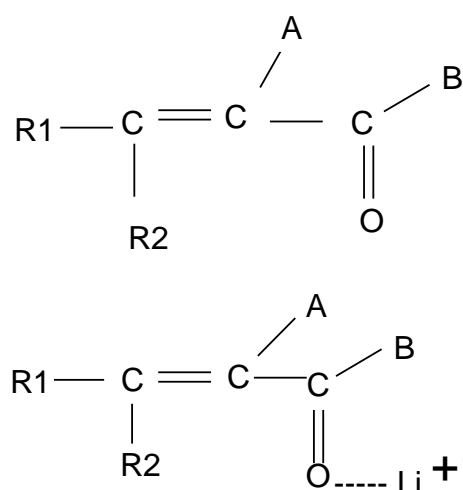


**Figure 4.2.2** General Chemical structure of  $\alpha,\beta$ -unsaturated carbonyl compounds and their  $O-Li^+$  complexes.

The  $\alpha,\beta$ -unsaturated carbonyl compounds studied in this theoretical work are listed in **Table 4.1.1** along with their respective names and proper abbreviation with optimization energies of the free bases ( $B_1$ ) and their  $B_1-Li^+$  complexes. Lithium cation affinities are defined as the negative value of the enthalpy change of reaction as  $B_1 + M^+ \leftrightarrow [B_1 - M^+]$ ,  $LCA = -\Delta H_{Li^+}$ .

The reactions are exothermic in each cases in gaseous as well as in aqueous phase. Affinities of each carbonyl compound for lithium cation are evaluated in both phases following equation (2) and it summarized in **Table 4.1.2**. The LCA value of six carbonyl derivatives shows different trend from gas to aqueous phase. Acrolein has lowest LCA ( $-48.98$  kcal/mole) in gas phase and exhibit weakest interaction enthalpy ( $-6.1221$  kcal/mole) with HNE ( $-6.1219$  kcal/mole) in aqueous media also. The respective quantum mechanical result ( $\Delta E_g$ ) of the selected bases indicate that, the gas phase LCA increases in the following order  $ACL < MVK \leq EMA < HNE < MA < ACR$ . Large variation has been observed in aqueous phase with lowering ligand – cation interaction enthalpy ( $\Delta E_{sol}$ ) where LCA increases in  $HNE \leq ACL < MVK < MA \leq EMA < ACR$  order. Acrylamide have the maximum affinity ( $-58.58$  kcal/mole) for  $Li^+$  cation in gas phase and it exhibit highest value ( $-8.94$  kcal/mole) in aqueous phase also. Presence of more electron releasing  $-NH_2$  substituent at carbonyl carbon increase the electron density on binding oxygen and enhance the ligand- metal interaction effectively. In gas phase effect of B = ( $-CH_3$  and  $-OC_2H_5$ ) substituent on LCA values is quite uniform for MVK and EMA ( $\pm 0.321$  kcal/mole) and +I effect of ‘A’ substituent ( $-CH_3$ ) at  $\alpha$  carbon of EMA is much less. The enhancement of LCA by  $-OCH_3$  is not much ( $-5.96$  kcal/mole) compared to  $-CH_3$  and  $-OC_2H_5$  at B. A comparison of LCA of six  $\alpha,\beta$ -unsaturated carbonyl compounds demonstrate clearly that conjugation effect of  $C=C$  and  $C=O$  is not maintain uniformity in both gas and aqueous phase and doughtily depend on B substituent. Gas phase affinity ( $\Delta E_g$ ) of HNE for  $Li^+$  cation enhanced by an inductive effect exhibited by the alkyl chain contiguous to carbonyl carbon contributes via bond-electron donation. O- $Li^+$  interaction enthalpy of each compounds decreased by  $+42.85$  to  $+49.63$  kcal/mole in aqueous phase compared to gas phase. Effect of B and A substituent on comparative LCA values in aqueous phase of three unsaturated carbonyl compounds MVK, MA and EMA ( $\pm 1.07$  kcal/mole) is much less. Electron shifting capacity of  $-NH_2$  group

## Chapter 4

towards oxygen ligand in ACR is arrested due to the hydrogen bond (N-----H) formation, decreases partial -ve charge on oxygen binding site and lower the affinity for  $\text{Li}^+$  (-8.94 kcal/mole). The comparative enthalpies (H), Gibbs free energies (G) of the studied  $\alpha,\beta$ -unsaturated carbonyl compounds obtained from the vibrational frequency analysis at B3LYP [6-311G (d,p)] level of theory are listed in **Table 4.1.3**. Frequencies analyses (with zero imaginary frequency) uncover the fact that all the optimized complexes at this level of theory correspond to the minima of potential energy surface. LCA ( $-\Delta H_{\text{Li}^+}^{298.15}$ ), LCB ( $-\Delta G_{\text{Li}^+}^{298.15}$ ) and entropy ( $\Delta S^{298.15}$ ) values of the complexes are also summarized in **Table 4.1.3**. We have calculated our LCA values again as total enthalpies of the reactants minus total enthalpies of the product [ $H_{\text{Li}^+} + H_{\text{ligand}} - H_{\text{Complex}}$ ] of the corresponding equilibrium reaction. For LCB it is the differences of Gibbs free energies between reactants and product. Work term  $\Delta(pV)$  is included in enthalpy by definition, therefore correction of work term is not necessary for LCA calculation by this way.<sup>37</sup> LCA values of the studied compounds are listed in **Table 4.1.2** and **4.1.3** are very close to each other in each compound only differ by 0.35 kcal/ mole to 5.67 kcal/ mole in gas phase and this differences become less than 1 kcal/ mole under solvation. Gibbs free energy describes the molecular association tendency of a molecular complex. Therefore role of entropy ( $\Delta S$ ) of the reaction process is very important. When two reactants formed single metal- ligand cationic complex, entropy of the system will loss. In our study entropy changes in the complex formation reaction of six unsaturated carbonyl derivatives are in the range of -21.86 cal /mole to -29.04 cal/ mole in the gas phase where it varies from -22.71 cal/ mole to -27.97 cal/mole in water. LCB values were evaluated from calculated Gibbs free energies summarized in **Table 4.1.3** Computed LCB values are negative and has a variation in the range -40.87 kcal/mole to -49.32 kcal/mole in gas phase, while energy difference is reduced in water (-0.943 kcal/mole to 2.13 kcal/mole) and positive values also appeared. On the basis of their LCA ( $-\Delta H_{\text{Li}^+}$ ) and LCB ( $-\Delta G_{\text{Li}^+}$ )

values the stability order of the studied complexes may be written as  $ACR > EMA \geq MA > MVK > HNE > ACL$  in gas phase, while in water it stand little bit different and it is  $ACR \geq MA > EMA > MVK > ACL \geq HNE$ . Minor discrepancy has been found in LCA values obtained from two different methods of calculation. Though in water, the order of stability remains same. We have already mentioned that generated atomic charges are not important in this quantum mechanical calculation. Computed net charge on carbonyl oxygen atom ( $q_{O^-}$ ) of the free bases and of the  $Li^+$  complexes as well as charge on lithium cation ( $q_{Li^+}$ ) of the lithium complexes obtained from Mulliken population analysis are summarized in **Table 4.1.4**. Charge on carbonyl oxygen atom is in the range of  $-0.2864$  to  $-0.3594$  and  $-0.3490$  to  $-0.4675$  in free bases in gas and aqueous phase respectively. It is seen that dipole moment is increased in solvent indicating higher charge separation in solvent which is expected for polar compounds. Computed net charges on oxygen is higher in water which support the fact of higher charge separation. In lithium complexes net charge carried by the  $Li^+$  cation varies in the range of  $0.7544$  to  $0.7925$  and  $0.8479$  to  $0.8746$  in gas and aqueous phase respectively. Electron density from the  $C=O$  double bond shifted to the cation and makes the interaction between  $Li^+$  and the ligand stronger during complex formation. **Table 4.1.4** also reports the Ligand to Metal charge transfer values ( $Q_{CT}$ ) [calculated from MPA results] at the equilibrium ground state. The partial charges on carbonyl oxygen of the free bases and on the alkali metal ion and on carbonyl oxygen of the metal complexes obtained from natural population analysis (NPA) both in gas phase and in aqueous phase are summarised in **Table 4.1.5**. In all cases  $Q_{CT}$  and  $\Delta q_{CT}$  values from **Table 4.1.4** and **Table 4.1.5** clear that, a significant charge transfer from Ligand to Metal ion has taken place. However the values obtained from both Mulliken population analysis (MPA) and NPA do not correlate properly. This is happen due to the higher functional sensitivity of the Mulliken population analysis where NPA is not overly sensitive to the methods.<sup>38</sup> It may be expect that charge transfer

## Chapter 4

values obtained from MPA and NPA will have good correlation to the evaluated LCA data of the complexes, but this is not the case.  $Q_{CT}$  results gave the stability order as  $ACR > MA \geq EMA > HNE > MVK > ACL$  in gas phase while in aqueous phase it follows  $ACR > MA > EMA > MVK > ACL \geq HNE$  decreasing order. Then it may be stated that MPA results provide not perfect but a good correlation with the evaluated LCA values in aqueous phase, a little deviation is observed in gas phase. Results obtained from NPA shows, while not perfect, there is a reasonable correlation between  $\Delta q_{CT}$  and LCA results. Since lithium cation form the bond with its 1s filled orbital in the ligand- cation interaction is largely ionic, so this is an ion-dipole attraction and ion induced dipole interaction rather than a covalent interaction. Some geometrical parameters like bond distance, bond angle are listed in **Table 4.1.6** and **Table 4.1.7** for gaseous and aqueous phase. Since the lithium-ligand interaction is electrostatic, the bond length between ligand and cation should be a supporting parameter to realize the strength of interaction. The gas phase optimized geometry around the carbonyl moiety of the selected carbonyl derivatives are almost similar, it slightly differs with their O-Li<sup>+</sup> bond distance ( $d_2$ ). The shortest bond distance (O-Li<sup>+</sup>) found in ACR complex [1.712Å]. With respect to their  $d_2$  results,  $\alpha,\beta$ -unsaturated compounds are in following order  $ACR > MA > HNE > EMA \geq MVK > ACL$ , the difference of bond distance varies just within  $\pm 0.031\text{Å}$ . In aqueous phase  $d_2$  increases little bit for all derivatives and lies within the range 1.88Å to 1.947Å, it may be due to the electronic relaxation effect in presence of solvent. The aqueous phase LCA of the six carbonyl derivatives can not be explained properly with only  $d_2$  distance taking into account. Analysis of the  $d_1$  bond lengths in selected compound shows that the substituent (A and B) contribution to the distance ( $d_1$ ) is distinctly less, they are almost same in each case. The  $d_1$  length of the free bases is little increased in their respective lithium complexes, in gas phase it increased from 0.032Å to 0.049Å and 0.015Å to 0.032Å in aqueous phase. Geometry optimization in aqueous phase applying PCM-SCRF model is a



time taking process. Gas phase optimized geometries are used as in initial input in aqueous phase optimization process. Alkali metal cation always prefers to form monodentate complex in solvent.<sup>39</sup> Geometrical structures are not affected markedly on solvation. The bond angle  $\angle \text{C-O-Li}^+$  and dihedral angle  $\tau (\text{C-C-O-Li}^+)$  in metal complexes exist within the range  $146.198^\circ$  to  $174.992^\circ$  and  $0.000$  to  $180.00^\circ$  in gas phase, it is  $137.3178^\circ$  to  $168.873^\circ$  and  $0.000^\circ$  to  $179.262^\circ$  in aqueous phase. The almost invariant optimized geometrical parameters at or around carbonyl ring tend to suggest that substituent effect on LCA of the six unsaturated carbonyl derivatives is difficult to predict exactly without considering the different electronic properties originates from far away centre of the bases.

#### 4.4 Conclusion

We compared the lithium cation affinities and some associated quantum mechanical parameter of six conjugated  $\alpha,\beta$ -unsaturated carbonyl derivatives of type-2-alkene in gas phase as well as in aqueous phase with the support of DFT/B3LYP method at 6-311G (d,p) basis set level. The evaluated gas-phase complexation free energies of lithium cation with Lewis bases can be rationalized by considering different electronic properties of the free bases and of their lithium complexes. Solvation factor markedly effect on interaction enthalpies, the evaluated values are less negative in aqueous phase. LCA values of the carbonyl compounds are obtained from refined equilibrium between inductive and resonance effect. Hence it is difficult to predict the LCA of unsaturated carbonyl derivatives in gas as well as in aqueous phase, it is possible to interpret on variation of LCA by discussing inductive, resonance effect and others electronic properties originates from complexes.

**Table 4.1.1** Computed total optimization energies (hartree) of the free bases ( $B_1$ ) and their  $O-Li^+$  complexes ( $B_1Li^+$ ) in hartree unit obtained from DFT[B3LYP] 6-311G(d,p) method.

Molecule	Total energy(hartree)			
	Gas Phase		Aqueous Phase	
	$B_1$	$B_1Li^+$	$B_1$	$B_1Li^+$
Acrolien(ACL)	-191.9682	-199.3321	-191.9741	-199.4635
4-hydroxy-2-nonenal(HNE)	-503.1551	-510.5261	-503.1644	-510.6538
Methyl vinyl ketone (MVK)	-231.3020	-238.6687	-231.3080	-238.7976
Acrylamide (ACR)	-247.3658	-254.7450	-247.3766	-254.8705
Methyl acrylate (MA)	-306.5414	-313.9176	-306.5515	-314.0427
Ethyl metharylate (EMA)	-385.2139	-392.5811	-385.2191	-392.7104

**Table 4.1.2** Calculated Lithium cation affinities (LCA) of six conjugated  $\alpha,\beta$ -unsaturated carbonyl derivatives in equilibrium ground state both in gas phase and solvent phase. Calculated as  $\Delta H^{298.15K} = \{(E_{B_1Li^+} - (E_{B_1} + E_{Li^+}) + \Delta(pV))$  Here LCA values are expressed in term of  $[\Delta E_g]$  for gas phase and  $[\Delta E_{sol}]$  for solvents.  $E_{Li^+}$  (Gas) = -7.2849 hartree,  $E_{Li^+}$  (Aqueous) = -7.4787 hartree [1 hartree = 627.5095 kcal/mole].

Molecule	Gas phase		Aqueous phase		
	(LCA) $\Delta E_g$		(LCA) $\Delta E_{sol}$		decrease by
	hartree	Kcal/mole	In hartree	Kcal/mole	Kcal/mole
ACL	-0.078	-48.98	-0.00975	-6.1221	42.85
HNE	-0.085	-53.37	-0.0097	-6.1219	47.25
MVK	-0.0808	-50.73	-0.0099	-6.24	44.49
ACR	-0.0933	-58.57	-0.0142	-8.94	49.63
MA	-0.0903	-56.69	-0.0115	-7.25	49.44
EMA	-0.0813	-51.04	-0.0116	-7.31	43.73

**Table 4.1.3** Obtained enthalpy, free energy of six  $\alpha,\beta$ -unsaturated carbonyl derivatives and Lithium Cation Affinities (LCA, in kcal/mol), and Lithium Cation Basicities (LCB, in kcal/mol) and entropies ( $\Delta S$ ) in cal/ mole by B3LYP/DFT method at 6-311G(d,p) level in gas and aqueous phase. LCA calculated as:  $H_{Li^+} + H_{free\ base} - H_{Complex}$ .

$$LCB \text{ calculated as: } G_{Li^+} + G_{Free\ base} - G_{Complex}$$

At 298.15<sup>0</sup> K

	<b>H</b>	<b>G</b>	<b>LCA (<math>\Delta H_{Li^+}</math>)</b>	<b>LCB (<math>\Delta G_{Li^+}</math>)</b>	<b><math>\Delta S</math></b>
<b>Gas phase:</b>					
Li <sup>+</sup>	-7.2825	-7.2976			
ACL	-191.9027	-191.9334	- 47.87	- 41.35	- 21.86
ACL - Li <sup>+</sup>	-199.2615	-199.2969			
<b>In Aqueous</b>					
Li <sup>+</sup>	-7.4763	-7.4914			
ACL	-191.9077	-191.9393	- 6.02	0.753	- 22.71
ACL- Li <sup>+</sup>	-199.3936	-199.4295			
<b>Gas phase</b>					
HNE	-502.9046	-502.9601	-49.13	- 40.47	- 29.04
HNE- Li <sup>+</sup>	-510.2654	-510.3222			
<b>In Aqueous</b>					
HNE	-502.9142	-502.9699	-5.33	2.13	- 25.02
HNE- Li <sup>+</sup>	-510.3990	-510.4579			
<b>Gas phase:</b>					
MVK	-231.2063	-231.2420	-50.38	- 43.48	- 23.14
MVK- Li <sup>+</sup>	-238.5691	-238.6089			
<b>In Aqueous</b>					
MVK	-231.2123	-231.2481	- 6.14	1.5	- 25.62
MVK- Li <sup>+</sup>	-238.6984	-238.7371			
<b>Gas phase:</b>					
ACR	-247.2839	-247.3195	- 57.1	- 49.32	- 26.09
ACR-Li+	-254.6574	-254.6957			
<b>In Aqueous</b>					
ACR	-247.2946	-247.3295	-7.96	- 0.125	- 26.27
ACR- Li+	-254.7836	-254.8211			
<b>Gas phase</b>					
MA	-306.4391	-306.4775	- 56.22	- 48.94	- 24.41
MA- Li+	-313.8112	-313.8531			
<b>In Aqueous:</b>					
MA	-306.4492	-306.4878	- 7.84	0.502	- 27.97
MA- Li+	-313.9380	-313.9784			
<b>Gas phase</b>					
EMA	- 385.0356	-385.0812	- 56.72	- 49.32	- 24.81
EMA- Li+	-392.4085	-392.4574			
<b>In Aqueous:</b>					
EMA	- 385.0448	-385.0903	-7.27	- 0.943	-21.22
EMA- Li+	-392.5327	-392.5815			

**Table 4.1.4** Obtained Mulliken net charges on Lithium ion ( $q_{Li^+}$ ) in lithium complexes ( $B_1Li^+$ ) and Ligand to Metal Charge Transfer ( $Q_{CT}$ ) in the complexes in equilibrium ground state in both gas phase and in solvent phase.

Molecule	$(q_{o-})$			$(Q_{CT})$	$(q_{o-})$			$(Q_{CT})$
	Gas Phase				Aqueous Phase			
	$B_1$	$B_1Li^+$	$q_{Li^+}$		$B_1$	$B_1Li^+$	$q_{Li^+}$	
ACL	-0.2864	-0.4207	0.7925	0.2075	-0.4675	-0.3801	0.8742	0.1258
HNE	-0.2944	-0.4444	0.7724	0.2276	-0.3520	-0.3848	0.877	0.123
MVK	-0.3022	-0.4570	0.7765	0.2235	-0.3574	-0.3919	0.8746	0.1254
ACR	-0.3594	-0.5146	0.7544	0.2456	-0.4316	-0.4618	0.8479	0.1521
MA	-0.3525	-0.4810	0.7643	0.2357	-0.3778	-0.4312	0.8545	0.1455
EMA	-0.3071	-0.5035	0.7666	0.2334	-0.3701	-0.4202	0.8561	0.1439

**Table 4.1.5** B3LYP/6-311G(d,p) Computed Partial Charges (units e) on the carbonyl oxygen ( $Q_{O^-}$ ) of the free bases( $B_1$ ) and charge on alkali metal ion( $Q_{Li^+}$ ) and on carbonyl oxygen ( $Q_{O^-}$ ) of the O- $Li^+$  complexes( $B_1Li^+$ ) and the Ligand to Metal Charge Transfer( $\Delta q_{CT}$ ) in Complexes Obtained from NPA analysis in both gas and aqueous phases.

Molecule	Gas Phase				Aqueous Phase			
	$Q_{O^-}$		$Q_{Li^+}$	$(\Delta q_{CT})$	$Q_{O^-}$		$Q_{Li^+}$	$(\Delta q_{CT})$
	$B_1$	$B_1Li^+$			$B_1$	$B_1Li^+$		
ACL	-0.505	-0.764	0.9584	0.0416	-0.567	-0.655	0.9780	0.022
HNE	-0.533	-0.781	0.9330	0.067	-0.553	-0.675	0.9783	0.0217
MVK	-0.549	-0.800	0.9505	0.0495	-0.597	-0.694	0.9744	0.0256
ACR	-0.604	-0.856	0.9471	0.0529	-0.671	-0.773	0.9704	0.0296
MA	-0.567	-0.815	0.9506	0.0494	-0.626	-0.727	0.9709	0.0291
EMA	-0.558	-0.819	0.9509	0.0491	-0.618	-0.713	0.9695	0.0305

\*The ligand to metal charge transfer ( $\Delta q_{CT}$ ) = [(Formal +1 charge on the metal ion) – (charge on the metal in the complex)].

**Table 4.1.6** Geometrical features of the free base [ $B_1$ ] and O- $Li^+$  complexes [ $B_1Li^+$ ]. (length in Å and angle in degree) in gas phase.

Molecule	$B_1$	$B_1Li^+$			
	$r(C-O)(d1)$	$r(C-O)(d1)$	$r(O-Li^+)(d2)$	$\angle C-O-Li^+$	$\angle C-C-O-Li^+$
ACL	1.208	1.237	1.743	174.992	180.0
HNE	1.212	1.248	1.729	162.022	176.073
MVK	1.213	1.245	1.735	168.842	179.934
ACR	1.22	1.257	1.712	173.045	0.0000
MA	1.203	1.242	1.72	146.198	179.999
EMA	1.208	1.24	1.737	154.277	172.567

**Table 4.1.7** Geometrical features of the free bases [B<sub>1</sub>] and O-Li<sup>+</sup> complexes [B<sub>1</sub>Li<sup>+</sup>]. (Bond length in Å and angle in degree) in aqueous phase.

Molecule	B <sub>1</sub>	B <sub>1</sub> Li <sup>+</sup>			
	r(C-O)d <sub>1</sub>	r(C-O)d <sub>1</sub>	r(O-Li <sup>+</sup> )d <sub>2</sub>	<C-O-Li <sup>+</sup>	<C-C-O-Li <sup>+</sup>
ACL	1.221	1.225	1.942	137.3178	179.262
HNE	1.21	1.228	1.947	147.312	177.974
MVK	1.219	1.227	1.925	168.873	179.947
ACR	1.230	1.242	1.882	165.8335	0.00
MA	1.212	1.225	1.904	147.442	179.862
EMA	1.212	1.225	1.944	139.1882	170.777

\*\*<C-O-Li<sup>+</sup>: 3c-8o-9Li (ACL), 20c-21o-28Li (HNE), 5c-8o-12Li (MVK), 3c-7o-11Li (ACR), 5c-7o-13Li (MA), 5c-6o-19Li (EMA). \*τ(C-C-O-Li<sup>+</sup>): 2c-3c-8o-9Li (ACL), 19c-20c-21o-28Li (HNE), 2c-5c-8o-12Li (MVK), 2c-3c-7o-11Li (ACR), 2c-5c-7o-13Li (MA), 2c-5c-6o-19Li (EMA).

**Table 4.1.8** Obtained dipole moment (p) of the free bases in gas and aqueous phase.

Molecule	Dipole moment (p)		Molecule	Dipole moment (p)	
	Gas	Solvent		Gas	Solvent
ACL	3.15	4.04	ACR	3.88	5.14
HNE	2.12	2.83	MA	4.32	5.56
MVK	2.70	3.51	EMA	1.78	5.51

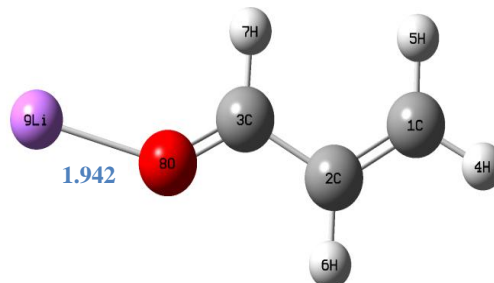
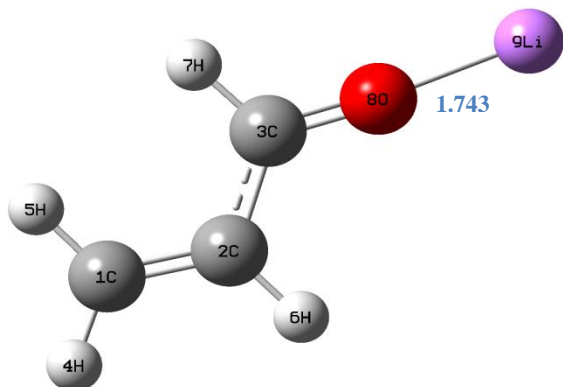
Chapter 4

$B_1Li^+$

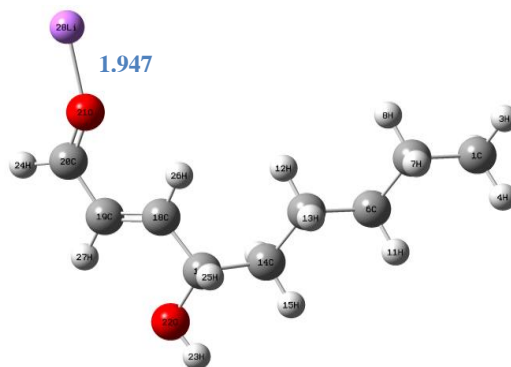
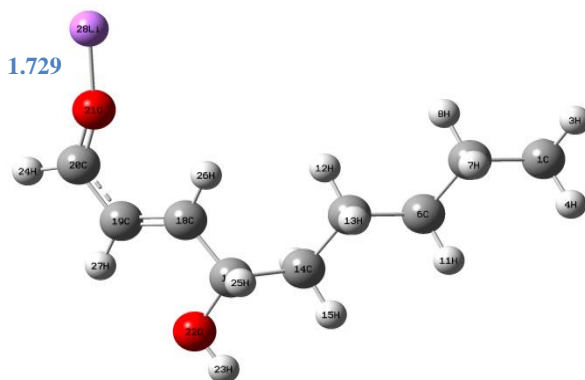
Gas phase

Aqueous phase

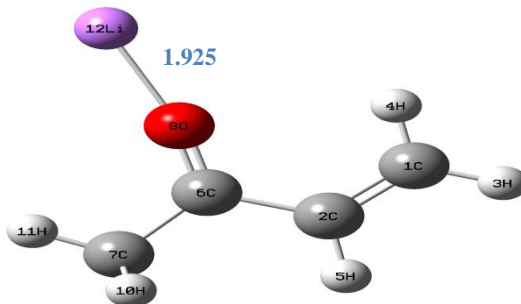
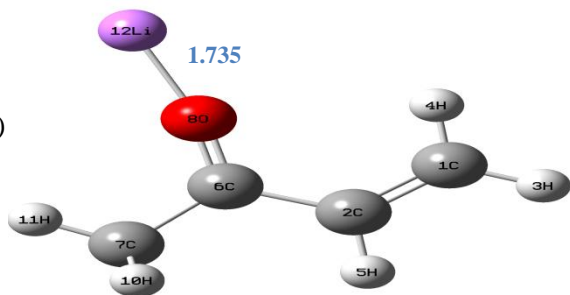
ACL ( $Li^+$ )



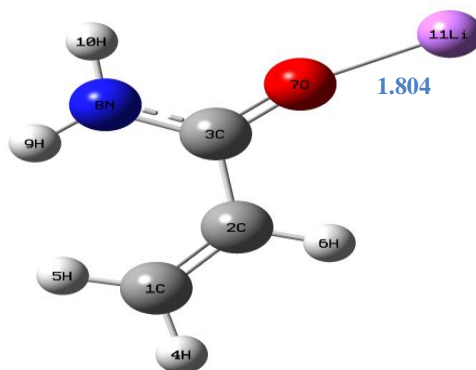
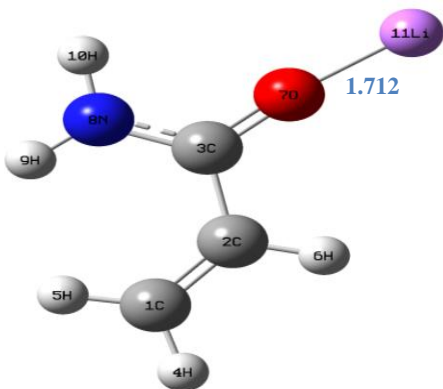
HNE ( $Li^+$ )



MVK ( $Li^+$ )



ACR ( $Li^+$ )



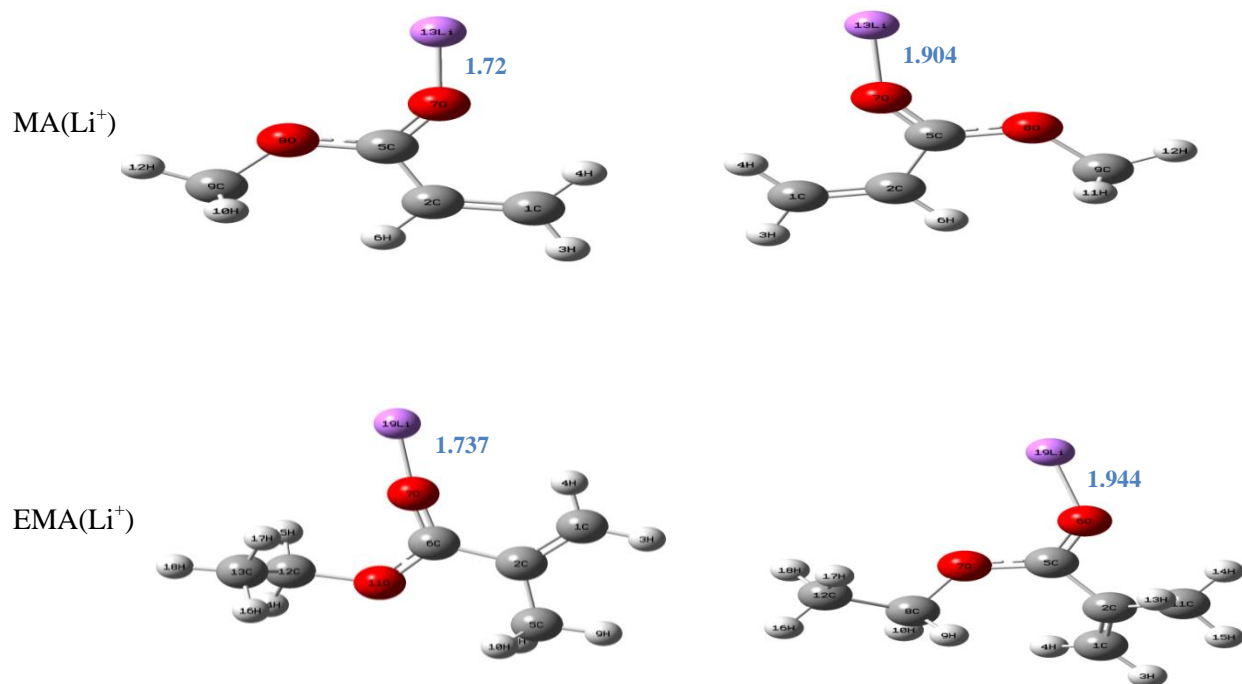


**Figure 4.2.3** Optimized geometrical structure of six  $\alpha,\beta$ -unsaturated carbonyl compounds in gas and aqueous phase. (Bond length in Å unit).

## 4.5 References

- (1) Poonia, N. S.; Bajaj, A. V. *Chem. Rev.* **1979**, *79*, 389.
- (2) Daniele, P.G.; Foti, C.; Gianguzza, A.; Prenesti, E.; Sammartano, S. *Coord. Chem. Rev.* **2008**, *252*, 1093.
- (3) Burk, P.; Sults, M-L.; Jaana, T. T. *Proc. Estonian Acad. Sci. Chem.* **2007**, *56*, 107.
- (4) Kaim, W.; Schwederski, B. *Bioinorganic Chemistry: Inorganic Elements in Chemistry of Life*, 1st ed., Wiley, Chichester, 1994.
- (5) Cowan, J. A. *Inorganic Biochemistry: An Introduction*, 2nd ed., Wiley, New York, 1997.
- (6) Allen, R. N.; Shukla, M. K.; Leszczynski, J. *Int. J. Quant. Chem.* **2006**, *106*, 2366.
- (7) Allen, R. N.; Shukla, M. K.; Burda, J. V.; Leszczynski, J. *J. Phys. Chem. A* **2006**, *110*, 6139.
- (8) Benzakour, M.; Cartier, A.; Mcharfi, M.; Daoudi, A. *J. Mol. Struct. (Theochem)* **2004**, *681*, 99.
- (9) Marino, T.; Russo, N.; Toscano, M. *J. Phys. Chem. B* **2003**, *107*, 2588.
- (10) Marino, T.; Russo, N.; Toscano, M. *Inorg. Chem.* **2001**, *40*, 6439.
- (11) Henderson, K. W.; Walther, D. S.; Williard, P. G. *J. Am. Chem. Soc.* **1995**, *117*, 8680.
- (12) (a) Woodin, R. L.; Houle, F. A.; Goddard, W. A., III. *Chem. Phys.* **1976**, *14*, 461. (b) Abboud, J.-L. M.; Yanez, M.; Elguero, J.; Liotard, D.; Essefar, M.; Mouhtadi, M. El.; Taft, R. W. *New J. Chem.* **1992**, *16*, 739. (c) Alcami, M.; Mo, O.; Yanez, M. *J. Phys. Chem.* **1989**, *93*, 3929. (d) Alcami, M.; Mo, O.; de Paz, J. L. G.; Yanez, *Theor. Chim. Acta* **1990**, *77*, 1. (e) Speers, P.; Laidig, K. E. *J. Chem. Soc., Perkin Trans.* **1994**, *2*, 799. (f) Alcami, M.; Mo, O.; Yanez, M.; Anvia, F.; Taft, R. W. *J. Phys. Chem.* **1990**, *94*, 4796. (g) Anvia, F.; Walsh, S.; Capon, M.; Koppel, I. A.; Taft, R. W.; de Paz, J. L. G.; Catalan, J. *J. Am. Chem. Soc.* **1990**, *112*, 5095. (h) Alcami, M.; Mo, O.; Yanez, M.



Modelling Intrinsic Basicities: The Use of the Electrostatic Potentials and Atoms-in-Molecules Theory. *In Molecular Electrostatic Potentials: Concepts and Applications*; Murray, J. S.; Sen, K., Eds.; Elsevier: Amsterdam, 1996.

- (13) Dzidic, I.; Kebarle, P. *J. Phys. Chem.* **1970**, *74*, 1466.
- (14) Sunner, J.; Kebarle, P. *J. Am. Chem. Soc.* **1984**, *106*, 6135.
- (15) Tissandier, M. D.; Cowen, K. A.; Feng, W. Y.; Gundlach, E.; Cohen, M. H.; Earhart, A. D.; Coe, J. V.; Tuttle, T. R., Jr. *J. Phys. Chem. A* **1998**, *102*, 7787.
- (16) Castleman, A. W.; Keesee, R. G. *Chem. Rev.* **1986**, *86*, 589.
- (17) Wieting, R. D.; Staley, R. H.; Beauchamp, J. L. *J. Am. Chem. Soc.* **1975**, *97*, 924.
- (18) Staley, R. H.; Beauchamp, J. L. *J. Am. Chem. Soc.* **1975**, *97*, 5920.
- (19) Woodin, R. L.; Beauchamp, J. L. *J. Am. Chem. Soc.* **1978**, *100*, 501.
- (20) Woodin, R. L.; Beauchamp, J. L. *Chem. Phys.* **1979**, *41*, 1.
- (21) Taft, R. W.; Anvia, F.; Gal, J.-F.; Walsh, S.; Capon, M.; Holmes, M. C.; Hosn, K.; Oloumi, G.; Vasanwala, R.; Yazdani, S. *Pure Appl. Chem.* **1990**, *62*, 17.
- (22) McLuckey, S. A.; Cameron, D.; Cook, R. G.; *J. Am. Chem. Soc.* **1981**, *103*, 1313.
- (23) Cook, R. G.; Patrick, J. S.; Kotiaho, T.; McLuckey, S. A. *Mass Spectrom. Rev.* **1994**, *13*, 287.
- (24) More, M. B.; Glendening, E. D.; Ray, D.; Feller, D.; Armentrout, P. B. *J. Phys. Chem.* **1996**, *100*, 1605.
- (25) Rodgers, M. T.; Armentrout, P. B. *J. Phys. Chem. A* **1997**, *101*, 1238.
- (26) Rodgers, M. T.; Armentrout, P. B. *J. Phys. Chem. A* **1997**, *101*, 2614.
- (27) Lin, C.-Y.; Dunbar, R. C. *Organometallics.* **1997**, *16*, 2691.
- (28) Pozniak, B. P.; Dunbar, R. C. *J. Am. Chem. Soc.* **1997**, *119*, 10439.
- (29) Senapati, U.; De, D.; De, B. R. *J. Mol. Struct. (Theochem)* **2007**, *808*, 157.
- (30) LoPachin, R. M.; Gavin, T. *Environ. Health Perspect.* **2012**, *120*, 12.

## Chapter 4

- (31) Lee, C.; Yang, W.; Parr, R. G. *Phys. Rev.* **1988**, *B37*, 785.
- (32) Hehre, W. J. *J. Chem. Phys.* **1969**, *51(6)*, 2657.
- (33) Frisch, M. J.; Trucks, G. W.; Schlegel, H. B.; Scuseria, G. E.; Robb, M. A.; Cheeseman, J. R.; Scalmani, G.; Barone, V.; Mennucci, B.; Petersson, G. A. et al. *Gaussian 09*, Revision A.02, Gaussian Inc., Wallingford, CT, 2009.
- (34) Tomasi, J.; Mennucci, B.; Cancès, E. *J. Mol. Struct. (Theochem)* **1999**, *464(1-3)*, 211.
- (35) Mulliken, R. S. *J. Chem. Phys.* **1955**, *23(10)*, 1833.
- (36) Boys, S. F.; Bernardi, F. *Mol. Phys.* **1970**, *19*, 553.
- (37) Del Bene, J. E.; Mettee, H. D.; Frisch, M. J.; Luke, B. T.; Pople, J. A. *J. Phys. Chem.* **1983**, *87*, 3279.
- (38) Varadwaj, P. R.; A. Varadwaj, A.; Marques, H. M. *J. Phys. Chem. A* **2011**, *115*, 5592.
- (39) Sille, J.; Gurraj, V.; Jezko, P.; Remko, M. *Acta Facultatis Pharmaceuticae Universitatis Comenianae*, Tomus LVII, 2010.

## **CHAPTER 5**

**Ground state sodium cation affinities (SCA) and associate parameters of a series of  $\alpha,\beta$ -unsaturated carbonyl compounds of type-2-alkene chemical class (ACL, HNE, MVK, ACR, MA and EMA ): A Comparative DFT based computational study in both gas and solvent phases.**



## Abstract

A detailed quantum mechanical study of ground state sodium cation ( $\text{Na}^+$ ) affinities (SCA) and some associate parameters of conjugated  $\alpha,\beta$ -unsaturated carbonyl compounds [acrolein(ACL), 4-hydroxy-2-nonenal (HNE), methyl vinyl ketone (MVK), Acrylamide (ACR), methyl acrylate (MA) and ethyl methacrylate (EMA)] has been computed in gas phase and in different solvents (water, DMSO,  $\text{CCl}_4$ ) phase using DFT [B3LYP] method employing 6-311G (d,p) basis set. Sodium complexes are stabilized by solvation in all cases. ACR exhibits the highest sodium cation affinity (SCA) in all medium. In gas phase, computed  $\text{Na}^+$  affinity of the compounds are in following order  $\text{ACR} > \text{MA} > \text{HNE} > \text{MVK} \geq \text{EMA} > \text{ACL}$  whereas upon solvation it shows different trend, follow  $\text{ACR} \geq \text{MA} > \text{EMA} \geq \text{MVK} > \text{ACL} \geq \text{HNE}$  order. Sodium cation basicity (SCB) has been calculated from Gibbs free energies obtained in frequency calculation at the same level of theory. Calculated SCA and SCB values in gas phase are higher in comparison to the solvent phases. Entropy of the complex formation reactions has been estimated. Atomic charges of the complexes have been calculated in two schemes MPA and NPA. The interactions sodium cation ( $\text{Na}^+$ ) with ligand is electrostatic ion-dipole interaction in all case. The local stereochemical disposition of the  $\text{Na}^+$  is found to be almost same in each case.

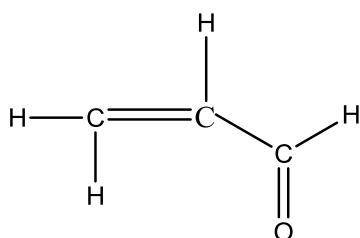
## 5.1 Introduction

The present work is part of a continuing effort from our laboratory to provide additional information in ion-molecular interaction in gas phase as well as in different solvent phases by means of sodium cation affinities (SCA), ligand-cation bond distance and charge on different atom including metal cation with other quantum mechanical parameters. The interaction of alkali metal cation (Lewis acid) with carbonyl compounds (Lewis base) extended the area of theoretical and computational research. It is known that a Lewis acid is an electron pair acceptor because of having one or more empty orbitals which make easier to complex formation by coordinating ligands. The reactivity of alkali metal cations towards ligand are quite simple compared to transition metal ion, it can form clusters or adducts which are ions 'solvated' by one or several ligands.<sup>1</sup> Due to easy production under vacuum, alkali metal ions became the first metal cations to studied in the gas phase. The bioinorganic chemistry of the alkali metal ions has been extensively reviewed.<sup>2</sup> Solid state crystal structures have been determined for many complexes of alkali metal ions in small peptides, nucleic acid constituents, carbohydrates and ionophore complexes.<sup>3</sup> Sodium occur in all known biological systems, generally functioning as electrolytes inside and outside cells.<sup>4</sup> Sodium is an essential nutrient that regulates blood volume, blood pressure, osmotic equilibrium and pH. The minimum physiological requirement for sodium is 500 milligrams per day.<sup>5</sup> Ion-molecule complexes helps to remove metal cation from contaminated area with their active involvement in molecular recognition processes.<sup>6</sup> Carbonyl compounds taken in this theoretical study are known as environmental pollutants and dietary contaminants. Exposure to these type-2 alkenes produce major toxicity in organ systems and to probable carcinogenicity in humans and laboratory animals.<sup>7-12</sup> Some experimental procedure like high pressure mass spectrometry HPMS,<sup>13-16</sup> ion cyclotron resonance (ICR)<sup>17-21</sup> or unimolecular dissociation–Cooke's kinetic method<sup>22-23</sup> has been employed for measuring most accurate alkali metal cation affinities. The ground state sodium cation affinity of a series of

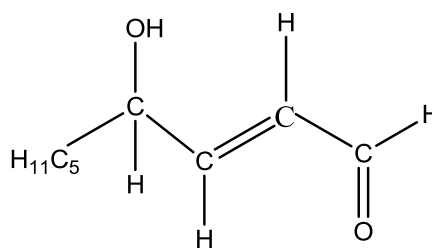
substituted acetophenones was reported earlier.<sup>24</sup> The Na<sup>+</sup> ion affinity of asparagine, glutamine, histidine and arginine were also studied theoretically.<sup>25</sup> Metal ion affinities and geometrical features of formohydroxamic acids derivatives have been investigated theoretically in gas and water phase.<sup>26</sup> On the basis of some previously evaluated<sup>27,28</sup> sodium ion affinities, it may be assessed that sodium will bind most preferentially with the acid function. Though several important functional groups have been studied, coverage might be not exhaustive and some key groups would be of considerable interest. To the best of our knowledge, no such computational studies were performed systematically for six selected carbonyl compounds to investigate comparative SCA values in different phases. In this chapter we have systematically analysed the structures, ground state sodium cation affinities, basicities and some other computed parameters of  $\alpha,\beta$ -unsaturated carbonyl derivatives  $RC(H) = C(A) - C(=O)B$  [A = -H, -CH<sub>3</sub>, B = -H, -NH<sub>2</sub>, -CH<sub>3</sub>, -OCH<sub>3</sub>, -OC<sub>2</sub>H<sub>5</sub>] both before and after complex formation in gas phase and in different solvents of low, medium and high dielectric constant ( $\epsilon$ ). The calculations have been carried out with the help of most reliable B3LYP[DFT] method using most accurate atom centred split valence with polarization function 6-311(d,p) basis set.<sup>29,30</sup> The compounds undertaken in the present study are acrolein(ACL), 4-hydroxy-2-nonenal (HNE), methyl vinyl ketone (MVK), Acrylamide (ACR), methyl acrylate (MA) and ethyl methacrylate (EMA). The gas phase SCA values are evaluated considering reaction between free base (B<sub>1</sub>) and metal cation (M<sup>n+</sup>) that is  $B_1 + M^{n+} \leftrightarrow [B_1 \cdots M^{n+}] \cdots$  (1). It was seen that sodium cation (Na<sup>+</sup>) interact with carbonyl oxygen ligand of the unsaturated carbonyl compounds and formed metal complexes in each case. Compounds have more than one donor atom (N and O in acryl amide) were optimized with free Na<sup>+</sup> (not directly bonded with carbonyl oxygen). We observed that, Na<sup>+</sup> cation prefers to bind with carbonyl oxygen (C=O) to form stable complexes. Before attempting the ion-molecular optimization in solvent phase, a detail idea of gas phase ion-molecular interaction energies, geometrical features are required.<sup>31</sup> We have observed the solvents effect on

## Chapter 5

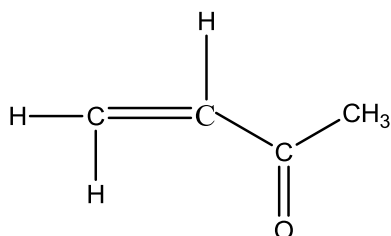
equilibrium geometry and atomic charge distribution of the complexes, because inclusion of solvents may change the geometrical and electronic parameters. The goal of our present study to supply a bunch of reliable quantum mechanical parameters including sodium cation affinities in gas phase and in three different solvents water ( $\epsilon = 78.39$ ), DMSO ( $\epsilon = 46.7$ ) and  $\text{CCl}_4$  ( $\epsilon = 2.228$ ). The data obtained from this theoretical analysis has been discussed comprehensively. It is expected that the model system chosen above will provide some initial insight into the binding of a univalent cation i.e.,  $\text{Na}^+$  to carbonyl oxygen of unsaturated compounds. Compounds studied in this theoretical calculation are listed below with their name and proper abbreviation.



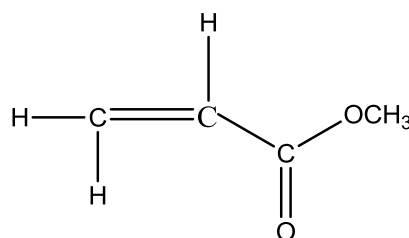
Acrolein (ACL)



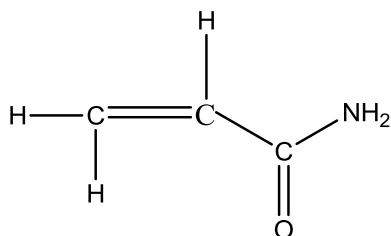
4-hydroxy-2-nonenal (HNE)



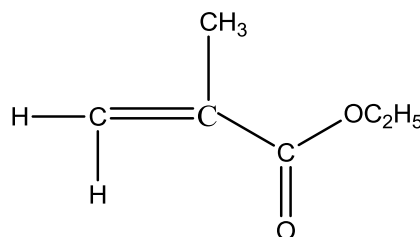
Methyl vinyl ketone (MVK)



Methyl acrylate (MA)



Acrylamide (ACR)



Ethyl methacrylate(EMA)

**Figure 5.2.1** Structure of several  $\alpha,\beta$ -unsaturated carbonyl compounds.



## 5.2 Computational details

The geometry of the six  $\alpha,\beta$ -unsaturated carbonyl compounds and their metal ion complexes in gas phase and different solvent phase has been completely optimized with hybrid B3LYP/DFT method using most accurate 6-311G(d,p) basis set of Gaussian'09' programme package.<sup>32</sup> In order to optimize these systems in solvents we used polarisation continuum model (PCM)<sup>33</sup> and water, DMSO and CCl<sub>4</sub> have been selected from given solvents list in the programme. Specifically three dielectric constants were utilised to create the solvents environment. Thermodynamics data of ion-molecule complexes (cation-Lewis base) obtained from B3LYP/DFT calculations at 6-311G(d,p) basis set level are very close to accuracy<sup>34</sup> and differed only by 10 KJoule/mole therefore DFT method can be used as an appropriate alternative to conventional *ab-initio* methods for investigating larger ion-molecular interactions. Mulliken population analysis<sup>35</sup> and NBO analysis (NPA only) are used to determine equivalent charges on all atoms of the free bases and their O-Na<sup>+</sup> complexes. Basis set superposition error (BSSE) were not made in this calculations. The magnitude of BSSE was evaluated at the B3LYP/ 6-311G (d,p) level for a small test set of molecules using counterpoise correction<sup>36</sup> and found to be small (0.5 Kcal/mol or less). Gibbs free energies (G) and enthalpies (H) were evaluated using unscaled frequencies calculation at the same level of basis set.

### 5.3 Results and discussion

A general geometrical structure of the studied  $\alpha,\beta$ -unsaturated carbonyl compounds and their O- $\text{Na}^+$  complexes are given bellow.

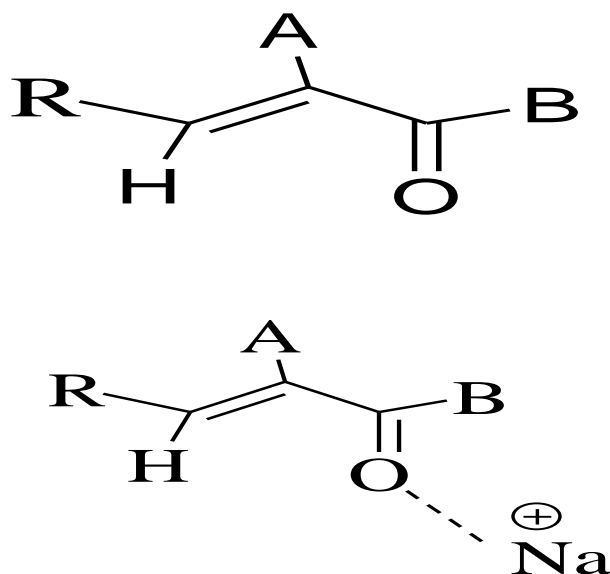


**Figure 5.2.2** General structures for conjugated  $\alpha,\beta$ -unsaturated carbonyl compounds of type-2-alkene chemical class. (R = -H or alkyl group, A = -H or - $\text{CH}_3$  and B = -H, - $\text{CH}_3$ , - $\text{OCH}_3$ , - $\text{NH}_2$ , - $\text{OC}_2\text{H}_5$ ).

The gas phase sodium cation affinities of the selected unsaturated carbonyl compounds has been evaluated as negative value of the enthalpy change ( $\Delta H^{298.15\text{K}}$ ) of the reaction  $\text{B}_1 + \text{Na}^+ \leftrightarrow \text{B}_1\text{Na}^+$ .---- (2) where SCA is defined as  $-\Delta H_{\text{Na}^+}$ . In the similar way sodium cation basicity (SCB) is defined as negative of the Gibbs free energy change associated with the above thermodynamic equation, where  $\text{SCB} = -\Delta G_{\text{Na}^+}$ . We also report the entropies ( $\Delta S^{298.15\text{K}}$ ) of the same reaction. The interaction enthalpy ( $\Delta H^{298.15\text{K}}$ ) for the metal ion-Lewis base complexes can also be obtained by following equation

$$\Delta H^{298.15\text{K}} = \{E^{298.15}(\text{B}_1\text{M}) - [E^{298.15}(\text{B}_1) + E^{298.15}(\text{M})]\} + \Delta(pV) \text{----- (3)}.$$

The compounds studied are listed in **Table 5.1.1** along with their respective abbreviated names and total energies of the free bases ( $\text{B}_1$ ) and their sodium complexes ( $\text{B}_1\text{Na}^+$ ) in gas

phase and in different solvents. **Table 5.1.2** reports the calculated sodium cation affinities (SCA) of the carbonyl compounds using equation (3). Where  $\Delta E_g$  are the gas phase SCA values and  $\Delta E_{(sol)}$  are the SCA in solvent phases. **Table 5.1.3** summarized the total enthalpies (H), Gibbs free energies (G), SCA and sodium cation basicity (SCB) results of the compounds. We observed that, SCA values of the compounds obtained in two different calculations do not differ significantly. It is very much expected for a thermodynamic equilibrium reaction. Difference of SCA values evaluated in two methods of calculation can be neglected considering minor computational errors. The calculated  $\Delta E_g$  values have a variation in the range of  $-34.67$  to  $-42.265$  kcal/mole in gas phase. In solvents,  $\Delta E_{1(sol)}$  varying in the range of  $-5.18$  to  $-7.43$  kcal/mole,  $-5.43$  to  $-7.68$  kcal/mole and  $-17.15$  to  $-22.24$  kcal/mole in water, DMSO and  $CCl_4$  respectively. Acrylamide (ACR) exhibits the highest affinity for sodium cation in both gas and in all solvent phases in comparison to other compounds in the series. Differences of SCA values of selected unsaturated carbonyl derivatives obtained due to the non-unique effect of conjugated double bond on binding oxygen. SCA values are also influenced by different substituent attached to carbonyl carbon and by the substituent at  $\alpha$ -carbon of the alkyl chain of the compound.

In Acrylamide,  $-NH_2$  group is present at carbonyl carbon. Lone pair electron of amide nitrogen helps to increase electron density on binding oxygen which enhance the ligand-cation interaction. Magnitudes of SCA's for all six compounds are found to be smaller in all solvents relative to the gas phase. Based on the  $\Delta E_{sol}$  values, SCA's are found to follow the order as  $ACR \geq MA > EMA \geq MVK > ACL \geq HNE$  in all solvents.

Sodium cation affinities of the compounds in solvent phase are in the order  $Water \leq DMSO < CCl_4$ .  $\Delta E_{1(sol)}$  values in DMSO observed little bit more ( $0.183$  kcal/mole to  $0.31$  kcal/mole) compared to water, while in carbon tetra chloride, it increased markedly. This trend indicates that, solvent polarity has marked influence on SCA values. In **Table 5.1.3**, total enthalpies

## Chapter 5

(H), Gibbs free energies (G) of the free bases and their O–Na<sup>+</sup> complexes and SCA as  $-\Delta H_{\text{Na}^+}$  and SCB as  $-\Delta G_{\text{Na}^+}$  are tabulated. [ $-\Delta H_{\text{Na}^+}$  has been calculated as difference between enthalpies of the product and reactants ( $\text{SCA} = H_{\text{Na}^+} + H_{\text{free base}} - H_{\text{complex}}$ ) and  $-\Delta G_{\text{Na}^+}$  has been calculated as difference between free energies of the product and reactants ( $\text{SCA} = G_{\text{Na}^+} + G_{\text{free base}} - G_{\text{complex}}$ )].

The SCA values reported in **Table 5.1.2** and **Table 5.1.3** are differ only by 0.03 to 2.35 kcal/mole in gas phase, while in solvents, this difference become distinctly less. The calculated SCA values of all unsaturated derivatives reported in **Table 5.1.2** and **Table 5.1.3** maintain same trend in both gas and different solvent phases. The computed Gibbs free energies ( $\Delta G_{\text{Na}^+}$ ) are negative and have a large energy difference from  $-27.79$  kcal/ mole to  $-34.32$  kcal/mole in gas phase. On solvation (water, DMSO), interaction Gibbs energies difference reduced a lot [(0.9412 to  $-0.3765$  kcal/mole in water and 0.5647 to  $-0.502$  kcal/mole in DMSO)] and positive value also obtain in some cases. In non-polar CCl<sub>4</sub> solvent,  $\Delta G_{\text{Na}^+}$  values has a variation in the range  $-9.78$  to  $-14.11$  kcal/mole clears the fact that SCB values are somehow influenced by solvent polarity.

We know, for molecular complexes, the associating tendency is described by Gibbs free energies. So it is important to know the significance of entropy in the process studied. Since a single cationic metal- ligand complex is formed from a couple of reactant, loss of entropy should be involved in the process which exactly happened in our study. From **Table 5.1.3** we observed that, entropy change due to complex formation of the studied carbonyl derivatives vary in the range of  $-20.42$  cal/ mole to  $-25.05$  cal/ mole in gas phase, it is  $-20.41$  to  $-22.92$  cal/ mole,  $-21.04$  to  $-23.13$  cal/mole and  $-20.40$  to  $-27.57$  cal/mole in aqueous, DMSO and CCl<sub>4</sub> respectively. Loss of entropy in the gas phase for six  $\alpha,\beta$ -unsaturated carbonyl complexes is differ by  $-4.63$  cal/mole only. This difference is reduced to  $-2.51$  cal/ mole in water,  $-2.09$  cal/mole in DMSO and  $-7.17$  cal/mole in CCl<sub>4</sub>.

We are unable to compare the energetic values obtained in this theoretical analysis due to the unavailability of exact experimental data of this class of compounds. However metal cation affinity, basicity values obtained from B3LYP level of theory provide good accuracy in comparison to experimental results.<sup>37, 38</sup>

Atomic charge on the atoms are non-unique, depend on the basis set used in the theoretical calculation<sup>39</sup> but till it used in theoretical calculations. **Table 5.1.4** reported the computed Mulliken net charge on the carbonyl oxygen atom of the free bases and the Na<sup>+</sup> complexes both in their equilibrium ground state in gas phase and in solvents. Mulliken net charge carried out by Na<sup>+</sup> cation of the metal complexes in different phases at the equilibrium ground state are tabulated in **Table 5.1.5**. Charge on oxygen atom of the free bases and of their metal complexes and charge on Na<sup>+</sup> cation in complexes are also evaluated by means of Natural Population Analysis (NPA). The calculated NPA results are listed in **Table 5.1.6**. The atomic charges obtained in Mulliken population analysis (MPA) by dividing orbital overlap equally by two shared atoms.

It is observed from **Table 5.1.4** and **Table 5.1.5**, the charge density on oxygen is higher in solvents relative to gas phase. Charge on Na<sup>+</sup> cation in sodium complexes vary in the range of 0.7544 to 0.7925 in gas phase, 0.8479 to 0.877 in water, 0.89 to 0.911 in DMSO and 0.8756 to 0.8933 in CCl<sub>4</sub>. The relative magnitudes of the charges on Na<sup>+</sup> cation indicate that, the bond formed by the sodium cation is largely ionic. Therefore the interactions between Na<sup>+</sup> cation and carbonyl oxygen of the Lewis base is predominantly an ion-dipole attraction and ion induced dipole interaction as well rather than a covalent interactions. Increases of dipole moment ( $\mu$  in Debye) in all solvents (**Table 5.1.8**) clearly indicate the higher charge separation in solution phase (as it is expected for polar molecules). The magnitudes of the charges also indicate that, both pre and post-complex correlations with local charge densities of the adjoining locality of the carbonyl oxygen sites are not strong. So sodium cation

## Chapter 5

affinities of the corresponding unsaturated carbonyl compounds (Lewis bases) cannot be explained properly considering the binding site properties only.

A significant ligand to metal charge transfer values ( $\Delta q_{CT}$ ) calculated from natural population analysis in both gas and different solvent phase are summarized in **Table 5.1.6a**. The extent of charge transfer ( $\Delta q_{CT}$ ) might have expected parallel to the alkali metal binding affinities of the compounds but this is not occurred. The NPA results gave uncooperatively MA  $\geq$  ACR  $>$  EMA  $>$  MVK  $>$  HNE  $>$  ACL in gas, MA  $>$  MVK  $>$  ACR = EMA  $>$  ACL  $>$  HNE in water, MA  $>$  ACR  $>$  MVK  $>$  EMA  $>$  HNE  $\geq$  ACL in DMSO and MA = EMA  $\geq$  MVK  $\geq$  ACR  $>$  HNE  $>$  ACL in CCl<sub>4</sub>. No direct correlation between SCA and ( $\Delta q_{CT}$ ) has been observed. It was seen from a previous study of dichalcogen-bridged complexes with divalent metal cation (Mn<sup>+2</sup>, Fe<sup>+2</sup>, Co<sup>+2</sup>, Ni<sup>+2</sup>, Cu<sup>+2</sup>, Zn<sup>+2</sup>) by Jeanvoine and Spezia<sup>40</sup> using B3LYP and MP2 method that, there was also no direct good correlation between ( $\Delta q_{CT}$ ) and binding affinities.

We observed the calculated NPA atomic charge on carbonyl oxygen and sodium cation in complexes is higher compared to MPA charges. Magnitudes of  $\Delta q_{CT}$  are smaller than  $Q_{CT}$  (**Table 5.1.5** and **Table 5.1.6a**). Although the relative order of charge transfer in MPA and NPA follows a parallel trend. Both  $\Delta q_{CT}$  and  $Q_{CT}$  values have been predicted to be highest in ACR in gas phase and it is found minimum for ACL which satisfy their obtained SCA results.

Optimized geometry of free base and complexes are shown in **Figure 5.2.3**. Important geometrical parameters like bond angle (in degree), bond distance (Å) and dihedral or torsion angle (in degree) of the optimized structures are summarized systematically in **Table 5.1.7**. The local stereochemical properties around the carbonyl moiety are found to be almost identical in each compound. The C = O bond length of the free bases elongated by 0.023 Å to 0.029 Å in complexes in the gas phase whereas in solvents atmosphere it is remain almost same (increased slightly by 0.001 to 0.015 Å).

In solvents, distance between carbonyl carbon and donor oxygen of the free bases and their  $\text{Na}^+$  complexes has a variation in the range 1.20 to 1.23 Å and 1.22 to 1.24 Å respectively. Analysis of the C = O bond length in each compounds are tend to suggest that, substituent's effect on bond length is marginal. Since the sodium-ligand interaction is electrostatic, the bond length between ligand and cation should be a supporting parameter to realize the strength of interaction. From **Table 5.1.7** it is seen that, O– $\text{Na}^+$  distance remains within the range from 2.092 to 2.22 Å in the gas phase. The O– $\text{Na}^+$  bond length is found to be shortest in ACR in gas phase as well as in all solvents. Thus it can be predicted partially that, ligand-cation interaction is stronger in ACR compared to other compounds.

Employing PCM type solvents model leads to increase of O– $\text{Na}^+$  bond distance of the given class of compounds. Ligand-cation bond lengths are elongated by 0.09 to 0.189 Å, 0.09 to 0.176 Å and 0.058 to 0.083 Å in aqueous, DMSO and  $\text{CCl}_4$  with an exception of MA complex in carbon tetra chloride where it is reduced by 0.02 Å. We also observed that O– $\text{Na}^+$  bond distances are reduced by 0.08 to 0.11 Å in  $\text{CCl}_4$  compared to other two solvents. This may be occurred in non-polar solvent where solvent particles compress the electron density between the nuclei of two bonding atom responsible for decreased bond length. The equilibrium geometrical optimized structures of the unsaturated carbonyl compounds obtained with DFT/B3LYP/6-311G(d,p) calculation in gas phase and in different solvents do not changed significantly. Concerning torsion angles [ $\tau$  (adjacent to carbonyl C–carbonyl C–carbonyl O –  $\text{Na}^+$  cation)] for all metal complexes, it should be noticed that except the sodium complex of ACR and EMA, all complexes have planar structure in all gas and solvent phases. ACR has non-planar structure in all medium (dihedral angles are  $13.5^\circ$ ,  $-4.18^\circ$ ,  $-5.82^\circ$  and  $3.24^\circ$ ). EMA has planar geometry in  $\text{CCl}_4$  ( $\tau = -178.86^\circ$ ) but in gas, water and DMSO, non planar structures have been obtained.

## Chapter 5

In ACL torsion angle ( $\tau$ ) is  $180^\circ$  in all medium, in HNE it is  $-175^\circ$  to  $172^\circ$ , in MVK,  $\tau = 179$  to  $180^\circ$  and which estimated  $-179^\circ$  in MA . The almost invariant stereochemistry around the complex formation site of bases forced to suggest that the entire contribution from different substituent effects to SCA cannot be described comprehensively without considering the contribution from far away centres.

We have analysed hardness ( $\eta$ ) as a single global parameter for all compounds in the equilibrium ground state in gas phase as well as in solvents. Hardness ( $\eta$ ) =  $[\epsilon_{\text{LUMO}} - \epsilon_{\text{HOMO}}]/2$  parameters are listed in **Table 5.1.8**.

Calculated  $\eta$  values clearly reflects that, EMA is more hard ( $\eta = 0.1137$  to  $0.1172$  hartree) in all medium while HNE exhibit lowest  $\eta$  values ( $0.0943$  to  $0.0964$  hartree) in gas and also in solvents. Compounds are stabilized in all solvents. The solvation energy ( $\Delta E_s$ ) of all studied  $\alpha,\beta$ -unsaturated compounds listed in **Table 5.1.9**. Solvation energy of the compounds follows the order water > DMSO > CCl<sub>4</sub> which fulfil the chemical expectation raised from the dielectric constant of the solvents.



## 5.4 Conclusion

The theoretical calculation of six  $\alpha,\beta$ -unsaturated carbonyl compounds using DFT [B3LYP] method at hybrid triple zeta 6-311G(d,p) basis set level provides a set of important data like SCA, SCB, entropy of the reactions process in gas phase as well as in different solvents. The applications of PCM-SCRF model in the study not influence markedly on geometrical structures of the compounds but it change a lot of chemical properties. The calculations indicate that  $\text{Na}^+$  cation prefer to bind with carbonyl oxygen of the studied bases. Sodium cation affinity is predicted to be highest in ACR in all medium of reactions. The interaction enthalpies, Gibbs free energies of the complexation reactions reduced in solvents in each case.

The SCA of the unsaturated compounds obtained from a delicate balance between inductive and resonance effect of different substituent or group present at the carbonyl carbon or any other position in the compound. Finally, from the different electronic properties of the complexes, we can conclude that the interactions are predominantly an ion-dipole attraction and ion-induced dipole interaction as well rather than covalent interaction.

**Table 5.1.1** Computed total energies (hartree) of the carbonyl derivatives and their sodium complexes ( $B_1Na^+$ ) for both gas phase and in different solvent phase at the equilibrium geometry of the ground state.

Molecule	Total energy (hartree)							
	Gas Phase		Aqueous Phase		DMSO		CCl <sub>4</sub>	
	B <sub>1</sub>	B <sub>1</sub> Na <sup>+</sup>	B <sub>1</sub>	B <sub>1</sub> Na <sup>+</sup>	B <sub>1</sub>	B <sub>1</sub> Na <sup>+</sup>	B <sub>1</sub>	B <sub>1</sub> Na <sup>+</sup>
ACL	-191.96	-354.11	-191.97	-354.23	-191.94	-354.22	-191.97	-354.17
HNE	-503.15	-665.30	-503.16	-665.42	-503.16	-665.41	-503.15	-665.36
MVK	-231.30	-393.44	-231.30	-393.56	-231.30	-393.56	-231.30	-393.51
ACR	-247.36	-409.52	-247.37	-409.63	-247.37	-409.63	-247.37	-409.58
MA	-306.54	-468.69	-306.55	-468.80	-306.55	-468.80	-306.54	-468.75
EMA	-385.21	-547.35	-385.21	-547.47	-385.21	-547.47	-385.20	-547.41

**Table 5.1.2** Calculated Sodium cation affinities (SCA) of six conjugated  $\alpha,\beta$ -unsaturated carbonyl derivatives in equilibrium ground state both in gas phase and solvents. SCA Calculated as  $\Delta H^{298.15K} = \{E^{298.15}(B_1M) - [E^{298.15}(B_1) + E^{298.15}(M)]\} + \Delta(pV)$ . Here SCA values are expressed in term of  $[\Delta E_g]$  for gas phase and  $[\Delta E_{sol}]$  for solvents.

$[E_{Na^+}(\text{Gas}) = -162.0874 \text{ hartree}, E_{Na^+}(\text{Aqueous}) = -162.2468 \text{ hartree}, E_{Na^+}(\text{DMSO}) = -162.2454 \text{ hartree}, E_{Na^+}(\text{CCl}_4) = -162.1764 \text{ hartree}]$ .

Molecule	Gas phase [ $\Delta E_g$ ], Kcal/mole	Solvent phase [ $\Delta E_{sol}$ ], Kcal/mole		
		water	DMSO	CCl <sub>4</sub>
ACL	-34.67	-5.367	-5.55	-17.15
HNE	-37.62	-5.18	-5.43	-17.91
MVK	-35.61	-5.43	-5.682	-17.60
ACR	-42.265	-7.43	-7.68	-22.24
MA	-41.70	-6.43	-6.74	-21.18
EMA	-35.42	-5.55	-5.80	-21.05

**Table 5.1.3** Obtained enthalpy, free energy of six  $\alpha,\beta$ -unsaturated carbonyl derivatives and Sodium Cation Affinities (SCA, in kcal/mole), Sodium Cation Basicities (SCB, in kcal/mole) and entropies ( $\Delta S$ ) in cal/mole by B3LYP/DFT method at 6-311G(d,p) level in gas and different solvents. SCA calculated as:  $H_{Na^+} + H_{free\ base} - H_{Complex}$ .

$$SCB \text{ calculated as: } G_{Na^+} + G_{Free\ base} - G_{Complex}$$

At 298.15<sup>0</sup> K

	<b>H</b>	<b>G</b>	<b>SCA</b> ( $\Delta H_{Na^+}$ )	<b>SCB</b> ( $\Delta G_{Na^+}$ )	<b><math>\Delta S</math></b>
<b>Gas phase:</b>					
Na <sup>+</sup>	-162.0851	-162.1018			
ACL	-191.9027	-191.9334	-33.88	-27.79	-20.42
ACL-Na <sup>+</sup>	-354.0418	-354.0795			
<b>Aqueous phase:</b>					
Na <sup>+</sup>	-162.2445	-162.2613			
ACL	-191.9077	-191.9393	- 5.39	1.25	-22.27
ACL-Na <sup>+</sup>	-354.1608	-354.1986			
<b>In DMSO:</b>					
Na <sup>+</sup>	-162.2431	-162.2599	-5.58	1.00	-22.08
ACL	-191.9076	-191.9392			
ACL-Na <sup>+</sup>	-354.1596	-354.1975			
<b>In CCl<sub>4</sub></b>					
Na <sup>+</sup>	-162.1741	-162.1908			
ACL	-191.9044	-191.9359	-17.005	-9.78	-24.24
ACL-Na <sup>+</sup>	-354.1056	-354.1423			
<b>Gas phase</b>					
HNE	-502.9046	-502.9601	-37.65	-31.31	-21.26
HNE-Na <sup>+</sup>	-665.0497	-665.1118			
<b>In Aqueous phase</b>					
HNE	-502.9142	-502.9699	-5.33	0.941	-21.033
HNE-Na <sup>+</sup>	-665.1672	-665.2297			
<b>In DMSO:</b>					
HNE	-502.9140	-502.9697	-5.64	0.7531	-21.44
HNE-Na <sup>+</sup>	-665.1661	-665.2284			
<b>In CCl<sub>4</sub></b>					
HNE	- 502.9086	-502.9641	-18.07	-11.10	-23.37
HNE-Na <sup>+</sup>	- 665.1115	-665.1726			
<b>Gas phase:</b>					
MVK	-231.2063	-231.2420	-35.51	- 29.053	-21.65
MVK-Na <sup>+</sup>	-393.3480	-393.3901			
<b>In Aqueous phase:</b>					
MVK	-231.2123	-231.2481	-5.584	1.06	-22.28
MVK-Na <sup>+</sup>	-393.4657	-393.5077			

Continued to next page

## Chapter 5

At 298.15<sup>0</sup> K

	H	G	SCA ( $\Delta H_{Na^+}$ )	SCB ( $\Delta G_{Na^+}$ )	$\Delta S$
<b>In DMSO:</b>					
MVK	-231.2122	-231.2480	-5.773	0.815	-22.09
MVK-Na <sup>+</sup>	-393.4645	-393.5066			
<b>In CCl<sub>4</sub></b>					
MVK	-231.2089	-231.2446	-17.63	-11.546	-20.40
MVK-Na <sup>+</sup>	-393.4111	-393.4538			
<b>Gas phase:</b>					
ACR	-247.2839	-247.3195	-40.72	-33.25	-25.05
ACR-Na <sup>+</sup>	-409.4339	-409.4743			
<b>In Aqueous phase</b>					
ACR	-247.2946	-247.3295	-6.96	-0.125	-22.92
ACR-Na <sup>+</sup>	-409.5502	-409.5910			
<b>In DMSO</b>					
ACR	-247.2945	-247.3294	-7.21	-0.313	-23.13
ACR-Na <sup>+</sup>	-409.5491	-409.5898			
<b>In CCl<sub>4</sub></b>					
ACR	-247.2885	-247.3238	-21.14	-14.11	-23.57
ACR-Na <sup>+</sup>	-409.4963	-409.5371			
<b>Gas phase</b>					
MA	-306.4391	-306.4775	-41.603	-34.324	-24.41
MA-Na <sup>+</sup>	-468.5905	-468.6340			
<b>In Aqueous phase:</b>					
MA	-306.4492	-306.4878	-6.463	-0.3765	-20.41
MA-Na <sup>+</sup>	-468.7040	-468.7497			
<b>In DMSO</b>					
MA	-306.4490	-306.4876	-6.777	-0.502	-21.04
MA-Na <sup>+</sup>	-468.7029	-468.7483			
<b>In CCl<sub>4</sub></b>					
MA	-306.4434	-306.4819	-21.021	-14.056	-23.36
MA-Na <sup>+</sup>	-468.6510	-468.6951			
<b>Gas phase</b>					
EMA	-385.0356	-385.0812	-37.776	-30.81	-23.36
EMA-Na <sup>+</sup>	-547.1809	-547.2321			
<b>In Aqueous phase</b>					
EMA	-385.0448	-385.0903	-5.647	0.753	-21.46
EMA-Na <sup>+</sup>	-547.2983	-547.3504			
<b>In DMSO</b>					
EMA	-385.0447	-385.0902	-5.898	0.5647	-21.67
EMA-Na <sup>+</sup>	-547.2972	-547.3492			
<b>In CCL<sub>4</sub></b>					
EMA	-385.0394	-385.0849	-20.833	-12.612	-27.57
EMA-Na <sup>+</sup>	-547.2467	-547.2958			

**Table 5.1.4** Calculated Mulliken net charge on oxygen atom ( $q_{O^-}$ ) in unit 'e' in free bases and in sodium complexes in equilibrium ground state both in gas phase and in different solvent phases.

Molecule	$(q_{O^-})$ Gas phase		$(q_{O^-})$ Solvent phase					
	Free base	Sodium complex	Water		DMSO		CCl <sub>4</sub>	
			Free base	Sodium complex	Free base	Sodium complex	Free base	Sodium complex
ACL	-0.2864	-0.4283	-0.4675	-0.3728	-0.4668	-0.3732	-0.4352	-0.3972
HNE	-0.2944	-0.4514	-0.3520	-0.3796	-0.3483	-0.3804	-0.3185	-0.4148
MVK	-0.3022	-0.4608	-0.3574	-0.3935	-0.3567	-0.3944	-0.3260	-0.4277
ACR	-0.3594	-0.5181	-0.4316	-0.4607	-0.4307	-0.4612	-0.3904	-0.4903
MA	-0.3525	-0.4173	-0.3778	-0.4249	-0.3770	-0.4253	-0.3424	-0.4503
EMA	-0.3071	-0.5099	-0.3701	-0.3974	-0.3691	-0.3981	-0.3339	-0.4373

**Table 5.1.5** Mulliken net charges (unit 'e') on sodium ion ( $q_{Na^+}$ ) in sodium complexes ( $B_1Na^+$ ) and Ligand to Metal Charge Transfer ( $Q_{CT}$ ) in the complexes in equilibrium ground state in both gas phase and in different solvent phase.

Molecule	$(q_{Na^+})$ Gas phase		$(q_{Na^+})$ Solvent phase					
	$B_1Na^+$	$Q_{CT}$	Water		DMSO		CCl <sub>4</sub>	
			$B_1Na^+$	$Q_{CT}$	$B_1Na^+$	$Q_{CT}$	$B_1Na^+$	$Q_{CT}$
ACL	0.7925	0.2075	0.8742	0.1258	0.9110	0.089	0.8933	0.1067
HNE	0.7724	0.2286	0.877	0.123	0.9116	0.088	0.8883	0.1117
MVK	0.7765	0.2235	0.8746	0.1246	0.909	0.091	0.8901	0.1099
ACR	0.7544	0.2456	0.8479	0.1521	0.896	0.104	0.8769	0.1231
MA	0.7643	0.2357	0.8545	0.1455	0.890	0.11	0.8764	0.1236
EMA	0.7666	0.2334	0.8561	0.1439	0.903	0.097	0.8756	0.1244

**Table 5.1.6** Computed Partial atomic Charges (units 'e') on the carbonyl oxygen ( $q_{O^-}$ ) of the free bases ( $B_1$ ) and charge on alkali metal ion ( $q_{Na^+}$ ) and on carbonyl oxygen ( $q_{O^-}$ ) of the  $O-Na^+$  complexes ( $B_1Na^+$ ) obtained from NPA analysis in both gaseous and different solvents.

Molecule	$(q_{O^-})$ Gas		$q_{Na^+}$	$(q_{O^-})$ Water		$q_{Na^+}$	$(q_{O^-})$ DMSO		$q_{Na^+}$	$(q_{O^-})$ CCl <sub>4</sub>		$q_{Na^+}$
	$B_1$	$B_1Na^+$	$B_1Na^+$	$B_1$	$B_1Na^+$	$B_1Na^+$	$B_1$	$B_1Na^+$	$B_1Na^+$	$B_1$	$B_1Na^+$	$B_1Na^+$
ACL	-0.505	-0.716	0.977	-0.567	-0.624	0.983	-0.566	-0.625	0.982	-0.538	-0.669	0.980
HNE	-0.521	-0.723	0.975	-0.553	-0.650	0.984	-0.554	-0.651	0.983	-0.535	-0.698	0.979
MVK	-0.549	-0.751	0.970	-0.597	-0.660	0.978	-0.597	-0.661	0.978	-0.570	-0.710	0.974
ACR	-0.604	-0.812	0.954	-0.671	-0.744	0.979	-0.683	-0.745	0.977	-0.649	-0.780	0.975
MA	-0.567	-0.679	0.953	-0.626	-0.686	0.974	-0.625	-0.687	0.974	-0.592	-0.729	0.973
EMA	-0.558	-0.759	0.964	-0.618	-0.689	0.979	-0.617	-0.690	0.979	-0.583	-0.727	0.973

**Table 5.1.6a** Charge Transfer ( $\Delta q_{CT}$ ) (unit e) in different phase. Calculated from the data of ( $q_{Na^+}$ ) listed in **Table 5.1.6** [The Ligand to Metal charge transfer ( $\Delta q_{CT}$ ) = [(Formal +1 charge on the metal ion) – (charge on the metal in the complex)] obtained in NPA.

Molecule	Gas	Water	DMSO	CCl <sub>4</sub>
	$\Delta q_{CT}$	$\Delta q_{CT}$	$\Delta q_{CT}$	$\Delta q_{CT}$
ACL	0.023	0.017	0.018	0.020
HNE	0.025	0.016	0.017	0.021
MVK	0.030	0.022	0.022	0.026
ACR	0.046	0.021	0.023	0.025
MA	0.047	0.026	0.026	0.027
EMA	0.036	0.021	0.021	0.027

**Table 5.1.7** Some selected geometrical features of six  $\alpha,\beta$ -unsaturated carbonyl derivatives and their sodium complexes at ground state equilibrium geometry. [Bond distance (carbonyl carbon-binding oxygen [ $r(\text{C-O})$ ] and binding oxygen- sodium cation  $r(\text{O-Na}^+)$  in Å,  $\angle$ carbonyl carbon-carbonyl oxygen-sodium ion ( $\angle\text{C-O-Na}^+$ ) and  $\tau(\text{C-C-O-Na}^+)$  angles in  $^\circ$ ].

Molecule	Gas phase		Solvent phase					
	$r(\text{C-O})$		water		DMSO		$\text{CCl}_4$	
	$B_1$	$B_1\text{Na}^+$	$B_1$	$B_1\text{Na}^+$	$B_1$	$B_1\text{Na}^+$	$B_1$	$B_1\text{Na}^+$
ACL	1.208	1.231	1.221	1.222	1.221	1.227	1.218	1.226
HNE	1.212	1.239	1.21	1.225	1.217	1.225	1.214	1.232
MVK	1.213	1.238	1.219	1.226	1.219	1.226	1.215	1.231
ACR	1.22	1.248	1.230	1.237	1.23	1.23	1.224	1.242
MA	1.203	1.229	1.212	1.22	1.212	1.221	1.206	1.226
EMA	1.208	1.237	1.212	1.22	1.211	1.22	1.20	1.227
		$r(\text{O-Na}^+)$	--	$r(\text{O-Na}^+)$	--	$r(\text{O-Na}^+)$	--	$r(\text{O-Na}^+)$
ACL	--	2.124	--	2.313	--	2.30	--	2.20
HNE	--	2.117	--	2.29	--	2.29	--	2.20
MVK	--	2.119	--	2.297	--	2.293	--	2.18
ACR	--	2.092	--	2.238	--	2.23	--	2.15
MA	--	2.22	--	2.31	--	2.31	--	2.20
EMA	--	2.107	--	2.27	--	2.27	--	2.19

Molecule	Gas phase		Solvent phase					
	$\angle\text{C-O-Na}^+$		Water		DMSO		$\text{CCl}_4$	
	$\angle\text{C-O-Na}^+$	$\tau(\text{C-C-O-Na}^+)$	$\angle\text{C-O-Na}^+$	$\tau(\text{C-C-O-Na}^+)$	$\angle\text{C-O-Na}^+$	$\tau(\text{C-C-O-Na}^+)$	$\angle\text{C-O-Na}^+$	$\tau(\text{C-C-O-Na}^+)$
ACL	174.228	180.00	134.082	180.00	134.946	180.00	151.525	180.00
HNE	159.216	-175.537	143.12	-175.537	143.146	-175.51	147.534	172.547
MVK	167.869	180.034	141.356	179.934	141.697	-179.96	162.248	179.939
ACR	170.425	13.5137	162.338	-4.189	163.175	-5.823	171.834	3.248
MA	103.925	-179.966	126.752	-179.995	126.639	-179.986	145.398	-179.966
EMA	164.829	13.001	164.829	13.0016	165.544	-13.235	149.544	-178.869

\*\* $\angle\text{C-O-Na}^+$ : 3C-8O-9Na<sup>+</sup> (ACL), 20C-21O-28Na<sup>+</sup> (HNE), 5C-8O-12Na<sup>+</sup> (MVK), 3C-7O-11Na<sup>+</sup> (ACR), 5C-7O-13Na<sup>+</sup>(MA), 5C-6O-19Na<sup>+</sup> (EMA).

\* $\tau(\text{C-C-O-Na}^+)$ : 2C-3C-8O-9Na<sup>+</sup> (ACL), 19C-20C-21O-28Na<sup>+</sup> (HNE), 2C-5C-8O-12Na<sup>+</sup> (MVK), 2C-3C-7O-11Na<sup>+</sup> (ACR), 2C-5C-7O-13Na<sup>+</sup> (MA), 2C-5C-6O-19Na<sup>+</sup> (EMA).

**Table 5.1.8** Selected computed parameters of six conjugated  $\alpha,\beta$ -unsaturated carbonyl derivatives in gas phase as well as in various solvent phase.

Molecule	Hardness ( $\eta = [(\epsilon_{\text{LUMO}} - \epsilon_{\text{HOMO}})/2]$ hartree)				Dipole moment(Debye)			
	Gas phase	Solvent phase			Gas phase	Solvent phase		
		Water	DMSO	CCl <sub>4</sub>		Water	DMSO	CCl <sub>4</sub>
ACL	0.0957	0.0982	0.0981	0.0968	3.15	4.04	4.032	3.54
HNE	0.0943	0.0964	0.0963	0.0952	2.12	2.83	2.82	2.40
MVK	0.0963	0.0983	0.0983	0.0971	2.70	3.51	3.49	3.03
ACR	0.1058	0.1099	0.1098	0.1076	3.88	5.14	5.12	4.40
MA	0.1083	0.1127	0.1127	0.1102	4.32	5.56	5.54	4.84
EMA	0.1137	0.1172	0.1172	0.1167	1.78	5.51	5.48	4.64

**Table 5.1.9** Calculated solvation energies (hartree) of the six  $\alpha,\beta$ -unsaturated carbonyl compounds by DFT/B3LYP method at 6-311 G(d,p) basis set level. Solvation energy ( $\Delta E_s$ ) = [(Total energy in solvent phase) – (Total energy in gas phase)].

Molecule	Solvation energy ( $\Delta E_s$ ) (hartree)		
	Water	DMSO	CCl <sub>4</sub>
ACL	- 0.0059	- 0.0058	- 0.0025
HNE	- 0.0093	- 0.0091	- 0.0040
MVK	- 0.0060	- 0.0059	- 0.0026
ACR	- 0.0108	- 0.0107	- 0.0047
MA	- 0.0101	- 0.0099	- 0.0043
EMA	- 0.0059	- 0.0093	- 0.0038

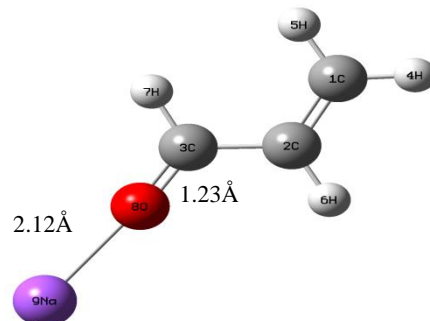
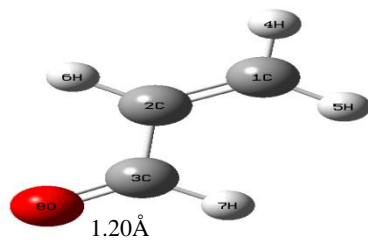


## Gas phase optimized structures

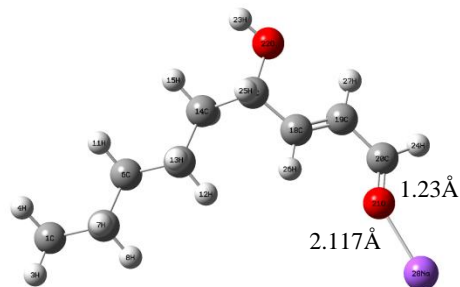
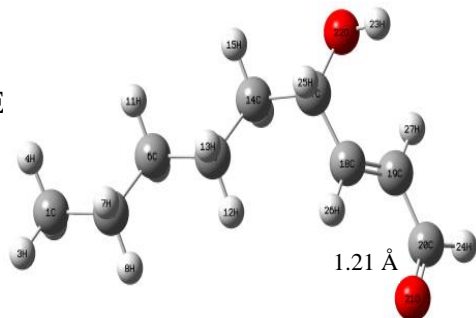
Free base

Na<sup>+</sup> Complex

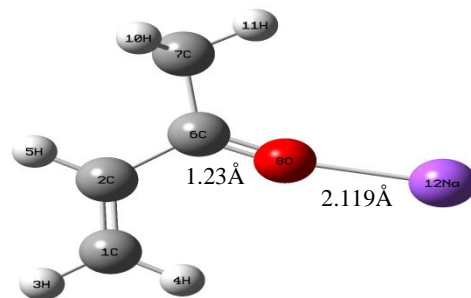
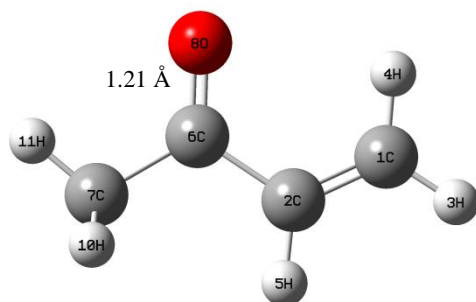
ACL



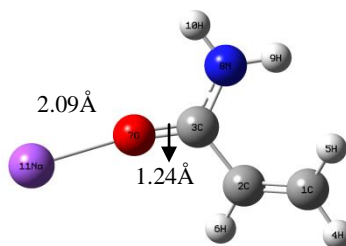
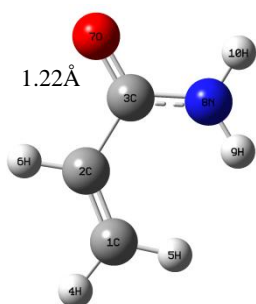
HNE



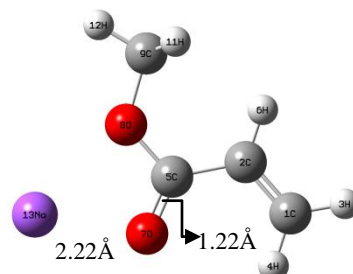
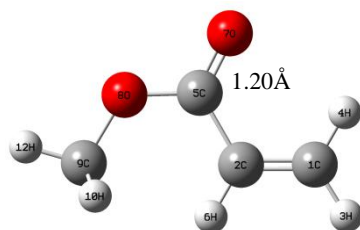
MVK



ACR

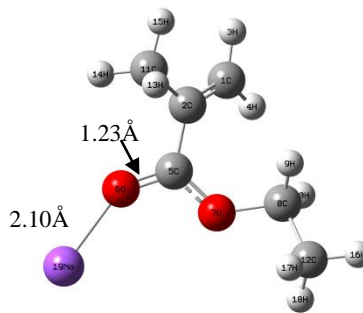
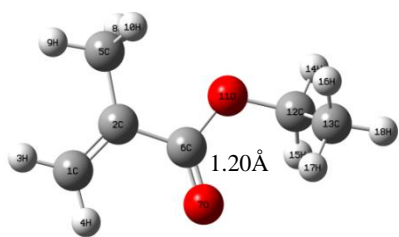


MA



Chapter 5

EMA

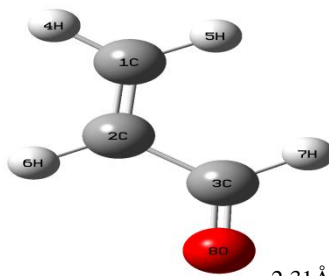
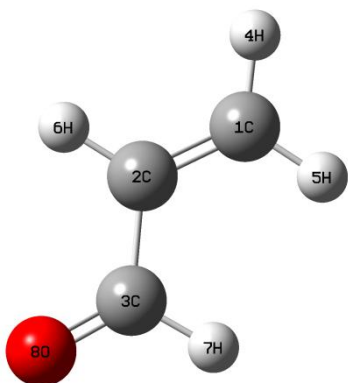


Aqueous phase optimized structures

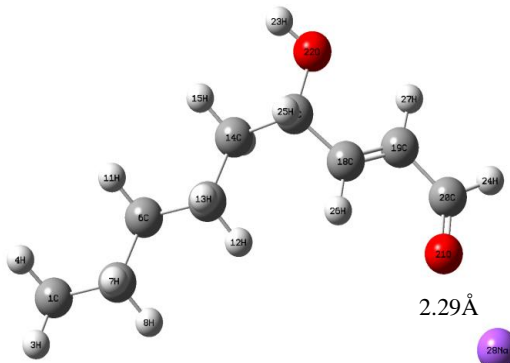
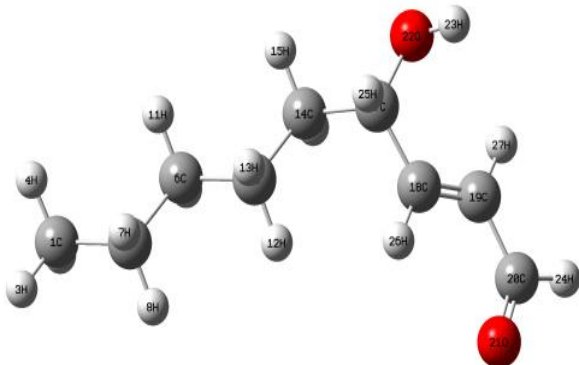
Free base

Na<sup>+</sup> complex

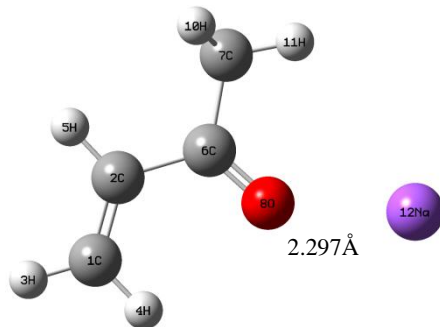
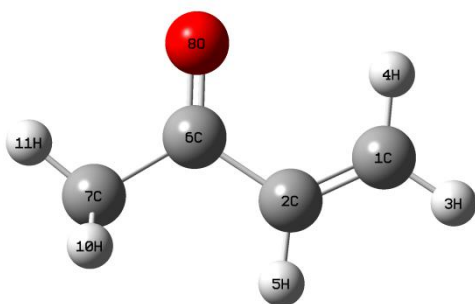
ACL

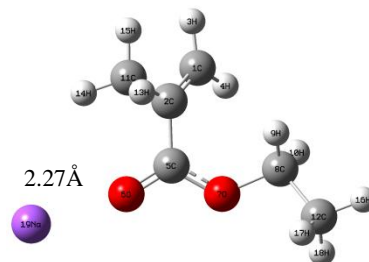
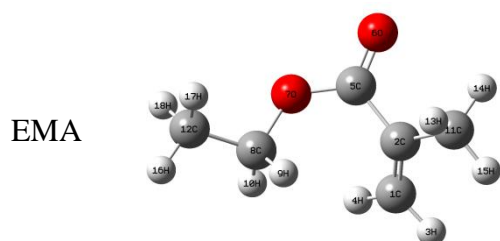
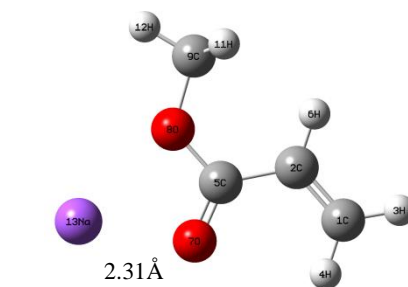
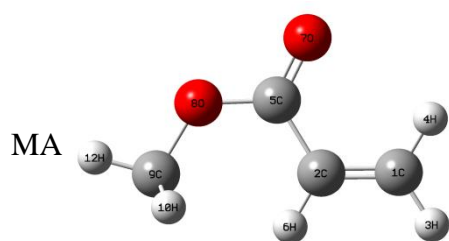
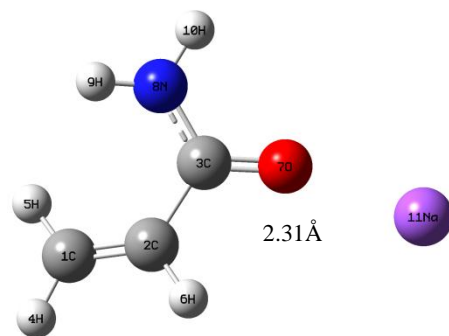
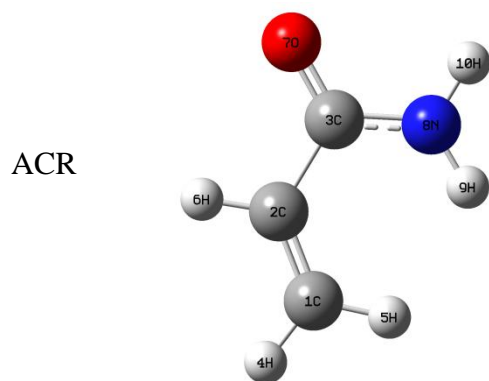


HNE



MVK

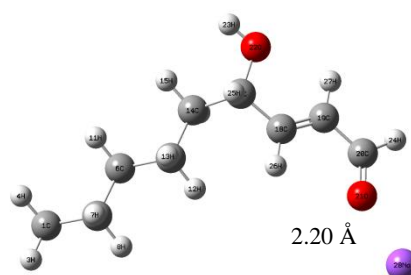
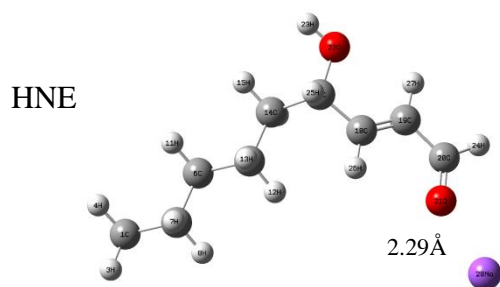
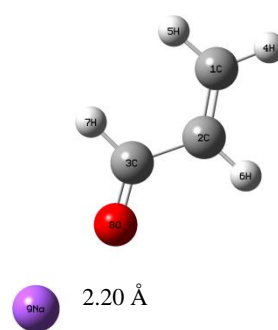
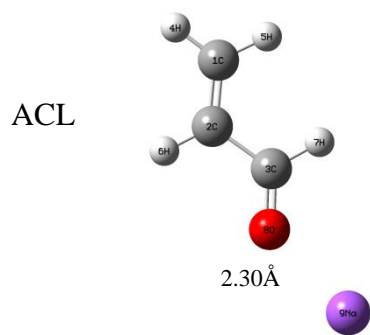




Optimized structure of the complexes in DMSO and CCl<sub>4</sub>

In DMSO

In CCl<sub>4</sub>



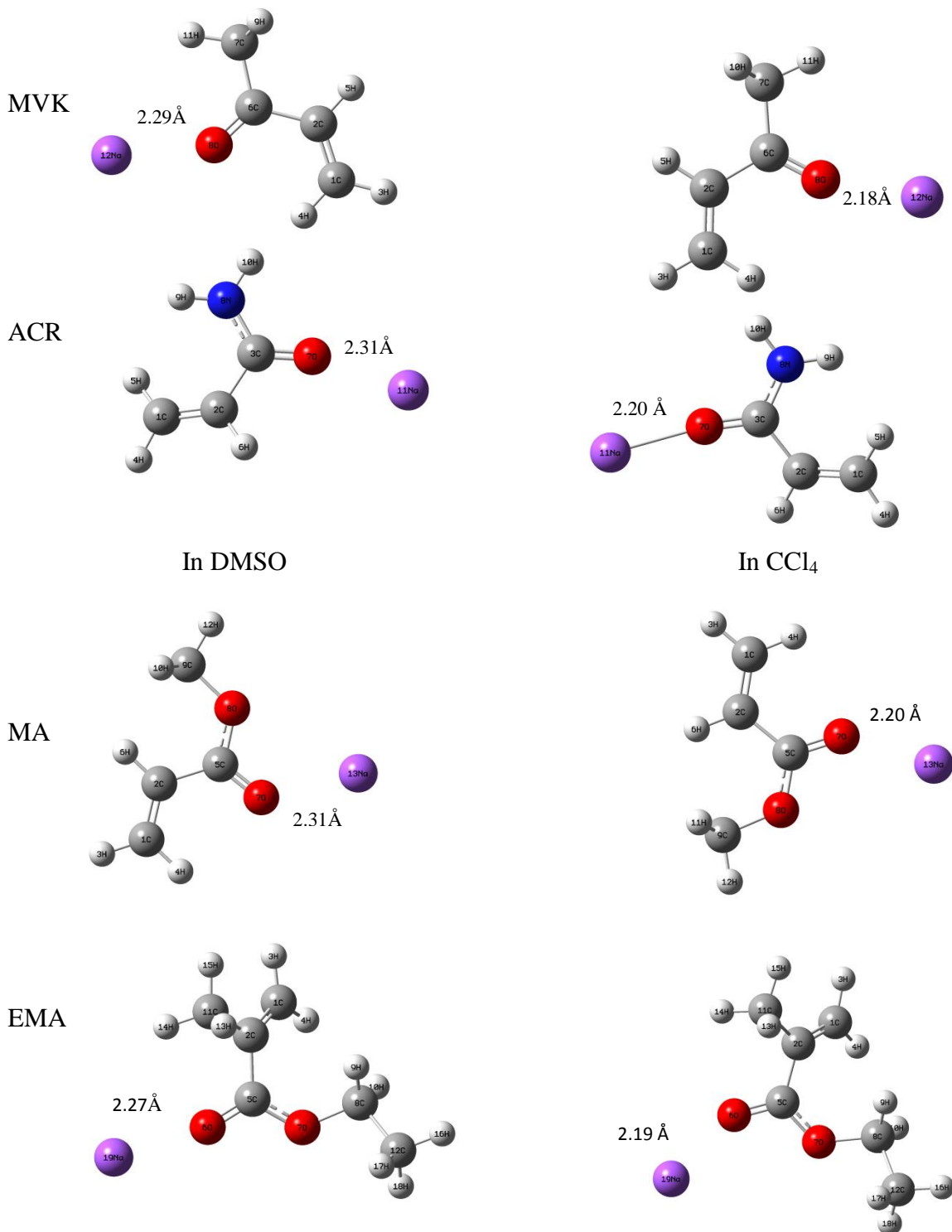


**Figure 5.2.3** Optimized structure of the studied  $\alpha,\beta$ -unsaturated carbonyl compounds and their O-Na<sup>+</sup> complexes in gas phase and in different solvents. [Optimized structures of the free bases in DMSO and CCl<sub>4</sub> are almost similar as they obtained in aqueous phase thus not given].

## 5.5 References

- (1) Burk, P.; Sults, M.-L.; Jaana, T.-T. *Proc. Estonian Acad. Sci. Chem.* **2007**, *56*(3), 107.
- (2) Aoki, K.; Murayama, K.; Ning-Hai, H. *Solid State Structures of Alkali Metal Ion Complexes Formed by Low-Molecular-Weight Ligands of Biological Relevance*. 2016.
- (3) In Astrid, Sigel; Helmut, Sigel; Roland K.O., Sigel. *The Alkali Metal Ions: Their Role in Life*. Metal Ions in Life Sciences. 16. Springer. pp. 27-101.
- (4) Winter, Mark. "WebElements Periodic Table of the Elements | Sodium | biological information". WebElements. Retrieved 13 January 2012.
- (5) Northwestern University. Archived from the original (PDF) on 23 August 2011. Retrieved 21 November 2011.
- (6) Ma, J. C.; Dongherty, D. A. *Chem. Rev.* **1997**, *97*, 1303.
- (7) LoPachin, R. M.; Barber, D. S.; Gavin, T. *Tox. Sci.* **2008**, *104*, 235-249.
- (8) Friedman, M. *J. Agric. Food Chem.* **2003**, *51*, 4504-4526.
- (9) LoPachin, R. M.; Gavin, T. *J. Agric. Food Chem.* **2008**, *56*, 5994-6003.
- (10) Stedman, R. L. *Chem. Rev.* **1968**, *68*, 153-207.
- (11) Parzefall, W. *Food Chem. Toxicol.* **2008**, *46*, 1360-1364.
- (12) Stevens, J. F.; Maier, C. S. *Mol. Nutr. Food Res.* **2008**, *52*, 7-25.
- (13) Dzidic, I.; Kebarle, P. *J. Phys. Chem.* **1970**, *74*, 1466-1474.
- (14) Sunner, J.; Kebarle, P. *J. Am. Chem. Soc.* **1984**, *106*, 6135-6139.
- (15) Tissandier, M. D.; Cowen, K. A.; Feng, W. Y.; Gundlach, E.; Cohen, M. H.; Earhart, A. D.; Coe, J. V.; Tuttle, T. R., Jr. *J. Phys. Chem. A* **1998**, *102*, 7787-7794.
- (16) Castleman, A. W.; Keesee, R. G. *Chem. Rev.* **1986**, *86*, 589-618.
- (17) Wieting, R. D.; Staley, R. H.; Beauchamp, J. L. *J. Am. Chem. Soc.* **1975**, *97*, 924-926.
- (18) Staley, R. H.; Beauchamp, J. L. *J. Am. Chem. Soc.* **1975**, *97*, 5920-5921.

## Chapter 5

- (19) Woodin, R. L.; Beauchamp, J. L. *J. Am. Chem. Soc.* **1978**, *100*, 501-508.
- (20) Woodin, R. L.; Beauchamp, J. L. *Chem. Phys.* **1979**, *41*, 1-9.
- (21) Taft, R. W.; Anvia, F.; Gal, J.-F.; Walsh, S.; Capon, M.; Holmes, M. C.; Hosn, K.; Oloumi, G.; Vasanwala, R.; Yazdani, S. *Pure Appl. Chem.* **1990**, *62*, 17-23.
- (22) McLuckey, S. A.; Cameron, D.; Cook, R. G. *J. Am. Chem. Soc.* **1981**, *103*, 1313-1317.
- (23) Cook, R. G.; Patrick, J. S.; Kotiaho, T.; McLuckey, S. A. *Mass Spectrom. Rev.* **1994**, *13*, 287-339.
- (24) Senapati, U.; De, D.; De, B. R. *Mol. Simul.* **2010**, *36*(6), 448-453.
- (25) Ping, W.; Gilles, O.; Chrys, W. *Int. J. Mass Spectrom.* **2008**, *269*, 34-45.
- (26) Sille, J.; Garaj, V.; Jezko, P.; Remco, M. *Acta Facultatis Pharmaceuticae Universitatis Comenianae* **2010**, *17*, 96-113.
- (27) Hoyau, S.; Norman, K.; McMohon, T. B.; Ohanessian, G. *J. Am. Chem. Soc.* **1990**, *121*, 8864.
- (28) Armentrout, P. B.; Rodgers, M. T. *J. Phys. Chem. A.* **2000**, *104*, 2238.
- (29) Lee, C.; Yang, W.; Parr, R. G. *Phys. Rev.* **1988**, *B37*, 785.
- (30) Hehre, W. J. *J. Chem. Phys.* **1969**, *51*(6), 2657.
- (31) Jensen, F. *J. Am. Chem. Soc.* **1992**, *114*, 9533-9537.
- (32) Frisch, M. J.; Trucks, G. W.; Schlegel, H. B.; Scuseria, G. E.; Robb, M. A.; Cheeseman, J. R.; Scalmani, G.; Barone, V.; Mennucci, B.; Petersson, G. A. Gaussian 09, Revision A.02; Gaussian Inc.: Wallingford, CT, 2009.
- (33) Tomasi, J.; Mennucci, B.; Cancès, E. *J. Mol. Struct. (Theochem)* **1999**, *464*(1-3), 211-226.
- (34) Remko, M.; Rode, B. M. *J. Mol. Struct. (Theochem)* **2000**, *505*, 269-281.
- (35) Mulliken, R. S. *I. J. Chem. Phys.* **1955**, *23*(10), 1833-1840.

- (36) Boys, S. F.; Bernardi, F. *Mol. Phys.* **1970**, *19*, 553.
- (37) Nagase, H.; Woessner, J. F. Jr. *J. Boil. Chem.* **1999**, *274*, 21491-21494.
- (38) Scolnick, L. R.; Clements, A. M.; Liao, J.; Crenshaw, L.; Heliberg, M.; May, J.; Dean, T. R.; Christianson, D. W. *J. Am. Chem. Soc.* **1997**, *119*, 850-851.
- (39) De, D.; Dalai, S.; De, B. R. *African Journal of Pure and Applied Chemistry*, **2010**, *4(9)*, 177-182.
- (40) Jeanvoine, Y.; Spezia, R. *J. Phys. Chem.* **2009**, *113*, 7878-7887.





## **CHAPTER 6**

**The proton affinities of a series of  $\beta$ -substituted Acrylamide in the ground state: A DFT based computational study.**



## Abstract

A detailed study of the proton affinities of a series of  $\beta$ -substituted acrylamides and their O-protonated counterparts has been performed by B3LYP (DFT) method using 6-311G (d,p) basis sets with complete geometry optimization both before and after protonation. The gas phase O-protonation is observed to be exothermic and the local stereochemical disposition of the proton is found to be almost the same in each case. The presence of  $\beta$ -substituent is seen to cause very little change of the proton affinities, relative to the unsubstituted acrylamides.

Computed proton affinities are sought to be correlated with a number of computed system parameters such as the Mulliken net charge on the carbonyl oxygen of the unprotonated bases, Mulliken net charge on the carbonyl oxygen and Mulliken net charge on the proton of the protonated bases. The overall basicity is explained by the distant atom contribution in addition to the contribution from the carbonyl group. The electron-releasing substituents are seen to increase the computed proton affinities (PAs) while the electron-withdrawing groups have an opposite effect as expected.

## 6.1 Introduction

The acid base interactions are of great importance in chemistry. These quantitative studies in the gas phase methods.<sup>1-9</sup> have the advantage of determining the intrinsic ground state acid base properties in the absence of complicating effects of solvation. For molecules containing carbonyl chromophores, protonation and hydrogen bonding are very much important. Recently the basicities of a series of substituted crotonaldehyde and acetophenone in their ground states have been theoretically calculated.<sup>10,11</sup> The systems were aliphatic and aromatic conjugated carbonyl systems. In an effort to understand the nature and origin of variation in the relative magnitude of the proton affinities to be expected in a series of aliphatic carbonyls, namely, acryl amide, the most toxicant air pollutant,<sup>12</sup> we have calculated the gas phase ground state proton affinities of a number of  $\beta$ -substituted acrylamides by B3LYP(DFT) method<sup>13,14</sup> using 6-311G(d,p) basis set. In this chapter, we have analysed the computed proton affinity values (PAs) to understand whether the pre-protonation charge distribution local to the chromophore or post-protonation relaxation of charge density or both are important in shaping the overall basicity of the acrylamides. We have also looked into the possible origin of the small shift in the proton affinities as one goes from the unsubstituted to the  $\beta$ -substituted acrylamides. In a particular state the possibility of correlating the proton affinity with the global hardness of the molecules is also explored. We have also calculated an important parameter softness to account for the stability of a molecule and the direction of acid-base reactions.

## 6.2 Computational details

Calculations were performed using Gaussian 03W software and B3LYP (DFT) method with 6-311G (d,p) basis sets. In all calculations complete geometry optimizations has been carried out on the molecules both before and after protonation.

## 6.3 Results and discussion

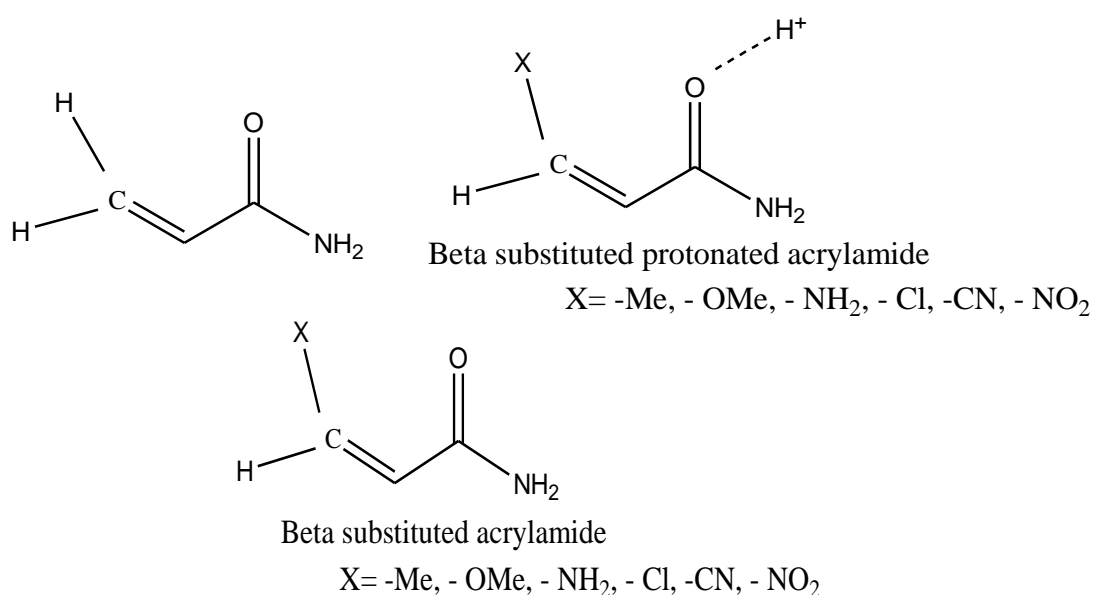


**Figure 6.2.1** Structure of Acrylamide, Beta substituted ACR and their Protonated Counterparts

The molecules studied theoretically are  $\beta$ -substituted acrylamides and its protonated species. The molecules studied are listed in **Table 6.1.1** along with their respective abbreviated names and computed total energies and proton affinities in DFT method using 6-311G (d,p) basis set. **Table 6.1.2** reports the computed Mulliken net charge on the carbonyl oxygen atoms at the equilibrium ground state of the unprotonated free base molecules as well as the computed Mulliken net charge carried out by proton and the Mulliken net charge on the carbonyl oxygen at the equilibrium ground state of the protonated bases. Atomic charge is not an observable quantum mechanical property. All methods for computing the atomic charges are necessarily arbitrary. Electron density among the atoms in a molecular system is being

partitioned. Mulliken population analysis computes charges by dividing orbital overlap equally between the two atoms involved. Therefore the values are non-unique. Still, it is widely used. From **Table 6.1.1** it is seen that the proton affinities (PAs) of all the  $\beta$ -substituted acrylamides are in the range  $-167.16$  kcal/mole to  $-229.29$  kcal/mole. Proton affinities (PAs) of all the  $\beta$ -substituted acrylamides indicate that the gas phase O-protonation is exothermic in each case. The electron-releasing substituents are seen to increase the computed PAs while electron-withdrawing groups have an opposite effect as expected. **Table 6.1.1** reveals that proton affinity is highest for  $\beta$ AACR,  $X = -\text{NH}_2$ .

From **Table 6.1.4** it is clear that lower softness value of  $\beta$ AACR,  $X = -\text{NH}_2$  and highest softness value of  $\beta$ NACR,  $X = -\text{NO}_2$  indicates  $\beta$ AACR is a hard base and favors protonation (since  $\text{H}^+$  is a hard acid). This is one of the reasons of highest PA of  $\beta$ AACR. A perusal of **Table 6.1.2** reveals that the computed net charge on the proton is small in each case and is in the range of  $0.2864$  e to  $0.365$  e showing that, a rather large migration of electron density to the added proton has taken place. The proton adds to the base, giving polar covalent sigma bond with a very extensive charge transfer. The base molecule carries the rest of the positive charge. The large degree of charge transfer results from the fact that  $\text{H}^+$  is a bare nucleus, with a very low energy unfilled  $1\text{S}$  orbital. These migrations is not local and originates from all over the molecule is clearly reflected in the computed net charges on the carbonyl oxygen atom of the protonated bases as shown in **Table 6.1.2**. The oxygen atom still carries a net negative charge, albeit depleted, relative to the unprotonated base. It is also seen that the charge density of O-atom before protonation is higher when X is an electron-releasing group. This favours protonation. The reverse is the case with electron-attracting group. This may be one of the reasons for the slight increase and decrease of PA values relative to unsubstituted acrylamides. It can therefore, be anticipated that the proton affinities of these carbonyl bases cannot be modelled or described by local properties of the carbonyl moiety only. It must be

shaped strongly by distant atom contribution in addition to the contribution from the carbonyl group.

Optimized structures of  $\beta$ -substituted acrylamides and their O-protonated counterparts in the ground state are shown in **Figure 6.2.5**. The local characteristics at or around the carbonyl moiety cannot model the substituent effects. This is again revealed from the data reported in **Table 6.1.3** where some of the selected computed geometrical parameters around the carbonyl group are listed. The O–H<sup>+</sup> bond length has a variation in the range of 0.9669 to 1.4448 Å for all the protonated bases. The C–O–H<sup>+</sup> bond angle is virtually within 102.8165 to 116.1180° in all the cases. Similarly, the torsion angle  $\tau$  (C–C–O–H<sup>+</sup>) shows only a small variation in all the cases. The C–O length of all the protonated bases increases except for  $\beta$ MyACR where it remains same even after protonation. The carbonyl ring near invariant stereochemistry around the protonation site of each base tends to suggest that the entire contribution from substituent effects to PA cannot be modelled properly unless contributions from far away centers are taken into account. It also points to the fact that “local” effects of the group must be very nearly identical in each case.

As the local parameter we have chosen the computed net charge density on the carbonyl oxygen atom of the unprotonated bases ( $q_{O^-}$ ) and the net charge density on the proton ( $q_{H^+}$ ) of the fully relaxed BH<sup>+</sup>. It is seen that the plot of the computed gas phase proton affinities (PAs) against the computed net charge density on the carbonyl oxygen atom of the unprotonated bases ( $q_{O^-}$ ) (**Figure 6.2.2**) is not linear. It is also seen that the plot of the computed gas phase proton affinities (PAs) versus  $q_{H^+}$  of the fully relaxed BH<sup>+</sup> (**Figure 6.2.3**) is not linear. We have also searched for the possibility of existence of correlation with a single global parameter of the entire molecule. As the global parameter we have chosen the hardness,  $\eta = (I - A)/2 = (\epsilon_{LUMO} \sim \epsilon_{HOMO})/2$  listed in **Table 6.1.4**. It is seen that no perfect correlation between the hardness and proton affinity in the series could be made. This is

further revealed from **Figure 6.2.4** where the gas phase proton affinity versus computed hardness is plotted which shows no linearity. Thus all these reveal marginal linearity of the computed PA's with respect to local and global parameters. This indicates that both pre- and post-protonation correlations with local charge densities in the immediate neighbourhood of the protonation site are weak.

## 6.4 Conclusion

The above computational study shows that gas phase O-protonation of  $\beta$ -substituted acrylamides and their O-protonated counterparts is spontaneous irrespective of their electron releasing or withdrawing nature. The overall proton affinity is explained by distant atom contribution in addition to the contribution from the carbonyl group. The carbonyl ring near invariant stereochemistry around the protonation site of each base tends to suggest that the entire contribution from substituent effects to PA cannot be modelled properly unless contributions from far away centers are taken into account.



**Table 6.1.1** Computed total energies of  $\beta$ -substituted acrylamide and their protonated complexes, proton affinities and gas phase basicities. (PA =  $E_{BH^+} - E_B$ ).

Molecule	Total energies (hartree)		PA (hartree)	PA (Kcal/mole)
	B	BH <sup>+</sup>		
ACR, X= -H	-247.3692	-247.7160	-0.3468	-217.62
$\beta$ MACR, X= -CH <sub>3</sub>	-286.6979	-287.0491	-0.3512	-220.38
$\beta$ MyACR, X= -OCH <sub>3</sub>	-361.7297	-361.9961	-0.2664	-167.16
$\beta$ AACR, X= -NH <sub>2</sub>	-302.7994	-303.1248	-0.3654	-229.29
$\beta$ CIACR, X = -Cl	-706.9850	-707.3301	-0.3451	-216.55
$\beta$ CNACR, X= -CN	-339.6279	-339.9596	-0.3317	-208.14
$\beta$ NACR, X= -NO <sub>2</sub>	-451.9159	-452.2472	-0.3313	-207.89

**Table 6.1.2** Computed net charge on O-atom ( $q_{O^-}$ ) [unit 'e'] of free base (B) and O-protonated base (BH<sup>+</sup>) and computed net charge on proton ( $q_{H^+}$ ) at the equilibrium ground state of protonated base (BH<sup>+</sup>) and free base (B).

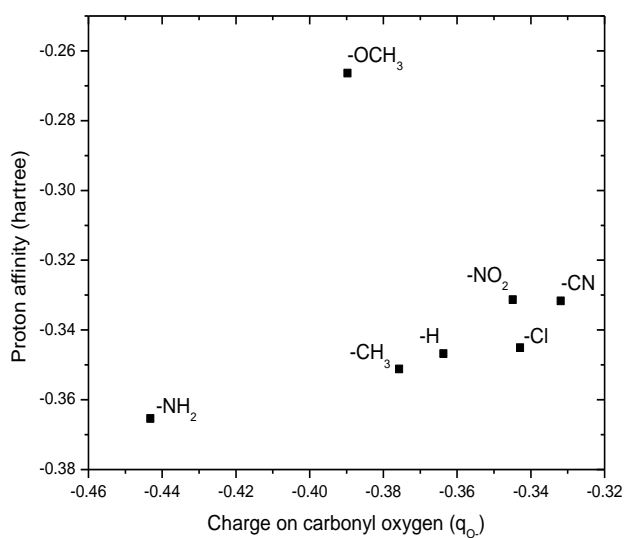
Molecule	Charge on Carbonyl Oxygen atom( $q_{O^-}$ )		Charge on Proton( $q_{H^+}$ )
	B	BH <sup>+</sup>	
ACR	-0.3637	-0.2457	0.3059
$\beta$ MACR	-0.3757	-0.2710	0.2951
$\beta$ MyACR	-0.3897	-0.2817	0.3651
$\beta$ AACR	-0.4432	-0.3436	0.2963
$\beta$ CIACR	-0.3429	-0.2316	0.2864
$\beta$ CnACR	-0.3319	-0.2471	0.3091
$\beta$ NACR	-0.3449	-0.2386	0.3070

**Table 6.1.3** Geometrical features of the free base and O-protonated base (length in Å and angle in degree).

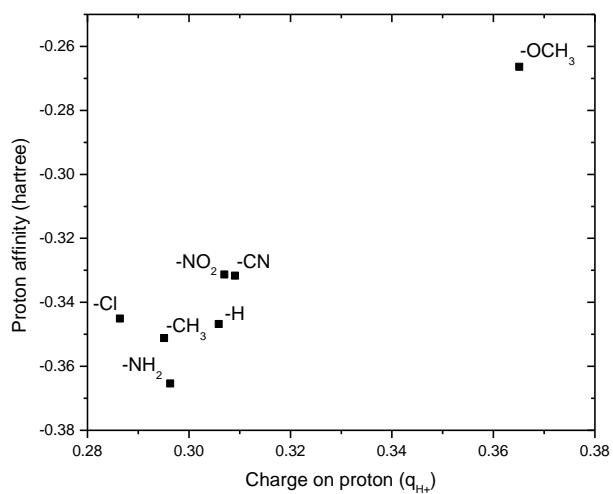
Molecule	Free base	O-protonated base			
	r(C–O)	r(C–O)	r(O–H <sup>+</sup> )	<C–O–H <sup>+</sup>	<C–C–O–H <sup>+</sup>
ACR	1.2183	1.3057	0.9679	113.2913	–5.4293
βMACR	1.2219	1.3105	0.9690	114.6336	180.0044
βMyACR	1.2232	1.2232	1.4448	102.8165	–174.3517
βAACR	1.2375	1.3328	0.9669	114.1474	–179.4498
βClACR	1.2155	1.3017	0.9770	112.3551	–0.0481
βCnACR	1.2152	1.3008	0.9703	116.1180	179.9410
βNACR	1.2188	1.3071	0.9708	115.1478	–179.9838

**Table 6.1.4** Computed hardness (hartree) and softness (hartree) of the free base (B) in the ground state by B3LYP (DFT) method using 6-311G (d,p) basis set. Hardness ( $\eta$ ) =  $[(\epsilon_{\text{LUMO}} - \epsilon_{\text{HOMO}})/2]$ 

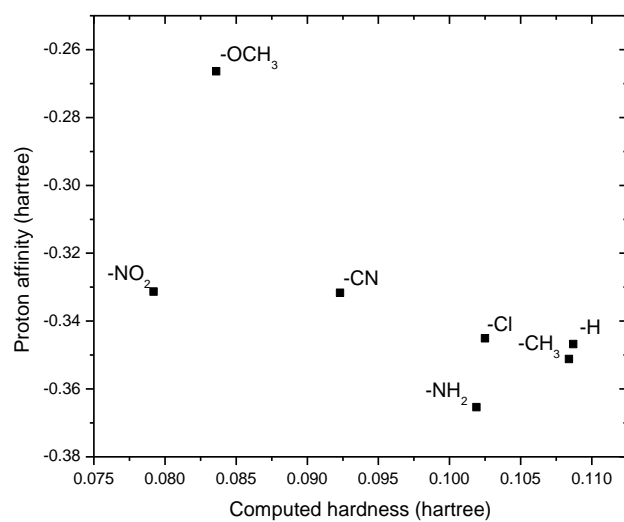
Molecule	$\epsilon_{\text{HOMO}}$	$\epsilon_{\text{LUMO}}$	$\eta$ (Hardness)	$S = 1/2\eta$ (Softness)
ACR	–0.2585	–0.0410	0.1087	4.5998
βMACR	–0.2509	–0.0341	0.1084	4.6125
βMyACR	–0.2205	–0.0533	0.0836	5.9808
βAACR	–0.2118	–0.0079	0.1019	4.9067
βClACR	–0.2587	–0.0537	0.1025	4.8780
βCnACR	–0.2756	–0.0910	0.0923	5.4171
βNACR	–0.2829	–0.1244	0.0792	6.3131



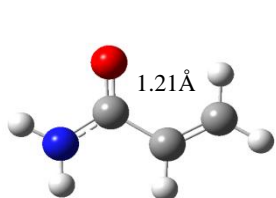
**Figure 6.2.2** Plot of gas phase ground state proton affinity vs. charge on the carbonyl oxygen atom of the free bases.



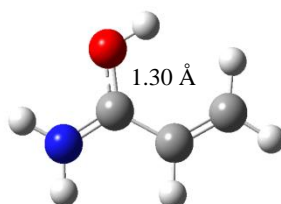
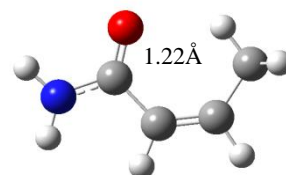
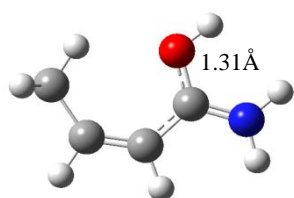
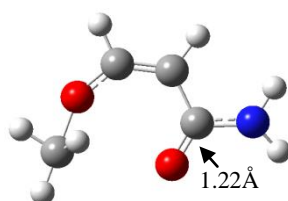
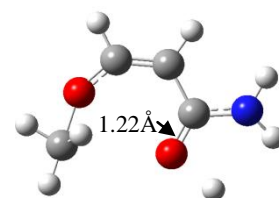
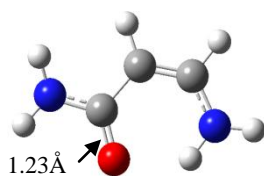
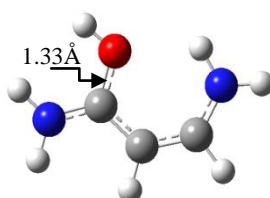
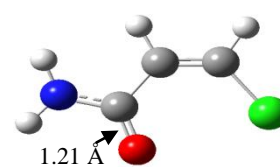
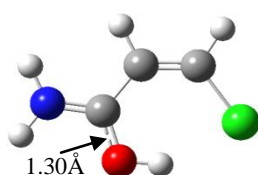
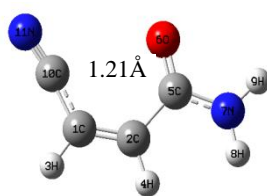
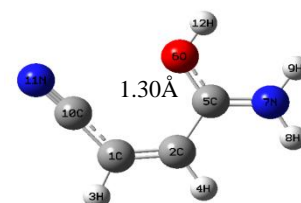
**Figure 6.2.3** Plot of gas phase ground state proton affinity vs. charge on the proton of the complex BH<sup>+</sup>.



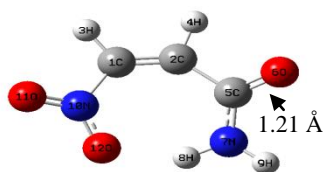
**Figure 6.2.4** Plot of gas phase ground state proton affinity vs. computed hardness.



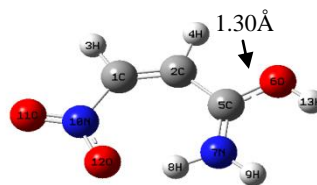
ACR

ACR(H<sup>+</sup>) $\beta$ MACR $\beta$ MACR(H<sup>+</sup>) $\beta$ MyACR $\beta$ MyACR(H<sup>+</sup>) $\beta$ AACR $\beta$ AACR(H<sup>+</sup>) $\beta$ CIACR $\beta$ CIACR(H<sup>+</sup>) $\beta$ CnACR $\beta$ CnACR(H<sup>+</sup>)

Chapter 6



$\beta$ NACR



$\beta$ NACR(H<sup>+</sup>)

**Figure 6.2.5** Optimized structures of  $\beta$ -substituted acrylamides and their O-protonated counterparts in the ground state.

## 6.5 References

- (1) Bhome, D. K.; Hemsworth, R. S.; Rundle, H. I.; Schiff, H. I. *J. Chem. Phys.* **1973**, *58*, 3504.
- (2) Beauchamp, J. L. *Interaction between Ions and Molecules*. (Plenum, New York) **1974**, pp. 413, 459, 489.
- (3) Yamadagni, R.; Kebarle, P. J. *J. Am. Chem. Soc.* **1973**, *96*, 3727.
- (4) Bhome, D. K.; Mackay, G. I.; Schiff, H. I.; Hemsworth, R. S. *J. Chem. Phys.* **1974**, *61*, 2175.
- (5) Solomon, J. J.; Meot Ner, M.; Fiele, F. M. *J. Am. Chem. Soc.* **1974**, *96*, 3727.
- (6) Long, J. I.; Franklin, J. L. *J. Am. Chem. Soc.* **1974**, *96*, 2320.
- (7) Brauman, J. I.; Blair, L. K. *J. Am. Chem. Soc.* **1970**, *92*, 5986.
- (8) Wieting, R. D.; Staley, R. H.; Beacchamp, J. L. *J. Am. Chem. Soc.* **1974**, *96*, 7552.
- (9) Staley, R. H.; Beacchamp, J. L. *J. Am. Chem. Soc.* **1975**, *96*, 3727.
- (10) Pandit, S.; De, D.; De, B. R. *J. Mol. Struct. (Theochem)* **2006**, *760*, 245.
- (11) Senapati, U.; De, D.; De, B. R. *Indian J. Chem.* **2008**, *47A*, 548.
- (12) Lopachin R. M.; Gavin T. *Environmental Health Perspectives.* **2012**, *120(12)*, 1650-1657
- (13) Frisch, M. J.; Trucks, G. W.; Schlegel, H. B.; Scuseria, G. E.; Robb, M. A.; Cheeseman, J. R.; Montgomery, J. A. Jr.; Vreven, T.; Kudin, K. N.; Burant, J. C.; Millam, J. M.; Iyengar, S. S.; Tomasi, J.; Barone, V.; Mennucci, B.; Cossi, M.; Scalmani, G.; Rega, N.; Petersson, G. A.; Nakatsuji, H.; Hada, M.; Ehara, M.; Toyota, K.; Fukuda, R.; Hasegawa, J.; Ishida, M.; Nakajima, T.; Honda, Y.; Kitao, O.; Nakai, H.; Klene, M.; Li, X.; Knox, J. E.; Hratchian, H. P.; Cross, J. B.; Adamo, C.; Jaramillo, J.; Gomperts, R.; Stratmann, R. E.; Yazyev, O.; Austin, A. J.; Cammi, R.; Pomelli, C.; Ochterski, J. W.; Ayala, P. Y.; Morokuma, K.; Voth, G. A.; Salvador, P.;

## Chapter 6

Dannenberg, J. J.; Zakrzewski, V. G.; Dapprich, S.; Daniels, A. D.; Strain, M. C.; Farkas, O.; Malick, D. K.; Rabuck, A. D.; Raghavachari, K.; Foresman, J. B.; Ortiz, J. V.; Cui, Q.; Baboul, A. G.; Clifford, S.; Cioslowski, J.; Stefanov, B. B.; Liu, G.; Liashenko, A.; Piskorz., P.; Komaromi, I.; Martin, R. L.; Fox, D. J.; Keith, T.; Al-Laham, M. A.; Peng, C. Y.; Nanayakkara, A.; Challacombe, M.; Gill, P. M. W.; Johnson, B.; Chen, W.; Wong, M. W.; Gonzalez, C.; Pople, J. A.; Gaussian, Inc., Wallingford, CT, 2004.

- (14) Lee, C.; Yang, W.; Parr, R. G.; *Phys. Rev.* **1988**, *B37*, 785; Becke, A. D. *J. Chem. Phys.* **1993**, *98*, 5648.



## **CHAPTER 7**

**The comparative basicities,  $\text{Li}^+$  and  $\text{Na}^+$  cation affinities of a series of heterocyclic molecules (Pyrrole, Furan, Thiophene and Pyridine) in the ground state. A DFTstudy.**



## Abstract

Ground state gas phase proton affinities, alkali metal cation ( $\text{Li}^+$ ,  $\text{Na}^+$ ) affinities and basicities of pyrrole, furan, thiophene and pyridine have been calculated computationally with the help of DFT /B3LYP method of calculation at hybrid triple zeta 6-311 G (d,p) basis set level. Different binding sites of pyrrole, furan and thiophene for protonation were observed. Proton affinity (PA) value of  $\text{C}_\alpha\text{-H}^+$  complexes of pyrrole, furan and thiophene are found higher compared to  $\text{C}_\beta\text{-H}^+$  and  $\text{X-H}^+$  complexes ( $\text{X} = \text{N}, \text{O}, \text{S}$ ). In case of pyridine, protonation occurred at hetero atom (N) and formed most stable protonated complex. Results are obtained in this calculation shows good agreement with experimental values. Alkali metal cation ( $\text{Li}^+$ ,  $\text{Na}^+$ ) affinity and basicity of the same molecules have been calculated at the same level of theory. Pyridine exhibits the highest affinity for  $\text{Li}^+$  and  $\text{Na}^+$  cation. The electronic properties of the complexes indicate that, proton formed polar co-valent sigma bond with binding site of the corresponding molecule whereas alkali metal cation ( $\text{Li}^+, \text{Na}^+$ ) –free molecule interactions are predominantly an ion-dipole attraction and the ion-induced dipole interaction as well rather than a covalent interaction. Computed proton, lithium and sodium affinities are sought to be correlated with a number of computed system parameters like the computed net charge on the binding atom of the free molecules and with the net charge on proton,  $\text{Li}^+$ , and  $\text{Na}^+$  of the protonated, lithium and sodium complexes.

## 7. 1 Introduction

Acid-base interactions are of great importance in chemistry. Quantitative studies in the gas phase provide the intrinsic acid–base properties free from interference from solvent molecules and counter ions. The most widespread study concerns different gas phase proton transfer equilibria.<sup>1</sup> Protonation reactions are very important in various organic reaction mechanism and it play important roles in bio-molecular process.<sup>2</sup> Though mass spectrometric studies can explain easily the thermodynamic and kinetic properties of protonation and deprotonation process but it is difficult to recognised the structural behaviour, some time more than one results are obtained.<sup>3</sup> The heterocyclic molecules have lately attracted attention due to their “shifted PKa values” upon complexation to metal ions, because it can rationalize the existence of nucleobases of differing protonation state at physiological P<sup>H</sup>.<sup>4</sup> The reactivity and positional selectivity for electrophilic substitution reactions of five membered N, O and S heterocyclic compounds was studied quantitatively.<sup>5,6</sup> It is also known that, heterocyclic compounds containing N, O or S hetero atoms (X) increased the reactivity of  $\alpha$ -carbon (next to hetero atom) and usually formed stable complexes. It was also seen<sup>5,6</sup> that, order of reactivity (N–hetero > O–hetero > S–hetero) does not maintain the sequence of positional selectivity (product ratio of  $\alpha$  and  $\beta$  substituted complex), it appeared as O–hetero > S–hetero > N–heterocyclic compounds. In the current work we have optimized H<sup>+</sup>–heterocyclic (pyrrole, furan, thiophene) complexes thrice (by changing the position of proton in initial input) to investigate proper binding sites for protonation and the most stable protonated complexes. Interestingly, in each heterocyclic molecule, more than one protonation sites (heteroatom, C <sub>$\alpha$</sub>  and C <sub>$\beta$</sub> ) are found. Lithium and sodium complexes of these molecules are optimized in two different ways. First time lithium and sodium directly bonded with X atom and secondly, they are non-bonded in the initial input. We observed that, Li<sup>+</sup> and Na<sup>+</sup> have two possible positions relative to hetero cyclic molecules (pyrrole, furan, thiophene

and pyridine). A number of experimental and theoretical studies were performed<sup>7-10</sup> with different heterocyclic molecules. To the best of our knowledge, a systematic and comprehensive comparative theoretical study on gas phase basicity, proton affinity (PA), alkali metal cation affinity and basicity of the above mentioned molecules are rather scarce. Otto Dopfer et al<sup>11</sup> were reported on protonation of heterocyclic molecules. Interaction of hydrogen molecules with complexes of lithium cation and N-containing heterocyclic anions have been studied earlier.<sup>12</sup> Some electronic properties of pyridine, pyrimidine, pyrazine and pyridazine have been studied<sup>13</sup> before by DFT method. LiNH<sub>2</sub> interaction with pyridine, furan and thiophene have been reported recently.<sup>14</sup> Stabilities and structures of five membered heterocyclic molecules containing N, O and S hetero atom were investigated by Hikora et al.<sup>15</sup> In an effort to understand the nature of bonding and origin of variation in the relative magnitude of the basicities, lithium cation affinities (LCA) and sodium cation affinities (SCA) to be expected in a series of heterocyclic compounds (pyrrole, furan, thiophene and pyridine), the most biologically important and deadly poisons, we have computationally studied the gas phase basicities, LCA and SCA of the above said molecules. The comparative study of proton affinity, Li<sup>+</sup> affinity and Na<sup>+</sup> affinity of these heterocyclic compounds in the ground state have been performed by DFT/ B3LYP method using 6-311G (d,p) basis set.

Alkali metal ions were the first metal cations to be studied in the gas phase for their coordination properties. This is due to their relatively easy production under vacuum. In contrast with the transition metal ions, their reactivity towards ligands is quite simple, in general, they form adducts, or clusters that can be considered as ions “solvated” by one or several ligands.<sup>16</sup> Recently the ground state basicities of a series of substituted crotonaldehyde and acetophenone in their ground state were reported in the literature.<sup>17,18</sup> The ground state Li<sup>+</sup> and Na<sup>+</sup> affinities of a series of substituted crotonaldehyde and acetophenone were also

## Chapter 7

reported in previous studies.<sup>19-21</sup> Gas phase methods<sup>22-30</sup> have the advantage for determining the intrinsic ground state, acid base properties in the absence of complicating effect of solvation. Therefore the present study have been undertaken to evaluate few important data in gas phase.

The purpose of the present work is not only to gathered information of the basicities, proton affinities,  $\text{Li}^+$  and  $\text{Na}^+$  affinities of the above said heterocyclic molecules by means of computational calculation but also to study on geometrical features of their protonated, lithium, and sodium complexes. We also reports more than one result about protonation and alkali metal cation interaction site (s) observed in our study.

Here we analyzed the PA, LCA and SCA values to understand whether the pre-complex charge distribution local to the molecules or post-complex relaxation of charge density or both are important for explaining the overall gas phase basicity and affinities of the molecules in a particular state.

Since the ion-molecule complexes are involved in molecular recognition process<sup>32</sup> and helps in removing metal cations from contaminated media. These studies may be used to gain insight into many important biological processes,<sup>33-36</sup> electron transfer process<sup>37,38</sup> and more complicated biological system.

In this work we have looked into the possible origin of the small shift in the proton,  $\text{Li}^+$  and  $\text{Na}^+$  affinities on the heterocyclic molecules and also focus our attention on the nature of bonding in protonated and alkali metal complexes.

### **7. 2 Computational details**

Standard quantum mechanical calculations (DFT) were performed at B3LYP/6-311G(d,p) level<sup>39</sup> using Gaussian O9W program package.<sup>31</sup> In all calculations, complete geometry

optimization has been carried out on the molecules both before and after protonation,  $\text{Li}^+$  complex and  $\text{Na}^+$  complex formation. It has been shown<sup>40</sup> B3LYP triple zeta calculations well reproduce the thermodynamic values of ion-molecule interactions with higher accuracy with respect to the experimental results. So this method is appropriate as an alternative to traditional *abinitio* method for studying these types of interactions. Frequencies were calculated at same levels. No scaling was applied to obtain DFT frequencies for the calculation of thermodynamic parameters (at 298.15°K) using standard procedures. Natural population analysis (NPA) has been applied to evaluate the partial atomic charge on atoms.

### 7. 3 Results and discussion

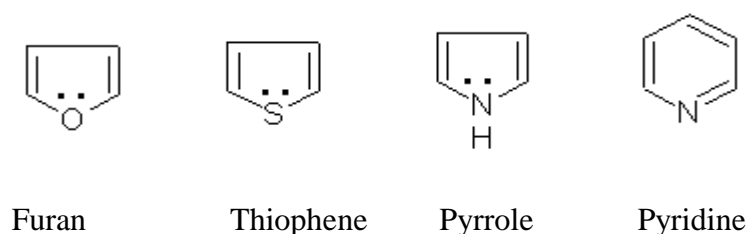


**Figure 7.2.1** General chemical structure of studied molecules

Gas phase proton affinity (PA), Lithium cation affinity (LCA) and Sodium cation affinity (SCA) is defined as negative value of enthalpy change ( $\Delta H$ ) of the following reaction



Where B represent the corresponding hetero cyclic molecule.

Gas phase basicity, Lithium cation basicity (LCB), Sodium cation basicity (SCB) is the negative value of free energy change ( $\Delta G$ ) of the same reaction 1, 2 and 3. Gas phase proton affinities have been calculated as  $[\text{H}_{\text{B1H}^+} - \text{H}_{\text{B1}}]$ ,  $[\text{H}_{\text{B2H}^+} - \text{H}_{\text{B2}}]$ ,  $[\text{H}_{\text{B3H}^+} - \text{H}_{\text{B3}}]$ ,  $[\text{H}_{\text{B4H}^+} - \text{H}_{\text{B4}}]$ . In the similar way gas phase basicities ( $\Delta G$ ) of the same molecules have been calculated as  $[\text{G}_{\text{B1H}^+} - \text{G}_{\text{B1}}]$ ,  $[\text{G}_{\text{B2H}^+} - \text{G}_{\text{B2}}]$ ,  $[\text{G}_{\text{B3H}^+} - \text{G}_{\text{B3}}]$ ,  $[\text{G}_{\text{B4H}^+} - \text{G}_{\text{B4}}]$ . Where B1= pyrrole, B2= furan, B3= thiophene, B4 = pyridine. H = Total enthalpy and G = Total Gibbs free energy at

## Chapter 7

298.15k. Gas phase alkali metal cation affinities (LCA and SCA) and basicities (LCB and SCB) have been calculated as  $MCA = [H_{BM}^+ - (H_B + H_M^+)]$ ..... (4) And  $MCB = [G_{BM}^+ - (GB + G_M^+)]$ ..... (5).

MCA = Metal cation affinity and MCB = Metal cation basicity.  $M^+$  = Lithium and sodium. B represents the hetero cyclic molecules B1, B2, B3 and B4. **Table 7.1.1** summarises the proton affinity and basicity values of the studied molecules obtained in this theoretical calculation.

In the present work, a significant incident is arise with more than one protonation sites for the 3 five membered heterocyclic molecules, protonation occurred at hetero atom and also at  $C_\alpha$  and  $C_\beta$  position.  $C_\alpha-H^+$  complexes of pyrrole, furan and thiophene are obtained as most stable compared to  $C_\beta-H^+$  and  $X-H^+$  complexes ( $X = N, O$  and  $S$ ). In case of pyridine we observed  $H^+$  prefers to bind with hetero atom (N) to form stable protonated complex. That means  $C_\alpha$  protonated complexes (for B1, B2, B3) reached to the global minima potential energy surface (PES) whereas  $C_\beta$  and  $X$ -protonated complexes corresponds to the comparatively higher energy local minima. For B4,  $X$ -protonated species corresponds to the global minima PES. From **Table 7.1.1** we observed that, both PA and  $\Delta G$  results of  $C_\alpha$  and  $C_\beta$  protonated species are seen to be much closer to each other. Difference of PA values between  $C_\alpha$  and  $C_\beta$  for pyrrole is  $<5$  kcal/ mole. It is slightly higher in case of furan ( $\approx 13$  kcal/mole) and thiophene ( $<10$  kcal/mole). Very interestingly we observed, PA values obtained in  $C_\beta - H^+$  complexes are more nearer to the literature results (Hunter, Lias. 1998), difference are only  $\pm 2.11, \pm 1.24$  and  $\pm 0.82$  kcal /mole for pyrrole, furan and thiophene respectively. Gas phase PA value of pyridine ( $-232.8$  kcal/mole) is also well agreed with the experimental data ( $-225.86$  kcal/mole, Hunter, Lias. 1998). Calculated gas phase basicities are in a good corresponds to the experimental ones (**Table 7.1.1**). In respect to the obtained  $\Delta G$  values of the  $C_\alpha-H^+$  complexes, the differences are  $\pm 9.1, \pm 2.53, \pm 13.04$  kcal/mole for B1, B2 and B3 and it is  $\pm 5.83$  kcal/mole for B4. The calculated difference in gas phase



basicities for protonation at  $C_\alpha$  and  $C_\beta$  site(s) are  $\pm 5.14$ ,  $\pm 0.0$  and  $\pm 9.14$  kcal/mole for B1, B2 and B3 respectively.

Considering all PA values of different protonated complexes of pyrrole, furan and thiophene, PA order can be written as  $C_\alpha - H^+ > C_\beta - H^+ > X - H^+$ . With the inclusion of pyridine in the series, PA order of the molecules ranked as pyridine  $>$  pyrrole  $>$  thiophene  $>$  furan. This order of stability (PA) of the  $C_\alpha$ ,  $C_\beta$  and X protonated complexes are well supported by NPA results. Partial NPA charges on binding proton in the complexes obtained from NPA procedure summarised in **Table 7.1.3**. The values of  $q_{CT}$  indicate that there is a significant transfer of charge from ligand to interacting proton. The extent of charge transfer is quite parallel to the complex stability for pyrrole and furan, minor discrepancy is observed in case of thiophene where  $q_{CT}$  values obtained little higher (0.798e) in  $X-H^+$  complex compared to  $C_\alpha-H^+$  complex. The  $q_{CT}$  values for pyrrole protonated complexes ( $C_\alpha$ ,  $C_\beta$  and N) are 0.729e, 0.694e and 0.544e. It is 0.724e, 0.678e and 0.413e in furan complexes and 0.701e, 0.682e and 0.798e in thiophene complexes. The origin of such discrepancy needs further exploration in case of thiophene complexes. **Table 7.1.2** summarised the Mullikan charges on some specific atom of the free molecules and their different protonated complexes. It is seen that, charge on proton binding atom slightly increased in complexes relative to their corresponding free molecules, that means they favours protonation according to this particular point of view. Mullikan charge (e) on hetero atom (X) in the  $X-H^+$  complexes vary in the range of 0.552e to  $-0.331e$ , Charge on  $C_\alpha$  in  $C_\alpha-H^+$  complexes has a variation in the range of  $-0.0143e$  to  $-0.38e$ , in case of  $C_\beta-H^+$  complexes,  $-0.187e$  to  $-0.256e$  of Mullikan charges are obtained on  $C_\beta$  atom. These Mullikan charges obtained in this calculation do not correlate properly with the complex stability or PA value of the corresponding complex. Our results suggest that, results obtained in Mullikan population analysis (MPA) are not very reliable to predict the exact protonation site(s) of the molecules.

## Chapter 7

The gas phase lithium and sodium cation affinity and basicity values of studied molecules are collected in **Table 7.1.4**. LCA and SCA's are calculated following equation 4, and LCB and SCB values are calculated with the help of equation 5. Calculated DFT results shows that, both LCA ( $-48.25$  kcal /mole) and SCA ( $-33.82$  kcal/mole) values are observed highest for pyridine then it followed by pyrrole (LCA =  $-42.79$  kcal/mole, SCA=  $-28.17$  kcal/mole), thiophene (LCA =  $-39.79$  kcal /mole, SCA=  $-25.85$  kcal /mole) and furan (LCA =  $-32.37$  kcal /mole, SCA=  $-21.64$  kcal /mole). On the basis of calculated LCA and SCA values, lithium and sodium complex stability of the studied heterocyclic molecules are stand in the order N-hetero > S- hetero > O- hetero. In the present study it is pyridine > pyrrole > thiophene > furan. As per result obtained in this work, the metal cation affinities or metal cation basicities are much lower than proton affinities and gas phase basicities. But order of metal cation affinity and basicity of the molecules are observed same as PA order.

Partial NPA charges on alkali metal cation ( $q_{Li^+}$  and  $q_{Na^+}$ ) of the metal complexes are summarised in **Table 7.1.5**.  $\Delta Q_{Li^+}$  and  $\Delta Q_{Na^+}$  results clear the fact of a significant charge transfer from ligand to metal cation. It may also be expected that, there will be a good correlation between extent of charge transfer and complex stability or metal cation affinity, but this is not found properly, instead the NPA results produced stability order as pyrrole > thiophene > pyridine > furan for lithium complexes. In case of sodium complexes this order appeared as pyrrole  $\geq$  pyridine > thiophene > furan.

Charges on the atom obtained from both MPA and NPA procedure tend to suggest that, two different Lewis acids  $H^+$  and alkali metal cation ( $Li^+$  and  $Na^+$ ) shows to the contrary in nature of bonding with ligand. Proton adds to the molecules gives a covalent sigma( $\sigma$ ) bond with extensive charge transfer where  $H^+$  retains with 0.202 to 0.587 unit of NPA charge. On the other hand the bond formed by alkali cations (with its filled 1S shell) is largely ionic in

nature. Thus the interactions are ion-dipole and ion induced dipole rather than covalent where  $\text{Li}^+$  cation retains with 0.896 to 0.975 e and  $\text{Na}^+$  contain 0.95e to 0.98e of positive charge in the complexes.

Some geometrical parameters for protonated and alkali metal ( $\text{Li}^+$  and  $\text{Na}^+$ ) complexes of the heterocyclic compounds are summarised in **Table 7.1.6**.

**Protonated complexes of pyrrole, furan, thiophene and pyridine:** Pyrrole, furan, thiophene are planar 5-membered heterocyclic molecules. They have three possible protonation sites X,  $\text{C}_\alpha$  and  $\text{C}_\beta$ . Pyridine is a planar 6-membered heterocyclic molecule. Single protonation site (N) has been found for pyridine in our study. Geometrical optimized structures obtained in B3LYP/6-311G (d,p) optimization process of all possible protonated complexes of these heterocyclic molecules are shown in **Figure 7.2.2**. From the data tabulated in **6a** part of **Table 7.1.6**, we observed that,  $\text{X-H}^+$  bond distance is largest in thiophene (1.362Å) and it is found shortest in furan (0.976Å). The  $\angle \text{C}_\alpha - \text{X-H}^+$  bond angle varies in the range 99.7° to 118.37°. Torsion angle ( $\tau$ )  $\angle \text{C}_\beta - \text{C}_\alpha - \text{X-H}^+$  of the complexes revealed that, five membered heterocyclic compounds lost their planarity due to the protonation at X atom, but pyridine remain planar even after  $\text{X-H}^+$  complex formation. Comparison of the geometrical parameters of  $\text{C}_\alpha - \text{H}^+$  and  $\text{C}_\beta - \text{H}^+$  complexes (except pyridine) of all four heterocyclic molecules (**Table 7.1.6b and 7.1.6c**) clears that, geometry of the complexes strongly affected by  $\text{H}^+$  interaction. Both 5 and 6 membered heterocyclic molecules become non-planar after protonation. The  $r(\text{C}_\alpha - \text{H}^+)$  and  $r(\text{C}_\beta - \text{H}^+)$  bond length remain almost same (1.09 to 1.1Å) and 1.1Å in each case. It has been seen in the present work, protonation at all three (X,  $\text{C}_\alpha$ ,  $\text{C}_\beta$ ) sites leads to elongation of  $\text{C}_\alpha - \text{X}$  bond length for pyrrole, furan and thiophene, it remain almost same in pyridine ( $\text{X-H}^+$ ) complex. Due to protonation at  $\text{C}_\alpha$  position of these three molecules,  $\text{C}_1 - \text{X}$  bond length elongated by 0.09Å, it

is 0.06 to 0.11 Å for X-protonated complexes. In case of  $C_\beta$  protonation,  $C_1$ -X bond distance increased by 0.05 Å and 0.04 Å for pyrrole and thiophene while it is decreased 0.1 Å for furan. Little contractions are observed in  $C_1$ - $C_2$  of X- protonated species whereas  $C_1$ - $C_2$  bond length elongated by 0.11 to 0.12 Å for  $C_\alpha$  protonation.  $C_\beta$  protonation induces small contractions of  $C_1$ - $C_2$  in pyrrole, thiophene (0.03 to 0.04 Å) and large elongation (0.11 Å) in furan. We observed,  $C_2$ - $C_3$  bond length increased 0.02 to 0.04 Å and 0.06 to 0.07 Å due to protonation at X and  $C_\beta$  position, while 0.06 to 0.07 Å contraction is observed due to  $C_\alpha$  protonation.

**Figure 7.2.3** shows the optimized structures of lithium and sodium complexes of four studied heterocyclic molecules. Lithium and sodium has different position (in plane, out of plane) depend on the types of heterocyclic molecules. For furan and pyridine, lithium complexes are found in plain (structure **b**, **d**) where a bond is formed between lithium cation and X hetero atom. The X- $Li^+$  bond distance is 1.84 Å and 1.91 Å for furan and pyridine respectively. Dihedral angle ( $\tau$ )  $\angle C-C-X-Li^+$  is found 179.7° and 179.99° in furan and pyridine complex. The out of plane structures are formed for pyrrole (**a**) and thiophene (**c**) where lithium remain above the ring but inclined to the hetero atom (N and S). The distance between X and  $Li^+$  is 2.19 Å and 2.46 Å for pyrrole and thiophene respectively. Out of plane structures are well supported by obtained  $\angle C-C-X-Li^+$  dihedral angle data of **Table 7.1.6d** (62.97° in pyrrole and 61.74° in thiophene). An in-plane structure of thiophene- $Li^+$  complex (**c1**) is also formed by bonding between S and lithium. The S- $Li^+$  bond distance and  $\tau \angle C-C-S-Li^+$  angle are found 2.33 Å and 179.99° respectively. An out-of-plane structure of furan- $Li^+$  complex is also obtained (**b1**) with same optimization energy (- 231.418 hartree) where lithium is inside the ring with the distance 2.16 Å and 2.24 Å from O and  $C_\alpha$  atom. The  $\tau \angle C-C-O-Li^+$  angle (66.47°) reveals the non-planarity of complex.

**Table 7.1.6e** summarised the geometrical parameters of sodium complexes of the same heterocyclic molecules. It is obvious from the results, furan and pyridine form in-plane structures (dihedral angle  $\angle\text{C-C-X-Na}^+ = 179.99^\circ$  and  $180.0^\circ$ ) while out-of-plane structures are obtained for pyrrole and thiophene ( $\tau = -66.14^\circ$  and  $66.8^\circ$ ). The X–Na<sup>+</sup> bond distances are found little higher in all complexes relative to X–Li<sup>+</sup> distances. The bond distance between sodium and X atom is 2.23Å and 2.3Å in furan and pyridine. In pyrrole and thiophene complexes, X–Na<sup>+</sup> distances are found larger; it is 2.87Å in pyrrole and 2.92Å in thiophene.

It is known that, isomers having lowest potential energies are most stable. But there is some exception with the conjugated cyclic planar ring systems. In these cases stability of the molecules depend on their resonance stabilisation energy. DFT method provides some important parameters like hardness ( $\eta$ ), chemical potential ( $\mu$ ), electrophilic index ( $\omega$ ) which are helps to predict the molecular stability and reactivity.<sup>41</sup> The absolute hardness ( $\eta$ ) is defined by  $(I - A)/2$ . Where I is the vertical ionisation energies and A mean the vertical electron affinity. According to Koopman's theory  $I = -\epsilon_{\text{HOMO}}$  (HOMO energy) and  $A = -\epsilon_{\text{LUMO}}$  (LUMO energies). Therefore  $\eta = (\epsilon_{\text{LUMO}} - \epsilon_{\text{HOMO}})/2$ . **Table 7.1.7** contain the values of HOMO and LUMO energies of the studied molecules and their hardness also. In order to understand the stability of the protonated complexes, we also summarized the hardness for the different protonated complexes in same Table. The higher HOMO energy is expected for a more reactive molecule in a reaction with electrophile<sup>42</sup>. The calculated HOMO energies are obtained in this work as pyridine ( $-7.09\text{eV}$ ) < thiophene ( $-6.6\text{eV}$ ) < furan  $-6.38$  < pyrrole ( $-5.75$ ). The HOMO–LUMO energy gap is lower in the protonated complexes relative to the unprotonated species in each case. In an effort to estimate the reactivity of these molecules computationally, we calculate the chemical potential ( $\mu$ ) and electrophilicity index ( $\omega$ ) of each molecule (**Table 7.1.8**). The calculated  $\mu$  and  $\omega$  values are seen lowest for pyrrole ( $-2.39$

ev and 0.840 ev) then followed by furan (-3.09 and 1.46 ev), thiophene (-3.05 and 2.05 ev) and pyridine (-4.02 and 2.61 ev).

## 7.4 Conclusion

From the above theoretical analysis, it can be well concluded that, pyrrole, furan and thiophene exhibits highest PA values when proton attacked at  $C\alpha$  position of the free molecules. Proton preferentially attacked at hetero atom (N) and formed most stable protonated complex of pyridine.  $C\beta$  – protonated complexes are also formed for three five-membered heterocyclic molecules [which can be rationalised by kinetic factor <sup>42</sup>]. PA and basicity results are obtained in this studied shows good agreement with the results found in literature. Protonation at all three position ( $C\alpha$ ,  $C\beta$ , X= N, O, S) leads to form non-planar structures of pyrrole, furan and thiophene. Only pyridine retains with planar form. N-hetero molecules (pyridine and pyrrole) exhibit more affinity and basicity as well for alkali metal cations ( $Li^+$  and  $Na^+$ ) compared to O and S- heterocyclic molecules. Furan and thiophene can form lithium complex with two different geometries. One in-plane and another is out-of-plane structure. Alkali-metal complexes of pyridine are exists with planar structures. Comparing three 5-membered heterocyclic molecules, only furan-sodium complex is planar. Pyrrole-lithium or pyrrole- sodium and thiophene-sodium complexes are found non-planar. Lower value of  $\mu$  and  $\omega$  characterised the more reactivity of the molecule. In the present study reactivity order of the molecules are pyrrole > furan > thiophene > pyridine.

**Table 7.1.1** Different gas phase proton affinities ( $\Delta E$ ) and basicities ( $\Delta G$ ) of pyrrole, furan, thiophene and pyridine obtained from B3LYP/ 6-311G (d,p) method of calculation.

Compound	$\Delta E$ (kcal/mole)	Experimental $\Delta E$ values (kcal/mole)	$\Delta G$ kcal/mole	Experimental $\Delta G$ values (kcal/mole)
Pyrrole(X-H <sup>+</sup> )	-197.5	-209.98*	-190.09	-201.86*
Pyrrole (C <sub><math>\beta</math></sub> - H <sup>+</sup> )	<b>-212.09</b>		-205.82	
Pyrrole (C <sub><math>\alpha</math></sub> - H <sup>+</sup> )	-217.7		-210.96	
Furan (X-H <sup>+</sup> )	-173.8	-192.0*	-171.68	-187.22*
Furan (C <sub><math>\beta</math></sub> - H <sup>+</sup> )	<b>-190.76</b>		-189.75	
Furan (C <sub><math>\alpha</math></sub> - H <sup>+</sup> )	-203.68		-189.75	
Thiophene(X-H <sup>+</sup> )	-179.9	-194.97*	-177.39	-187.63*
Thiophene (C <sub><math>\beta</math></sub> - H <sup>+</sup> )	<b>-194.15</b>		-191.13	
Thiophene (C <sub><math>\alpha</math></sub> - H <sup>+</sup> )	-204.8		-200.67	
Pyridine(X-H <sup>+</sup> )	<b>-232.8</b>	-225.86*	-224.08	-218.25*

X= N, O, S. \* Ref. Hunter, E. P.; Lias, S. G. 1998, *J. Phy. Chem.* 27(3), 413-656.

**Table 7.1.2** Mulliken atomic charges (e) on some selected atoms of the free and protonated complexes of pyrrole, furan, thiophene and pyridine.

Compound	atom	Free compound	(X- H <sup>+</sup> ) complex	C $\alpha$ -H <sup>+</sup> complex	C $\beta$ - H <sup>+</sup> complex
Pyrrole	N	-0.327	-0.331	-0.304	-0.258
	C $\alpha$	0.042	0.0321	-0.0479	----
	3C $\beta$	-0.174	-0.0615	----	-0.251
	11 <sub>H+</sub>	--	0.3202	0.223	0.22
Furan	O	-0.229	-0.2787	-0.152	-0.102
	C $\alpha$	0.065	0.161	-0.0143	----
	2C $\beta$	-0.165	-0.114	----	-0.256
	10 <sub>H+</sub>	--	0.392	0.237	0.244
Thiophene	S	0.263	0.552	0.49	0.573
	C $\alpha$	-0.289	-0.269	-0.38	----
	3C $\beta$	-0.082	-0.0094	----	-0.187
	10 <sub>H+</sub>	--	0.1839	0.251	0.234
Pyridine	N	-0.292	-0.316	----	----
	C $\alpha$	----	0.213	----	----
	C $\beta$	-0.177	-0.198	----	----
	12 <sub>H+</sub>	----	0.294	----	----

\*In case of pyridine, proton always attack at hetero atom (N) so charge on  $\alpha$  or  $\beta$  carbon not given.



**Table 7.1.3** Partial atomic charges on H<sup>+</sup> ion [ $q_{H^+}$ ] (in e unit) in different protonated complex obtained from NPA procedure and charge transfer ( $q_{CT}$ ) from compound to added proton.

Protonated complex	Charge on proton ( $q_{H^+}$ )	Charge transfer ( $q_{CT}$ )
Pyrrole (X-H <sup>+</sup> )	0.456	0.544
Pyrrole (C <sub>α</sub> -H <sup>+</sup> )	0.271	<b>0.729</b>
Pyrrole (C <sub>β</sub> -H <sup>+</sup> )	0.306	0.694
Furan (X-H <sup>+</sup> )	0.587	0.413
Furan (C <sub>α</sub> -H <sup>+</sup> )	0.276	<b>0.724</b>
Furan (C <sub>β</sub> -H <sup>+</sup> )	0.322	0.678
Thiophene (X-H <sup>+</sup> )	0.202	0.798
Thiophene (C <sub>α</sub> -H <sup>+</sup> )	0.299	<b>0.701</b>
Thiophene (C <sub>β</sub> -H <sup>+</sup> )	0.318	0.682
Pyridine (X-H <sup>+</sup> )	0.44	<b>0.56</b>

\*Charge transfer calculated as [Normal charge of proton (1) -  $q_{H^+}$ ]

**Table 7.1.4** Ground state gas phase lithium cation affinities (LCA), basicities (LCB) and sodium cation affinities (SCA), basicities (SCB) of pyrrole, furan, thiophene and pyridine obtained from B3LYP/ 6-311G (d,p) method of calculation.

Compound	LCA	LCB	SCA	SCB
	Kcal/mole	Kcal/mole	Kcal/mole	Kcal/mole
Pyrrole	-42.79	-35.2	-28.17	-21.38 (-14.4)
Furan	-32.37	-28.8	-21.64	-18.51
Thiophene	-39.59	-31.24	-25.85	-18.32
Pyridine	-48.25	-40.97	-33.82	-26.79 (-20.4)

\*Values noted in the parenthesis are experimental results

**Table 7.1.5** Partial atomic charges on metal cation [ $q_{Li^+}$  and  $q_{Na^+}$ ] (in e unit) in different alkali metal complexes and ligand to metal charge transfer ( $\Delta Q_{Li^+}$  and  $\Delta Q_{Na^+}$ ) obtained from NPA procedure.

Compound	Li <sup>+</sup> complex	Charge transfer ( $\Delta Q_{Li^+}$ )	Na <sup>+</sup> complex	Charge transfer ( $\Delta Q_{Na^+}$ )
	$q_{Li^+}$		$q_{Na^+}$	
Pyrrole	0.896	0.104	0.965	0.035
Furan	0.975	0.025	0.98	0.02
Thiophene	0.93	0.07	0.95	0.05
Pyridine	0.96	0.04	0.967	0.033

\*Charge transfer calculated as [Normal charge of metal cation (1) –  $q_M^+$ ] M = Lithium and Sodium.

**Table 7.1.6** Some important geometrical features [bond length in Å, bond angle in degree, dihedral angle ( $\tau$ ) in degree] of the protonated and alkali metal ( $Li^+$  and  $Na^+$ ) complexes of pyrrole, furan, thiophene and pyridine in the ground state.

#### 6a. (X–H<sup>+</sup>) complexes

Complexes	X–H <sup>+</sup>	$\angle C_\alpha-X-H^+$	$\tau (C_\beta-C_\alpha-X-H^+)$
Pyrrole (X–H <sup>+</sup> )	1.028	111.19	+120.53, – 120.52
Furan (X–H <sup>+</sup> )	0.976	119.92	+ 146.38, –146.34
Thiophene (X–H <sup>+</sup> )	1.362	99.70	+105.85, –105.92
Pyridine (X–H <sup>+</sup> )	1.10	118.37	+180.01, – 180.0

#### 6b. (C<sub>α</sub>-H<sup>+</sup>) complexes

Complexes	C <sub>α</sub> -H <sup>+</sup>	$\angle C-C_\alpha-H^+$	$\tau (C-C-C_\alpha-H^+)$
Pyrrole (C <sub>α</sub> -H <sup>+</sup> )	1.09	113.0	118.6
Furan (C <sub>α</sub> -H <sup>+</sup> )	1.09	114.7	116.8
Thiophene (C <sub>α</sub> -H <sup>+</sup> )	1.09	112.7	–119.4
Pyridine (C <sub>α</sub> -H <sup>+</sup> )	1.11	110.0	126.7

6c. (C<sub>β</sub>-H) complexes

Complexes	C <sub>β</sub> -H <sup>+</sup>	< C- C <sub>β</sub> -H <sup>+</sup>	τ (C-C- C <sub>β</sub> -H <sup>+</sup> )
Pyrrole (C <sub>β</sub> -H <sup>+</sup> )	1.10	113.6	-120.01
Furan (C <sub>β</sub> -H <sup>+</sup> )	1.102	114.7	119.58
Thiophene (C <sub>β</sub> -H <sup>+</sup> )	1.103	112.8	-124.5
Pyridine (C <sub>β</sub> -H <sup>+</sup> )	----	---	----

6d. (X-Li<sup>+</sup>) complexes

Lithium complexes	X-Li <sup>+</sup>	< C-X-Li <sup>+</sup>	τ (C-C- X-Li <sup>+</sup> )
Pyrrole	2.19	73.67	62.97
Furan (In-plane)	1.84	126.87	179.7
Furan (out-of-plane)	2.16	75.15	66.47
Thiophene (out of plane)	2.46	64.11	61.74
Thiophene (in-plane)	2.33	133.38	179.99
Pyridine	1.91	121.12	179.99

6e. (X-Na<sup>+</sup>) complexes

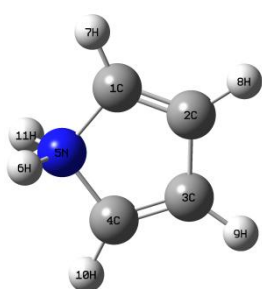
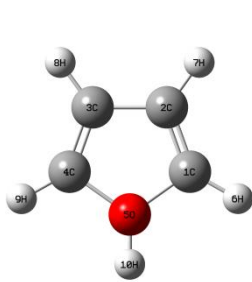
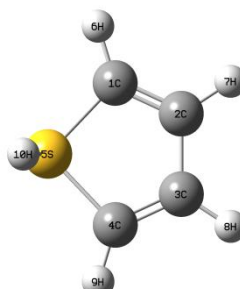
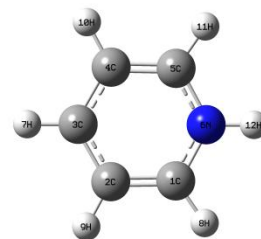
Sodium complexes	X-Na <sup>+</sup>	< C-X-Na <sup>+</sup>	τ (C-C- X-Na <sup>+</sup> )
Pyrrole	2.87	73.16	- 63.14
Furan	2.23	126.89	179.99
Thiophene	2.92	67.76	66.80
Pyridine	2.3	121.27	180.0

**Table 7.1.7** Computed hardness ( $\eta$ ) =  $(I - A)/2 = (\epsilon_{\text{LUMO}} - \epsilon_{\text{HOMO}})/2$  of the protonated complexes in the ground state.  $\epsilon_{\text{HOMO}}$  and  $\epsilon_{\text{LUMO}}$  energies are in hartree unit. (1 hartree = 27.21ev)

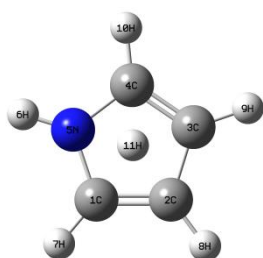
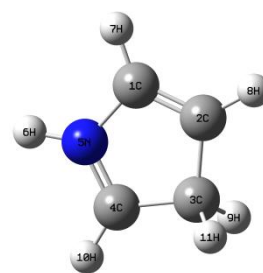
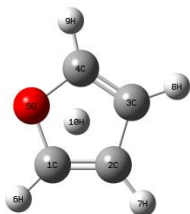
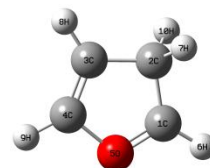
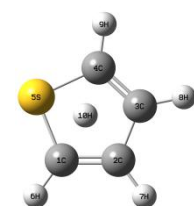
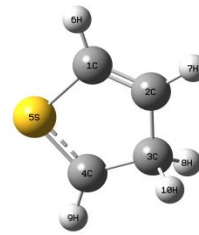
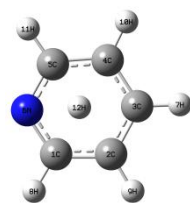
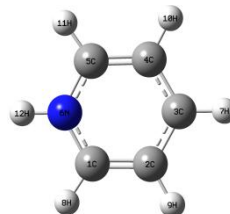
Free molecules	$\epsilon_{\text{HOMO}}$	$\epsilon_{\text{LUMO}}$	$\eta$ (ev)
Pyrrole	-0.2124	0.0365	3.38
Furan	-0.2347	0.00676	3.28
Thiophene	-0.2425	-0.0182	3.05
Pyridine	-0.2609	-0.0348	3.07
Protonated complexes	$\epsilon_{\text{HOMO}}$	$\epsilon_{\text{LUMO}}$	$\eta$ (ev)
Pyrrole ( $\text{C}_\alpha\text{-H}^+$ )	-0.4898	-0.2849	2.78
Pyrrole ( $\text{C}_\beta\text{-H}^+$ )	-0.4693	-0.2781	2.60
Furan ( $\text{C}_\alpha\text{-H}^+$ )	-0.5298	-0.3211	2.83
Furan ( $\text{C}_\beta\text{-H}^+$ )	-0.4982	-0.3171	2.46
Thiophene ( $\text{C}_\alpha\text{-H}^+$ )	-0.4893	-0.3183	2.32
Thiophene ( $\text{C}_\beta\text{-H}^+$ )	-0.4803	-0.3142	2.25
Pyridine ( $\text{X-H}^+$ )	-0.4845	-0.2648	2.98

**Table 7.1.8** Calculated chemical potential ( $\mu$ ) =  $(\epsilon_{\text{LUMO}} + \epsilon_{\text{HOMO}})/2$  and electrophilicity ( $\omega$ ) =  $\mu^2 / 2\eta$  of the heterocyclic molecules in the ground state. Unit in ev).

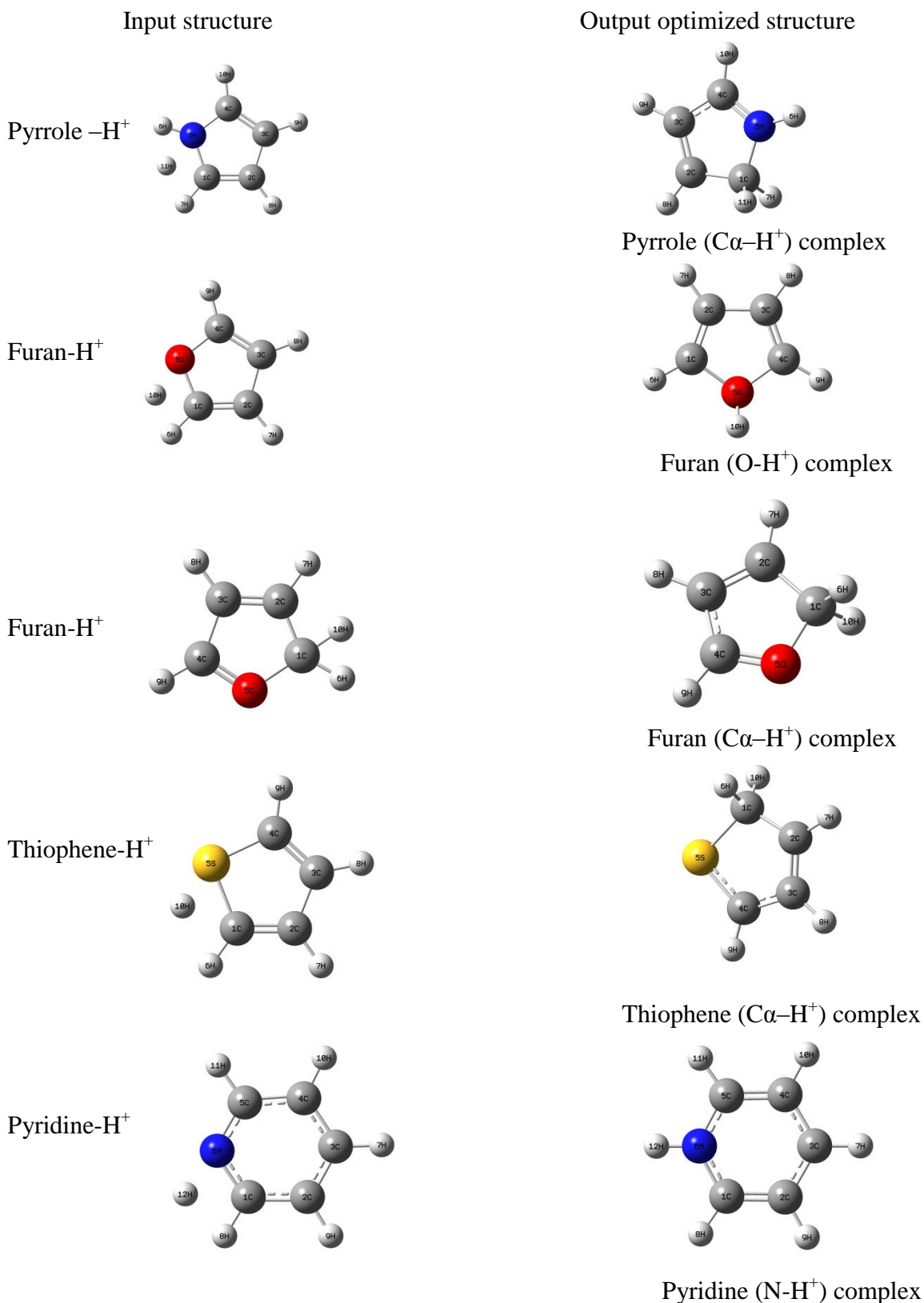
Compound	$\mu$ (ev)	$\omega$ (ev)	$\eta$ (ev)
Pyrrole	-2.39	0.840	3.38
Furan	-3.09	1.46	3.28
Thiophene	-3.54	2.05	3.05
Pyridine	-4.02	2.61	3.07

Pyrrole (X-H<sup>+</sup>)Furan (X-H<sup>+</sup>)Thiophene (X-H<sup>+</sup>)Pyridine (X-H<sup>+</sup>)

Path –I: Gas phase optimized structures (Proton directly bonded with hetero[X] atom in initial input. X= N, O, S

Initial input [Pyrrole-H<sup>+</sup>]Pyrrole (C<sub>β</sub>-H<sup>+</sup>) complexInitial input [Furan-H<sup>+</sup>]Furan (C<sub>β</sub>-H<sup>+</sup>) complexInitial input [Thiophene-H<sup>+</sup>]Thiophene (C<sub>β</sub>-H<sup>+</sup>) complexInitial input [Pyridine-H<sup>+</sup>]Pyridine (N-H<sup>+</sup>) complex

Path –II: Gas phase optimized structures (Proton placed inside the ring in initial input.



Path –III: Gas phase optimized structures (Proton placed outside the ring in between X and  $\alpha$ -C in initial input).

**Figure 7.2.2** Optimized structures of the protonated complexes (different sites of protonation) pyrrole, furan, thiophene and pyridine.

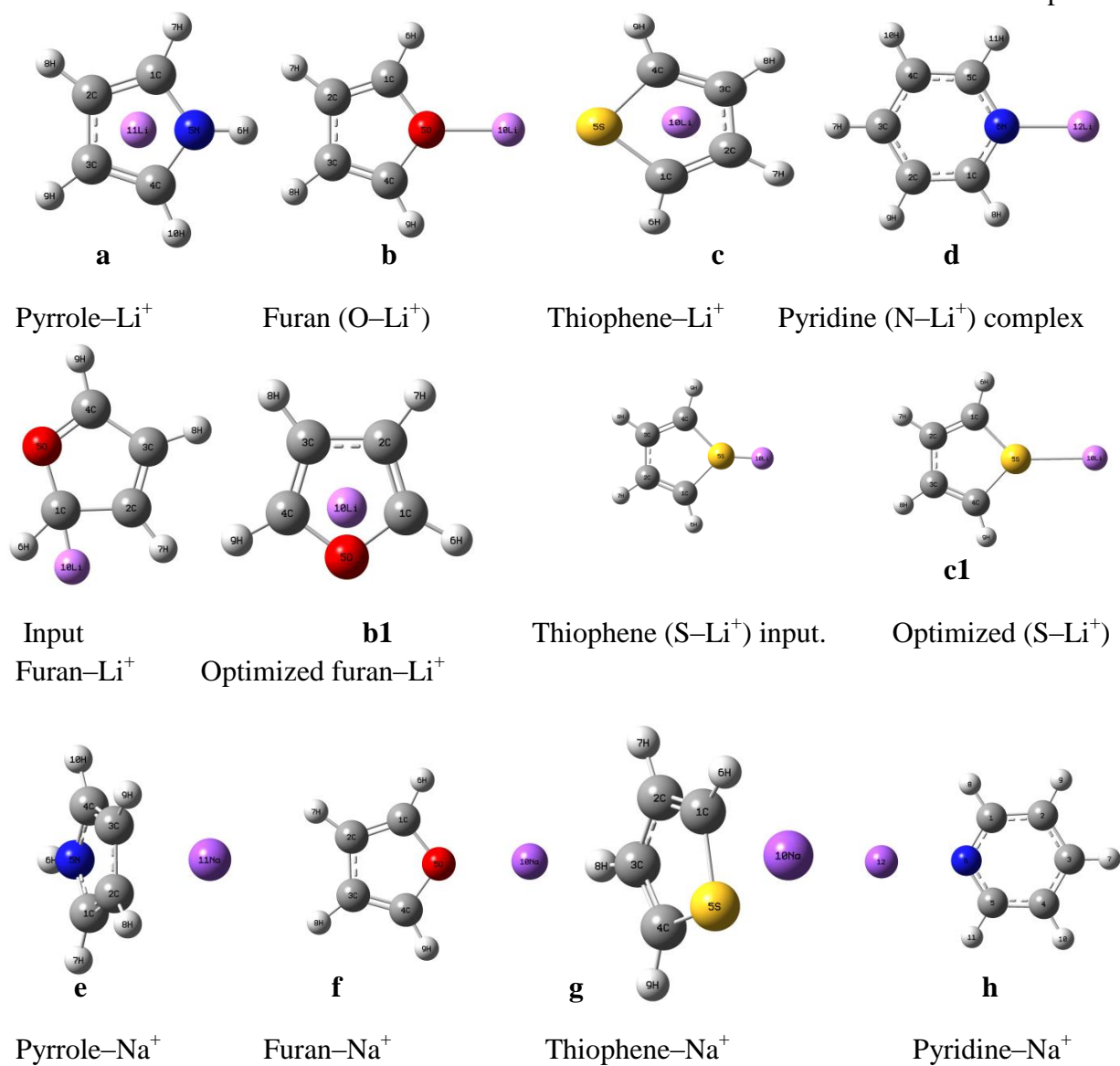


**Figure 7.2.3** Optimized structures of Li<sup>+</sup> and Na<sup>+</sup> complexes of pyrrole, furan, thiophene and pyridine.

**a: out-of-plane, b: In-plane, b1: out-of-plane, c: out-of-plane, c1: In-plane d: In-plane, e: out-of-plan, f: out-of-plane, g: In-plane, h: out-of-plane, i: In-plane.**

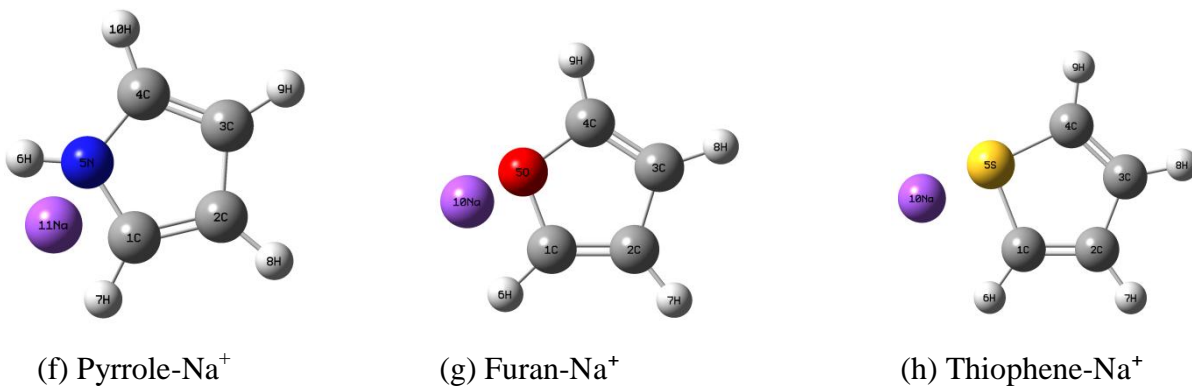


**Figure 7.2.4** Geometry of sodium complexes before optimisation.

## 7.5 References

- (1) (a) Hunter, E. P.; Lias, S. G. *J. Phys. Chem. Ref. Data* **1998**, *27*, 413. (b) NIST WebBook,
- (2) Smith, M. B.; March, J. *Advanced Organic Chemistry: Reactions, Mechanisms and Structure*, Wiley, New York, 2001.
- (3) Kuck, D. *Mass Spectrom. Rev.* **1990**, *9*, 583.
- (4) Roitzsah, M. R.; Lippert, B. *J. Am. Chem. Soc.* **2004**, *126*, 2421.
- (5) Marino, G. *Adv. Heterocycl. Chem.* **1971**, *13*, 235.
- (6) Marino, G. *Chem. Heterocycl. Comp.* **1973**, *9*, 537.
- (7) Larson, J. W.; McMahon, T. B. *J. Am. Chem. Soc.* **1982**, *104*, 6255.
- (8) Meot-Ner, M. *J. Am. Chem. Soc.* **1984**, *106*, 1257.
- (9) Meot-Ner, M.; Ross, M. M.; Campana, J. E. *J. Am. Chem. Soc.* **1985**, *107*, 4839.
- (10) Valencia, D.; Klimova, T.; Isidoro, G.-C. *Fuel*, **2012**, *100*, 177.
- (11) Lorenz, U. J.; Lemaire, J.; Maitre, P.; Crestoni, M.-E.; Fornani, S.; Dopfer, O. *Int. J. Mass Spectrom.* **2007**, *267*, 43.
- (12) Sun, Y.; Sun, H. *J. Mol. Model.* **2013**, *19*, 1641.
- (13) Salman, S. R. *Chemistry of material Research* **2014**, *6(4)*, 53.
- (14) Junyang, W. U.; Yan, H.; Chen, H.; Zhong, A.; Cao, W. *Comp. Theor. Chem.* **2012**, *1000*, 52.
- (15) Hiraoka, K.; Takimoto, H.; Yamabe, S. *J. Am. Chem. Soc.* **1987**, *109*, 7346.
- (16) Burk, P.; Koppel, I. A.; Koppel, I.; Kurg, R.; Gal, J.-F.; Maria, P.-C.; Herreros, M.; Notario, R.; Abboud, J.-L. M.; Anvia, F.; Taft, R. W. *J. Phys. Chem. A* **2000**, *104*, 2824.
- (17) Pandit, S.; De, D.; De, B. R. *J. Mol. Struct. (Theochem)* **2006**, *760*, 245.
- (18) Senapati, U.; De, D.; De, B. R. *Indian J. Chem.* **2008**, *47A*, 548.



- (19) Pandit, S.; De, D.; De, B. R. *J. Mol. Struct. (Theochem)* **2007**, 819, 160.
- (20) Senapati, U.; De, D.; De, B. R. *J. Mol. Struct. (Theochem)* **2007**, 808, 157.
- (21) Senapati, U.; De, D.; De, B. R. *Mol. Simul.* **2010**, 36(6), 448.
- (22) Bhome, D. K.; Hemsworth, R. S.; Rundle, H. I.; Schiff, H. I. *J. Chem. Phys.* **1973**, 58, 3504.
- (23) Beauchamp, J. L. *Interaction between Ions and Molecules*. (Plenum, New York) **1974**, pp. 413, 459, 489.
- (24) Yamadagni, R.; Kebarle, P. J. *J. Am. Chem. Soc.* **1973**, 96, 727.
- (25) Bhome, D. K.; Mackay, G. I.; Schiff, H. I.; Hemsworth, R. S. *J. Chem. Phys.* **1974**, 61, 2175.
- (26) Solomon, J. J.; Meot Ner, M.; Fiele, F. M. *J. Am. Chem. Soc.* **1974**, 96, 3727.
- (27) Long, J. W.; Franklin, L. L.; *J. Am. Chem. Soc.* **1974**, 96, 2320.
- (28) Brauman, J. I.; Blair, L. K. *J. Am. Chem. Soc.* **1970**, 92, 5986.
- (29) Wieting, R. D.; Staley, R. H.; Beauchamp, J. L. *J. Am. Chem. Soc.* **1974**, 96, 7552.
- (30) Staley, R. H.; Beauchamp, J. L. *J. Am. Chem. Soc.* **1975**, 96, 3727.
- (31) Frisch, M. J.; Trucks, G. W.; Schlegel, H. B.; Scuseria, G. E.; Robb, M. A.; Cheeseman, J. R.; Scalmani, G.; Barone, V.; Mennucci, B.; Petersson, G. A.; Nakatsuji, H.; Caricato, M.; Li, X.; Hratchian, H. P.; Izmaylov, A. F.; Bloino, J.; Zheng, G.; Sonnenberg, J. L.; Hada, M.; Ehara, M.; Toyota, K.; Fukuda, R.; Hasegawa, J.; Ishida, M.; Nakajima, T.; Honda, Y.; Kitao, O.; Nakai, H.; Vreven, T.; Montgomery, J. A. Jr.; Peralta, J. E.; Ogliaro, F.; Bearpark, M.; Heyd, J. J.; Brothers, E.; Kudin, K. N.; Staroverov, V. N.; Kobayashi, R.; Normand, J.; Raghavachari, K.; Rendell, A.; Burant, J. C.; Iyengar, S. S.; Tomasi, J.; Cossi, M.; Rega, N.; Millam, J. M.; Klene, M.; Knox, J. E.; Cross, J. B.; Bakken, V.; Adamo, C.; Jaramillo, J.; Gomperts, R.; Stratmann, R. E.; Yazyev, O.; Austin, A. J.; Cammi, R.; Pomelli, C.;

## Chapter 7

Ochterski, J. W.; Martin, R. L.; Morokuma, K.; Zakrzewski, V. G.; Voth, G. A.; Salvador, P.; Dannenberg, J. J.; Dapprich, S.; Daniels, A. D.; Farkas, O.; Foresman, J. B.; Ortiz, J. V.; Cioslowski, J.; Fox, D. J.; Gaussian 09, Revision A.02, Gaussian, Inc., Wallingford CT, 2009.

- (32) Ma, J. C.; Dongherty, D. A. *Chem. Rev.* **1997**, *97*, 1303.
- (33) Karlin, S.; Zuker, M.; Brocchieri, L. *J. Mol. Biol.* **1994**, *239*, 227.
- (34) Livnah, O.; Stura, E. A.; Johnson, D. L.; Middleton, S. A.; Mulchany, L. S.; Wrighton, N. C.; Dower, W. J.; Jolliffe, L. K.; Wilson, I. A. *Science* **1996**, *255*, 306.
- (35) Cervenansky, C.; Engstorm, A.; Karlsoon, E. *Eur. J. Biochem.* **1995**, *229*, 270.
- (36) Novotny, J.; Bruccoleri, R. E.; Saul, F. A. *Biochemistry* **1989**, *28*, 4735.
- (37) Lippard, S. J.; Berg, J. M. *Principles of Bioinorganic Chemistry*, University Science Books, Mill Valley, CA, **1994**.
- (38) Kaim, W.; Schwederski, B. *Bioinorganic Chemistry: Inorganic Elements in the Chemistry of Life*, Wiley, Chichester, **1994**.
- (39) Lee, C.; Yang, W.; Parr, R. G. *Phys. Rev.* **1988**, *B37*, 785.
- (40) Ventura, O. N.; Rama, J. B.; Turi, L.; Dannenberg, J. J. *J. Phys. Chem.* **1995**, *99*, 131.
- (41) Geerlings, P.; De Proft, F.; Langenaeker, W. *Chem. Rev.* **2003**, *103*, 1793.
- (42) Angelini, G.; Laguzzi, G.; Sparapani, C.; Speranza, M. *J. Am. Chem. Soc.* **1984**, *106*,

## **CHAPTER 8**

**The ground state Cu<sup>2+</sup>ion affinities of Glycine, Alanine and Cysteine in gas and aqueous phase: A DFT based computational study.**



## Abstract

A detail study of  $\text{Cu}^{2+}$  ion affinities of the amino acids namely Glycine (Gly), Alanine (Ala) and Cysteine (Cys) and their  $\text{Cu}^{2+}$  complexes have been investigated using density functional theory. Interactions of  $\text{Cu}^{2+}$  ion with oxygen, nitrogen and sulphur (for cysteine) of the selected amino acids have been optimized. The results show that complex formation reactions are exothermic in both gas and aqueous phase and the local stereochemical disposition of  $\text{Cu}^{2+}$  ion is almost the same in each amino acid. The computed  $\text{Cu}^{2+}$  affinity for both O- $\text{Cu}^{2+}$  and N- $\text{Cu}^{2+}$  interaction in gas phase is in this order  $\Delta E_{\text{Cys}} > \Delta E_{\text{Ala}} > \Delta E_{\text{Gly}}$ . In aqueous phase  $\text{Cu}^{2+}$  ion affinity for O- $\text{Cu}^{2+}$  interaction follow the same order as above, whereas in N- $\text{Cu}^{2+}$  interaction it differs as  $\Delta E_{\text{Ala}} \geq \Delta E_{\text{Cys}} > \Delta E_{\text{Gly}}$ . In N- $\text{Cu}^{2+}$  interaction Zwitterterionic complexes ( $\text{Cu}^{2+}$  bind with both nitrogen and carbonyl oxygen atom) have been formed. The optimization energies are estimated to be lower relative to the other interactions and the  $\text{Cu}^{2+}$  ion affinities have been predicted more. The results have been well supported by the natural population analysis (NPA) of the atoms and hardness parameters. The charge, energetics, structural and electronic properties of the complexes indicate that the interaction between the  $\text{Cu}^{2+}$  with the carbonyl oxygen and the amino nitrogen of free amino acids is predominantly a covalent interaction in gas phase and which becomes more ionic in aqueous phase.

## 8.1 Introduction

Glycine, alanine and cysteine have important roles as model systems due to the small in structure compared to the other amino acids. They contain a carboxyl group (COOH), an amino group (NH<sub>2</sub>) and a side group (R). The side group increases gradually from glycine (R = H) to alanine (R = CH<sub>3</sub>) and to cysteine (R = CH<sub>2</sub>SH). Copper ion is responsible for oxidation, dioxygen transport and charge transfer.<sup>1</sup> It also plays an important role in many bio-chemical processes. The metal binding affinity to the biological fragments has remarkable attention from both experimental<sup>2-6</sup> and theoretical<sup>7-11</sup> points of view. The role of a metal ion in bio-chemical process can be known from thermodynamic properties of metal ion-protein interaction.<sup>12</sup> In gaseous phase, binding energies for Cu<sup>+</sup> ion-amino acid complexes have been studied earlier. The Cu<sup>+</sup> ion affinities for glycine, serine and cysteine also have been studied theoretically by Hoyau.<sup>13</sup> The metal ions (Mg<sup>2+</sup>, Ca<sup>2+</sup>, Ni<sup>2+</sup>, Cu<sup>2+</sup> and Zn<sup>2+</sup>) effect and ion affinities for arginine complexes have been reported by Remko<sup>14</sup> where arginine showed strongest affinity by Cu<sup>2+</sup> cation. Interaction of Cu<sup>+</sup> and Cu<sup>2+</sup> ions with  $\alpha$ -alanine system has been reported by Nino Russo.<sup>15</sup>

The stability of the metal complexes and preferable binding sites are different, depending on the nature of the cation. In general, open-shell system Cu<sup>2+</sup> (d<sup>9</sup>) is less stable than Cu<sup>+</sup> (d<sup>10</sup>) system, but this is not true always. However, in aqueous phase Cu<sup>+</sup> ion disproportionate to Cu<sup>2+</sup> with an unusual oxidation state and become less stable than Cu<sup>2+</sup> state. Different theoretical studies on amino acids– copper complexes found in literature.<sup>16,17</sup> So far, detailed, systematic comparative studies on the interactions between Cu<sup>2+</sup> with glycine or alanine or cysteine are rather scarce.

To the best of our knowledge, no more theoretical works have been performed on Cu<sup>2+</sup> – amino acid complexes in gas phase as well as in aqueous phases together. A systematic study

on metal ion-amino acid complexation is important for better understanding of metal-protein binding mechanism in living systems. Therefore, in order to investigate the nature of binding interactions of  $\text{Cu}^{2+}$  ion with three amino acids glycine, alanine and cysteine and to obtain some quantitative idea about relative  $\text{Cu}^{2+}$  ion affinities, we have performed a DFT study on the  $\text{Cu}^{2+}$  – glycine,  $\text{Cu}^{2+}$  – alanine and  $\text{Cu}^{2+}$  – cysteine complexes. The conformational behaviour of amino acids is essential to understand their dynamic role in protein formation. However, amino acids have a zwitterionic structure in their solid state. Consequently, to obtain the neutral structure of amino acids, studies are required in the gas and aqueous phases. The solvent effect on the energetics and geometries of the complexes has been observed carefully in the present work. We have also focused our attention on the binding sites of the amino acid with  $\text{Cu}^{2+}$  ion and on the optimized geometrical structure of the complexes.

## 8.2 Computational details

DFT calculations were performed at the B3LYP level with 6-311G (d,p) internal basis set for all atoms using the Gaussian 09W program<sup>18</sup> package. In order to understand the structural behaviour of the free bases and different  $\text{Cu}^{2+}$  complexes, we carried out PCM<sup>19</sup> (polarisable continuum model) geometry optimization process at the same level of theory. Water was used as solvent. Both natural population analysis (NPA) and Mulliken population analysis<sup>20</sup> were applied to determine equivalent charges on atoms of the free bases and their metal complexes. The natural atomic charges have been calculated to analyze the nature of the bonding of  $\text{Cu}^{2+}$ -amino acids complexes.

It has been shown that the density functional method provides accurate results for many transition metal-containing systems<sup>21-23</sup>. Hence this method is suitable for studying metal ion complexes. Unrestricted open shell methods were used to calculate the  $\text{Cu}^{2+}$  systems.

## Chapter 8

Equilibrium geometries for all the structures were fully optimized without any symmetry restrictions.

In order to minimise basis set super position error (BSSE), final energetic were obtained at 6-311(G) d,p basis set level. Use of 6-311(G) d,p basis set ensures that the magnitude of the computed BSSE values is small, it is (2.0 to 2.5 kcal / mole) for complexes. Since this is a comparative study and energetic values discussed in this paper are relative to a particular species. Therefore errors occurred in the results will be cancelled and does not affect more on  $\text{Cu}^{2+}$  affinities of the complexes and stability order as well. Thus we neglected this in our study.

### 8.3 Results and Discussion

We have studied the interaction of  $\text{Cu}^{2+}$  ion with N atom of amino group ( $\text{Cu}^{2+}$  directly bonded with N in initial input) and O atom of carbonyl group ( $\text{Cu}^{2+}$  directly bonded with carbonyl O in initial input) of each amino acid. In addition to  $\text{N-Cu}^{2+}$  and  $\text{O-Cu}^{2+}$  interactions, we have studied the interaction of  $\text{Cu}^{2+}$  with S atom of  $\text{CH}_2\text{SH}$  side group in cysteine. The optimization energy is found to be lowest in  $\text{N-Cu}^{2+}$  case compared to  $\text{O-Cu}^{2+}$  or  $\text{S-Cu}^{2+}$ . The highest  $\text{Cu}^{2+}$  ion affinity to nitrogen indicates that  $\text{Cu}^{2+}$  ion preferably bind with  $-\text{NH}_2$  group of amino acids to form stable complexes. This is because of the lone pair of nitrogen is loosely bind and lone pair of carbonyl oxygen atom are more tightly bind, then  $\text{Cu}^{2+}$  ion interact more easily with amino N atom. The stability of co-ordinated complexes depends on the hard-soft nature of metal and ligand (according to HSAB theory). Being borderline acid,  $\text{Cu}^{2+}$  ion forms most stable complex with borderline donor nitrogen. This is exactly seen in our study. Results obtained from  $\text{S-Cu}^{2+}$  complexes of cysteine are not discussed widely, because comparatively lower minimum optimization energies are found from  $\text{O-Cu}^{2+}$ ,  $\text{N-Cu}^{2+}$  optimization process. Computed total energies (hartree) of the free



amino acids (B) and their complexes (B-Cu<sup>2+</sup>) and the computed Cu<sup>2+</sup> ion affinities ( $\Delta E$ , kcal/mole) are tabulated in **Table 8.1.1** in both phases. In both phases,  $\Delta E$  values are higher for N-Cu<sup>2+</sup> complex than that of O-Cu<sup>2+</sup> complex. The  $\Delta E$  values are increased by -20.269, -14.872, -19.603 kcal/mole in gas phase and it is -6.275, -38.027, -26.293 kcal/mole in aqueous phase for glycine, alanine and cysteine respectively.

**Table 8.1.2** summarised the computed net charge on carbonyl O (>C = O) atom and N atom of amino group of the free amino acids and their complexes in their ground state in gas and aqueous phases. It also reports the computed net charge on Cu<sup>2+</sup> at the ground state of Cu<sup>2+</sup> complexes in the both phases. The computed net charge on the Cu<sup>2+</sup> vary in the range of 0.9187 to 1.0637 e in gas phase, on solvation, the values are slightly increased and they are in the range of 1.2918 to 1.3654 e. The values of the atomic charges on Cu in O-Cu<sup>2+</sup> complexes indicate that some migration of electron density to the metal ion has taken place. Similarly for N-Cu<sup>2+</sup> complexes, the computed net charge on the Cu vary in the range of 1.1708 to 1.3805 e in gas and it ranges from 1.4932 to 1.5099 e in aqueous phase. This migration is not local and originates from all over the molecule which is clearly reflected from the computed net charge on O and N atom of the Cu<sup>2+</sup> complexes. The carbonyl O atom and amino N still carries a net negative charge, which is increased relative to the free amino acids in both phases.

The important component of the valence interaction is the charge transfer (CT). We have used this quantity to determine the degree of valence interaction in the present cation-dipole complexes (B-Cu<sup>2+</sup>). The calculated atomic charges and the net amount of CT from the base to Cu<sup>2+</sup> are given in **Table 8.1.3**. We have seen that the degree of CT increases from gas phase to aqueous phase. We also observed that, for the N-Cu<sup>2+</sup> complexes, the degree of CT is more than that of O-Cu<sup>2+</sup> complexes. The results revealed that the N-Cu<sup>2+</sup> interactions are more ionic.

The partial NPA charges on metal ion in all the metal-amino acid complexes and ligand to metal charge transfer ( $Q_{CT}$ ) in both gas and in aqueous phases are summarized in **Table 8.1.4**. The results show that there is a significant charge transfer from ligand to metal ion. A good correlation between extent of charge transfer and complex stability were observed. In both phases, the extent of charge transfer in both complexes follow the decreasing order as cysteine > alanine > glycine. This is well supported by the computed  $Cu^{2+}$  affinity values.

We have searched for the possibility of the existence of correlation with a single global parameter of the entire molecule. As the global parameter, we have chosen the hardness,  $\eta = (I - A)/2 = (\epsilon_{LUMO} \sim \epsilon_{HOMO})/2$  listed in **Table 8.1.7**. In both phases hardness values of glycine and alanine are almost same and it is found to be slightly less for cysteine. Obtained  $\eta$  values clear that, a perfect correlation between the hardness and  $Cu^{2+}$  ion affinity in the series could be made. In this series, glycine has the highest  $\eta$  value whereas its  $Cu^{2+}$  ion affinity is lowest.

It also shows that both pre- and post-complex correlations with local charge densities in the immediate neighbourhood of the complex formation site are weak. Therefore it can be anticipated that the  $Cu^{2+}$  ion affinities of these amino acids cannot be modelled or described by local properties of the carbonyl moiety of the carboxyl group and amino group of the amino acids only. At this level of calculation, while not perfect, there is a good linear correlation between the charge on oxygen and nitrogen of the free amino acids with the  $Cu^{2+}$  affinities. Still it must be shaped strongly by distant atom contribution in addition to the contribution from the carbonyl and amino group respectively.

In **Table 8.1.5** and **Table 8.1.6** we have highlighted some important optimized geometrical parameters of the free amino acids and their complexes. The local stereochemical

characteristics at or around the carbonyl moiety of carboxyl group and  $-\text{NH}_2$  group of amino acids are almost same in both phases. The C–O bond length is found to be almost same for all the amino acids. The  $\angle \text{C–C–O}$  bond angles for free amino acids are very nearly identical, which are reported in the range  $122.666^\circ$  to  $125.148^\circ$  and  $123.189^\circ$  to  $125.5^\circ$  in gas and aqueous phase respectively. In both phases the C–O and C–N bond length is increased upon  $\text{Cu}^{2+}$  ion complex formation relative to the free amino acids. The O– $\text{Cu}^{2+}$  bond length is found to be almost same for all the complexes. In O– $\text{Cu}^{2+}$  complexes (where carbonyl oxygen directly involved in the bonding with  $\text{Cu}^{2+}$  ion) the O– $\text{Cu}^{2+}$  bond distance decreased little bit ( $0.027$  to  $0.047\text{\AA}$ ) from gas to aqueous phase. Similarly, the N– $\text{Cu}^{2+}$  bond distance in N– $\text{Cu}^{2+}$  complexes (where nitrogen directly involved in the bonding with  $\text{Cu}^{2+}$  ion) also decreased by  $0.06$  to  $0.19\text{\AA}$  from gas to aqueous phase. The  $\angle \text{C–C–O}$  bond angles are also found to be almost identical for all the complexes. Similarly, the torsion angle  $\tau(\text{C–C–O–Cu}^{2+})$  is nearly identical for  $\text{Cu}^{2+}$  complexes of glycine and alanine and these are  $-178.611^\circ$  and  $-179.998^\circ$  showing loss of planarity. For cys– $\text{Cu}^{2+}$  complex the  $\tau$  value is  $174.860^\circ$  which reveal its planar structure. Exact reverse cases are observed in aqueous phase. The carbonyl chromophore of carboxyl group near invariant stereochemistry round the complex formation site of each free amino acid tend to suggest that, the entire contribution to  $\text{Cu}^{2+}$  ion affinity cannot be modelled properly unless contribution from far away centres are taken into account. We observed from the geometrical structures of corresponding  $\text{Cu}^{2+}$  complexes of three amino acids, they form monocoordinated species when  $\text{Cu}^{2+}$  ion directly bonded with carboxyl oxygen in gas as well as in aqueous phase. We also observed, bicoordinated (with N and O atom) optimized geometries are formed in aqueous phase when  $\text{Cu}^{2+}$  ion is directly bonded with amino nitrogen in the initial input. Optimized geometries in the gas phase and aqueous phase of the studied amino acids and their different  $\text{Cu}^{2+}$  complexes are shown in **Figure 8.2.1**. From **Table 8.1.1** we observed that, gas phase  $\Delta E$  values of the amino acids in

## Chapter 8

O–Cu<sup>2+</sup> interactions vary in the range –205.948 to –226.342 kcal /mole and in aqueous phase it ( $\Delta E$  value) varies in the range of – 67.143 to –78.689 kcal /mole. For N–Cu<sup>2+</sup> interactions  $\Delta E$  values are in the range of –226.217 to –245.983 kcal /mole and –73.418 to –107.115 kcal /mole in gas and aqueous phase respectively. From **Table 8.1.1** it is also clear that the amino acids and their complexes are stabilised in water. The dipole moment of amino acid is increased in water indicating that the charge separation is higher in water as is expected for a polar molecule. This is supported by the data from **Table 8.1.2** where it is found that the charge density on O-atoms and N-atoms are much more increased than that in the gas phase. From  $\Delta E$  values, it is clear that the gas phase and aqueous phase O–Cu<sup>2+</sup> and N–Cu<sup>2+</sup> complex formation turns to be exothermic. **Table 8.1.2** shows that the charge densities on the carbonyl oxygen atom and amino nitrogen atom before the complex formation are almost similar. In the complexes, the charge density on carbonyl oxygen atom ( $q_{O-}$ ) and amino nitrogen atom ( $q_{N-}$ ) has been increased for all the amino acids in both phases. The magnitude of charges of the complexes indicate that, interaction of Cu<sup>2+</sup> with the carbonyl oxygen atom and amino nitrogen atom in the ground state is predominantly a covalent interaction in gas phase. This also shows that both pre- and post-complex correlations with local charge densities in the immediate neighbourhood of the complex formation site are weak. It can therefore be anticipated that the Cu<sup>2+</sup> ion affinities of these amino acids cannot be modelled or described by local properties of the carbonyl and amino group only. The Cu<sup>2+</sup> ion affinities must be shaped strongly by distant atom contribution in addition to the contribution from the carbonyl group and amino group.

## 8.4 Conclusion

From the above theoretical studies, it can be concluded that, the gas phase and aqueous phase  $\text{Cu}^{2+}$  ion affinity of amino acids are spontaneous. The electronic properties of the complexes indicate that there is pre-dominance of co-valent and ionic interaction in gas and aqueous phase respectively. Complexes formed (Zwitterionic) due to  $\text{N-Cu}^{2+}$  interactions are more stable than that of  $\text{O-Cu}^{2+}$  complexes in both phases. The overall reactivity is fully explained by the distant atom contribution in addition to the contribution from the carbonyl moiety of carboxyl group and amino group of amino acids.

**Table 8.1.1** Computed total energies (hartree) of the free amino acids and their  $\text{Cu}^{2+}$  complexes ( $\text{BCu}^{2+}$ ) and  $\text{Cu}^{2+}$  ion affinities [ $\Delta E$ ] in hartree unit for both gas and aqueous phase at the equilibrium geometry of the ground state.  $E_{\text{Cu}^{2+}(\text{gas})} = -1639.3973$  hartree,  $E_{\text{Cu}^{2+}(\text{aqueous})} = -1639.9410$  hartree. 1 hartree = 627.5095 Kcal/ mole = 27.2116 ev.

Molecule	Gas phase			Aqueous Phase		
	Total energy(hartree)		$\Delta E$ (kcal/mole)	Total energy(hartree)		$\Delta E$ (kcal/mole)
	<b>B</b>	<b>BCu<sup>2+</sup> (O–Cu<sup>2+</sup>)</b>		<b>B</b>	<b>BCu<sup>2+</sup> (O–Cu<sup>2+</sup>)</b>	
Glycine	-284.5149	-1924.2404	-205.948	-284.5248	-1924.5728	-67.143
Alanine	-323.8334	-1963.5781	-217.996	-323.8466	-1963.8977	-69.088
Cysteine	-722.0495	-2361.8075	-226.342	-722.0621	-2362.1285	-78.689
Molecule	<b>B</b>	<b>BCu<sup>2+</sup> (N–Cu<sup>2+</sup>)</b>		<b>B</b>	<b>BCu<sup>2+</sup> (N–Cu<sup>2+</sup>)</b>	
Glycine	-284.5149	-1924.2727	-226.217	-284.5248	-1924.5828	-73.418
Alanine	-323.8334	-1963.6018	-232.868	-323.8466	-1963.9583	-107.115
Cysteine	-722.0495	-2361.8388	-245.983	-722.0621	-2362.1704	-104.982
Molecule	<b>B</b>	<b>BCu<sup>2+</sup> (S–Cu<sup>2+</sup>)</b>		<b>B</b>	<b>BCu<sup>2+</sup> (S–Cu<sup>2+</sup>)</b>	
Cysteine	-722.0495	-2361.7997	-221.761	-722.0621	-2362.1184	-72.351

**Table 8.1.2** Computed net mulliken charge (unit 'e') on O-atom ( $q_{O^-}$ ) and charge on N-atom ( $q_{N^-}$ ) of free amino acids and their  $Cu^{2+}$  complexes and the computed net charge on  $Cu^{2+}$  ion ( $q_{Cu^{2+}}$ ) of  $BCu^{2+}$  and also dipole moment,  $\mu$  (debye unit) of amino acids for both gas phase and aqueous phase in the equilibrium ground state.

Molecule	$q_{O^-}$ (Gas Phase)		$q_{O^-}$ (Aq. Phase)		Gas phase	Aq. phase	$\mu$ in gas phase	$\mu$ in aq. phase
	B	$BCu^{2+}(O-Cu^{2+})$	B	$BCu^{2+}(O-Cu^{2+})$	$q_{Cu^{2+}}$	$q_{Cu^{2+}}$	B	B
Glycine	-0.3369	-0.4859	-0.3772	-0.4730	1.0637	1.3654	2.0037	2.9458
Alanine	-0.3171	-0.4949	-0.3631	-0.5039	1.0237	1.2918	4.1481	5.9648
Cysteine	-0.3162	-0.4747	-0.3634	-0.4998	0.9187	1.3368	2.0393	2.7745
Molecule	$q_{N^-}$ (Gas Phase)		$q_{N^-}$ (Aq.Phase)		Gas phase	Aq. phase	$\mu$ in gas phase	$\mu$ in aq. phase
	B	$BCu^{2+}(N-Cu^{2+})$	B	$BCu^{2+}(N-Cu^{2+})$	$q_{Cu^{2+}}$	$q_{Cu^{2+}}$	B	B
Glycine	-0.4534	-0.7200	-0.4632	-0.6904	1.3805	1.5099	3.2456	5.3375
Alanine	-0.4513	-0.7038	-0.4623	-0.6770	1.3654	1.5019	4.8014	6.6653
Cysteine	-0.4215	-0.6728	-0.4317	-0.6821	1.1708	1.4932	4.0578	13.2029

**Table 8.1.3** Computed atomic charges (unit 'e') in the complexes and the amount of charge transfer (CT).

$BCu^{2+}(O-Cu^{2+})$ Gas phase	$q_{Cu^{2+}}$	$q_{O^-}$	$q_{CT}$	$BCu^{2+}(O-Cu^{2+})$ Aq. phase	$q_{Cu^{2+}}$	$q_{O^-}$	$q_{CT}$
Glycine	1.0637	-0.4859	0.5778	Glycine	1.3654	-0.4730	0.8924
Alanine	1.0237	-0.4949	0.5288	Alanine	1.2918	-0.5039	0.7879
Cysteine	0.9187	-0.4747	0.4440	Cysteine	1.3368	-0.4998	0.8370
$BCu^{2+}(N-Cu^{2+})$ Gas phase	$q_{Cu^{2+}}$	$q_{N^-}$	$q_{CT}$	$BCu^{2+}(N-Cu^{2+})$ Aq. phase	$q_{Cu^{2+}}$	$q_{N^-}$	$q_{CT}$
Glycine	1.3805	-0.7200	0.6605	Glycine	1.5099	-0.6904	0.8195
Alanine	1.3654	-0.7038	0.6616	Alanine	1.5019	-0.6770	0.8249
Cysteine	1.1708	-0.6728	0.4980	Cysteine	1.4932	-0.6821	0.8111

**Table 8.1.4** Natural net charges (Units e) on  $\text{Cu}^{2+}$  ion ( $q_{\text{Cu}^{2+}}$ ), Oxygen atom ( $q_{\text{O}^-}$ ) and Nitrogen atom ( $q_{\text{N}^-}$ ) and ligand to metal charge transfer ( $Q_{\text{CT}}$ ) of O- $\text{Cu}^{2+}$  complexes and N- $\text{Cu}^{2+}$  complexes (Zwitterionic) in gas and aqueous phase respectively obtained from NPA analysis.

O- $\text{Cu}^{2+}$ complex	Gas phase			Aqueous phase		
	$q_{\text{Cu}^{2+}}$	$q_{\text{O}^-}$	$Q_{\text{CT}}$	$q_{\text{Cu}^{2+}}$	$q_{\text{O}^-}$	$Q_{\text{CT}}$
Glycine	0.6347	-0.3483	1.365	0.9453	-0.3049	1.054
Alanine	0.5932	-0.3540	1.40	0.8656	-0.3336	1.134
Cysteine	0.4800	-0.3504	1.52	0.9149	-0.2885	1.085
N- $\text{Cu}^{2+}$ complex	Gas phase			Aqueous phase		
	$q_{\text{Cu}^{2+}}$	$(q_{\text{N}^-})$	$Q_{\text{CT}}$	$q_{\text{Cu}^{2+}}$	$(q_{\text{N}^-})$	$Q_{\text{CT}}$
Glycine	1.041	-0.3634	0.959	1.143	-0.3543	0.857
Alanine	1.022	-0.3642	0.978	1.132	-0.3525	0.868
Cysteine	0.795	-0.4093	1.205	1.120	-0.3512	0.88

**Table 8.1.5** Geometrical features of the free amino acids and their  $\text{Cu}^{2+}$  complexes in gas phase (length in Å and angle in degree).

Molecule	B		BCu <sup>2+</sup> (O-Cu <sup>2+</sup> )			
	r (C-O)	<C-C-O	r(C-O)	r (O-Cu <sup>2+</sup> )	<C-C-O	<C-C-O-Cu <sup>2+</sup>
Glycine	1.204	125.148	1.230	1.927	119.931	-178.611
Alanine	1.199	123.519	1.233	1.922	120.052	-179.998
Cysteine	1.200	122.666	1.227	1.906	119.748	174.860
Molecule	B		BCu <sup>2+</sup> (N-Cu <sup>2+</sup> )			
	r (C-N)	<C-C-N	r(C-N)	r (N-Cu <sup>2+</sup> )	<C-C-N	<C-C-N-Cu <sup>2+</sup>
Glycine	1.45	110.154	1.47	1.9556	105.867	-0.1428
Alanine	1.44	108.346	1.52	1.9586	106.555	200.6756
Cysteine	1.449	112.398	1.50	2.0262	111.944	-151.1961



**Table 8.1.6** Geometrical features of the free molecule and their  $\text{Cu}^{2+}$  complexes in aqueous phase (Bond length in Å, bond angle and torsion angle ( $\tau$ ) in degree).

Molecule	B		$\text{BCu}^{2+}$			
	r (C-O)	<C-C-O	r(C-O)	r (O-Cu <sup>2+</sup> )	<C-C-O	$\tau$ <C-C-O-Cu <sup>2+</sup>
Glycine	1.207	125.500	1.224	1.880	121.861	179.921
Alanine	1.204	124.560	1.232	1.895	119.226	179.149
Cysteine	1.206	123.189	1.243	1.879	122.140	-177.736
Molecule	B		$\text{BCu}^{2+}$ (N-Cu <sup>2+</sup> )			
	r (C-N)	<C-C-N	r(C-N)	r (N-Cu <sup>2+</sup> )	<C-C-N	$\tau$ <C-C-N-Cu <sup>2+</sup>
Glycine	1.43	110.919	1.44	1.949	109.001	-0.1818
Alanine	1.42	108.896	1.50	1.939	106.595	-23.124
Cysteine	1.426	112.796	1.48	1.879	122.140	-149.853

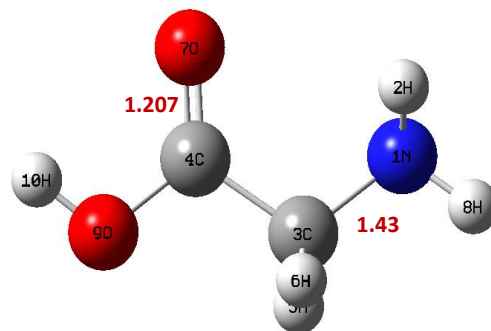
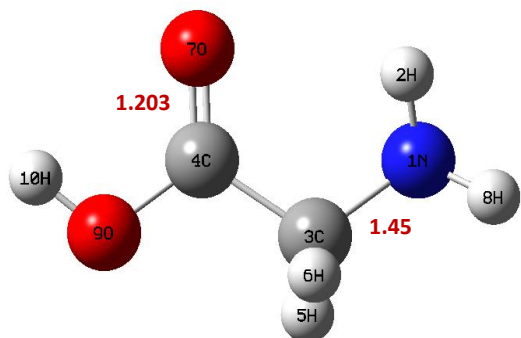
**Table 8.1.7** Computed hardness [hartree (h)] of the free molecules in gas and aqueous phase.

Molecule	Gaseous phase			Aqueous phase		
	$\epsilon_{\text{HOMO}}(\text{h})$	$\epsilon_{\text{LUMO}}(\text{h})$	$\eta(\text{h})$	$\epsilon_{\text{HOMO}}(\text{h})$	$\epsilon_{\text{LUMO}}(\text{h})$	$\eta(\text{h})$
Glycine	-0.24567	-0.0009	0.1223	-0.2531	0.0004	0.1267
Alanine	-0.25106	-0.0067	0.1221	-0.2547	-0.0051	0.1248
Cysteine	-0.26227	-0.0192	0.1214	-0.2589	-0.0112	0.1238

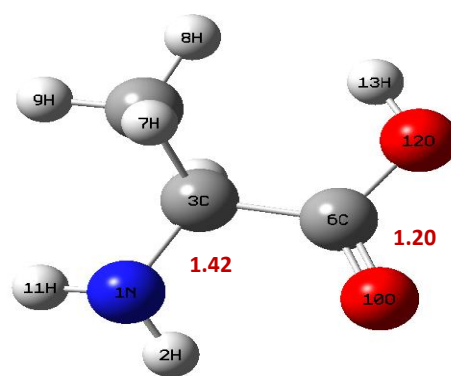
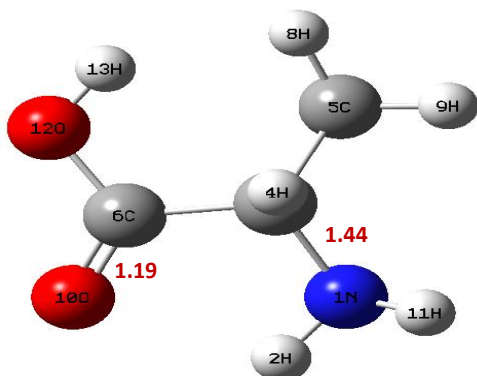
Gas phase

Aqueous phase

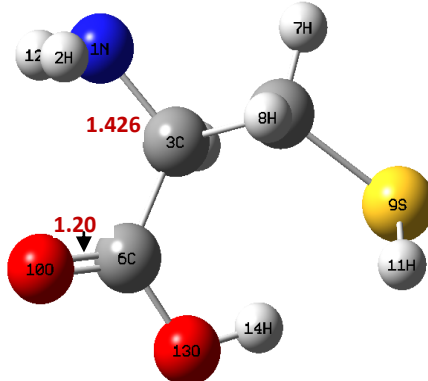
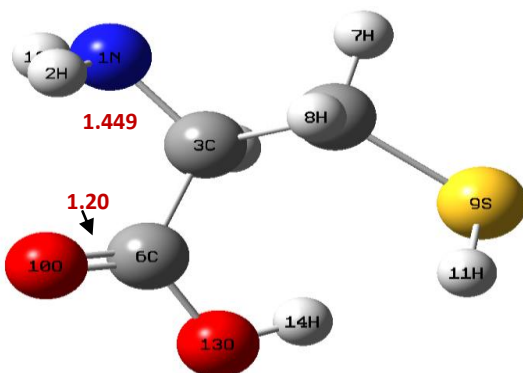
Glycine



Alanine

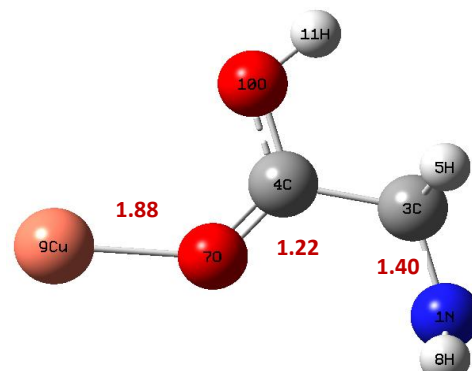
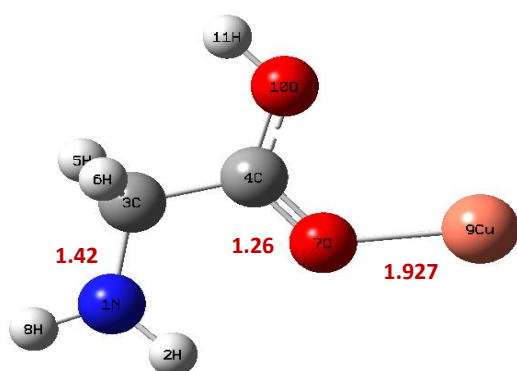
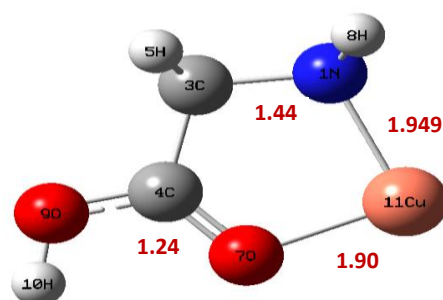
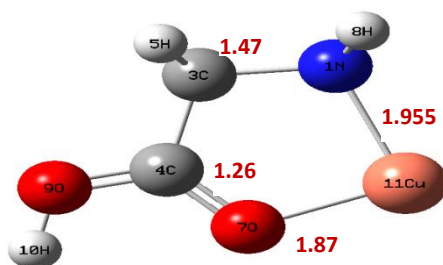
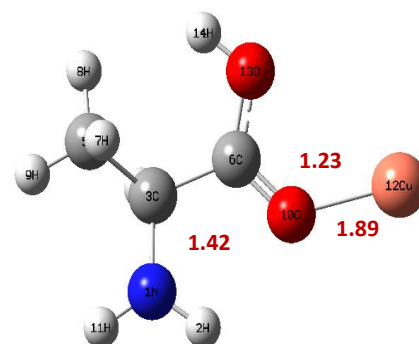
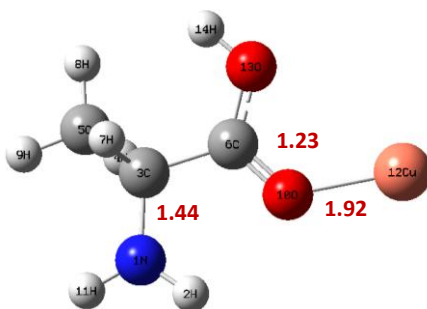
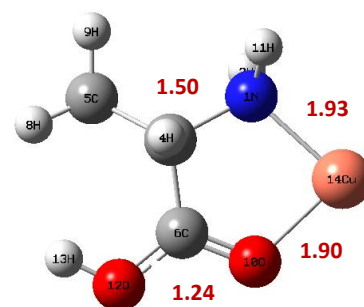
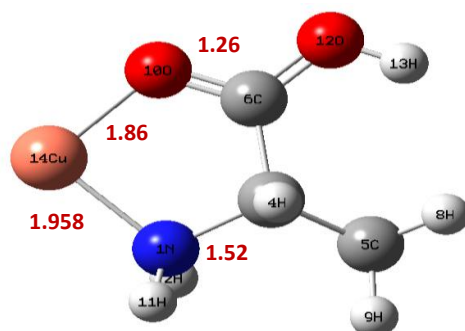


Cysteine



Gas phase

Aqueous phase

Glycine  
(O-Cu<sup>2+</sup>)Glycine  
(N-Cu<sup>2+</sup>-O)Alanine  
(O-Cu<sup>2+</sup>)Alanine  
(N-Cu<sup>2+</sup>-O)

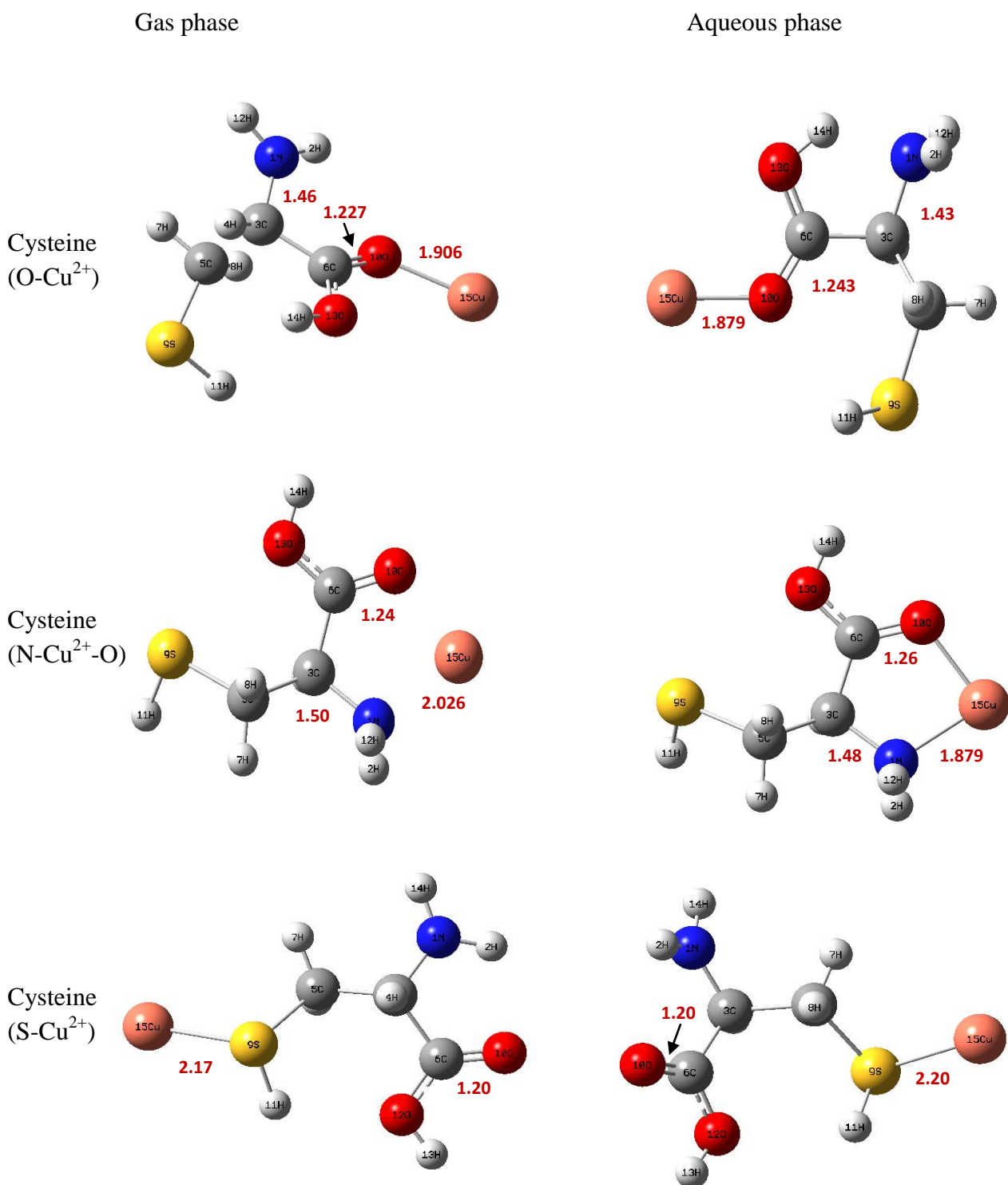


**Figure 8.2.1** Optimized structure of neutral glycine, alanine and cysteine and there different Cu<sup>2+</sup> complexes in gas and aqueous phase.(Bond distance is in angstrom (Å) unit).

## 8. 5 References

- (1) Lippard, S. J.; Berg, J. M. *Principles of Bioinorganic Chemistry*, (University Science Books, Mill Valley, CA & references therein) 1994.
- (2) Grese, R. P.; Cerny, R. L.; Gross, M. L. *J. Am. Chem. Soc.* **1989**, *111*, 2865.
- (3) Hu, P.; Gross, M. L. *J. Am. Chem. Soc.* **1992**, *114*, 9153.
- (4) Hu, P.; Gross, M. L. *J. Am. Chem. Soc.* **1993**, *115*, 8821.
- (5) More, M. B.; Ray, D.; Armentrout, P. B. *J. Phys. Chem. A* **1997**, *101*, 4254.
- (6) Lee, S.-W.; Kim, H. S.; Beauchamp, J. L. *J. Am. Chem. Soc.* **1998**, *120*, 3188.
- (7) Cerda, B. A.; Wesdemiotis, C. *J. Am. Chem. Soc.* **1996**, *118*, 11884.
- (8) Cerda, B. A.; Hoyau, S.; Ohanessian, G.; Wesdemiotis, C. *J. Am. Chem. Soc.* **1998**, *120*, 2437.
- (9) Hoyau, S.; Ohanessian, G. *Chem. Eur. J.* **1998**, *4*, 1561.
- (10) Luna, A.; Morizur, J. P.; Tortajada, J.; Alcamí, M.; Mo, O.; Yanez, M. *J. Phys. Chem. A* **1998**, *102*, 4652.
- (11) Spöner, J.; Burda, J. V.; Sobat, M.; Leszczynski, J.; Hobza, P. *J. Phys. Chem. A* **1998**, *102*, 5951.
- (12) Liedl, K. R.; Rode, B. M. *Chem. Phys. Lett.* **1992**, *197*, 181.
- (13) Hoyau, S.; Ohanessian, G. *J. Am. Chem. Soc.* **1997**, *119*, 2016.
- (14) Remko, M.; Fitz, D.; Rode, B. M. *J. Phys. Chem. A* **2008**, *112*, 7652.
- (15) Marino, T.; Russo, N.; Toscano, M. *J. Mass Spectrom.* **2002**, *37*, 786-791.
- (16) Marino T, Russo N, Tocci E & Toscano M, *Int J Quantum Chem*, 84 (2001) 264.
- (17) Cerda, B. A.; Wesdemiotis, C. *J. Am. Chem. Soc.* **1995**, *117*, 9734.
- (18) Frisch, M. J.; Trucks, G. W.; Schlegel, H. B.; Scuseria, G. E.; Robb, M. A.; Cheeseman, J. R.; Scalmani, G.; Barone, V.; Mennucci, B.; Petersson, G.A.; et al. *Gaussian 09, Revision A.02*, Gaussian, Inc., Wallingford, CT, 2009.

## Chapter 8

- (19) Tomasi, J.; Mennucci, B.; Cancès, E. *J. Mol. Struct. (Theochem)* **1999**, *464(1-3)*, 211–226.
- (20) Mulliken, R. S. *J. Chem. Phys.* **1955**, *23(10)*, 1833-1840.
- (21) Blomberg, M. R. A.; Siegbahn, P. E. M.; Svensson, M. *J. Phys. Chem. A* **1996**, *104*, 9546.
- (22) Holthausen, M. C.; Mohr, M.; Koch, W. *Chem. Phys. Lett.* **1995**, *240*, 245.
- (23) Rodriguez-Santiago, L.; Sodupe, M.; Branchadell, V. *J. Chem. Phys.* **1996**, *105*, 9966.

## CHAPTER 9

**Proton affinities of a series of  $\alpha,\beta$ -unsaturated carbonyl compounds of type-2-alkene (ACL, HNE, MVK, ACR, MA, EMA), in the gas and aqueous phase in their low-lying excited triplet state. A DFT/PCM-SCRF approach.**





## Abstract

DFT [B3LYP] / 6-311G(d,p) calculations were performed to quantify triplet state proton affinities (PA) and transition energies of a series of  $\alpha,\beta$ -unsaturated carbonyl compounds and their O-protonated counterparts in gas phase as well as in aqueous phase. In order to evaluate structural behaviour and different quantum mechanical properties in water we studied our optimization process using PCM-SCRF method at the same level of theory of the relevant low-lying excited state. The gas phase O-protonation turns out to be exothermic in each case and the local stereochemical disposition of the proton is found to be almost the same in each case. PA values of the different compounds are affected by substituent present at the carbonyl carbon. Different electrochemical properties (+R, +I, effect) originate from carbonyl chain are seen to cause change of the proton affinities. Acrylamide show the highest PA in both phases. In each case protonation at carbonyl oxygen is observed to be more energetically favourable compared to protonation at other probable binding sites present. Computed proton affinities of the compounds in gas phase are in the following order  $ACR \geq EMA > HNE > MVK > MA > ACL$ , while in aqueous phase the PA order is ranked differently. Charge density on binding oxygen and on added proton is recorded from both Mulliken population analysis (MPA) and natural population analysis (NPA). PA values are sought to be correlated with the computed hardness of the unprotonated species in the relevant excited state. The proton induced shifts (PIS) are in general red shifts for the low-lying excited triplet state. The overall reactivity is explained by distant atom contribution in addition to the contribution from the carbonyl group.

## 9.1 Introduction

Ion-molecule interactions are now a growing interest in the field of both experimental and theoretical research in chemistry. Proton transfer reactions are of considerable importance in chemistry. Excited state proton transfer is very important in biological process.<sup>1</sup> By definition, an acid is an electron acceptor whereas base is an electron donor, so there may have a relationship between charge density distribution and acid–base properties. Acid- base properties of a molecule may change from one electronic state to another due to the extensive molecular charge redistribution in different electronic state. Basic chemistry of a carbonyl chromophore in ground state is largely independent of the nature of alkyl or aryl group present at carbonyl carbon. By changing the electronic nature of the low-lying excited state these alkyl or aryl groups markedly influence the chemical and physical nature of the carbonyl chromophore at the lowest excited state. Excited state proton transfer process on guanine and some related species has been investigated theoretically.<sup>2,3</sup> Basicity of some proto-typical carbonyls in ground and low-lying excited state has been reported earlier.<sup>4</sup> Gas phase methods<sup>5-13</sup> have the advantage for determining inherent acid–base properties in ground state avoiding solvent effect. In presence of solvent, excited state acid-base properties of a molecule can be measured utilizing absorption and fluorescence spectral data in conjugation with Forster cycle.<sup>14-17</sup> Different computational studies<sup>18-20</sup> have been performed to investigate gas phase basicities of organic molecules in the excited state. Excited state proton affinities and vertical excitation energies of 1,5 and 1,8- di-amino naphthalenes were computed with the help of B3LYP / 6-31G(d,p) and CIS/ 6-31G(d,p) method of calculations.<sup>21</sup> In last few years the basicities, of a series of substituted aliphatic conjugated carbonyl system (chrotonaldehyde)<sup>22,23</sup> in ground state and their low-lying excited state and proton affinities of a series of aromatic conjugated carbonyl system (aceto phenone)<sup>24</sup> in their lowest excited triplet state has been studied theoretically. In this current work a series of conjugated  $\alpha,\beta$ -

unsaturated carbonyl derivatives of type-2-alkene chemical class has been investigated using DFT/ B3LYP method at most reliable 6-311G(d,p) basis set at relevant low-lying excited triplet state. Compounds investigated in this study are acrolein (ACL), 4-hydroxy-2-nonanol (HNE), methyl vinyl ketone (MVK), acryl amide (ACR), methyl acrylate (MA) and ethylmethacrylate (EMA). A ground state comparative study of proton affinities of the same compounds were previously reported.<sup>25</sup> These unsaturated compounds selected in this work are considered as environmental pollutants. It is also recognized that electrophilic  $\alpha,\beta$ -unsaturated carbonyl derivatives of the type-2 alkene chemical class cause broad organ system toxicity by forming covalent Michael-type adducts with amino acids.<sup>26-28</sup>

The purpose of the present work is to deliver comparative data base for proton affinities and basicities of the carbonyl compounds involved in bio-molecular process in their low-lying excited triplet state in both gas and aqueous phase.

It was observed that several energetic values obtained in DFT/ B3LYP calculation are reached to the global minima potential energy surface than those obtained in *ab-initio* (Hartree-Fock) study, therefore H-F results are not taken into account. The optimized geometry of the protonated complexes tend to suggest that proton ( $H^+$ ) added to the compound prefers to bind with carbonyl oxygen in all complexes with lowest optimization energy. Both Mulliken population analysis (MPA) and natural population analysis (NPA) have been applied for evaluating the charge density on carbonyl oxygen of the unprotonated bases and of their protonated complexes and charge on added proton of the protonated complexes. We have analysed the transition energies ( $^1S_0 \rightarrow T_1$ ) to understand whether the pre protonation charge distribution local to the chromophore or post protonation relaxation of charge density or both are important in explaining the overall basicity of each compound in a particular state. We have also analysed the kind and extent of spectral shift caused by protonation. In a particular state the possibility of correlating the PA values with the global

hardness of the molecules are also explored. Following are the Chemical structures (**Figure 9.2.1**) of investigated unsaturated carbonyl compounds with their proper name and abbreviation.

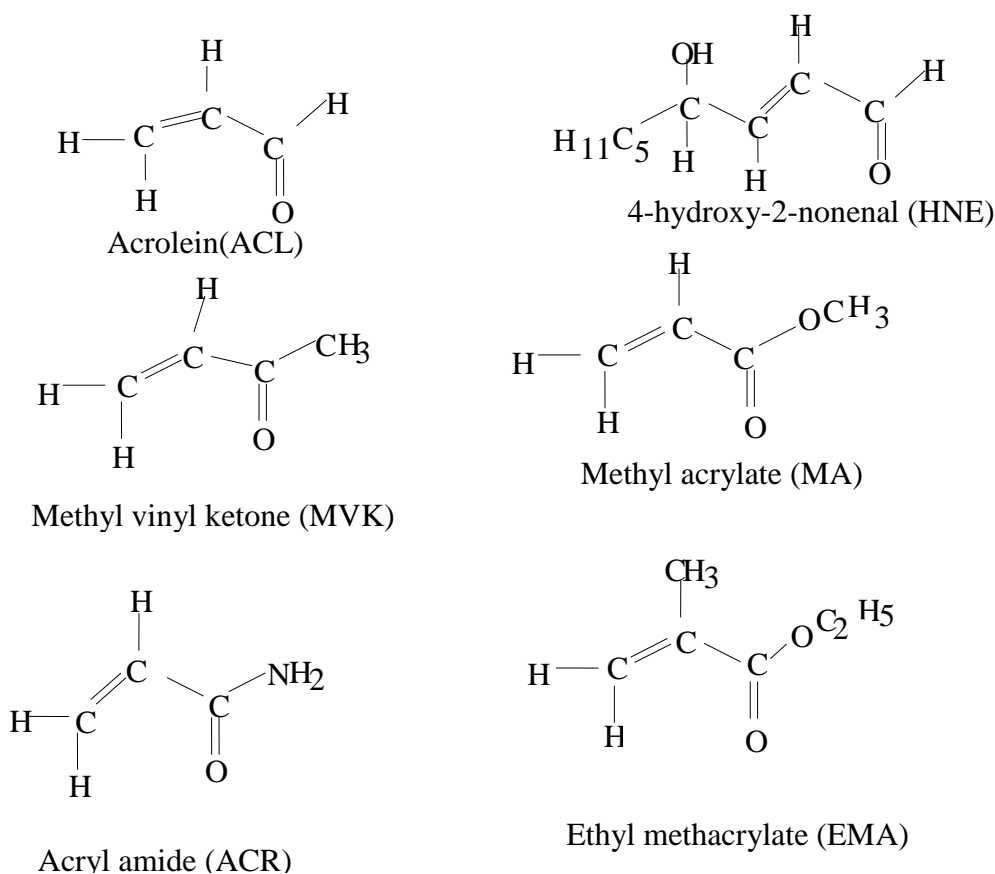


**Figure 9.2.1** Structure of several conjugated  $\alpha,\beta$ -unsaturated carbonyl compounds

## 9.2 Computational details

The geometry of the six  $\alpha,\beta$ -unsaturated carbonyl compounds has been fully optimized with most accurate DFT/B3LYP method<sup>29</sup> at 6-311G(d,p) basis set level of Gaussian '09' program package.<sup>30</sup> In order to verify geometrical behaviour PA's and other computed parameters in solvent we used SCRF-PCM<sup>31</sup> (Polarisable Continuum Model) model for geometry optimization at same level of theory. Water has been selected as solvent from the solvent list

given in Gaussian program. The charge density on atoms (carbonyl oxygen and added proton) of the optimized structures was calculated in both MPA<sup>32</sup> and NPA<sup>33</sup> framework. Basis set superposition error was found to be small therefore results are not included in this current work. To obtain the thermodynamic parameters (enthalpies, Gibbs free energies at 298.15 K) frequency calculations were performed for all neutral, protonated complexes at the same level of theory.

### 9.3 Results and discussion

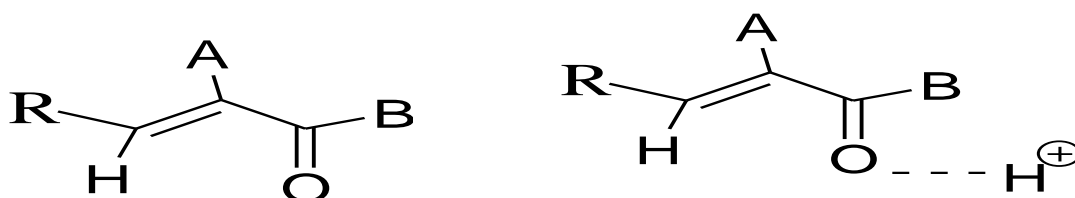


**Figure 9.2.2** General neutral and protonated structures for conjugated  $\alpha,\beta$ -unsaturated carbonyl compounds of type-2-alkene chemical class. (R = -H or alkyl group, A = -H or -CH<sub>3</sub> and B = -H, -CH<sub>3</sub>, -OCH<sub>3</sub>, -NH<sub>2</sub>, -OC<sub>2</sub>H<sub>5</sub>).

The proton affinity of a base is defined as negative enthalpy change ( $-\Delta H^{298.15k}$ ) of a thermodynamic equilibrium reaction:  $B_1 + H^+ \leftrightarrow [B_1H^+]$  and basicity is defined as the negative of the free energy change ( $-\Delta G^{298.15k}$ ) associated with the same reaction. So affinity and basicity can be characterised as

$$PA (\Delta H) = H^{298.15k} [(B_1H^+) - (B_1)] \dots \dots (1), \text{ basicity } (\Delta G) = G^{298.15k} [(B_1H^+) - (B_1)] \dots (2).$$

PA of the compound can be obtain computationally according to Maksic and co-workers<sup>34,35</sup> that is  $PA = [E_{tot} (B_1H^+) - E_{tot} (B_1)] \dots (3)$ .

Both gas and aqueous phase total energies of six  $\alpha,\beta$ -unsaturated carbonyl compounds and of their O-protonated complexes in low-lying excited triplet state are summarized in **Table 9.1.1**. Evaluated PA values [following equation (3)] of the studied compounds are tabulated in **Table 9.1.2**. It is observed that PA's of different carbonyl compounds has a variation in the

## Chapter 9

range  $-223.35$  kcal /mole to  $-199.29$  kcal /mole in the gas phase while in aqueous phase the PA's span is increased and it is of  $-272.61$  to  $-256.11$  kcal/mole. It is clear from the obtained values that conjugated double bond effect on PA's are not uniform. Presence of different substituent (B) at the carbonyl carbon and at any other positions (A at  $\alpha$ - carbon) of the alkyl chain of the compounds are markedly influence the proton affinities. It is seen that in both phases Acryl amide (ACR) exhibits the highest PA values ( $-223.35$  kcal /mole and  $-272.61$  kcal /mole in gas and aqueous phase respectively). The PA value of ACL is predicted to be lowest ( $-199.29$  kcal /mole) in the gas phase. In aqueous phase, HNE exhibits the lowest PA value ( $-252.563$ kcal/mole) in the series in this particular electronic state. Lone pair electron of nitrogen of  $-\text{NH}_2$  may increase the electron density on binding oxygen thus the  $\text{O}-\text{H}^+$  interaction in ACR is enhanced.

Effect of B (**Figure 9.2.2**) on PA in the low-lying triplet state are in the following increasing order  $-\text{H}$  (in ACL)  $< -\text{CH}_3 < -\text{OCH}_3 < -\text{H}$  (in HNE)  $< -\text{OC}_2\text{H}_5 \leq -\text{NH}_2$ . On salvation, this effect on PA's ranked slightly different and it is  $-\text{H}$  (in HNE)  $< -\text{H}$  (in ACL)  $< -\text{CH}_3 < -\text{OC}_2\text{H}_5 < -\text{OCH}_3 \leq -\text{NH}_2$ . We observed that, gas phase PA value of EMA is comparatively higher than that of MA and MVK. This is may be the cause of double substituent effect (B =  $-\text{OC}_2\text{H}_5$  and A =  $-\text{CH}_3$ ). Both +I and +R effects (B) originate from A and B of EMA makes the  $\text{O}-\text{H}^+$  interaction more strong compared to MA and MVK. The enhancement of  $-\text{OCH}_3$  and  $-\text{CH}_3$  attached at carbonyl carbon of the unsaturated compounds are less than  $-\text{OC}_2\text{H}_5$  resulted less PA for MVK ( $-211.49$  kcal/mole) and MA ( $-209.61$  kcal/mole). Excited state (low-lying) PA of HNE compound ( $-217.18$  kcal /mole) obtained little more (approx 6 to 8 kcal /mole) compared to MVK and MA. This trend may be explained by the Inductive effect (+I) exhibited by the long alkyl group ( $\text{C}_5\text{H}_{11}$ ) linked to the carbonyl carbon, contributes by means of bond electron donation to enhance the  $\text{O}-\text{H}^+$  interaction. Computed PA values of the unsaturated compounds are predicted little more in water. Proton affinity values in

aqueous phase increases in the following order  $\text{HNE} < \text{ACL} < \text{MVK} < \text{EMA} < \text{MA} \leq \text{ACR}$ . Different PA order appeared in this phase may be due to electronic relaxation effect in presence of solvation. The change of PA order (with higher values) of the same bases in solution phase is expected, because ions can become modified with the change of phase since the gas phase environment differs from that of the solvent phase. It was already revealed from a previous investigation<sup>36</sup> that, the order of basicity in solution differs from that in the gas phase. **Table 9.1.2** also clear the fact that, excited (low-lying) state proton affinities are comparatively higher in gas as well as in the solvent phase compared to that obtained in ground state. Exceptionally, PA of ACL and HNE in this state is observed little smaller relative to the ground state. This tendency has been investigated in earlier study<sup>37,38</sup> which can be attributed to the phenomenon of redistribution of charges in the excited state in comparison to ground state.<sup>38</sup> Gas phase basicities were evaluated from calculated free energies (G) following above equation (2). The total Gibbs free energies and evaluated basicities of the unsaturated carbonyl compounds in both gas and aqueous phases are collected in **Table 9.1.3**. It was observed that basicity values are closer to corresponding PA in each case, they differs only by  $\pm 4.48$  to  $\pm 8.81$  kcal/mole in gas phase and  $\pm 4.77$  to  $\pm 9.12$  kcal/mole in aqueous. The order of the basicities of the compounds is not parallel to their PA's data. Little discrepancy in order has been found between ACR and EMA in gas phase and between MA and ACR in aqueous phase. **Table 9.1.4** reports the computed Mulliken net charge on carbonyl oxygen atom of the free and protonated complexes and also the net charge on added proton of the protonated complexes in both phases in this particular state. Since Mulliken population analysis (MPA) is more method sensitive, we have tested another procedure (NPA) for evaluating partial charge on atoms. **Table 9.1.5** summarized the partial charges on the same atoms obtained in the frame of natural population analysis (NPA). From the  $Q_{\text{CT}}$  and  $q_{\text{CT}}$  values of **Table 9.1.4** and **Table 9.1.5** clears that, in both phases a

## Chapter 9

significant charge transfer from ligand to proton has taken place. One might have expected that, transferred charge will be parallel to the proton affinity of the complexes. But this is not the case; both  $Q_{CT}$  and  $q_{CT}$  gave unexpected order in gas and aqueous phase. Charges obtained from NPA are comparatively higher compared to MPA. MPA charge on proton of the protonated complexes varies in the range of +0.2961 to +0.3145 and +0.3179 to +0.3335 in gas and aqueous phase respectively while NPA results shows 0.50 to 0.51e natural charges on added proton in the gas phase and it is little bit higher in water (0.51e to 0.52e). This charge migration is not local and originates from all over the compound. It is observed that there is no direct correlation between NPA or MPA results and complex stability. The  $Q_{CT}$  results are given in **Table 9.1.4**. According to the calculated results ( $Q_{CT}$ ) stability order of the complexes can be written as  $HNE \geq MA > ACR > EMA > ACL > MVK$  and  $MA \geq ACR > MVK \geq EMA > ACL > HNE$  in the gas and aqueous phase respectively. NPA results shows different trend in gas as well as in water, it is  $HNE > MA \geq ACL > MVK > EMA$  and  $ACR \geq ACL > MA > MVK = HNE > EMA$ . This is tending to suggest that NPA results are also method sensitive. Functional sensitivity of NPA results was observed previously<sup>39</sup>. So further exploration is in need to resolve such a major discrepancy.

The optimized geometrical structures of the studied carbonyl compounds in gas and aqueous phases are presented in **Figure 9.2.3** and **Figure 9.2.4** respectively.

**Table 9.1.6** and **Table 9.1.7** exposed some important geometrical features around the functional carbon in the low-lying excited state. It is obvious from the results tabulated in **Table 9.1.6** and **7** that optimized geometry of the compounds not changed markedly from gas to aqueous phase. C=O bond distance elongated slightly from unprotonated bases to protonated complexes. It is 0.004 to 0.09Å in gas and quite similar 0.004 to 0.085Å in aqueous phase. The O-H<sup>+</sup> bond distance has a variation in the range of 0.967 to 0.9766Å and 0.9672 to 0.9743Å in gas and aqueous phase respectively. In both phases <C-O-H<sup>+</sup> bond



angle of all protonated complexes remain in between  $110.869^\circ$  to  $118.76^\circ$  in gas phase. The range is reduced on aqueous environment ( $110.59^\circ$  to  $113.77^\circ$ ). Among six unsaturated compounds HNE, MVK and EMA shows planarity in both phases with  $\tau(\text{C-C-O-H}^+)$  dihedral angle  $-179.98^\circ$ ,  $179.99^\circ$  and  $-179.51^\circ$  in gas phase,  $178.28^\circ$ ,  $-179.99^\circ$  and  $-179.60^\circ$  in aqueous. In both phases optimized geometries of ACL, ACR and MA provide non planar structure. The almost invariant stereochemistry around the binding oxygen site tend to suggest that, PA's of the studied compounds cannot be predicted properly unless considering the contributions from distant atom. **Table 9.1.8** reports the computed transition energies ( $^1\text{S}_0 \rightarrow \text{T}_1$ ) as state energies differences and shifts due to protonation. The proton induced shifts (PIS) are red shift in all cases with an exception of ACL, in which it is blue shift. On aqueous environment, the proton induced shift (PIS) for ACL and HNE show blue shift whereas other unsaturated carbonyl bases of the series show red shifts. These trends of PIS refer to gas phase protonation of the isolated compounds without any additional effects due to solvation. It is seen from the data recorded in **Table 9.1.9**, the low-lying excited state dipole moment ( $\mu$ ) of the ACL, HNE and MVK are reduced relative to that of the ground state in both gas and aqueous phase whereas it ( $\mu$ ) has been estimated to be higher in ACR, MA and EMA than that in the ground state. This increase of dipole moment in these three carbonyl compounds may be caused by the shifting of electron density from different substituent ( $-\text{NH}_2$ ,  $-\text{OCH}_3$  and  $-\text{OC}_2\text{H}_5$ ) to carbonyl chromophore.

## 9.4 Conclusion

From the current theoretical study it can be concluded that both gas and aqueous phase protonation of the studied  $\alpha$   $\beta$ -unsaturated carbonyl compounds in low-lying excited state is spontaneous. Acryl amide (ACR) exhibits the highest PA values ( $-223.35$  kcal/mole and  $-272.61$  kcal/mole in gas and aqueous phase respectively). The proton affinity values are little higher in this particular electronic state relative to their ground state in both gas and aqueous

## Chapter 9

phase. Reverse trend also found due to the redistribution of electron density on atoms from one electronic state to another ( $S_0 \rightarrow T_1$ ). Effects of conjugated double on PA's are not uniform. Presence of different substituent (B) at the carbonyl carbon and at any other positions (A at  $\alpha$ -carbon) of the alkyl chain of the compounds are influenced the proton affinities markedly. Dipole moment of several unsaturated compounds is reduced in low-lying excited state compared to their ground state values. PIS are red shifts in general with the exception of ACL in gas phase and both ACL and HNE in aqueous phase. Overall PA values of the investigated bases cannot be predicted properly without considering the contribution from distant atom along with the contribution from carbonyl moiety.

**Table 9.1.1** Computed total energies (hartree) of the free bases ( $B_1$ ) and their protonated complexes ( $B_1H^+$ ) at the equilibrium geometry of the low-lying excited triplet state.

Molecule	Total Energy (hartree)		Total Energy (hartree)	
	Gas phase		Aqueous phase	
	$B_1$	$B_1H^+$	$B_1$	$B_1H^+$
Acrolin(ACL)	-191.8663	-192.1839	-191.8695	-192.2786
4-hydroxy-2-nonenal(HNE)	-503.0539	-503.40	-503.0843	-503.4869
Methyl vinyl ketone (MVK)	-231.1978	-231.5358	-231.2015	-231.6218
Acrylamide (ACR)	-247.2466	-247.6035	-247.2580	-247.6934
Methyl acrylate (MA)	-306.4280	-306.7630	-306.4378	-306.8725
Ethyl methacrylate (EMA)	-385.1056	-385.4615	-385.1150	-385.5385

**Table 9.1.2.** Evaluated proton affinities [ $\Delta E_g$  or  $\Delta E_s = (E_{B_1H^+} - E_{B_1})$ ] for both gas and solvent phases at the equilibrium geometry of the lowest excited triplet state. 1 hartree = 627.5095 kcal/mole.

Molecule	Gas phase		Aqueous Phase	
	PA		PA	
	$\Delta E_g$ (hartree)	$\Delta E_g$ (kcal/mole)	$\Delta E_g$ (hartree)	$\Delta E_g$ (kcal/mole)
ACL	-0.3176	-199.29	-0.4091	-256.11
HNE	-0.3461	-217.18	-0.4026	-252.63
MVK	-0.338	-211.49	-0.4203	-263.14
ACR	-0.3569	-223.35	-0.4354	-272.61
MA	-0.335	-209.61	-0.4347	-272.17
EMA	-0.3559	-222.73	-0.4235	-265.15

**Table 9.1.3** Obtained Gibbs free energies of six  $\alpha,\beta$ -unsaturated carbonyl compounds and basicities ( $\Delta G$ ) in kcal/mol) by B3LYP/DFT method at 6-311G(d,p) level in gas and aqueous phase at the equilibrium geometry of low-lying excited triplet state.

Basicity calculated as:  $G(B_1H^+) - G(B_1)$  in Kcal /mole.

Compound	Gas Phase		Aqueous Phase	
	Free energy [G]	$\Delta G$	Free energy [G]	$\Delta G$
	[hartree]	[kcal/mole]	[hartree]	[kcal/mole]
ACL	-191.8364		-191.8397	
		-191.7		-248.74
ACL-H <sup>+</sup>	-192.1419		-192.2361	
HNE	-502.869		-502.89	
		-212.6		-247.86
HNE- H <sup>+</sup>	-503.2078		-503.2850	
MVK	-231.1418		-231.1456	
		-204.37		-255.77
MVK- H <sup>+</sup>	-231.4675		-231.5532	
ACR	-247.2044		-247.2163	
		-214.54		-263.49
ACR-H <sup>+</sup>	-247.5463		-247.6362	
MA	-306.3724		-306.3809	
		-201.11		-263.8
MA-H <sup>+</sup>	-306.6929		-306.8013	
EMA	-384.9959		-385.0054	
		-216.23		-257.52
EMA-H <sup>+</sup>	-385.3405		-385.4158	

**Table 9.1.4** Computed Mulliken net charge (unit e) on oxygen atom ( $q_{O^-}$ ) of free bases ( $B_1$ ) and O-protonated complexes ( $B_1H^+$ ) and computed Mulliken net charge on added proton ( $q_H^+$ ) of the protonated complexes ( $B_1H^+$ ) and Ligand to Proton Charge Transfer ( $Q_{CT}$ ) at the equilibrium geometry of low-lying excited state.

Molecule	Gas Phase			$Q_{CT}$	Aqueous Phase			$Q_{CT}$
	$(q_{O^-})$		$q_H^+$		$(q_{O^-})$		$q_H^+$	
	$B_1$	$B_1H^+$			$B_1$	$B_1H^+$		
ACL	-0.1335	-0.1438	0.3117	0.6883	-0.1481	-0.1811	0.3316	0.6684
HNE	-0.1986	-0.2556	0.2999	0.7001	-0.2989	-0.3423	0.3335	0.6665
MVK	-0.1581	-0.2148	0.3145	0.6855	-0.1737	-0.2314	0.33	0.670
ACR	-0.3684	-0.2763	0.3082	0.6918	-0.4503	-0.3075	0.3212	0.6788
MA	-0.3044	-0.2023	0.2961	0.7039	-0.3726	-0.2226	0.3179	0.6821
EMA	-0.3157	-0.2539	0.3098	0.6902	-0.3802	-0.2709	0.3232	0.6768

\*Charge Transfer calculated as {[formal charge on proton (+1)] - [Charge obtained on proton]} in the complex.

**Table 9.1.5** Partial atomic charges (unit e) on carbonyl oxygen ( $Q_{O^-}$ ) of the free bases ( $B_1$ ) and their O-Protonated complexes ( $B_1H^+$ ), Partial charges on added proton ( $Q_H^+$ ) of the protonated complexes ( $B_1H^+$ ) obtained from NPA and Ligand to Proton Charge Transfer ( $q_{CT}$ ) at the equilibrium geometry of low-lying excited state.

Molecule	Gas Phase			$q_{CT}$	Aqueous Phase			$q_{CT}$
	$(Q_{O^-})$		$Q_H^+$		$(Q_{O^-})$		$Q_H^+$	
	$B_1$	$B_1H^+$			$B_1$	$B_1H^+$		
ACL	-0.1770	-0.4692	0.5080	0.492	-0.1912	-0.4961	0.520	0.48
HNE	-0.1870	-0.5774	0.5030	0.497	-0.2050	-0.5529	0.524	0.476
MVK	-0.2004	-0.5428	0.5112	0.4888	-0.2174	-0.5503	0.524	0.476
ACR	-0.595	-0.6032	0.5089	0.4911	-0.6774	-0.6226	0.516	0.484
MA	-0.5109	-0.5573	0.5050	0.495	-0.5856	-0.5726	0.522	0.478
EMA	-0.5546	-0.5905	0.5178	0.4822	-0.6181	-0.5985	0.5268	0.4732

\* Charge Transfer calculated as [(formal charge on proton (+1)) - (Charge obtained on proton in the complex)].

**Table 9.1.6** Geometrical features of the free base and O-protonated base (length in Å and angle in degree) in gas phase at equilibrium geometry of the low-lying excited state.

Molecule	Free Base	O-Protonated Base			
	r(C-O)	r(C-O)	r(O-H+)	<C-O-H+	<C-C-O-H+
ACL	1.31	1.308	0.9743	114.85	0.00
HNE	1.33	1.33	0.9766	118.76	-179.98
MVK	1.315	1.319	0.9717	113.036	179.99
ACR	1.23	1.32	0.9670	113.33	0.00
MA	1.236	1.31	0.9675	113.49	-0.0279
EMA	1.214	1.30	0.9728	110.86	-179.51

**Table 9.1.7** Geometrical features of the free base and O-protonated base (length in Å and angle in degree) in aqueous phase.

Molecules	Free Base	O-Protonated Base			
	r(C-O)	r(C-O)	r(O-H+)	<C-O-H+	<C-C-O-H+
ACL	1.310	1.308	0.9743	113.77	0.00
HNE	1.296	1.31	0.9706	111.75	178.28
MVK	1.315	1.31	0.9719	112.57	-179.99
ACR	1.245	1.32	0.9672	111.94	0.00
MA	1.238	1.30	0.9742	111.24	-0.0098
EMA	1.223	1.308	0.9731	110.59	-179.60

**Table 9.1.8** Computed adiabatic transition energies ( $1s_0 \rightarrow T_1$ ) (hartree) and proton-induced shifts (PIS, hartree) in the low-lying excited triplet state.

Molecule	Gas Phase			Aqueous Phase		
	Transition Energy		PIS	Transition Energy		PIS
	B	BH <sup>+</sup>		B	BH <sup>+</sup>	
ACL	0.1019	0.105	0.0031	0.1046	0.1481	0.0435
HNE	0.1012	0.0979	-0.0033	0.0801	0.0915	0.0114
MVK	0.1042	0.0998	-0.0044	0.1065	0.0999	-0.0066
ACR	0.1192	0.1106	-0.0086	0.1186	0.1101	-0.0085
MA	0.1134	0.1126	-0.0008	0.1137	0.0894	-0.0243
EMA	0.1083	0.0885	-0.0198	0.1047	0.0838	-0.0209

**Table 9.1.9** Estimated dipole moment ( $\mu$ ) of six  $\alpha,\beta$ -unsaturated carbonyl compounds in gas phase as well as in aqueous phase at low-lying excited state ( $T_1$ ) and ground state.

Molecule	Gas phase		Aqueous Phase	
	Dipole moment ( $\mu$ )		Dipole moment ( $\mu$ )	
	Ground state	Low-lying excited state	Ground state	Low-lying excited state
ACL	3.15	0.833	4.04	0.991
HNE	2.12	1.68	2.83	1.79
MVK	2.7	2.01	3.51	2.60
ACR	3.88	3.97	5.14	5.21
MA	4.32	4.35	5.56	5.71
EMA	1.78	4.22	5.51	5.76

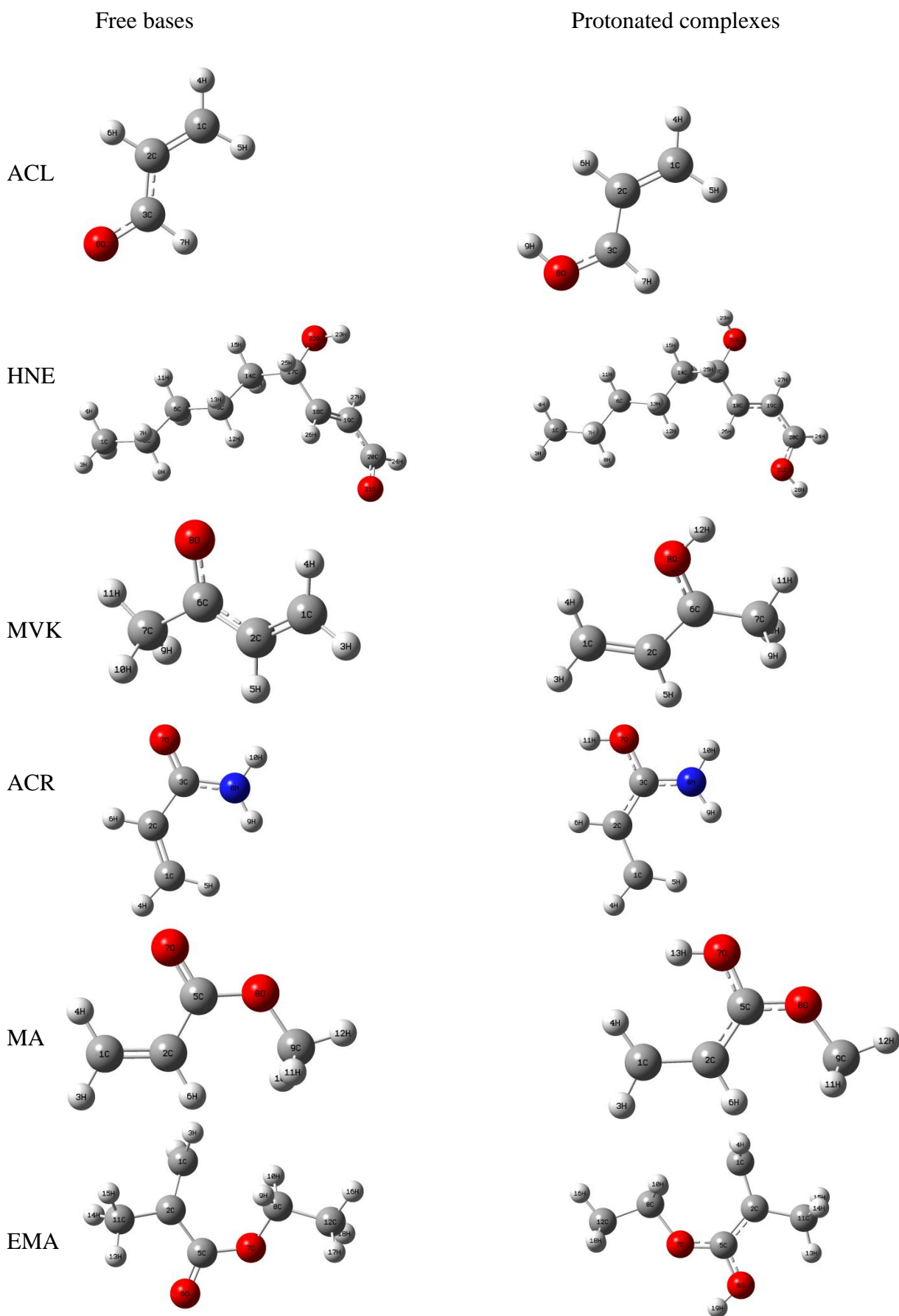


**Figure 9.2.3** Optimized geometries of the studied carbonyl compounds in gas phase.



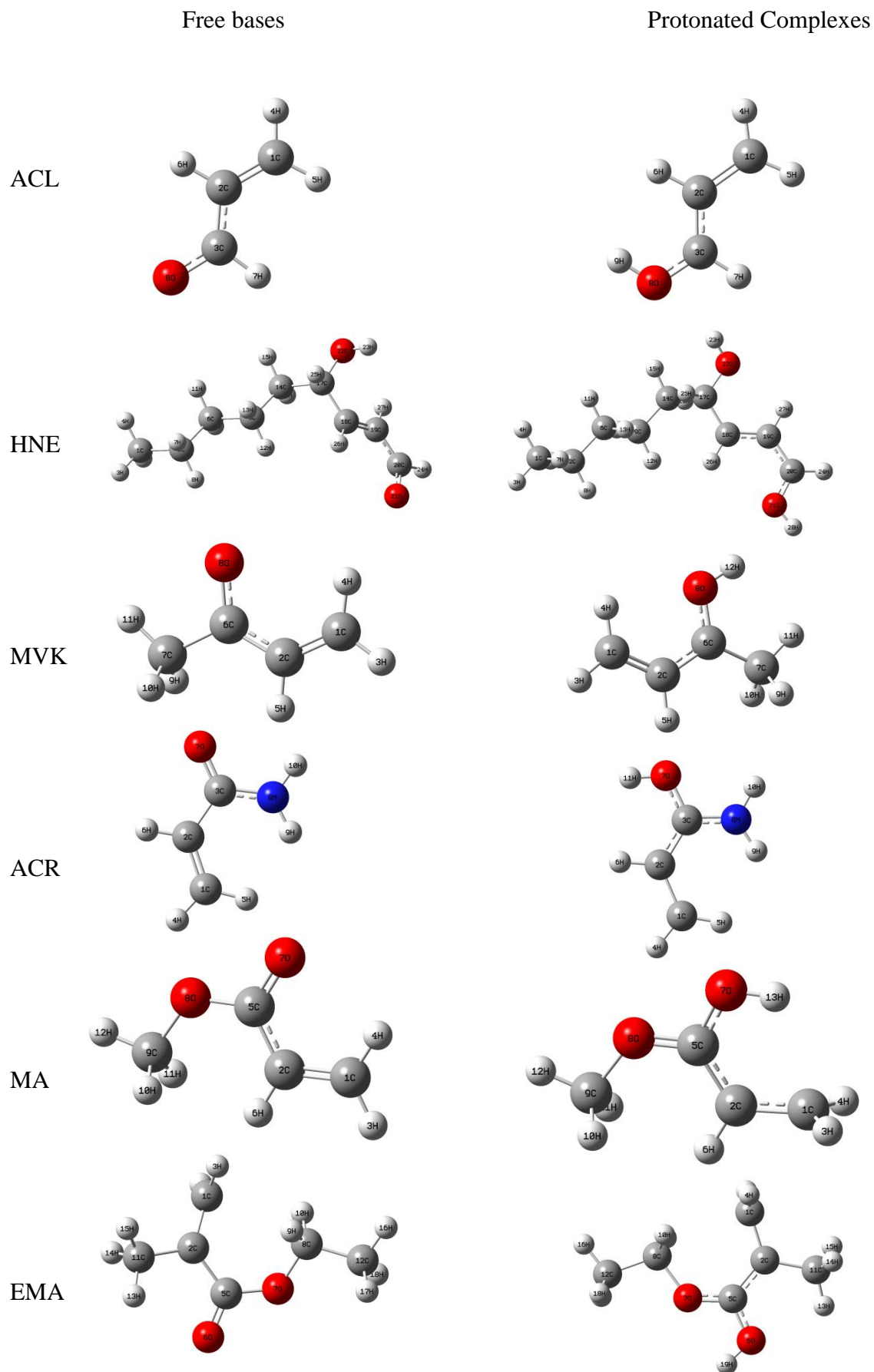


Figure 9.2.4 Optimized geometries of the studied carbonyl compounds in aqueous phase.

## 9.5 References

- (1) Rucker, J.; Cha, Y.; Jonsson, T.; Grant, K. L.; Klinman, J. P. *Biochemistry* **1992**, *31*, 11489.; Beveridge, A. J.; Heywood, G. C. *ibid.* **1993**, *32*, 3325.; Rose, I. A.; Kuo, D. J. *ibid.* **1992**, *31*, 5887.; Silverman, D. N.; Lindskog, S. *Acc. Chem. Res.* **1988**, *21*, 30.
- (2) Shukla, M. K.; Leszozynsky, J. *J. Phys. Chem. A* **2005**, *109*, 7775.
- (3) Aquino, A. J. A.; Lisohka, H.; Haettig, C. *J. Phys. Chem. A* **2005**, *109*, 3201.
- (4) Bhattacharya, S. P.; Medhi, C. *Proc. Indian acad. Sci. (Chem. Sci.)* **1993**, *105*(3), 195.
- (5) Bhome, D. K.; Hemsworth, R. S.; Rundle, H. I.; Schiff, H. I. *J. Chem. Phys.* **1973**, *58*, 3504.
- (6) Beauchamp, J. L. *Interaction between Ions and Molecules*. (Plenum, New York) **1974**, pp. 413, 459, 489.
- (7) Yamadagni, R.; Kebarle, P. J. *J. Am. Chem. Soc.* **1973**, *96*, 3727.
- (8) Bhome, D. K.; Mackay, G. I.; Schiff, H. I.; Hemsworth, R. S. *J. Chem. Phys.* **1974**, *61*, 2175.
- (9) Solomon, J. J.; Meot, M. N.; Field, F. M. *J. Am. Chem. Soc.* **1974**, *96*, 3727.
- (10) Long, J. W.; Franklin, J. L. *J. Am. Chem. Soc.* **1974**, *96*, 2320.
- (11) Brauman, J. I.; Blair, L. K. *J. Am. Chem. Soc.* **1970**, *92*, 5986; Yamadagni, R.; Kebarle, P. J. *J. Am. Chem. Soc.* **1973**, *96*, 3727.
- (12) Wieting, R. D.; Staley, R. H.; Beauchamp, J. L. *J. Am. Chem. Soc.* **1974**, *96*, 7552.
- (13) Staley, R. H.; Beauchamp, J. L. *J. Am. Chem. Soc.* **1975**, *97*, 5920.
- (14) Forster, T. Z. *Electrochem.* **1950**, *54*, 42.
- (15) Ottolenghi, M. *Acc. Chem. Res.* **1973**, *6*, 153.
- (16) Saeva, F. D.; Olin, G. R. *J. Am. Chem. Soc.* **1975**, *97*, 5630.
- (17) Ireland, J. F.; Wyatt, P. A. H. *Adv. Phys. Org. Chem.* **1976**, *12*, 138.

- (18) Antol, I.; Eckert-Maksić, M.; Lischka, H. *J. Phys. Chem. A* **2004**, *108*, 10317.
- (19) Mishra, H.; Maheshwary, S.; Tripathi, H. B.; Sathyamurthy, N. *J. Phys. Chem. A* **2005**, *109*, 2746.
- (20) Ibanez, G. A.; Labadie, G.; Escandar, G. M.; Olivieri, A. C. *J. Mol. Struct. (Theochem)* **2003**, *645*, 61.
- (21) Takehira, K.; Sugawara, Y.; Kowase, S.; Tobita, S. *Photochem. Photobiol. Sci.* **2005**, *4*, 287.
- (22) Pandit, S.; De, D.; De, B. R. *J. Mol. Struct. (Theochem)* **2006**, *760*, 245.
- (23) Pandit, S.; De, D.; De, B. R. *J. Mol. Struct. (Theochem)* **2006**, *778*, 1.
- (24) Senapati, U.; De, D.; De, B. R. *J. Mol. Struct. (Theochem)* **2007**, *808*, 153.
- (25) Mandal, B.; Senapati, U.; De, B. R. *Indian Journal of Advances in Chemical Science* **2016**, *4(4)*, 401.
- (26) Barber, D. S.; LoPachin, R. M. *Toxicol. Appl. Pharmacol.* **2004**, *201*, 120.
- (27) Barber, D. S.; Stevens, S.; LoPachin, R. M. *Toxicol. Sci.* **2007**, *100*, 156.
- (28) LoPachin, R. M.; Schwarcz, A. I.; Gaughan, C. L.; Mansukhani, S.; Das, S. *Neuro Toxicology* **2004**, *25*, 349.
- (29) Lee, C.; Yang, W.; Parr, R. G. *Phys. Rev.* **1988**, *B37*, 785.
- (30) Frisch, M. J.; Trucks, G. W.; Schlegel, H. B.; Scuseria, G. E.; Robb, M. A.; Cheeseman, J. R.; Scalmani, G.; Barone, V.; Mennucci, B.; Petersson, G. A. et al. Gaussian 09, Revision A.02, Gaussian Inc., Wallingford, CT, 2009.
- (31) Tomasi, J.; Mennucci, B.; Cancès, E. *J. Mol. Struct. (Theochem)* **1999**, *464(1-3)*, 211.
- (32) Mulliken, R. S. *J. Chem. Phys.* **1955**, *23(10)*, 1833.
- (33) Glendening, E. E.; Reed, A. E.; Carpenter, J. E.; Weinhold, F. NBO (Natural Bond Orbital), Vol. 5.
- (34) Maksić, Z. B.; Kovačević, B. *J. Phys. Chem. A* **1998**, *102*, 7324.

## Chapter 9

- (35) Maksić, Z. B.; Kovačević, B.; Kovaček, D. *J. Phys. Chem. A* **1997**, *101*, 7446.
- (36) Ma'an, H. A.; Nadja, B. C.; George S. J.; Christie G. E. *J. Mass Spectrom.* **2000**, *35*, 784.
- (37) Goeller, A. H.; Strehlow, D.; Hermann, G. *Chem. Phys. Chem.* **2005**, *6*, 1259.
- (38) Antol, I.; Eckert-Maksić, M.; and Klessinger, M. *J. Mol. Struct. (Theochem)* **2003**, *664/665*, 309.
- (39) Sannigrahi, A. B.; Nandi, P. K. *Chem. Phys. Lett.* **1993**, *204*, 73.

## **CHAPTER 10**

**Low-lying excited state lithium cation affinities (LCA) and associate parameters of a series of  $\alpha,\beta$ -unsaturated carbonyl compounds of type-2-alkene chemical class (ACL, HNE, MVK, ACR, MA and EMA ): A Comparative DFT based computational study in both gas and solvent phases.**



## Abstract

Quantum mechanical properties of several conjugated  $\alpha$ ,  $\beta$  unsaturated carbonyl compounds and interactions with lithium cation (Carbonyl O–Li<sup>+</sup>) were studied at the low-lying excited triplet state by means of high level DFT/6-311G(d,p) method. Lithium cation affinities (LCA) and lithium cation basicities (LCB) of the unsaturated compounds have been evaluated in gas phase as well as in aqueous phase. In order to quantify the LCA, LCB and different stereochemical nature of the free bases and their lithium complexes in aqueous phase, the optimization process have been carried out with SCRF–PCM model at the same theoretical level. Lithium cation affinity and basicity values of each compound reduced in solvent (water) enormously. The LCA and LCB value for 4-hydroxy-2-nonenal (HNE) is found to be highest in gas phase whereas methyl vinyl ketone shows the highest affinity for lithium cation in aqueous phase. In both phases acrolien (ACL) exhibits lowest lithium cation affinity and basicity. Natural population analysis (NPA) has been applied to evaluate partial atomic charges on binding oxygen and metal cation. Correlation between Charge transfer (Ligand to metal) and LCA values has been searched in both phases. Lithium induced shifts (LIS) at this electronic state have been measured from states (Low-lying excited state – ground state) energy difference.

## 10.1 Introduction

Cation affinity values are very important to understand the reactivity of an acids-base reaction.<sup>1-3</sup> Metal ion play important roles in almost one third of enzymes.<sup>4</sup> Alkali metal cations were first studied in gas phase because of their Lewis acid properties. Metal ion associations to unsaturated carbonyl compounds drawn more attention for their  $\pi$ -cation interactions.<sup>5</sup> In chapter 4, lithium cation affinities (LCA), lithium cation basicities (LCB) and some other quantum mechanical properties of six  $\alpha,\beta$ -unsaturated carbonyl compounds namely acrolein (ACL), 4-hydroxyl-2-nonenal (HNE), methyl vinyl ketone (MVK), Acrylamide (ACR), methyl acrylate (MA) and ethyl methacrylate (EMA) have been discussed in the ground state at same level of theory. The properties of the carbonyl compounds may vary in different electronic state (ground state to low-lying excited triplet state) due to electronic transition. Because at low-lying excited state, redistribution of electron densities caused by electronic transition modify the acid-base properties of the compounds. So a detailed knowledge about involved low-lying excited state is required for better considerate. The accurate theoretical data of these studied unsaturated carbonyl compounds at low-lying excited state are rarely available. We performed this calculation to provide some systematic quantum mechanical properties including LCA and LCB in both gas and aqueous phases at the relevant state. Quantum mechanical values obtained in ground and low-lying excited state has been discussed comparatively. It was observed previously, ion-molecule interactions are consistently involved in molecular recognition process.<sup>6</sup> Different experimental technique like high pressure mass spectrometry [HPMS]<sup>7-10</sup> or energy resolved collision induced dissociation [CID]<sup>11-13</sup> were employed to evaluate most accurate alkali metal cation affinities of several carbonyl bases. In recent years computational investigation of electronically excited state has been applied on protonated and alkali metal complexes of formamide.<sup>14</sup> The  $\text{Li}^+$  affinities of a series of substituted acetophenones in their low-lying



excited triplet state were reported earlier.<sup>15</sup> Previous investigations have stimulated to study the  $\text{Li}^+$  cation interaction with few biologically important unsaturated carbonyl compounds. The compounds chosen in present work are structurally related have extensive industrial utility and are pervasive environmental pollutants.<sup>16</sup> The gas phase lithium cation affinity (LCA) is defined as negative enthalpy change ( $-\Delta H$ ) corresponds to the thermodynamic equilibrium

$\text{B}_1 + \text{Li}^+ \leftrightarrow [\text{B}_1 - \text{Li}^+]$ .... (1). Where  $\text{B}_1$  treated as carbonyl base,  $\text{LCA} = -\Delta H_{\text{Li}^+}$  at 298.15K temperature. Lithium cation basicity (LCB) is defined as negative Gibbs free energy change ( $-\Delta G_{\text{Li}^+}$ ) of the same reaction at same temperature. The interaction enthalpy of a metal ion–Lewis base interaction also can be obtain as

$\Delta H^{298.15\text{k}} = \{E_{\text{tot}}^{298.15}(\text{B}_1\text{M}) - [E_{\text{tot}}^{298.15}(\text{B}_1) + E_{\text{tot}}^{298.15}(\text{M})]\} + \Delta(pV)$  .... (2). Where  $\text{B}_1$  = Carbonyl base and  $\text{M}$  = Metal cation (here  $\text{Li}^+$ ) and  $\Delta(pV) = RT$ . In the current work LCA values have been calculated following both equation (1) and (2) just to verify similarities of the data obtained in two ways. Lithium cation basicity of the compounds obtained from Gibbs free energies following equation (1). It is true that, a detailed knowledge of optimized geometry and energy of a metal ion–ligand interaction is required before attempting the theoretical optimization in solvent phase.<sup>17</sup> Since polar systems are stabilizes more in polar solvent (water) then equilibrium geometry and charge distribution may be effected on solvation. In order to describe the structural behaviour and energetic properties in aqueous phase we used most successful SCRF- PCM model<sup>18</sup> for geometry optimization. Besides LCA, LCB values, we also report the entropy change of the corresponding reactions as  $\Delta S^{298.15}$  at low-lying excited triplet state in both gas and aqueous phases. Ligand to metal charge transfer ( $q_{\text{CT}}$ ) from NPA results have been analysed to understand the complex stability in this particular state. We have also observed the mode of spectral shift caused by complex formation in the relevant state. A unified view of the quantum mechanical properties

of these six systems is emphasized and discussed. Compounds investigated in present study are given below with their name and abbreviation.

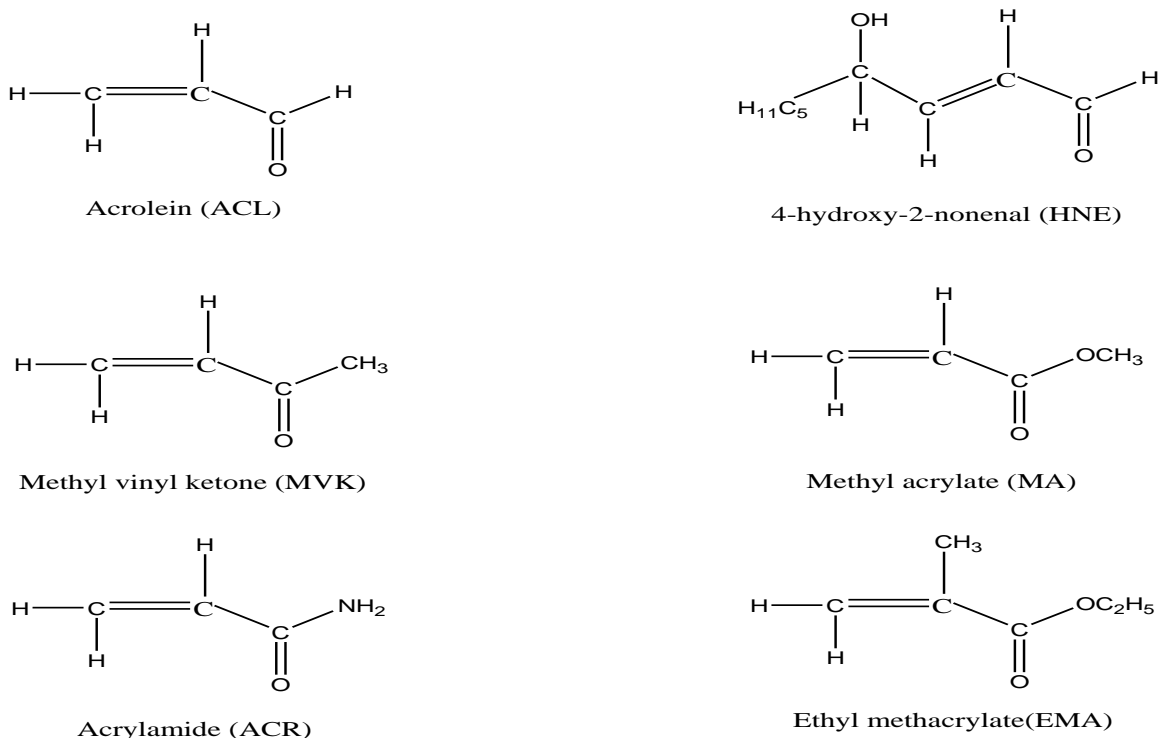


**Figure 10.2.1** Structure of several  $\alpha,\beta$ -unsaturated carbonyl compounds.

## 10.2 Computational details

We performed these theoretical calculations employing most reliable density functional theory (DFT/ B3LYP)<sup>19</sup> method at hybrid 6–311G(d,p) basis set level of Gaussian ‘09’ programme package.<sup>20</sup> Complete geometry optimization process in aqueous phase has been carried out using SCRF- PCM<sup>18</sup> model at the same level of theory. Water has been selected as solvent from the given list of solvents. A dielectric constant of 78.39 was utilized to simulate the aqueous atmosphere. Charge density on carbonyl oxygen of the free bases and of the lithium complexes and also the charge on  $\text{Li}^+$  of the complexes were evaluated from NPA.<sup>21</sup> The magnitude of basis set superposition error (BSSE) was evaluated at the same level of theory and found to be small. Therefore no corrections were made. Enthalpies, Gibbs free energies were obtained from standard frequency calculation. It was found from frequency

calculations at B3LYP/ 6-311G(d,p) level, all carbonyl compounds and their  $\text{Li}^+$  complexes were optimized with zero number of imaginary frequencies. .

### 10.3 Results and discussion

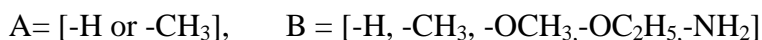
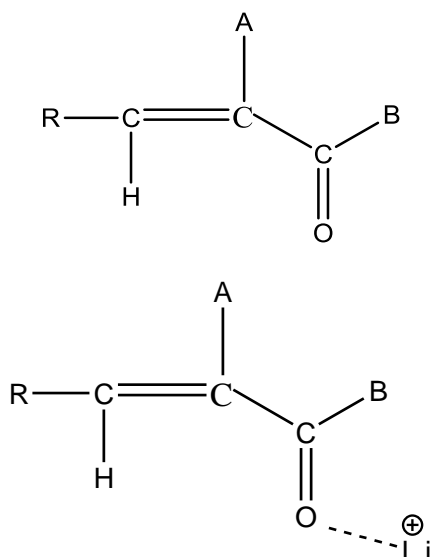


**Figure 10.2.2** General Chemical structure of  $\alpha,\beta$ -unsaturated carbonyl compounds and their  $\text{O-Li}^+$  complexes.

In previous chapter we have already discussed the proton affinities and basicities of the same set of unsaturated carbonyl derivatives at low-lying excited triplet state. Here we have analysed important lithium cation affinities (LCA), lithium cation basicities (LCB) and some other properties of six  $\alpha$   $\beta$ -unsaturated carbonyl compounds obtained in DFT/6-311G(d,p) calculations. **Table 10.1.1** summarizes the total optimization energies (hartree) of the free bases and their  $\text{O-Li}^+$  complexes and the obtained LCA ( $\Delta E_g$  and  $\Delta E_{\text{sol}}$ ) values (Kcal /mole) with their proper name and abbreviation. The LCA values reported in **Table 10.1.1** have been calculated using equation (2) where we substituted  $\Delta(pV) = RT$ . [ $T = 298.15 \text{ K}$ ]. It is seen that, gas phase LCA values vary in the range of  $-46.49 \text{ kcal /mole}$  to  $-80.5 \text{ kcal /mole}$  while in aqueous phase the LCA values are dropped largely remains in the range of  $-3.63 \text{ kcal$

/mole to  $-16.37$  kcal/mole. In both phases ACL have lowest affinity ( $-46.49$  kcal/mole) for lithium cation. The highest gas phase affinity ( $-80.5$  kcal/mole) exhibited by HNE whereas in aqueous phase MVK shows maximum affinity value ( $-16.5$  kcal/mole) for lithium. The LCA values calculated from enthalpies (H) (Obtained in frequency calculations) following equation (1) as  $-\Delta H_{Li^+} = H_{Li^+} + H_{free\ base} - H_{Complex}$  (at  $298.15^\circ$  K) are found to be almost same in each compound as their values tabulated in **Table 10.1.1**. In **Table 10.1.2** we summarized the relative free energies (G), enthalpies (H), LCA, LCB and entropy ( $\Delta S^{298.15k}$ ) of the corresponding complex formation reaction. We found that there is a marginal discrepancy between the values obtained in Table 1 and 2. It is  $\pm 0.5$  kcal/mole to  $\pm 2.64$  kcal/mole in gas phase and  $\pm 0.07$  kcal /mole to  $\pm 1.19$  kcal/mole in aqueous phase. The LCA values of six  $\alpha,\beta$ -unsaturated carbonyl compounds in the low-lying excited triplet state are obtained in the following decreasing order HNE > MA > ACR > EMA > MVK > ACL in the gas phase while it ranked differently on solvation and it is MVK > ACR > EMA > MA > HNE > ACL. Electronic relaxation effect caused by solvation may be responsible for the almost reversed order of LCA in water. The computed Gibbs free energies were utilized to calculate LCB ( $-\Delta G_{Li^+}$ ) values of the compounds. LCB values are calculated as  $-\Delta G_{Li^+} = G_{Li^+} + G_{free\ base} - G_{Complex}$ . The LCB values predicted in this study vary in the range of  $-38.9$  kcal/mole to  $-68.52$  kcal/mole in gas phase and on solvation it is reduced (from  $-8.91$  kcal/mole to  $4.07$  kcal/mole) and in some case positive values also appears. We observed that, low-lying excited state LCA values of the compounds in both phases are higher relative to ground state values with the exception of ACL(in gas phase) and ACL, HNE (in aqueous) where it obtained little bit lower. This trend already found in some previous study.<sup>22,23</sup> It happens due to the reorganisation of atomic charges in the low-lying excited state compared to ground state.

Gibbs free energy (G) mainly described the molecular association tendency; therefore change of entropy of a complexation reaction is important. When a single metal cation – complex is formed from a pair of reactants, loss of entropy is involved. In the present theoretical study  $\Delta S^{298.15\text{ K}}$  for complex formation reactions vary in the range of  $-22.94$  cal/mole to  $-43.56$  cal/mole in the gas phase and energy difference is reduced upon solvation ( $-24.38$  cal/mole to  $-28.006$  cal/mole). Partial atomic charges on carbonyl oxygen and on lithium cation of alkali-metal complexes and Ligand to Metal Charge Transfer ( $Q_{CT}$ ) in gas and solvent phases are tabulated in **Table 10.1.3**. Calculated  $Q_{CT}$  values from NPA results clearly indicate that, there is a significant charge transfer from ligand to metal ion. According to the obtained  $Q_{CT}$  results, conjugated carbonyl compounds are found in the following decreasing order  $HNE > ACR > MVK > EMA > MA > ACL$  in gas phase, upon solvation it ranked slightly different. In both phases  $Q_{CT}$  results (from NPA) are not fully parallel to the obtained LCA values of the compounds. LCA values of HNE, EMA and ACL are well supported by  $Q_{CT}$  results in gas phase and in aqueous phase  $Q_{CT}$  results satisfy the LCA order of MA and ACL.

The migration of charge is not local and originates from all over the molecule. In lithium complexes  $Li^+$  cation retains with 0.888e to 0.97e unit of positive charge in gas and aqueous phases. The large atomic charges on  $Li^+$  in the complexes indicate that, bond ( $O-Li^+$ ) formed by lithium cation with the ligands in low-lying excited state are largely ionic in nature, that means the interactions are ion-dipole and ion induced dipole rather than covalent interactions. Geometry optimization in low-lying excited state induces large effects in molecular structure.

The optimized geometries of the free base and their lithium complexes are presented in **Figure 10.2.3** and **10.2.4**. Most important stereochemical parameters at or around the carbonyl moiety of the optimized free bases and their lithium complexes are tabulated in **Table 10.1.4** and **Table 10.1.5**. It is seen that  $C = O$  bond length of ACR, MA and EMA increased slightly in  $O-Li^+$  complex (0.04 to 0.11 Å) relative to their free bases while in ACL,

HNE and MVK complexes C = O bond distance decreased by 0.035 to 0.065 Å. Employing PCM type of solvent model the C = O bond length elongated by 0.01 to 0.44 Å in HNE, ACR, MA, EMA, exceptionally it is decreased in ACL and MVK by 0.05 to 0.073 Å. We have observed that, O–Li<sup>+</sup> bond lengths in the complexes elongated by 0.16 to 0.21 Å upon solvation, which is an expected physical property. The <C–O–Li<sup>+</sup> bond angle has a variation in the range of 134.54 to 167.65° and 120.27 to 167.02° in gas and aqueous phase respectively. The values of the  $\tau(\text{C–C–O–Li}^+)$  dihedral angles reveals that, lithium complex of HNE and ACR has non planar configuration in both phases. We have seen that, lithium complexes of ACL, MVK, MA and EMA have planar geometrical configuration, where dihedral angles  $\tau(\text{C–C–O–Li}^+)$  are estimated to be 175° to 180° and 166° to 180° in gas and aqueous phases respectively. Concerning the geometries of six different optimized complexes, we have seen HNE favours to form bidentate specie in gas as well as in aqueous phase. It is known that, due to solvation alkali metal cation preferred to form open mono-dentate complexes, but alkali cation generally oscillate between two state (bi-dentate and mono-dentate) during optimization process, then it is difficult to predict the most stable complexes even it optimized because of proximate energetic stability. In HNE, Li<sup>+</sup> cation preferred bidentate binding mode (Li<sup>+</sup> bind with both carbonyl oxygen and hydroxyl oxygen) having  $\tau(\text{C–C–O–Li}^+)$  angle 134.16° and –17.59° in gas and aqueous phase respectively. The almost same stereochemical properties around carbonyl ring tend to suggest that, the LCA values of the studied compounds cannot be modelled accurately only considering the local effects. It also can be stated that different electronic properties [(Inductive (+I), resonance (+R, –R) effects)] of the entire molecule effects on lithium cation affinity values.

We have calculated the adiabatic transition energies from the state energies differences. Computed transition (<sup>1</sup>S<sub>0</sub> → T<sub>1</sub>) energies (hartree) in low-lying excited triplet state and shifts due to lithium cation interactions summarized in **Table 10.1.6**. We observed that, in gas

phase, lithium induced shifts (LIS) are red shifts in ACR, MA and EMA whereas ACL, HNE and MVK show blue shifts. In aqueous phase ACL and HNE show blue shifts, while red shifts found in rest four compounds. It is seen from the data recorded in **Table 10.1.7**, the dipole moment ( $\mu$ ) of the ACL, HNE and MVK are reduced in low-lying excited state ( $T_1$ ) relative to that of the ground state in both gas and aqueous phase whereas  $\mu$  of ACR, MA and EMA has been estimated to be higher than that in the ground state. This increase of dipole moment in these three carbonyl compounds may be due to the shifting of electron density from different substituent ( $-\text{NH}_2$ ,  $-\text{OCH}_3$  and  $-\text{OC}_2\text{H}_5$ ) to carbonyl chromophore.

## 10.4 Conclusion

From the present theoretical study, we can conclude that, lithium cation affinity (LCA) values of the investigated unsaturated carbonyl compounds are higher in low-lying excited triplet state compared to that in the ground state. Interaction between carbonyl oxygen and lithium cation is electrostatic ion dipole, ion induced dipole interactions rather than covalent interactions.  $\text{Li}^+$  cation prefers bidentate bonding mode with HNE in both gas and aqueous phase while other carbonyl compounds favours to form monodentate complex with lithium cation. The application of SCRF-PCM method leads to considerable changes in LCA values of the compounds. In gas phase, lithium induced shifts (LIS) are red shifts in ACR, MA and EMA and ACL, HNE and MVK shows blue shifts on  $^1\text{S}_0 \rightarrow \text{T}_1$  electronic transition energies. Blue shift effect on electronic transition energies have been found in ACL and HNE due to lithium complex formation.

**Table 10.1.1** Computed total energies (hartree) of the free bases ( $B_1$ ) and their lithium complexes ( $B_1Li^+$ ) and lithium cation affinities ( $LCA$ ) =  $\Delta H^{298.15K} = \{E^{298.15}(B_1Li^+) - [E^{298.15}(B_1) + E^{298.15}(Li^+)]\} + \Delta(pV)$  for both gas & aqueous phase at the equilibrium geometry of the low-lying excited triplet state.  $E_{Li^+}(Gas) = -7.2849$  hartree,  $E_{Li^+}(Aqueous) = -7.4787$  hartree. [ $LCA = \Delta E_g$  for gas phase and  $\Delta E_{Sol}$  for aqueous phase]

Molecule	Total energy (hartree)		$\Delta E_g$ kcal/mole	Total energy (hartree)		$\Delta E_{Sol}$ kcal/mole
	Gas Phase			Aqueous Phase		
	$B_1$	$B_1Li^+$	$B_1$	$B_1Li^+$		
Acrolin(ACL)	-191.8663	-199.2253	-46.49	-191.8695	-199.3541	-3.70
4-hydroxy-2-nonenal(HNE)	-503.0539	-510.4671	-80.50	-503.0843	-510.5703	-4.58
Methyl vinyl ketone (MVK)	-231.1978	-238.5641	-51.07	-231.2015	-238.7065	-16.50
Acrylamide (ACR)	-247.2466	-254.6308	-62.31	-247.2580	-254.7536	-10.60
Methyl acrylate (MA)	-306.4280	-313.8233	-69.27	-306.4378	-313.9293	-8.032
Ethyl methacrylate (EMA)	-385.1056	-392.4863	-60.11	-385.1150	-392.6074	-8.59



**Table 10.1.2** Obtained enthalpy, free energy of six  $\alpha,\beta$ -unsaturated carbonyl derivatives and Lithium Cation Affinities (LCA, kcal/mol), Lithium Cation Basicities (LCB, kcal/mol) and entropies ( $\Delta S$ ), cal/ mole by B3LYP/DFT method at 6-311G(d,p) level in gas and aqueous phase at low-lying excited triplet state.

LCA calculated as:  $H_{Li^+} + H_{free\ base} - H_{Complex}$ .

LCB calculated as:  $G_{Li^+} + G_{Free\ base} - G_{Complex}$

Gas phase data at 298.15K.

	<b>H</b>	<b>G</b>	$\Delta H_{Li^+}$	$\Delta G_{Li^+}$	$\Delta S$
	(hartree)	(hartree)	(kcal/mole)	(kcal/mole)	(cal/mole)
ACL	-191.8035	-191.8364	-45.99	-38.90	-23.77
ACL- Li <sup>+</sup>	-199.1593	-199.1960			
HNE	-502.8065	-502.869	-79.50	-68.52	-36.82
HNE-Li <sup>+</sup>	-510.2157	-510.2758			
MVK	-231.1061	-231.1538	-51.01	-43.54	-25.05
MVK-Li <sup>+</sup>	-238.4699	-238.5088			
ACR	-247.1688	-247.2144	-59.67	-46.68	-43.56
ACR-Li <sup>+</sup>	-254.5464	-254.5864			
MA	-306.3315	-306.3724	-67.20	-59.67	-25.25
MA-Li <sup>+</sup>	-313.7211	-313.7651			
EMA	-384.9485	-384.9959	-59.11	-52.27	-22.94
EMA-Li <sup>+</sup>	-392.3252	-392.3768			

Continued.....

Aqueous phase data at 298.15K.

	<b>H</b> (hartree)	<b>G</b> (hartree)	$\Delta H_{Li^+}$ (kcal /mole)	$\Delta G_{Li^+}$ (kcal /mole)	$\Delta S$ (cal /mole)
ACL	-191.8067	-191.8397	-03.63	04.07	-25.82
ACL- Li <sup>+</sup>	-199.2888	-199.3246			
HNE	-502.819	-502.890	-05.77	01.81	-25.42
HNE-Li <sup>+</sup>	-510.3196	-510.3785			
MVK	-231.1099	-231.1456	-16.37	-08.91	-25.02
MVK-Li <sup>+</sup>	-238.6123	-238.6512			
ACR	-247.1791	-247.2163	-09.85	-01.50	-28.006
ACR-Li <sup>+</sup>	-254.6711	-254.7101			
MA	-306.3410	-306.3809	-07.78	0.4392	-27.56
MA-Li <sup>+</sup>	-313.8297	-313.8716			
EMA	-384.9581	-385.0054	-07.96	-0.690	-24.38
EMA-Li <sup>+</sup>	-392.4471	-392.4979			

**Table 10.1.3** Partial atomic charges (unit 'e') on carbonyl oxygen( $Q_{O^-}$ ) of the free bases and of the metal complexes ( $B_1Li^+$ ) and charges on alkali metal cation ( $Q_{Li^+}$ ) of the metal complexes( $B_1Li^+$ ) obtained in NPA analysis of DFT/6-311G(d,p) method and Ligand to Metal Charge Transfer ( $Q_{CT}$ ) [unit 'e'] in both phases at low-lying excited (triplet) state.

Molecule	Gas Phase			$Q_{CT}$	Aqueous Phase			$Q_{CT}$
	$(Q_{O^-})$		$Q_{Li^+}$		$(Q_{O^-})$		$Q_{Li^+}$	
	$B_1$	$B_1Li^+$			$B_1$	$B_1Li^+$		
ACL	-0.177	-0.733	0.954	0.046	-0.191	-0.627	0.976	0.024
HNE	-0.187	-0.635	0.888	0.112	-0.205	-0.608	0.923	0.077
MVK	-0.200	-0.787	0.940	0.06	-0.217	-0.682	0.972	0.028
ACR	-0.595	-0.875	0.941	0.059	-0.677	-0.796	0.967	0.033
MA	-0.510	0.806	0.951	0.049	-0.585	-0.705	0.969	0.031
EMA	-0.554	-0.822	0.946	0.054	-0.618	-0.718	0.965	0.035

\*Charge Transfer calculated as {[formal charge on proton (+1)] – [Charge obtained on proton]} in the complex.

**Table 10.1.4** Geometrical features of the free bases [B<sub>1</sub>] and O-Li<sup>+</sup> complexes [B<sub>1</sub>Li<sup>+</sup>]. (Bond length in Å and bond angles, dihedral angles (τ) are in degree) in gas phase at low-lying excited triplet state.

Molecule	B <sub>1</sub>	B <sub>1</sub> Li <sup>+</sup>			
	r(C-O)	r(C-O)	r(O-Li <sup>+</sup> )	<C-O-Li <sup>+</sup>	τ<C-C-O-Li <sup>+</sup>
ACL	1.31	1.275	1.736	167.655	180.0
HNE	1.31	1.245	1.743	134.546	134.16
MVK	1.315	1.276	1.728	165.746	177.965
ACR	1.23	1.270	1.691	176.088	0.00
MA	1.236	1.247	1.734	156.667	179.556
EMA	1.214	1.254	1.739	145.995	175.144

**Table 10.1.5** Geometrical features of the free bases [B<sub>1</sub>] and O-Li<sup>+</sup> complexes [B<sub>1</sub>Li<sup>+</sup>]. in aqueous phase at low-lying excited triplet state. (Bond length in Å and bond angles, dihedral angles (τ) are in degree).

Molecule	B <sub>1</sub>	B <sub>1</sub> Li <sup>+</sup>			
	r(C-O)	r(C-O)	r(O-Li <sup>+</sup> )	<C-O-Li <sup>+</sup>	τ<C-C-O-Li <sup>+</sup>
ACL	1.31	1.267	1.92	167.0233	180.0
HNE	1.241	1.285	1.97	135.95	-17.59
MVK	1.315	1.242	1.92	120.278	-179.83
ACR	1.245	1.255	1.85	176.02	0.00
MA	1.238	1.246	1.89	147.456	179.73
EMA	1.223	1.237	1.93	131.579	166.37

**Table 10.1.6** Computed adiabatic transition energies (1<sub>S<sub>0</sub></sub>→T<sub>1</sub>) (hartree) and lithium-induced shifts (LIS, hartree) in the lowest excited triplet state.

Molecule	Gas Phase			Aqueous Phase		
	Transition Energy		LIS	Transition Energy		LIS
	B	B <sub>1</sub> Li <sup>+</sup>		B	B <sub>1</sub> Li <sup>+</sup>	
ACL	0.1019	0.1068	0.0049	0.0542	0.1094	0.0048
HNE	0.1012	0.1015	0.0003	0.0801	0.1213	0.0034
MVK	0.1042	0.1046	0.0004	0.1065	0.0911	-0.0154
ACR	0.1192	0.1142	-0.005	0.1186	0.1169	-0.0017
MA	0.1134	0.0943	-0.0191	0.1137	0.1134	-0.0003
EMA	0.1083	0.0948	-0.0135	0.1047	0.0974	-0.0073

**Table 10.1.7** Estimated dipole moment ( $\mu$ ) of six  $\alpha$   $\beta$ -unsaturated carbonyl compounds in gas phase as well as in aqueous phase at low-lying excited state ( $T_1$ ) and ground state.

Molecule	Gas phase		Aqueous Phase	
	Dipole moment ( $\mu$ )		Dipole moment ( $\mu$ )	
	Ground state	Low-lying excited state	Ground state	Low-lying excited state
ACL	3.15	0.833	4.04	0.991
HNE	2.12	1.68	2.83	1.79
MVK	2.7	2.01	3.51	2.60
ACR	3.88	3.97	5.14	5.21
MA	4.32	4.35	5.56	5.71
EMA	1.78	4.22	5.51	5.76

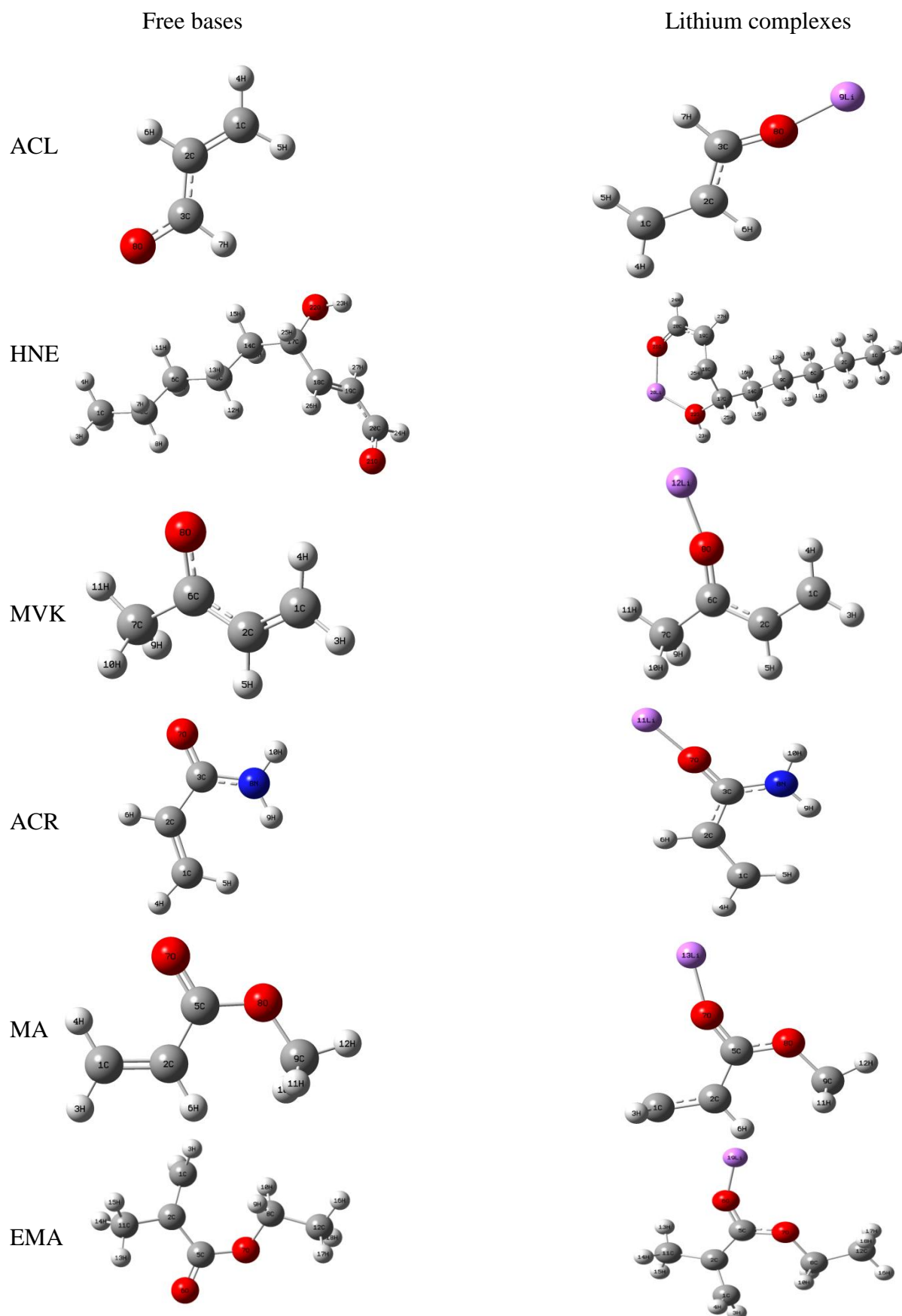


**Figure 10.2.3** Optimized geometries of free bases and their O-Li<sup>+</sup> complexes in gas phase.

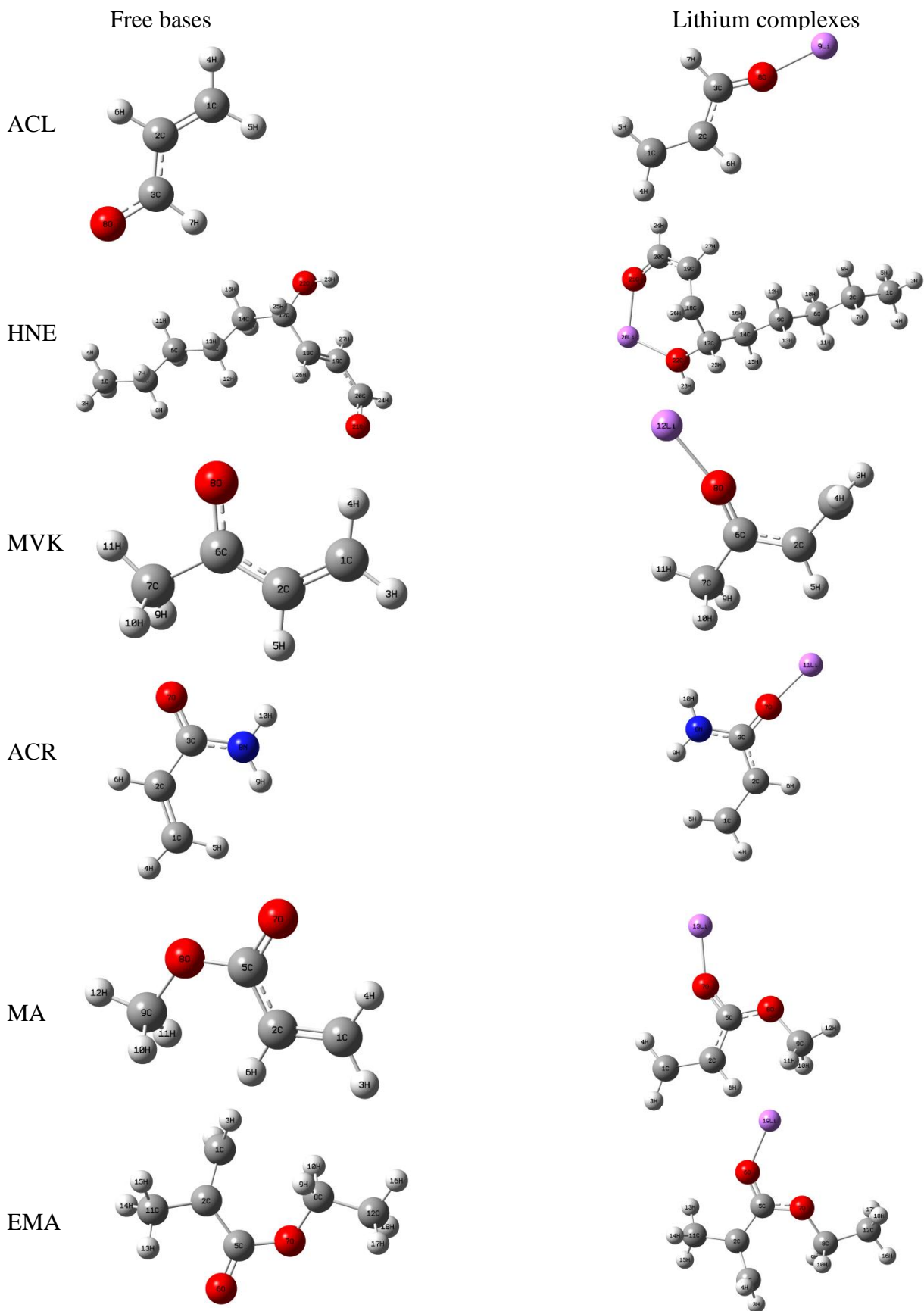


**Figure 10.2.4** Optimized geometries of free bases and their O-Li<sup>+</sup> complexes in aqueous phase.

## 10.5 References

- (1) Larionov, E.; Zipse, H. *WIREs Comp. Mol. Sci.* **2011**, *1*, 601–619.
- (2) Denmark, S. E.; Beutner, G. L. *Angew. Chem. Int. Ed.* **2008**, *47*, 1560–1638.
- (3) De Rycke, N.; Couty, F.; David, O. R. P. *Chem. Eur. J.* **2011**, *17*, 12852–12871.
- (4) Silva, J. J. R. F. D.; Williams, R. J. P. *The Biological Chemistry of the Elements*, Clarendon Press: Oxford. 1991.
- (5) Corral, I.; Mo, O.; Yancz, M. *Int. J. Mass Spectrom.* **2006**, *255*, 20.
- (6) Ma, J. C.; Dongherty, D. A. *Chem. Rev.* **1997**, *97*, 1303.
- (7) Dzidic, I.; Kebarle, P. *J. Phys. Chem.* **1970**, *74*, 1466–1474.
- (8) Sunner, J.; Kebarle, P. *J. Am. Chem. Soc.* **1984**, *106*, 6135–6139.
- (9) Tissandier, M. D.; Cowen, K. A.; Feng, W. Y.; Gundlach, E.; Cohen, M. H.; Earhart, A. D.; Coe, J. V.; Tuttle, T. R. Jr. *J. Phys. Chem. A* **1998**, *102*, 7787–7794.
- (10) Castleman, A. W.; Keesee, R. G. *Chem. Rev.* **1986**, *86*, 589–618.
- (11) More, M. B.; Glendening, E. D.; Ray, D.; Feller, D.; Armentrout, P. B. *J. Phys. Chem.* **1996**, *100*, 1605–1614.
- (12) Rodgers, M. T.; Armentrout, P. B. *J. Phys. Chem. A* **1997**, *101*, 1238–1249.
- (13) Rodgers, M. T.; Armentrout, P. B. *J. Phys. Chem. A* **1997**, *101*, 2614–2625.
- (14) Antol, I.; Barbatti, M.; Mirjana, E.-M.; Lischka, H. *Monatsh Chem.* **2008**, *139*, 319–328.
- (15) Senapati, U.; De, D.; De, B. R. *J. Mol. Struct. (Theochem)* **2009**, *894*, 71–74.
- (16) Lopochin, R. M.; Gavin, T. *Environmental Health Perspectives*, **2012**, *120* (12), 1650–1657.
- (17) Jensen, F. *J. Am. Chem. Soc.* **1992**, *114*, 9533–9537.
- (18) Tomasi, J.; Mennucci, B.; Cancès, E. *J. Mol. Struct. (Theochem)* **1999**, *464*(1-3), 211–226.

## Chapter 10

- (19) Lee, C.; Yang, W.; Parr, R. G. *Phys. Rev.* **1988**, *B37*, 785.
- (20) Frisch, M. J.; Trucks, G. W.; Schlegel, H. B.; Scuseria, G. E.; Robb, M. A.; Cheeseman, J. R.; Scalmani, G.; Barone, V.; Mennucci, B.; Petersson, G. A.; Nakatsuji, H.; Caricato, M.; Li, X.; Hratchian, H. P.; Izmaylov, A. F.; Bloino, J.; Zheng, G.; Sonnenberg, J. L.; Hada, M.; Ehara, M.; Toyota, K.; Fukuda, R.; Hasegawa, J.; Ishida, M.; Nakajima, T.; Honda, Y.; Kitao, O.; Nakai, H.; Vreven, T.; Montgomery, Jr., J. A.; Peralta, J. E.; Ogliaro, F.; Bearpark, M.; Heyd, J. J.; Brothers, E.; Kudin, K. N.; Staroverov, V. N.; Kobayashi, R.; Normand, J.; Raghavachari, K.; Rendell, A.; Burant, J. C.; Iyengar, S. S.; Tomasi, J.; Cossi, M.; Rega, N.; Millam, J. M.; Klene, M.; Knox, J. E.; Cross, J. B.; Bakken, V.; Adamo, C.; Jaramillo, J.; Gomperts, R.; Stratmann, R. E.; Yazyev, O.; Austin, A. J.; Cammi, R.; Pomelli, C.; Ochterski, J. W.; Martin, R. L.; Morokuma, K.; Zakrzewski, V. G.; Voth, G. A.; Salvador, P.; Dannenberg, J. J.; Dapprich, S.; Daniels, A. D.; Farkas, O.; Foresman, J. B.; Ortiz, J. V.; Cioslowski, J.; Fox, D. J. *Gaussian 09, Revision A.02*, Gaussian, Inc., Wallingford CT, 2009.
- (21) Glendening, E. E.; Reed, A. E.; Carpenter, J. E.; Weinhold, F. *NBO (Natural Bond Orbital)*, v. 5.0
- (22) Goeller, A. H.; Strehlow, D.; Hermann, G. *Chemphyschem.* **2005**, *6*, 1259–1268.
- (23) Antol, I.; Eckert-Maksić, M.; Klessinger, M. *J. Mol. Struct. (Theochem)* **2003**, *664–665*, 309–317.



## **CHAPTER 11**

**The proton affinities of a series of heterocyclic compounds pyrrole, furan, thiophene and pyridine in their low-lying excited triplet state: A DFT based comparative study**



## Abstract

Gas phase proton affinities(PAs), basicities ( $\Delta G$ ) and transition energies( $^1S_0 \rightarrow T_1$ ) of a series of heterocyclic molecules (pyrrole, furan, thiophene and pyridine) and their protonated counterparts have been investigated using density functional theory (Becke, Lee, Yang and Parr [B3LYP]) method at 6-311G(d,p) basis set level with complete geometry optimization in their low-lying excited triplet state. As in the case of ground states, the gas phase protonation turns out to be exothermic in each case. Geometry and electronic structures of the protonated complexes have been searched extensively. According to the calculated results, the proton affinity is predicted to be  $-222.13$  kcal/mole for pyridine. Proton affinities have been obtained more due to protonation at  $C_\alpha$  ( $C_1$ ) position of pyrrole, thiophene relative to the protonation at  $C_\beta$  and hetero (atom) sites. In furan, protonation at hetero atom ( $X = O$ ) leads to  $O-C_1$  bond breaking where PA value is determined to be  $-206.45$  kcal/mole. Computed proton affinities are sought to be correlated with the number of computed system parameters such as the net computed charge on the atoms (participating in protonation) of the free molecules and protonated species, charge on the proton of the protonated species and the computed hardness ( $\eta$ ) of the unprotonated species in their relevant excited states. The proton induced shifts (PIS) are in general red shifts for the lowest excited triplet states.

## 11.1 Introduction

The electron donor and acceptor definition of acidity and basicity introduces the idea that, there must be some relation between the molecular electron density distribution and the acid-base properties. This also implies that this property may vary from state to state of the same molecule due to some electronic transitions which are accompanied by extensive reorganization of molecular electronic charge distribution. Absorption and fluorescence spectral data in conjunction with Forster cycle<sup>1-4</sup> are utilized for the experimental determination of acid-base properties of molecules in excited states in presence of solvents. Gas phase methods<sup>5-7</sup> which ignore the complicating effects of solvation, have been successfully applied to determine the gas phase acid-base properties of molecules in excited states. Absolute proton affinity (PA) provides important information about electrophilic reactivity.<sup>8</sup> Intrinsic acid-base properties of a molecules or compounds may be reflected by their PA values. Gas phase PA and basicity ( $\Delta G$ ) are of considerable interest in the field of theoretical chemistry research.<sup>9</sup> PA can be utilised to determine the stability of ion-molecule complexes.<sup>10,11</sup> Pyrrole, furan and thiophene ( $C_4H_5N$ ,  $C_4H_4O$  and  $C_4H_4S$ ) are planar five membered (FM) aromatic heterocyclic molecules having  $C_{2v}$  point group. Pyridine ( $C_5H_5N$ ) is a prototypical planar ( $C_{2v}$  point group) six membered (SM) aromatic base. These heterocyclic molecules are widely known as basic units of different biological compounds.<sup>12-</sup>  
<sup>14</sup> The derivative of this five or six membered heterocyclic compounds involved in various bio-molecular and medicinal activities<sup>15-20</sup> such as anticancer, antitumor and so on. In the previous chapter (7), we have discussed on comparative PA, alkali metal cation ( $Li^+$ ,  $Na^+$ ) affinities and basicities of the same class of molecules in their equilibrium ground state. In this chapter, the effects of the change of electronic state ( $^1S_0$  to  $T_1$ ) on the PA, gas phase basicities ( $\Delta G$ ) and geometrical parameters have been investigated using quantum mechanical calculations. The PA values of furan and thiophene were determined theoretically<sup>21</sup> at the R1-

MP2/ aug-cc-pVDZ level of calculation. DFT/ MRCI computational method were employed to explore the ground and low-lying excited states of thiophene.<sup>22</sup> Various computational methods have been applied to investigate the radiationless deactivation of photo-excited furan.<sup>23</sup> Geometries and some electronic properties of low-lying triplet states of aniline has been studied computationally.<sup>24</sup> So far systematic and comprehensive studies on the ion-molecular reactions (protonation) of low-lying excited triplet state of a series of heterocyclic compounds (pyrrole, furan, thiophene and pyridine) are rather scarce. We are therefore compelled to turn to theory to obtain some quantitative idea about the relative proton affinities of these heterocyclic compounds in this particular state employing DFT/ B3LYP method<sup>25,26</sup> of calculation at 6-311G(d,p) basis set level of Gaussian 09W program package.<sup>27</sup> Recently the basicities of a series of substituted crotonaldehyde and acetophenone in their ground states and lowest excited triplet state have been theoretically calculated.<sup>28-31</sup> Ground state proton affinities of the same set of hetero cyclic molecules have been studied<sup>32</sup> earlier. We have analysed the PA values, transition energies of these molecules in various aspects, e.g., different protonation sites [ $C\alpha$ ,  $C\beta$  and hetero atoms (N, O or S)] have been considered to understand the most stable protonated complex in this electronic state. The natural charges of the atoms have been evaluated by means of natural population analysis (NPA). Finally a comparison has been drawn between ground state and low-lying excited state molecular properties of the studied molecules. We have also analysed the kind and extent of spectral shift caused by protonation. In a particular state the possibility of correlating the PA values with the global hardness of the molecules is also explored.

## 11.2 Computational details

All calculations were carried out using Gaussian O9W program package.<sup>27</sup> The molecular structures were optimized by the most accurate and reliable DFT/ B3LYP method at 6-311G (d,p) basis set level. In all calculations complete geometry optimization has been carried out on the molecules both before and after protonation. Unscaled vibrational frequency calculations were performed (at 298.15K) at the same level of theory. The optimized structures are used in these frequency calculations. Proton affinity (PA) has been calculated as  $(H_{BH^+} - H_B)$  and gas phase basicity  $(\Delta G) = (G_{BH^+} - G_B)$ , H= Total enthalpy, G = Total Gibbs free energy.

## 11.3 Results and Discussion

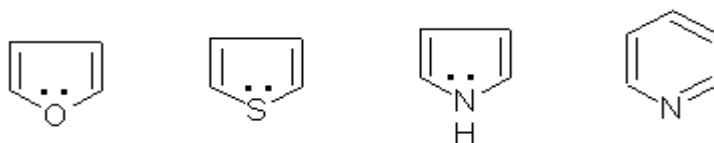


**Figure 11.2.1** General structure of studied molecules.

The gas phase basicity of a molecule defined as negative free energy change ( $\Delta G$ ) of a protonation reaction like  $B + H^+ \leftrightarrow [BH^+]$ .... (1). Proton affinity (PA) is defined in terms of negative enthalpy change ( $\Delta H$ ) associated with the same reaction at 298.15k temperature. Where B represent the molecules studied in the present work. Gas phase proton affinities have been calculated as  $[H_{B_1H^+} - H_{B_1}]$ ,  $[H_{B_2H^+} - H_{B_2}]$ ,  $[H_{B_3H^+} - H_{B_3}]$ ,  $[H_{B_4H^+} - H_{B_4}]$ . In the similar way, gas phase basicities ( $\Delta G$ ) of the same molecules have been calculated as  $[G_{B_1H^+} - G_{B_1}]$ ,  $[G_{B_2H^+} - G_{B_2}]$ ,  $[G_{B_3H^+} - G_{B_3}]$ ,  $[G_{B_4H^+} - G_{B_4}]$ . Where B1 = pyrrole, B2 = furan, B3 = thiophene, B4 = pyridine and G = Total Gibbs free energy. The molecules studied are listed in **Table 11.1.1** along with their respective names and their different proton affinity and gas phase basicity values obtained due to protonation occurred at different sites ( $C_\alpha$ ,  $C_\beta$  and X

hetero atoms) at the lowest excited triplet state. In case of pyridine,  $H^+$  preferentially attacked at N atom and gives more PA value ( $-222.13$  kcal/mole). Protonation at  $^1C\alpha$  carbon of pyridine provide little less PA value ( $-220.88$  kcal/mole). Five-membered heteroatomic systems, pyrrole, furan and thiophene have two different carbon sites attracting the incoming proton. We observed that, protonation can also occurred at X hetero atoms [X = N (pyrrole), O (furan) and S (thiophene)]. According to calculated results, it has been seen that, proton affinity values due to protonation at  $C\alpha$  and  $C\beta$  position are differ only by  $\pm 3.76$  kcal/mole. Proton affinity of thiophene is predicted to be  $-215.23$  kcal/mole) and  $-210.21$  kcal/mole for  $C\alpha$  and  $C\beta$  protonation. PA values are obtained little lower for pyrrole and thiophene in their X- protonated complexes. However, protonation of furan occurred at hetero oxygen atom accompanied with  $-206.45$  kcal/mole PA and provide O–C<sub>1</sub> bond opened optimized geometry (optimized geometry **I of Figure 11.2.1**). The proton affinity values are predicted to be  $-203.31$  and  $-208.96$  kcal/mole, due to protonation at  $^1C\alpha$  and  $^2C\beta$  sites of furan.

Calculated gas phase basicity ( $\Delta G$ ) results (**Table 11.1.1**) are found much closer to their PA values, In some cases two results are obtained almost identical. The  $\Delta G$  values are obtained exactly same with their PA results for protonated complexes of pyridine,  $C\beta$  and X- protonated complexes of thiophene. As per our results, PA and  $\Delta G$  values are differs by  $\pm 4.89$  to  $\pm 6.15$  kcal/mole in pyrrole complexes. These differences are found to be much lower ( $\pm 0.62$  to  $0.63$  kcal/mole) in furan complexes and  $C\alpha$  complexes of thiophene.

In comparison to the ground state PA results, low-lying excited triplet state PA values of the studied FM heterocyclic molecules are obtained higher. In case of pyridine, PA value at this particular electronic state is predicted to be lower than the ground state result, which can be attributed to the phenomenon of redistribution of charges in the low-lying excited state.

In **Table 11.1.2**, we summarised the Mulliken atomic charges on some specific atoms (protonation site) of the neutral and protonated complexes of the studied molecules. Partial

atomic charges (natural charge) on added proton and ligand to proton charge transfer ( $q_{CT}$ ) obtained from NPA procedure is tabulated in **Table 11.1.3**. The corresponding MPA values of charge transfer ( $Q_{CT}$ ) are also included in **Table 11.1.2** for the sake of comparison. Both  $Q_{CT}$  and  $q_{CT}$  results indicate that, there is a significant charge transfer from ligand to added proton. One might have expected the extent of charge transfer to parallel complex stability, but this is not occurred in the present cases. The calculated charge transfer ( $Q_{CT}$  and  $q_{CT}$ ) results provide same order of stability of the complexes of pyrrole, furan and thiophene. It is  $C\alpha-H^+ \geq C\beta-H^+ > X-H^+$  for pyrrole and furan. In case of thiophene, we observed this order obtained as  $X-H^+ > C\alpha-H^+ \geq C\beta-H^+$ .

Geometry of the five-member hetero atomic systems (pyrrole, furan and thiophene) and SM hetero cyclic pyridine have planar geometry at ground state with  $C_{2v}$  point group. The geometric parameters of all protonated complexes of the studied molecules have been tabulated in **Table 11.1.4 (4a, 4b, 4c)** and **Table 11.1.5**. Protonation at hetero atom (X) of all the molecules provide (**Table 11.1.4a**)  $X-H^+$  bond length 0.098Å to 1.39Å in the range. The  $\angle C-X-H^+$  bond angle shows the variation in the range of 101.42 to 120.51° and dihedral angle  $\tau(C\beta-C\alpha-X-H^+)$  is observed 120.76 and 92.64° for pyrrole and thiophene which are found to be 179.99° and 179.97° in furan and pyridine respectively. In  $C\alpha-H^+$  complexes (**Table 11.1.4b**), bond distance between  $C\alpha$  and excess proton ( $H^+$ ) is found to be same (1.09Å) in each cases. The  $\angle C-C\alpha-H^+$  bond angle in all complexes remains in between 110.8 and 114.17° and dihedral angle  $\tau(C-C-C\alpha-H^+)$  has a variation in the range of 115.51 to 120.3°. **Table 11.1.4c** highlighted the structural parameters of  $C\beta-$  protonated complexes. We observed, the  $C\beta-H^+$  bond length is identical (1.1Å) in each complex. Bond angle ( $\angle C-C\beta-H^+$ ) and dihedral angle ( $\tau(C-C-C\beta-H^+)$ ) of these complexes varies within 110.65 to 112.03° and -122.91 to 121.39° respectively.



Comparison of the structural parameters of optimized unprotonated and various protonated complexes of the studied molecules demonstrate the large effects of protonation on geometry of the molecules. We observed, geometrical parameters are varies widely with the variation of the site of protonation (**Table 11.1.5**). Optimized geometry of various protonated complexes are presented in **Figure 11.2. 2**.

#### **Optimized geometry of X–H<sup>+</sup> complexes:**

Protonation at X atom accompanied with the elongation of C4–X bond distance in pyrrole (0.07Å), large contraction is observed in furan (0.11Å) while it remain almost same in thiophene ( $\pm 0.01\text{Å}$ ). The C5–X bond distance in pyridine is also contracted by 0.07Å. C1–X bond length in pyrrole and pyridine protonated species are estimated 1.49Å and 1.46Å which are 0.07Å larger than the unprotonated molecules. Proton attacked at the O atom of furan leads to the O–C1 bond breaking mechanism and C1–O bond length is observed enormously large 2.89Å.

In addition, C1–C2 bond length, in pyrrole and pyridine protonated systems, is increased by 0.03 and 0.1Å whereas in furan and thiophene, this bond distance is decreased by 0.14 and 0.02Å. Concerning the bond angles ( $\angle\text{C2–C2–C3}$ ), a larger alteration has been observed in furan [106°(neutral) to 125°(protonated)], in pyrrole, thiophene and pyridine systems, minor alteration (0 to 3°) is found for this particular bond angle. Taking care of the (C1–X–C4) bond angle of three FM heterocyclic species, a huge contraction has been found in furan [105°(neutral) to 82°(complex)] whereas in pyrrole, thioophene and pyridine, it remains almost equal (1° to 4° change observed).

#### **Optimized geometry of C $\alpha$ –H<sup>+</sup> complexes:**

In comparison with geometry parameters of optimized unprotonated molecules, C1–X bond distances are elongated by 0.06Å, 0.09Å, 0.07Å and 0.02Å in protonated complexes of

pyrrole, furan, thiophene and pyridine respectively. On the other hand, C5–X bond length is largely shortened (0.12Å) in pyridine and 0.04Å to 0.06Å contractions have been observed in three FM heterocyclic complexes. In addition, C1–C2 bond distance obtained higher in pyrrole (0.06Å), and pyridine (0.16Å) protonated systems, but in thiophene and furan complexes, C1–C2 bond distance is shortened by 0.03Å and 0.01Å respectively. No such remarkable alteration has been found of C1–C2–C3 bond angles in all four heterocyclic protonated species relative to the unprotonated molecules. In contrary, large changes related to C1–X–C4 bond angle in FM heterocyclic protonated systems and C1–X–C5 bond angle of pyridine, which have been estimated to be 114°, 111°, 94° and 133° in pyrrole, furan, thiophene and pyridine respectively.

#### **Optimized geometry of C<sub>β</sub>–H<sup>+</sup> complexes:**

We have estimated the C4–X bond length 1.43Å and 1.81Å in pyrrole and thiophene protonated complexes, which are slightly higher than corresponding bond length in neutral systems. Large contraction (0.11Å) of this bond is found in furan complex compared to its unprotonated species (1.28Å). The C1–X bond length in both protonated pyrrole and thiophene is shortened by 0.11Å and it is slightly elongated (0.02Å) in furan. Protonation at C<sub>β</sub> do not effects effectively on C1–C2 bond distances of pyrrole and furan, but in case of thiophene complex, C1–C2 distance decreased by 0.07Å. As per our estimated values, no large changes have been found in <C1–C2–C3 bond angles in C<sub>β</sub>–H<sup>+</sup> complexes of pyrrole and thiophene (1° to 2°), in furan complex, it shifted 106° to 100°. The <C1–X–C4 bond angles are in the range of 91 to 111° which are found 88° to 107° in optimized unprotonated molecules.

**Electronic Transition Energies:** There are plenty of reports<sup>33-36</sup> about different electronic transition energies of these five or six membered heterocyclic molecules or their protonated complexes presented in literature. In this theoretical study, we have determined the adiabatic

transition energies ( ${}^1S_0 \rightarrow T_1$ ) as state energy difference. The results have been applied to find out the kind of shifts [proton induced shifts (PIS)] due to protonation. These results are tabulated in **Table 11.1.6 (6a, 6b, 6c)**. On the basis of our calculated results, the PIS are predicted to be red shift in all cases. These data refer to the gas phase protonation of the isolated base molecules without any additional effects caused by solvation.

We have searched for the possibility of existence of correlation with a single global parameter of the entire molecule in the relevant state. As the global parameter we have chosen the hardness ( $\eta$ ). The absolute hardness ( $\eta$ ) is defined by  $(I - A)/2$ . Where  $I$  is the vertical ionisation energies and  $A$  mean the vertical electron affinity. According to Koopmans's theory  $I = -\epsilon_{\text{HOMO}}$  (HOMO energy) and  $A = -\epsilon_{\text{LUMO}}$  (LUMO energies). Therefore  $\eta = (\epsilon_{\text{LUMO}} \sim \epsilon_{\text{HOMO}})/2$ . **Table 11.1.7** contain the values of HOMO and LUMO energies of the studied molecules and calculated hardness at lowest-excited triplet state along with the respective ground state values. From **Table 11.1.7**, it is seen that, the triplet state  $\eta$  values are lower compared to their ground state which favour protonation, in general.

In comparison to the ground state singlet computed values, the net atomic charge on hetero atom of the neutral heterocyclic molecules little bit increased in three FM systems, while in case of B4 it decreases slightly ( $-0.292 e$  to  $-0.201e$ ). This indicates that both pre-and post-protonation correlations with local charge densities in the immediate neighbourhood of the protonation site are weak.

## 11.4 Conclusion

The proton affinity and different electronic properties of pyrrole, furan, thiophene and pyridine have been investigated extensively at low-lying excited triplet state. From the present theoretical study it can be well concluded that, the gas phase proton affinities of the pyrrole, furan, thiophene and pyridine are spontaneous. Proton affinity values are predicted to be higher in all three FM heterocyclic systems relative to their ground state. Little deviation has been observed in pyridine where PA value obtained little less ( $\sim 10$  kcal/mole) compared to the ground state. Protonation at  $C\alpha$  and  $C\beta$  sites provides the more stable protonated complexes of pyrrole, thiophene than the N or S protonated. Proton attacked at O atom of neutral furan gives ring opened (O–C1 bond breaking) planar structure (Torsion angle  $179.99^\circ$ ). Protonation leads to loss of planarity for FM hetero systems (Except O-protonated furan) whereas pyridine retained with planer geometry even after protonation (N-protonated). Protonation at any sites (C or X = N, O, S) insert massive effect on geometrical features of the molecules. Proton Induced Shifts (PIS) are red shifts in all cases. The overall reactivity is fully explained by distant atom contribution in addition to the contribution from the hetero atoms of the free bases.

**Table 11.1.1** Different gas phase proton affinities ( $\Delta E$ ) and basicities ( $\Delta G$ ) of pyrrole, furan, thiophene and pyridine obtained from B3LYP/ 6-311G (d,p) method of calculation in low-lying triplet state.

Compound	( $\Delta E$ ) (kcal/mole)	( $\Delta G$ ) kcal/mole
Pyrrole(X-H <sup>+</sup> )	-209.96	-205.07
Pyrrole (C <sub><math>\beta</math></sub> -H <sup>+</sup> )	-226.9	-221.38
Pyrrole (C <sub><math>\alpha</math></sub> -H <sup>+</sup> )	-223.14	-216.99
Furan (X-H <sup>+</sup> )	-206.45	-207.07
Furan (C <sub><math>\beta</math></sub> -H <sup>+</sup> )	-208.96	-208.33
Furan (C <sub><math>\alpha</math></sub> -H <sup>+</sup> )	-203.31	-203.94
Thiophene(X-H <sup>+</sup> )	-193.27	-193.27
Thiophene (C <sub><math>\beta</math></sub> -H <sup>+</sup> )	-210.21	-210.21
Thiophene (C <sub><math>\alpha</math></sub> -H <sup>+</sup> )	-215.23	-214.6
Pyridine(X-H <sup>+</sup> )	-222.13	-222.13
Pyridine (C <sub><math>\alpha</math></sub> -H <sup>+</sup> )	-220.88	-220.88

**Table 11.1.2** Mullikan atomic charges (e) on some selected atoms of the free and protonated complexes of pyrrole, furan, thiophene and pyridine in their low-lying triplet state and Charge transfer (Q<sub>CT</sub>) obtained from MPA analysis.

Compound	atom	Free compound	(X-H <sup>+</sup> ) complex	Q <sub>CT</sub>	C <sub><math>\alpha</math></sub> -H <sup>+</sup> complex	Q <sub>CT</sub>	C <sub><math>\beta</math></sub> -H <sup>+</sup> complex	(Q <sub>CT</sub> )
Pyrrole	N	-0.424	-0.329	<b>0.69</b>	-0.279	<b>0.797</b>	-0.157	<b>0.797</b>
	C <sub><math>\alpha</math></sub>	0.038			-0.03		---	
	3C <sub><math>\beta</math></sub>	-0.143			---		-0.205	
	11 <sub>H+</sub>	---	0.31		0.203		0.203	
Furan	O	-0.293	-0.146	<b>0.7</b>	-0.162	<b>0.783</b>	-0.12	<b>0.78</b>
	C <sub><math>\alpha</math></sub>	0.056			0.002		---	
	2C <sub><math>\beta</math></sub>	-0.156			---		-0.187	
	10 <sub>H+</sub>	---	0.3		0.217		0.22	
Thiophene	S	0.172	0.562	<b>0.864</b>	0.571	<b>0.764</b>	0.556	<b>0.79</b>
	C <sub><math>\alpha</math></sub>	-0.274			-0.373		---	
	3C <sub><math>\beta</math></sub>	-0.067			---		-0.149	
	10 <sub>H+</sub>	---	0.136		0.236		0.21	
Pyridine	N	-0.201	-0.366	<b>0.707</b>	.....	<b>0.707</b>	.....	<b>0.707</b>
	C <sub><math>\alpha</math></sub>	0.013						
	C <sub><math>\beta</math></sub>	0.013						
	12 <sub>H+</sub>	---	0.293					

\*In case of pyridine, proton preferentially attacked at hetero atom (N) so charge on  $\alpha$  or  $\beta$  carbon not given.

**Table 11.1.3** Partial atomic charges on  $H^+$  ion [ $q_{H^+}$ ] (in e unit) in different protonated complexes obtained from NPA procedure and charge transfer ( $q_{CT}$ ) from compound to added proton.

Protonated complex	Charge on proton ( $q_{H^+}$ )	Charge transfer ( $q_{CT}$ )
Pyrrole ( $X-H^+$ )	0.237	0.763
Pyrrole ( $C_\alpha-H^+$ )	0.145	0.855
Pyrrole ( $C_\beta-H^+$ )	0.168	0.832
Furan ( $X-H^+$ )	0.25	0.75
Furan ( $C_\alpha-H^+$ )	0.143	0.857
Furan ( $C_\beta-H^+$ )	0.179	0.821
Thiophene ( $X-H^+$ )	0.142	0.858
Thiophene ( $C_\alpha-H^+$ )	0.149	0.851
Thiophene ( $C_\beta-H^+$ )	0.168	0.832
Pyridine ( $X-H^+$ )	0.213	0.787

\*Charge transfer calculated as [Normal charge of proton (1) –  $q_{H^+}$ ]

**Table 11.1.4** Some important geometrical features [bond length in Å, bond angle in degree, dihedral angle ( $\tau$ ) in degree] of the protonated complexes of pyrrole, furan, thiophene and pyridine in the low-lying excited state.

#### 11.1.4a. ( $X-H^+$ ) complexes

Complexes	$X-H^+$	$\angle C_\alpha-X-H^+$	$\tau (C_\beta-C_\alpha-X-H^+)$
Pyrrole ( $X-H^+$ )	1.03	112.05	120.76
Furan ( $X-H^+$ )	0.98	113.2	0.014 and 179.99
Thiophene ( $X-H^+$ )	1.39	101.42	92.64
Pyridine ( $X-H^+$ )	1.01	120.51	179.97

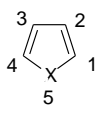
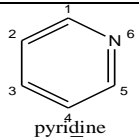
**11.1.4b.** ( $C_{\alpha}-H^+$ ) complexes

Complexes	$r(C_{\alpha}-H^+)$ in Å	$\angle C-C_{\alpha}-H^+$ in °	$\tau(C-C-C_{\alpha}-H^+)$
Pyrrole ( $C_{\alpha}-H^+$ )	1.09	114.17	117.69
Furan ( $C_{\alpha}-H^+$ )	1.09	115.45	115.51
Thiophene ( $C_{\alpha}-H^+$ )	1.09	113.9	-117.59
Pyridine ( $C_{\alpha}-H^+$ )	1.09	110.8	120.3

**11.1.4c.** ( $C_{\beta}-H^+$ ) complexes

Complexes	$r(C_{\beta}-H^+)$ in Å	$\angle C-C_{\beta}-H^+$ in °	$\tau(C-C-C_{\beta}-H^+)$
Pyrrole ( $C_{\beta}-H^+$ )	1.1	112.03	-121.11
Furan ( $C_{\beta}-H^+$ )	1.1	111.71	121.39
Thiophene ( $C_{\beta}-H^+$ )	1.1	110.65	-122.91
Pyridine ( $C_{\beta}-H^+$ )	----	---	----

**Table 11.1.5** Low-lying excited triplet state optimized geometry parameters of unprotonated pyrrole, furan, thiophene and pyridine and their protonated complexes. Calculated as B3LYP/6-311G (d,p) level of theory. Bond lengths are given in angstrom unit (Å), bond angles are in degree. B1= Pyrrole, B2= Furan, B3= Thiophene, B4= Pyridine. X= N, O and S

					
	<b>B1 (X-H<sup>+</sup>)</b>	<b>B2(X-H<sup>+</sup>)</b>	<b>B3(X-H<sup>+</sup>)</b>	<b>B4(X-H<sup>+</sup>)</b>	
C1-C2	1.47 (1.44)	1.35 (1.49)	1.44 (1.46)	C1-C2	1.46 (1.36)
C4-X	1.49 (1.42)	1.28 (1.39)	1.78 (1.79)	C5-X	1.32 (1.39)
C1-X	1.49 (1.42)	2.89*(1.41)	1.78 (1.79)	C1-X	1.46 (1.39)
<C1-C2-C3	109(108)	125 (106)	113 (113)	<C1-C2-C3	122 (119)
<C1-X-C4	103(107)	82 (105)	89 (88)	<C1-X-C5	120 (117)
	<b>B1 (C<math>\alpha</math>-H<sup>+</sup>)</b>	<b>B2 (C<math>\alpha</math>-H<sup>+</sup>)</b>	<b>B3 (C<math>\alpha</math>-H<sup>+</sup>)</b>		<b>B4(C<math>\alpha</math>-H<sup>+</sup>)</b>
C1-C2	1.50	1.48	1.43	C1-C2	1.52
C4-X	1.36	1.31	1.75	C5-X	1.27
C1-X	1.48	1.5	1.86	C1-X	1.41
<C1-C2-C3	108	106	114	<C1-C2-C3	122.4
< C1-X-C4	114	111	94	< C1-X-C5	133.9
	<b>B1 (C<math>\beta</math>-H<sup>+</sup>)</b>	<b>B2 (C<math>\beta</math>-H<sup>+</sup>)</b>	<b>B3 (C<math>\beta</math>-H<sup>+</sup>)</b>		
C1-C2	1.43	1.49	1.39		
C2- C3	1.5(1.34)	1.48 (1.34)	1.49 (1.34)		
C3-C4	1.5(1.47)	1.42 (1.42)	1.49 (1.46)		
C4-X	1.43	1.28	1.81		
C1-X	1.31	1.43	1.68		
<C1-C2-C3	109	100	115		
<C1-X-C4	111	108	91		

\*C1–5O bond opening, Bond distance observed 2.89Å.

\*\*C $\alpha$ -H<sup>+</sup> complexes, protonation occurred at C1 and C $\beta$ -H<sup>+</sup> complexes, protonation occurred at C3. Values are in the parenthesis obtained from unprotonated optimized species.



**Table 11.1.6**

**11.1.6a** Computed adiabatic transition energies ( ${}^1S_0 \rightarrow T_1$ ) (hartree) and proton induced shifts (PIS, hartree) in the lowest excited triplet state of X – protonated complexes. (X= N, O, S)

Compound ( ${}^1S_0 \rightarrow T_1$ )	Transition energy		PIS
	B	BH <sup>+</sup>	
B <sub>1</sub> (X = N)	0.1417	0.093	-0.0487
B <sub>2</sub> (X = O)	0.1254	0.06	-0.0654
B <sub>3</sub> (X = S)	0.1185	0.0864	-0.0321
B <sub>4</sub> (X = N)	0.1420	0.1389	-0.0031

**11.1.6b.** Computed adiabatic transition energies ( ${}^1S_0 \rightarrow T_1$ ) (hartree) and proton induced shifts (PIS in hartree) at the lowest excited triplet state of C $\alpha$  – protonated complexes.

Compound ( ${}^1S_0 \rightarrow T_1$ )	Transition energy		PIS
	B	BH <sup>+</sup>	
B <sub>1</sub> (X = N)	0.1417	0.106	-0.0357
B <sub>2</sub> (X = O)	0.1254	0.113	-0.0124
B <sub>3</sub> (X = S)	0.1185	0.087	-0.0315
B <sub>4</sub> (X = N)	0.1420	0.0456	-0.096

**11.1.6c** Computed adiabatic transition energies ( ${}^1S_0 \rightarrow T_1$ ) (hartree) and proton induced shifts (PIS in hartree) in the lowest excited triplet state of C $\beta$ –protonated complexes.

Compound ( ${}^1S_0 \rightarrow T_1$ )	Transition energy		PIS
	B	BH <sup>+</sup>	
B <sub>1</sub> (X = N)	0.1417	0.091	-0.0507
B <sub>2</sub> (X = O)	0.1254	0.086	-0.0394
B <sub>3</sub> (X = S)	0.1185	0.079	-0.0395
B <sub>4</sub> (X = N)	0.1420	....	....

**Table 11.1.7** Computed hardness ( $\eta$ ) =  $(I - A)/2 = (\epsilon_{LUMO} \sim \epsilon_{HOMO})/2$  of the free molecules in the lowest excited triplet state along with their ground state results.

Compound	$\epsilon_{HOMO}$ (hartree)	$\epsilon_{LUMO}$ (hartree)	$\eta$ (ev)
B <sub>1</sub> (X = N)	-0.0722 (-0.2124)	0.0469 (0.0365)	1.62 (3.38)
B <sub>2</sub> (X = O)	-0.1341 (-0.2347)	0.0244 (0.0067)	2.15 (3.28)
B <sub>3</sub> (X = S)	-0.1228 (-0.2425)	0.0069 (-0.0182)	1.76 (3.05)
B <sub>4</sub> (X = N)	-0.1437 (-0.2609)	-0.01391 (-0.0348)	1.765 (3.07)

\*Results obtained in ground state calculation written in parenthesis.

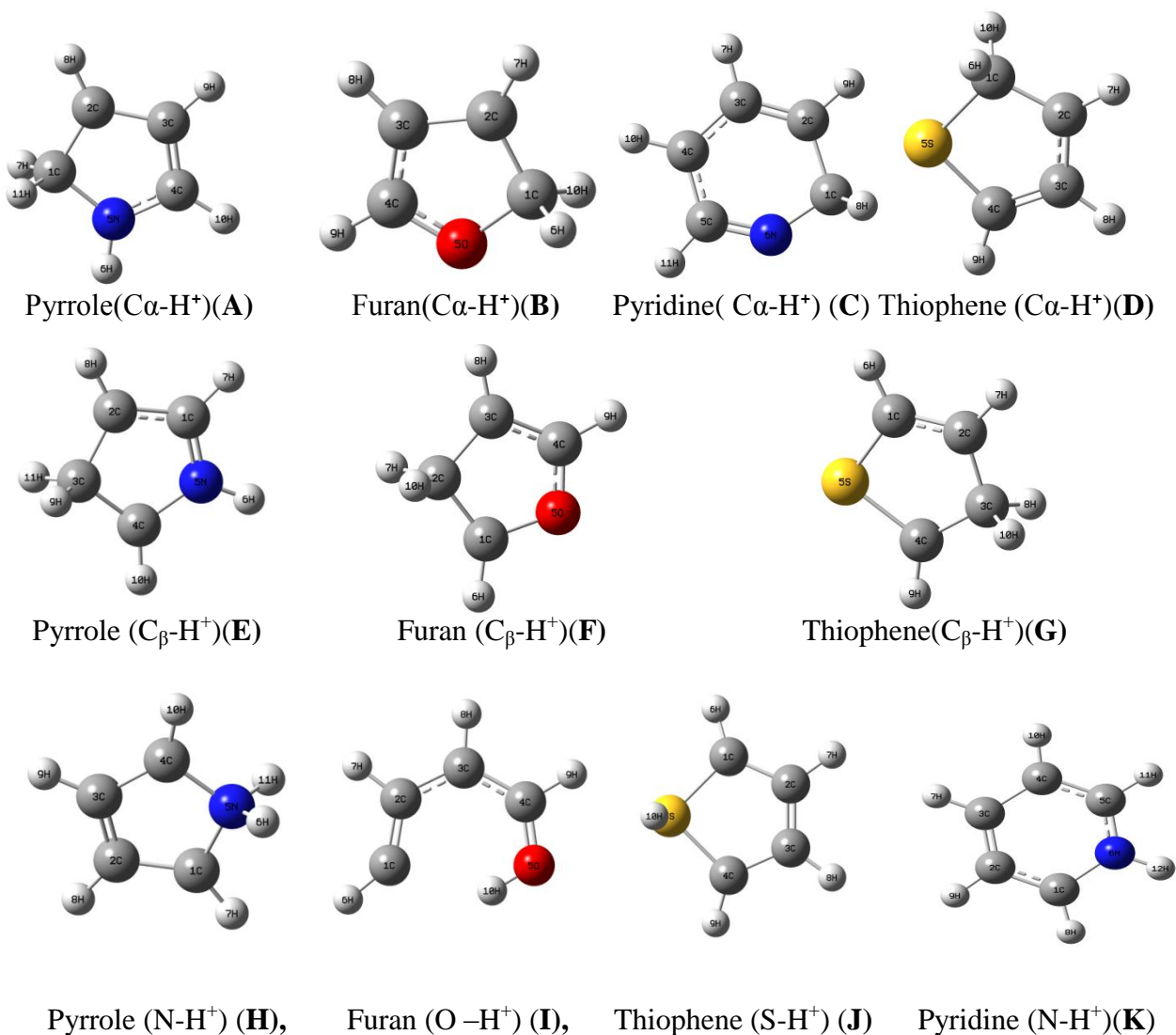


**Figure 11.2.2** Various protonated optimized complexes of the studied heterocyclic molecules at low-lying excited triplet state.

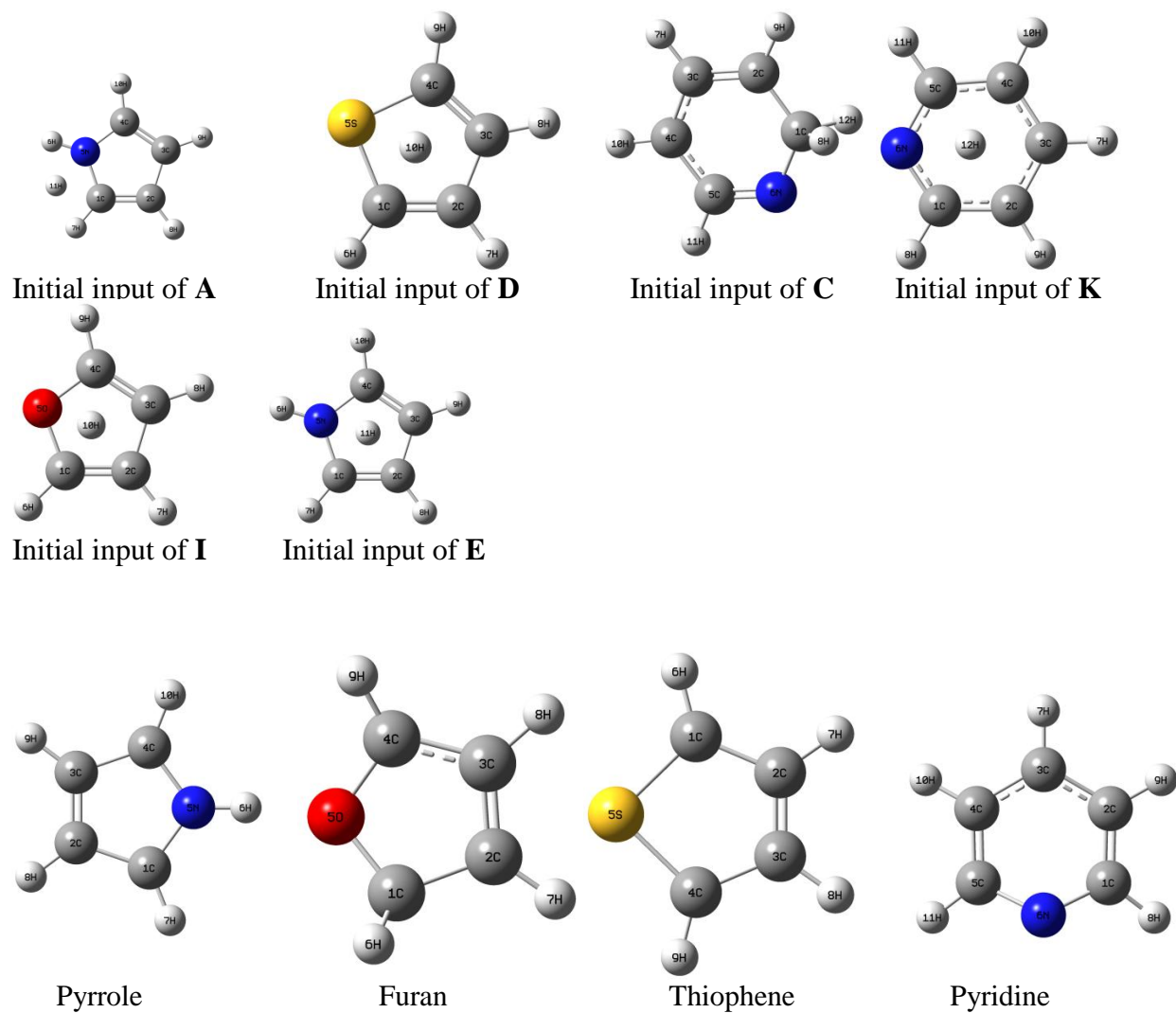


**Figure 11.2.3** [Un- protonated optimized geometries of the studied heterocyclic Compound]

## 11. 5 References

- (1) Forster, T. Z. *Electrochem.* **1950**, *54*, 42-53.
- (2) Ottolenghi, M. *Acc. Chem. Res.* **1973**, *6*, 153.
- (3) Saeva, F. D.; Olin, G. R. *J. Am. Chem. Soc.* **1975**, *97*, 5630.
- (4) Ireland, J. F.; Wyatt, P. A. H. *Adv. Phys. Org. Chem.* **1976**, *12*, 138.
- (5) Beauchamp, J. L. *Interaction between Ions and Molecules*. (Plenum, New York) **1974**, pp. 413, 459, 489.
- (6) Brauman, J. I.; Blair, L. K. *J. Am. Chem. Soc.* **1970**, *92*, 5986.
- (7) Frieiser, B. S.; Beacchamp, J. L. *J. Am. Chem. Soc.* **1977**, *99*, 3214.
- (8) Eskert-Maksic, M.; Antol, I.; Klessinger, M.; Maksic, Z. B. *J. Phys. Org. Chem.* **1999**, *12*, 597.
- (9) Martin, J-L-M.; Frankois, J. P.; Gijbels, R. *J. Comput. Chem.* **1989**, *10*, 346.
- (10) Lee, I. C.; Masel, R. I. *J. Phys. Chem. B* **2002**, *106*, 3902.
- (11) Lee, I. C.; Masel, R. I. *Catal. Lett.* **2002**, *83*, 43.
- (12) Lipshutz, B. H. *Chem. Rev.* **1986**, *86*, 795.
- (13) Klessinger, M.; Michl, J. *Excited state and photochemistry in organic molecules*, **1985**, New York.
- (14) Michl, J.; Bonacic-Koutecky, V. *Electronic aspects of organic photochemistry*, *Wiley-Interscience*, **1990**.
- (15) Helala, M. H.; Salem, M. A.; Gouda, M. A.; Ahmed, N. S.; El-Sherif, A. A. *Spectrochim. Acta Part A: Mol. Biomol. Spectrosc.* **2015**, *147*, 73-83.
- (16) Wardakhan, W. W.; Abdel-Salam, O. M. E.; Elmegeed, G. E. *Acta Pharm.* **2008**, *58*, 1-14.
- (17) Abdel Aziz, Y. M.; Said, M. M.; El Shihawy, H. A.; Abouzid, K. A. M. *Bioorg. Chem.* **2015**, *60*, 1-12.

- (18) Patpi, S. R.; Yogeewari, L. P. P.; Sriram, D.; Jain, N.; Sridhar, B.; Murthy, R.; Devi, T. A.; Kalivendi, S. V.; Kantevar, S. *J. Med. Chem.* **2012**, *55*, 3911-3924.
- (19) Wang, S. B.; Deng, X. Q.; Zheng, Y.; Yuan, Y. P.; Quan, Z. S.; Guan, L. P. *Eur. J. Med. Chem.* **2012**, *56*, 139-144.
- (20) Nasr, T.; Bondock, S.; Eid, S. *Eur. J. Med. Chem.* **2014**, *84*, 491-504.
- (21) Omidyan, R.; Salehi, M.; Heidari, Z. *Photochem. Photobio. Sci.* **2015**, *14*, 2261-2269.
- (22) Salzmann, S.; Kleinschmidt, M.; Tatchen, J.; Weinkauff, R.; Marian, C. M. *Phys. Chem. Chem. Phys.* **2008**, *10*, 380-392.
- (23) Stenrup, M.; Larson, A. *Chem. Phys.* **2011**, *379*, 6-12.
- (24) Hou, X-J.; Quan, P.; Holtzl, T.; Veszpre' mi, T.; Nguyen, M. T. *J. Phys. Chem. A* **2005**, *109*, 10396-10402.
- (25) Lee, C.; Yang, W.; Parr, R. G. *Phys. Rev.* **1988**, *B37*, 785;
- (26) Becke, A. D. Density-functional thermochemistry. III. The role of exact exchange, *J. Chem. Phys.* **1993**, *98*, 5648-5652.
- (27) Frisch, M. J.; Trucks, G. W.; Schlegel, H. B.; Scuseria, G. E.; Robb, M. A.; Cheeseman, J. R.; Scalmani, G.; Barone, V.; Mennucci, B.; Petersson, G. A.; Nakatsuji, H.; Caricato, M.; Li, X.; Hratchian, H. P.; Izmaylov, A. F.; Bloino, J.; Zheng, G.; Sonnenberg, J. L.; Hada, M.; Ehara, M.; Toyota, K.; Fukuda, R.; Hasegawa, J.; Ishida, M.; Nakajima, T.; Honda, Y.; Kitao, O.; Nakai, H.; Vreven, T.; Montgomery, J. A. Jr.; Peralta, J. E.; Ogliaro, F.; Bearpark, M.; Heyd, J. J.; Brothers, E.; Kudin, K. N.; Staroverov, V. N.; Kobayashi, R.; Normand, J.; Raghavachari, K.; Rendell, A.; Burant, J. C.; Iyengar, S. S.; Tomasi, J.; Cossi, M.; Rega, N.; Millam, J. M.; Klene, M.; Knox, J. E.; Cross, J. B.; Bakken, V.; Adamo, C.; Jaramillo, J.; Gomperts, R.; Stratmann, R. E.; Yazyev, O.; Austin, A. J.; Cammi, R.; Pomelli, C.; Ochterski, J. W.; Martin, R. L.; Morokuma, K.; Zakrzewski, V. G.; Voth, G. A.;

## Chapter 11

Salvador, P.; Dannenberg, J. J.; Dapprich, S.; Daniels, A. D.; Farkas, O.; Foresman, J. B.; Ortiz, J. V.; Cioslowski, J.; Fox, D. J. *Gaussian 09, Revision A.02*, Gaussian, Inc., Wallingford CT, **2009**.

- (28) Pandit, S.; De, D.; De, B. R. *J. Mol. Struct. (Theochem)* **2006**, 760, 245-246.
- (29) Pandit, S.; De, D.; De, B. R. *J. Mol. Struct. (Theochem)* **2006**, 778, 1-3.
- (30) Senapati, U.; De, D.; De, B. R. *Indian J. Chem.* **2008**, 47A, 548-550.
- (31) Senapati, U.; De, D.; De, B. R. *J. Mol. Struct. (Theochem)* **2007**, 808, 153-155.
- (32) Mandal, B.; Panda, B. K.; Sengupta, S. *Indian J. Sci.* **2014**, 8, 16-20.
- (33) Flicker, W. M.; Mosher, O. A.; Kuppermann, A. *J. Chem. Phys.* **1976**, 64, 1315-1321.
- (34) Derric. P. J.; Asbrink, L.; Edqvist, O.; Jonsson, B. -O.; Lindholm, E. *Int. J. Mass. Spectrom. Ion Phys.* **1971**, 6, 161-175.
- (35) Buemi, G.; Zuccarello, F.; Romeo, G. *J. Mol. Struct. (Theochem)* **1983**, 94, 115-126.
- (36) Christiansen, O.; Jorgensen, P. *J. Am. Chem. Soc.* **1998**, 120, 3423-3430.

## **CHAPTER 12**

**The lithium affinities of a series of heterocyclic compounds pyrrole, furan, thiophene and pyridine in their low-lying excited triplet state: A DFT based comparative study**





## Abstract

Comparative gas phase lithium cation affinities (LCA) basicities (LCB) and transition energies of a series of heterocyclic compounds (pyrrole, furan, thiophene and pyridine) and their  $\text{Li}^+$  complexes have been calculated using DFT/ B3LYP method at the most reliable 6-311G(d,p) basis set level. Complete geometry optimization process has been carried out at low-lying excited triplet state. As in the case of ground states, the gas phase  $\text{Li}^+$  complex formation turns out to be exothermic in each case. LCA value is predicted to be highest for pyridine. Geometries, Charge transfer have been estimated for all the systems. Natural population analysis (NPA) procedure has been applied to evaluate the natural charges on atoms of both free and  $\text{Li}^+$  complexes. Different interaction sites (C or X = N, O, S) of the molecules have been examined to find out the more stable complexes. Three different isomers of thiophene  $-\text{Li}^+$  complexes have been predicted. Computed lithium affinities are also sought to be correlated with the number of computed system parameters such as charge on the  $\text{Li}^+$  of the  $\text{Li}^+$  complexes and the computed hardness ( $\eta$ ) of the free bases in their relevant excited states. Chemical potential ( $\mu$ ), electrophilic index ( $\omega$ ) of the studied heterocyclic systems have been measured. The lithium induced shifts (LIS) at this electronic state have been measured from state energy differences. Obtained LIS are in general red shifts for the lowest excited triplet states.

## 12.1 Introduction

Ion-molecule complexes are frequently involved in molecular recognition processes<sup>1</sup> and these interactions are also expected to be involved in many important biological processes,<sup>2-5</sup> electron transfer processes<sup>6,7</sup> and more complicated biological systems. Important experimental method namely collision induced dissociation (CID) has been applied earlier to obtain the reliable thermodynamic properties of various organic, organometallic and metal-ligand complexes.<sup>8-12</sup> It is well known that, there is an excellent correlation of physical and chemical phenomenon with intermolecular weak interactions like hydrogen bond,<sup>13</sup>  $\pi$ -cation interactions,<sup>14</sup> lithium bond.<sup>15</sup> Pyrrole, furan, thiophene and pyridine are most common heterocyclic molecules of five or six membered ring contain one hetero atom N or O or S. They have a wide range of utilisation in the field of medicinal or pharmaceutical chemistry. Lithium cation affinity and basicity of these biologically significant aromatic heterocyclic molecules have been estimated at ground state (spin multiplicity 1) in our previous work (chapter 7). In the present study, we focus our interest to evaluate some thermodynamic and electronic properties due to interaction of lithium cation of the same set of molecules in their low-lying excited triplet state.  $\text{Li}^+$  complexes of some important organic and inorganic molecules or compounds were studied both theoretically and experimentally.<sup>16-20</sup> The  $\text{Li}^+$  ion affinity introduces the idea that, there must be some relation between the molecular electron density distribution and the affinity. This is also implies that, this properties of the same molecules may vary from state to state due to some electronic transitions which are accompanied by extensive reorganization of molecular electronic charge distribution. In order to examine the relative lithium cation affinities ( $\text{LCA} = \Delta E$ ), basicities structural behaviour of these heterocyclic compounds at the low-lying excited triplet state, DFT/B3LYP method<sup>21,22</sup> of calculations were performed employing most useful and reliable 6-311G(d,p) basis set of Gaussian'09' program package.<sup>23</sup> Recently the  $\text{Li}^+$  affinities of a series of substituted

acetophenone in their ground and lowest excited triplet state were reported<sup>24,25</sup> in literature. Proton affinities of a series of heterocyclic compounds (pyrrole, furan, thiophene and pyridine) in the ground and excited triplet state<sup>26,27</sup> have been investigated previously. A computational study<sup>28</sup> on lithium bond interaction of furan and thiophene were performed by Yuan Kun et.al in 2008. We have analysed the computed  $\text{Li}^+$  affinity, basicity values and transition energies to understand whether the pre-complex formation charge distribution local to the binding atom or post-complex relaxation of charge density or both are important in shaping the overall reactivity in a particular state. In this theoretical study we have searched for the different isomers of the  $\text{Li}^+$  complexes of the studied heterocyclic systems and also set our goal to observe how structures and stability of the studied molecules are influenced by the binding of lithium cation. Another metal cation interaction ( $\text{Na}^+$ ) has been included to recognize the effect of the size or charge on geometries and binding properties of the studied molecules. Sodium cation affinities and different computed electronics and structural parameters (obtained due to  $\text{Na}^+$  interactions with the heterocyclic molecules) are included in this study for the sake of comparison. We have also analysed the kind and extent of spectral shift caused by  $\text{Li}^+$ -complex formation in the relevant state. In a particular state, the possibility of correlating the  $\text{Li}^+$  affinity with the global hardness of the molecules is also explored.

## 12.2 Computational details

All calculations were performed with the help of DFT/ B3LYP method employing 6-311G (d,p) basis set of Gaussian 'O9'W program package<sup>23</sup>. It was already established that, B3LYP method of calculations provide most accurate results of geometry optimization of molecules<sup>29</sup>. In all calculations complete geometry optimization has been carried out on the molecules both before and after metal- complex formation. To obtain Enthalpies (H) and Gibbs free energies (G), vibrational frequencies (unscaled) were calculated at the same level

of theory at the temperature of 298.15K. To obtain partial atomic charges on atoms of the free molecules and their alkali metal complexes, we have applied NPA<sup>30</sup> (Natural Population Analysis) procedure. Mulliken charges on atoms are obtained by default with optimized results of the studied molecules.

## 12.3 Results and discussion

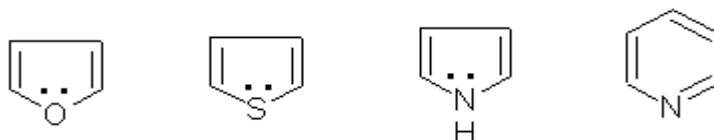


**Figure 12.2.1** General structures of studied molecules.

Lithium cation affinity (LCA) and Sodium cation affinity (SCA) is defined as negative value of enthalpy change ( $\Delta H$ ) of the following reaction



Where 'B' representing the corresponding hetero cyclic molecule.

Gas phase Lithium cation basicity (LCB), Sodium cation basicity (SCB) is the negative value of free energy change ( $\Delta G$ ) of the same reaction 1, 2. Gas phase alkali metal cation affinities (LCA and SCA) and basicities (LCB and SCB) have been calculated as  $MCA = [H_{BM}^+ - (H_B + H_M^+)]$ ..... (3) And  $MCB = [G_{BM}^+ - (G_B + G_M^+)]$ ..... (4). G and H = Total Gibbs free energy and total enthalpy of the reaction respectively at 298.15K. MCA = Metal cation affinity and MCB = Metal cation basicity.  $M^+$  = Lithium and sodium. B represents the hetero cyclic molecules B1, B2, B3 and B4. Where B1= pyrrole, B2= furan, B3= thiophene, B4 = pyridine.

**Table 12.1.1** summarises the lithium and sodium cation affinity and basicity values of the studied molecules obtained in this theoretical calculation. It is found that, LCA and LCB values are comparatively higher than SCA and SCB results in each case. According to the calculated results, LCA value is predicted to be highest ( $-45.49$  kcal/mole) in pyridine.

Among three five membered (FM) heterocyclic systems (pyrrole, furan and thiophene), pyrrole exhibits more affinity towards  $\text{Li}^+$  ( $-40.22$  kcal/mole) than furan ( $-38.59$  kcal/mole) and thiophene. In case of thiophene,  $\text{Li}^+$  has three different positions relative to the five membered ring, two out-of-plane and one in-plane.

In out-of-plane structures [**Fig 12.2.3 (C<sub>1</sub> and C<sub>2</sub>)**], LCA is estimated to be more ( $-34.19$  kcal/mole and  $-33.57$  kcal/mole) compared to the LCA result ( $-26.04$  kcal/mole) of in-plane structure [**Fig 12.2.3 (C)**] of  $\text{Li}^+$ -thiophene complex. Calculated LCB values are obtained in the range of  $-37.90$  kcal/mole to  $-18.44$  kcal/mole. We have observed that, SCA is also predicted to be highest in pyridine ( $-30.68$  kcal/mole) then it followed by pyrrole ( $-28.55$  kcal/mole), furan ( $-27.17$  kcal/mole) and thiophene ( $-23.15$  kcal/mole). Gas phase SCB values of these molecules remain in the range of  $-23.97$  to  $-15.06$  kcal/mole. We have also observed that, lowest excited triplet state LCA, LCB or SCA, SCB values are predicted to be lower in all cases compared to their ground state results. The only exception is furan shows little bit higher affinity and basicity values in this electronic state than in the ground state. This trend may be attributed to the redistribution or reorganization of electronic charge due to electronic transition in a particular electronic state.

In **Table 12.1.3** we have tabulated the computed Mulliken atomic charges on some important atoms of the free molecules and their alkali metal complexes along with the ligand to metal charge transfer (unit e)  $Q_{\text{ICT}}$  (for  $\text{Li}^+$  complexes) and  $Q_{\text{2CT}}$  (for  $\text{Na}^+$  complexes) obtained in Mulliken population analysis (MPA). In all cases the values of  $Q_{\text{ICT}}$  and  $Q_{\text{2CT}}$  clears the fact of a significant charge transfer from ligands to metal ion. Orders of the extent charge transfer results are not parallel to the LCA or SCA order of the studied molecules. They obtained in the following order thiophene > pyridine  $\approx$  pyrrole > furan in both lithium and sodium complexes. The natural charges (unit e) on metal ( $\text{Li}^+$  and  $\text{Na}^+$ ) in metal complexes obtained from natural population analysis (NPA) are summarised in **Table 12.1.2**. The corresponding

NPA results [ligand to metal charge transfer results ( $\Delta Q_{Li^+}$  and  $\Delta Q_{Na^+}$ )] are tabulated in this table for the sake of comparison. The magnitudes of the charges on metal ions in two different scheme are little different. Results obtained in NPA are somewhat higher than MPA. In lithium complexes, charge on  $Li^+$  varies in the range of 0.653 e to 0.833 e (MPA) whereas NPA results are remains within 0.879 e to 0.972 e. Charge on  $Na^+$  in sodium complexes are found in the span of 0.805 e to 0.889 e (MPA) and 0.937 e to 0.979 e (NPA). However, the magnitude of extent of charge transfer in MPA and NPA are different but the relative order of the charge transfer follows a similar trend. The magnitude of atomic charges on  $Li^+$  and  $Na^+$  of the complexes indicate that the interactions between  $Li^+$ ,  $Na^+$  and heterocyclic systems in low-lying excited triplet state are predominantly an ion-dipole attraction and ion-induced dipole interaction as well rather than a covalent interaction. This is also reveals that, both pre- and post-complex correlation with local charge densities in the immediate neighbourhood of the complex formation site are week. So it can therefore be imagined that, both LCA's and SCA's cannot be describe by the local properties of at or around the hetero atom moiety only. We have seen from **Table 12.1.2** and **Table 12.1.3**, computed net charges on hetero atoms ( $X = N, O, S$ ) are increasing in lithium and sodium complexes relative to their corresponding charges in free systems.

**Table 12.1.4** and **Table 12.1.5** reported some important geometrical parameters like bond length (in Å), bond angle, and dihedral angle (in degree) of optimized lithium and sodium complexes of the studied molecules. Optimized structures of the  $Li^+$  complexes are presented in **Figure 12.2.3**. It is known from the literature, all these three FM and one six-membered (SM) heterocyclic systems are planar having  $C_{2v}$  point group. We observed in our study, lithium bind with the hetero atom ( $X = N, O$  and  $S$ ) of the each free molecule to form complexes. In case of thiophene, three different lithium complexes [**Figure 12.2.3 (C, C<sub>1</sub> and C<sub>2</sub>)**] formed. In structure C lithium directly bonded with S atom and in other complexes

lithium is above the ring. In  $C_1$  structure lithium slightly inclined to S atom whereas in  $C_2$  structure lithium inclined little bit more to  ${}^1C\alpha$  atom.

The  $X-Li^+$  bond distance in lithium complexes is found to be shorter in furan (1.82Å) compared to pyrrole (1.95Å) pyridine (1.9Å) and thiophene (2.28Å)  $X-Li^+$  complexes. The  $C_1$  and  $C_2$  complex of thiophene provide  $X-Li^+$  bond length 2.39 and 2.41Å respectively (See **Table 12.1.4**). In this table we also include the  $r({}^1C\alpha-Li^+)$  bond length of each complex. Since thiophene provides more than one geometries of  $Li^+$ -complex ( $C_1$  and  $C_2$ ), it is important to find out the proper position of lithium above the FM ring. In  $C_1$  geometry the distance between  ${}^1C\alpha$  and  $Li^+$  is found to be larger (2.51Å) compared to the same in  $C_2$  geometry (2.27Å). In pyrrole, furan and pyridine  $r({}^1C\alpha-Li^+)$  bond lengths are observed 2.28, 2.88 and 2.84Å respectively. Concerning the bond angles, ( $\angle C_1-X-Li^+$ ) vary in the range of 63.3° to 134.4° in all complexes. The dihedral or torsion angles  $\tau(C_2-C_1-X-Li^+)$  is found to be 179.9° and 180.0° in  $X-Li^+$  complex of thiophene and pyridine respectively. In pyrrole, furan and thiophene ( $C_1$  and  $C_2$ ) complexes,  $\tau(C_2-C_1-X-Li^+)$  angles are found 95.27°, 142.8°, 55.7° and -67.9° respectively.

The optimized geometries obtained due to interaction of sodium cation ( $Na^+$ ) are presented in **Figure 12.2.4** and some important geometrical parameters like bond length, bond angle and dihedral angle of the complexes are collected in **Table 12.1.5**. It is seen that,  $r(X-Na^+)$  bond lengths are remarkably longer in each case relative to their  $r(X-Li^+)$  distances. In case of pyrrole and thiophene,  $Na^+$  is above the ring (**Figure 12.2.2 E and G**) whereas in furan and pyridine complexes sodium cation is found closer to hetero atom (O and N). The distance between sodium and hetero atom is predicted to be 2.35 and 2.77Å in pyrrole and thiophene. In furan and pyridine this bond distances are 2.20 and 2.28Å. The  $\angle C_1-X-Na^+$  bond angle in all complexes vary in the range of 77.2° to 120.0°. A large variation has been observed in dihedral angle  $\tau(C_2-C_1-X-Na^+)$ , it is ranges from 62.18° to 180.0°.

The optimized geometries of the free heterocyclic molecules taken in this theoretical study are presented in **Figure 12.2.2**. Comparison of the structural parameters of free heterocyclic molecules and their various  $\text{Li}^+$  and  $\text{Na}^+$  complexes demonstrates the immense effects of  $\text{Li}^+$  and  $\text{Na}^+$  interactions on the geometry of the molecules, clearly depends on the site of interactions. The optimized geometric parameters of free molecules and complexes are listed in **Table 12.1.6**. Comparing the data with parameters of the free molecules, we have seen that lithium and sodium cation interaction induced changes in different bond distance. The  $\text{C}_1 - \text{C}_2$  bond length is elongated by 0.03 to 0.07 Å in alkali metal complexes of pyrrole and pyridine. The same bond lengths remain almost unchanged ( $\pm 0$  to 0.01 Å) in different lithium and sodium complexes of thiophene. In furan complexes, it is contracted slightly by 0.04 Å. The  $\text{C}_2 - \text{C}_3$  distances are found to be almost same in all three FM heterocyclic metal complexes. Interestingly,  $\text{Li}^+$  interaction induces 0.05 Å elongation of  $\text{C}_2 - \text{C}_3$  bond length in pyridine but a large contraction (0.08 Å) of the same bond has been observed in pyridine- $\text{Na}^+$  complex. In both lithium and sodium complexes of pyrrole and furan, the distance between  $\text{C}_4$  and X atom elongated by 0.03 to 0.05 Å relative to the free molecules but  $\text{C}_4 - \text{X}$  bond distance of free thiophene molecule (1.79 Å) not changes remarkably even after lithium or sodium complex formation (1.78 to 1.8 Å). The  $\text{C}_5 - \text{X}$  bond length in pyridine- $\text{Li}^+$  complex enlarged upto 0.08 Å whereas it is contracted upto 0.09 Å in pyridine- $\text{Na}^+$  complex. In addition, Lithium cation interaction accompanied with large contraction of  $\text{C}_1 - \text{X}$  bond length (upto 0.08 Å) of pyridine, in contrary, the  $\text{C}_1 - \text{X}$  bond distance in  $\text{Na}^+$  complex elongated by 0.07 Å. Concerning FM heterocyclic systems,  $\text{C}_1 - \text{X}$  bond length enlarged by 0.02 Å to 0.04 Å in lithium and sodium complexes of pyrrole and furan relative to their neutral systems. In all thiophene complexes bond length of  $\text{C}_1 - \text{X}$  are predicted almost equivalent (1.78 to 1.80 Å) to the free molecule (1.79 Å).



Concerning bond angles, no such larger alterations have been found in  $\angle C_1-C_2-C_3$  which have been reported to be  $106^\circ$ ,  $106^\circ$ ,  $113^\circ$  and  $119^\circ$  in the pyrrole, furan, thiophene and pyridine respectively before complex formation. We have estimated this angle in lithium and sodium complexes  $0^\circ$  to  $3^\circ$  larger than corresponding bond angles in free heterocyclic systems. In comparison to the values of optimized free FM heterocyclic systems, the  $C_1-X-C_4$  bond angles altered by  $\pm 1^\circ$  to  $\pm 3^\circ$  in alkali metal complexes. In case of lithium and sodium complexes of pyridine  $C_1-X-C_5$  angle is estimated  $115^\circ$  which have been obtained  $117^\circ$  in free optimized pyridine system.

We have searched for the possibility of existence of correlation with a single global parameter of the entire molecule in the relevant electronic state. As the global parameter we have chosen the hardness,  $\eta = (I \sim A)/2 = (\epsilon_{LUMO} \sim \epsilon_{HOMO})/2$  listed in **Table 12.1.7** along with their respective ground state values. From **Table 12.1.7** it is seen that,  $\eta$  values are predicted to be lower in low-lying excited triplet state compared to their respective ground state which favour  $Li^+$  and  $Na^+$  complex formation, in general. As we know, hardness is associated with the stability of a chemical system<sup>31</sup> therefore this parameter is commonly used as a criterion of chemical reactivity and stability.<sup>32</sup> According to the DFT/B3LYP (6-311G d,p) calculated results, the  $\eta$  value is predicted to be highest in furan (2.15ev), which have been reported 1.62 ev, 1.76 ev and 1.765 ev in pyrrole, thiophene and pyridine. No perfect correlation between affinities (LCA and SCA) and the hardness ( $\eta$ ) have been found in this particular state. In an effort to estimate the reactivity of these molecules computationally, we have calculated the chemical potential ( $\mu$ ) and the global electrophilicity index ( $\omega$ ) of each molecule in low-lying excited triplet state (**Table 12.1.8**). The calculated  $\mu$  and  $\omega$  values are estimated to be lowest in pyrrole ( $-0.344$  ev and  $0.0365$  ev) then followed by furan ( $-1.49$  and  $0.516$  ev), thiophene ( $-1.57$  and  $0.7$  ev) and pyridine ( $-2.14$  and  $1.29$  ev). In this theoretical study, we have determined the adiabatic transition energies ( $^1S_0 \rightarrow T_1$ ) as state energy difference. The results have been applied to find out the kind of shifts [lithium

induced shifts (LIS) and sodium induced shifts (SIS)] due to  $\text{Li}^+$  and  $\text{Na}^+$  interactions. These results are tabulated in **Table 12.1.9**. On the basis of our calculated results, the lithium and sodium induced shifts are predicted to be red shift in all cases with the exception of  $\text{C}_1$  and  $\text{C}_2$  complex formation reactions of thiophene where blue shifts have been predicted due to  $\text{Li}^+$  interactions. These data refer to the gas phase lithium and sodium complexation of the isolated molecules without any additional effects caused by solvation.

## 12.4 Conclusion

From the present theoretical study it can be well concluded that the gas phase lithium affinities of the pyrrole, furan, thiophene and pyridine are spontaneous. Low-lying excited triplet state LCA or SCA values are lower in all cases relative to their ground state singlet with the exception of furan molecule. LCB or SCB values of the five or six membered heterocyclic systems are lower than their corresponding LCA or SCA values and the differences are 5.77 kcal/mole to 13.1 kcal/mole. Thiophene may have three different isomers of lithium complexes (**Fig 12.2.3 C, C<sub>1</sub>, C<sub>2</sub>**) in low-lying excited triplet state. LCA and LCB value of the molecules are estimated higher compared to their SCA and SCB values. The geometry of the studied five and six heteroatom systems have planar structures belong to the  $\text{C}_{2v}$  point group. It should be noticed that,  $\text{Li}^+$  and  $\text{Na}^+$  complexes of pyrrole, furan and thiophene (**Complex structure C<sub>1</sub> and C<sub>2</sub>**) have nonplanar configuration. Thiophene ( $\text{S-Li}^+$ ) complex(C) and lithium and sodium complex of pyridine retained with planar geometry. The electronic properties of the complexes clearly indicate that, interactions are predominantly electrostatic. That is bond formed by the  $\text{Li}^+$  and  $\text{Na}^+$  with the ligands are ionic in nature rather than covalent. Red shifts effect on  $\text{S}_0 \rightarrow \text{T}_1$  electronic transition energies have been predicted due to interactions of lithium and sodium cations with all four heterocyclic systems (except  $\text{C}_1$  and  $\text{C}_2$  complex of thiophene). The overall reactivity is fully explained by distant atom contribution in addition to the contribution from the hetero atoms of the free bases.

**Table 12.1.1** Gas phase lithium cation affinities (LCA), basicities (LCB) of pyrrole, furan, thiophene and pyridine obtained from B3LYP/ 6-311G (d,p) method of calculation in low-lying triplet state.  $LCA = [H_{BLi}^+ - (H_{Li}^+ + H_B)]$  and  $LCB = [G_{BLi}^+ - (G_{Li}^+ + G_B)]$ .

Compound	LCA	LCB	Compound	SCA	SCB
	Kcal/mole	Kcal/mole		Kcal/mole	Kcal/mole
Pyrrole-Li <sup>+</sup>	-40.22 (-42.79)	-27.1 (-35.2)	Pyrrole-Na <sup>+</sup>	-28.55 (-28.17)	-15.06 (-21.38)
Furan-Li <sup>+</sup>	-38.59 (-32.37)	-31.59 (-28.8)	Furan-Na <sup>+</sup>	-27.17 (-21.64)	-20.51 (-18.51)
Thiophene(S-Li <sup>+</sup> ) Structure C	-26.04	-18.44	Thiophene-Na <sup>+</sup>	-23.15 (-25.85)	-17.38 (-18.32)
Thiophene-Li <sup>+</sup> Structure C <sub>1</sub>	-34.19 (-39.59)	-25.97 (-31.24)			
Thiophene-Li <sup>+</sup> Structure C <sub>2</sub>	-33.57	-26.60			
Pyridine-Li <sup>+</sup>	-45.49 (-48.25)	-37.9 (-40.97)	Pyridine-Na <sup>+</sup>	-30.68 (-33.82)	-23.97 (-26.79)

\* Values written in the parenthesis are of their corresponding ground state singlet results.

**Table 12.1.2** Partial atomic charges on alkali metal cations [ $q_{Li}^+$  and  $q_{Na}^+$ ] (in e unit) in alkali metal complexes and ligand to metal charge transfer ( $\Delta Q_{Li}^+$  and  $\Delta Q_{Na}^+$ ), charges on hetero atoms (X= N, O, S) of the free molecules and their lithium, sodium complexes obtained from NPA procedure.

Compound	Free heterocyclic	Li <sup>+</sup> complex		Charge transfer ( $\Delta Q_{Li}^+$ )	Na <sup>+</sup> complex		Charge transfer ( $\Delta Q_{Na}^+$ )
	$q_X^-$	$q_X^-$	$q_{Li}^+$		$q_X^-$	$q_{Na}^+$	
Pyrrole	-0.680	-0.82	0.949	0.051	-0.771	0.970	0.03
Furan	-0.551	-0.739	0.972	0.028	-0.691	0.979	0.021
Thiophene	0.215	0.051	0.873 (C)	0.127	0.225	0.937	0.063
		0.266	0.879 (C <sub>1</sub> )	0.121			
		0.266	0.881 (C <sub>2</sub> )	0.119			
Pyridine	-0.194	-0.742	0.958	0.042	-0.678	0.965	0.035

\*Charge transfer calculated as [Formal charge of metal cation (1) -  $q_M^+$ ] M= Lithium and sodium.

**Table 12.1.3** Mulliken atomic charges (e) on some selected atoms of the free molecules (pyrrole, furan, thiophene and pyridine) and their lithium and sodium complexes of in the low-lying triplet state.

Compound	Atoms	Mulliken atomic charges				
		Free molecules	Li <sup>+</sup> -Complexes	Charge transfer (Q <sub>1 CT</sub> )	Na <sup>+</sup> complexes	Charge transfer (Q <sub>2 CT</sub> )
Pyrrole	N	-0.424	-0.475		-0.458	
	Li <sup>+</sup>	---	0.775	0.225	...	
	Na <sup>+</sup>	...	...	...	0.851	0.149
	<sup>1</sup> C $\alpha$	0.038	-0.106	...	-0.042	
Furan	O	-0.293	-0.469	...	-0.442	
	Li <sup>+</sup>	---	0.833	0.167	...	
	Na <sup>+</sup>			...	0.889	0.121
	<sup>1</sup> C $\alpha$	0.056	0.078	...	0.231	
Thiophene	S	0.172	0.271 (C) 0.301(C <sub>1</sub> ) 0.306 (C <sub>2</sub> )	...	0.233	...
	Li <sup>+</sup>	---	0.712 (C) 0.653 (C <sub>1</sub> ) 0.655 (C <sub>2</sub> )	0.288 (C) 0.347(C <sub>1</sub> ) 0.345 (C <sub>2</sub> )	...	...
	Na <sup>+</sup>	...	...	...	0.805	0.195
	<sup>1</sup> C $\alpha$	-0.274	-0.271 (C <sub>1</sub> ) -0.349 (C <sub>2</sub> )	...	-0.287	
Pyridine	N	-0.201	-0.541	...	-0.535	
	Li <sup>+</sup>	---	0.775	0.225	...	
	Na <sup>+</sup>			...	0.863	0.137
	<sup>1</sup> C $\alpha$	0.013	0.219	...	0.204	

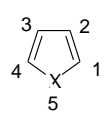
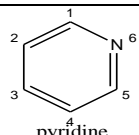
**Table 12.1.4** Low-lying excited triplet state geometrical parameters of the lithium complexes of pyrrole, furan, thiophene and pyridine obtained from B3LYP/6-311G (d,p) calculation.

Lithium complexes	X-Li <sup>+</sup> in Å	<sup>1</sup> C $\alpha$ -Li <sup>+</sup> in Å	< C <sub>1</sub> -X -Li <sup>+</sup>	$\tau$ (C <sub>2</sub> -C <sub>1</sub> - X-Li <sup>+</sup> ) in°
Pyrrole	1.95	2.28	114.0	95.27
Furan	1.82	2.88	123.6	142.8
Thiophene (out of plane)	2.39 (C <sub>1</sub> )	2.51(C <sub>1</sub> )	71.8(C <sub>1</sub> )	55.7(C <sub>1</sub> )
	2.41 (C <sub>2</sub> )	2.27 (C <sub>2</sub> )	63.3 (C <sub>2</sub> )	-67.9(C <sub>2</sub> )
Thiophene (in-plane)	2.28 (C)	3.76 (C)	134.5	179.99
Pyridine	1.9	2.84	124.0	180.0

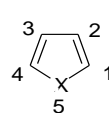
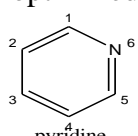
**Table 12.1.5** Geometrical parameters of the sodium complexes of pyrrole, furan, thiophene and pyridine low-lying excited triplet state obtained from B3LYP/6-311G (d,p) calculation.

Sodium complexes	X-Na <sup>+</sup> in Å	< C <sub>1</sub> -X-Na <sup>+</sup> in °	τ (C <sub>2</sub> -C <sub>1</sub> -X-Na <sup>+</sup> ) in °
Pyrrole	2.35	92.5	71.6
Furan	2.20	121.9	137.2
Thiophene	2.77	77.2	62.18
Pyridine	2.28	120.0	180.0

**Table 12.1.6** Low-lying excited triplet state optimized geometry parameters of free pyrrole, furan, thiophene and pyridine and their lithium complexes. Calculated at B3LYP/ 6-311G (d,p) level of theory. Bond lengths are given in angstrom unit (Å), bond angles are in degree. B1= Pyrrole, B2= Furan, B3= Thiophene, B4= Pyridine. X= N, O and S.

		<b>B1 (X-Li<sup>+</sup>)</b>	<b>B2(X-Li<sup>+</sup>)</b>	<b>B3(X-Li<sup>+</sup>)</b>	<b>B3-Li<sup>+</sup> (C<sub>1</sub>)</b>		<b>B4(X-Li<sup>+</sup>)</b>
C <sub>1</sub> -C <sub>2</sub>		1.48 (1.44)	1.45 (1.49)	1.46 (1.46)	1.47	C <sub>1</sub> -C <sub>2</sub>	1.42 (1.36)
C <sub>2</sub> -C <sub>3</sub>		1.35 (1.34)	1.34 (1.34)	1.34 (1.34)	1.35	C <sub>2</sub> -C <sub>3</sub>	1.47 (1.42)
C <sub>4</sub> -X		1.46 (1.42)	1.44 (1.39)	1.78 (1.79)	1.8	C <sub>5</sub> -X	1.47 (1.39)
C <sub>1</sub> -X		1.46 (1.42)	1.44 (1.41)	1.78 (1.79)	1.8	C <sub>1</sub> -X	1.31 (1.39)
<C <sub>1</sub> -C <sub>2</sub> -C <sub>3</sub>		108(106)	109(106)	114(113)	113	<C <sub>1</sub> -C <sub>2</sub> -C <sub>3</sub>	119 (119)
<C <sub>1</sub> -X-C <sub>4</sub>		103(107)	106 (105)	91(88)	89	<C <sub>1</sub> -X-C <sub>5</sub>	115 (117)

Values written in the parenthesis are obtained in free optimized molecules.

		<b>B1-Na<sup>+</sup></b>	<b>B2-Na<sup>+</sup></b>	<b>B3Na<sup>+</sup></b>		<b>B4-Na<sup>+</sup></b>
C <sub>1</sub> -C <sub>2</sub>		1.47 (1.44)	1.45 (1.49)	1.46 (1.46)	C <sub>1</sub> -C <sub>2</sub>	1.43 (1.36)
C <sub>2</sub> -C <sub>3</sub>		1.35 (1.34)	1.34 (1.34)	1.35 (1.34)	C <sub>2</sub> -C <sub>3</sub>	1.34 (1.42)
C <sub>4</sub> -X		1.45 (1.42)	1.43 (1.39)	1.79 (1.79)	C <sub>5</sub> -X	1.3 (1.39)
C <sub>1</sub> -X		1.45 (1.42)	1.43 (1.41)	1.79 (1.79)	C <sub>1</sub> -X	1.46 (1.39)
<C <sub>1</sub> -C <sub>2</sub> -C <sub>3</sub>		108.7(106)	108(106)	113 (113)	<C <sub>1</sub> -C <sub>2</sub> -C <sub>3</sub>	120 (119)
<C <sub>1</sub> -X-C <sub>4</sub>		104(107)	104 (105)	89(88)	<C <sub>1</sub> -X-C <sub>5</sub>	115 (117)

Values written in the parenthesis are obtained in free optimized molecules.

**Table 12.1.7** Computed hardness ( $\eta$ ) =  $(I - A)/2 = (\epsilon_{\text{LUMO}} - \epsilon_{\text{HOMO}})/2$  of the free molecules in the lowest excited triplet state.

Compound	$\epsilon_{\text{HOMO}}$ (hartree)	$\epsilon_{\text{LUMO}}$ (hartree)	$\eta$ (ev)
B <sub>1</sub> (X = N)	-0.0722 (-0.2124)	0.0469 (0.0365)	1.62 (3.38)
B <sub>2</sub> (X = O)	-0.1341 (-0.2347)	0.0244 (0.0067)	2.15 (3.28)
B <sub>3</sub> (X = S)	-0.1228 (-0.2425)	0.0069 (-0.0182)	1.76 (3.05)
B <sub>4</sub> (X = N)	-0.1437 (-0.2609)	-0.01391 (-0.0348)	1.765 (3.07)

\*Values written in the parenthesis are of their corresponding ground state singlet results.

**Table 12.1.8** Calculated chemical potential ( $\mu$ ) =  $(\epsilon_{\text{LUMO}} + \epsilon_{\text{HOMO}})/2$  and electrophilicity ( $\omega$ ) =  $\mu^2 / 2\eta$  of the heterocyclic molecules in the low-lying excited triplet state. Unit in ev).

Compound	$\mu$ (ev)	$\omega$ (ev)	$\eta$ (ev)
Pyrrole	-0.344 (-2.39)	0.0365(0.840)	1.62
Furan	-1.49 (-3.09)	0.516 (1.46)	2.15
Thiophene	-1.57 (-3.54)	0.700 (2.05)	1.76
Pyridine	-2.14 (-4.02)	1.29 (2.61)	1.765

\*Data written in the parenthesis are their corresponding ground state singlet results.

**Table 12.1.9** Computed adiabatic transition energies ( $^1S_0 \rightarrow T_1$ ) (hartree) and lithium induced shifts (LIS, hartree) and sodium induced shifts (SIS) in the lowest excited triplet state

Compound ( $^1S_0 \rightarrow T_1$ )	Transition energy			LIS	SIS
	B	B $\text{Li}^+$	B $\text{Na}^+$		
B <sub>1</sub> (X = N)	0.1417	0.131	0.127	-0.0107	-0.147
B <sub>2</sub> (X = O)	0.1288	0.1125	0.1134	-0.0129	-0.012
B <sub>3</sub> (X = S)	0.1185	0.109 (Fig 12.2. 3. C)	0.116	-0.0095	-0.0025
B <sub>3</sub> (X = S)	0.1185	0.122 (Fig 12.2. 3. C1)	.....	0.0035	.....
B <sub>3</sub> (X = S)	0.1185	0.121(Fig 12.2. 3. C <sub>2</sub> )		0.0025	.....
B <sub>4</sub> (X = N)	0.1420	0.1403	0.141	-0.0017	-0.001

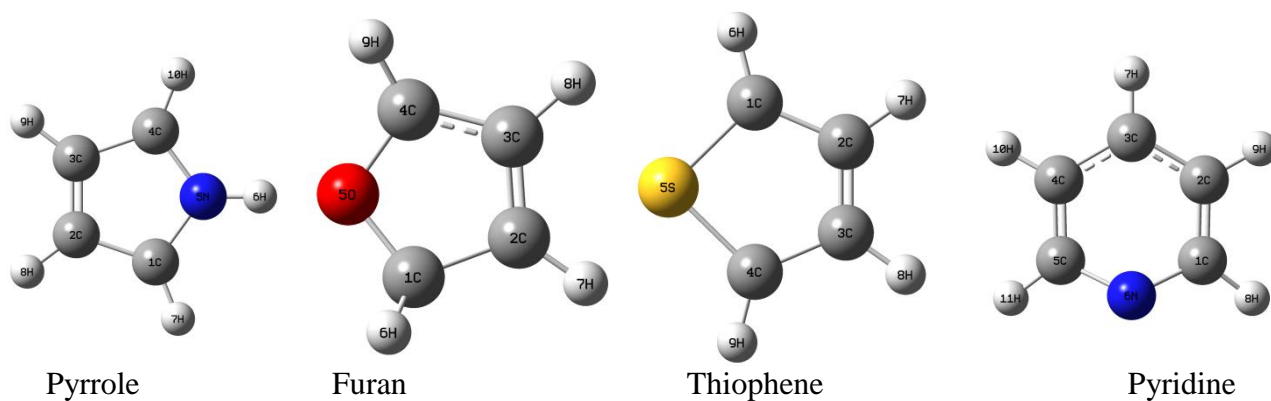


**Figure 12.2.2** Optimized geometries of the free heterocyclic molecules.

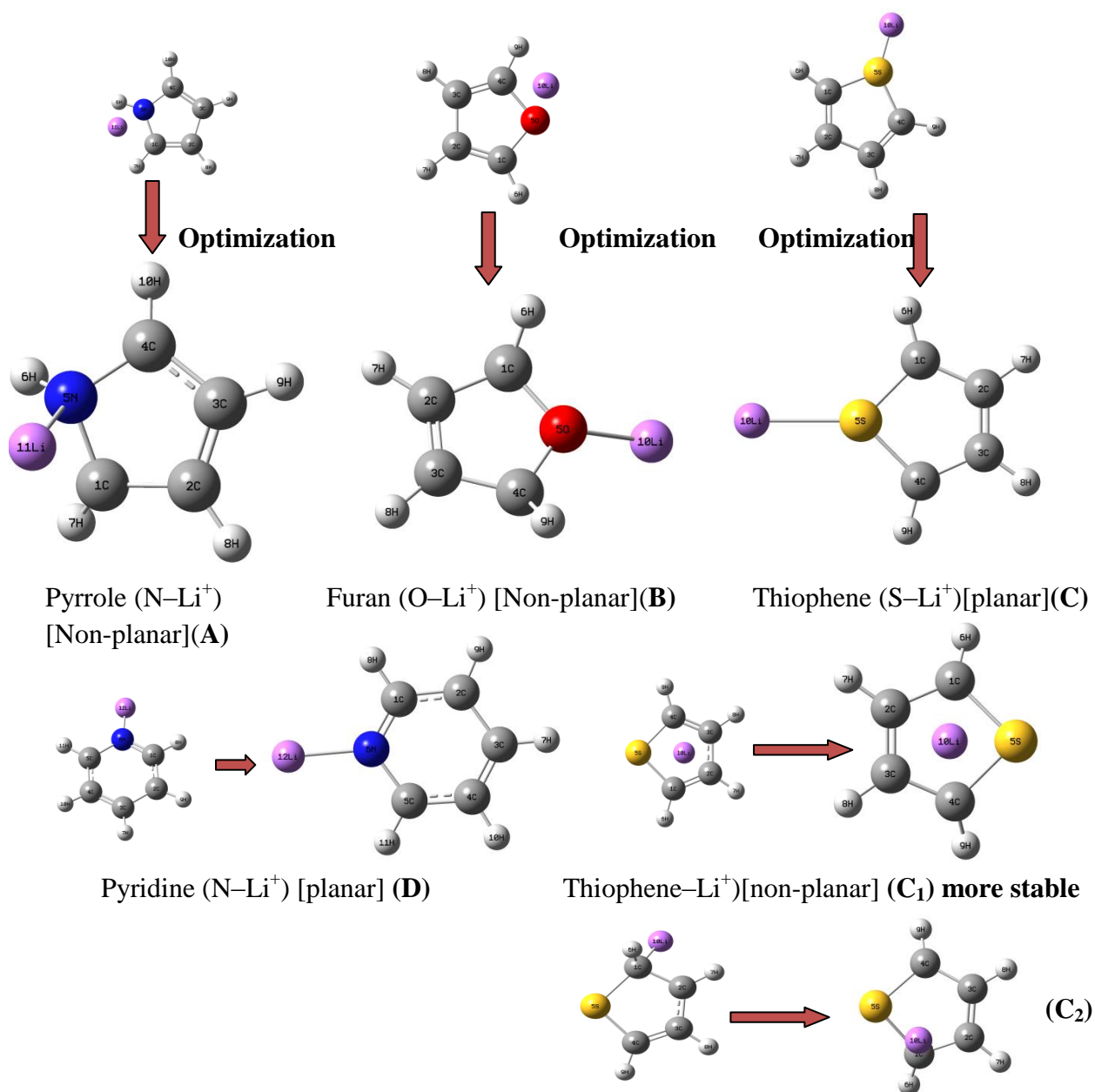
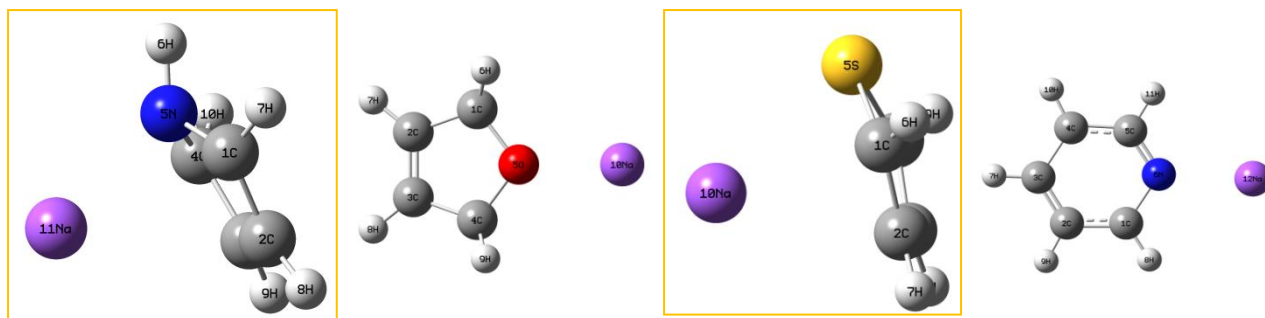


**Figure 12.2.3** Optimized geometry of various lithium complexes of the studied molecules.



Pyrrole–Na<sup>+</sup> (**E**)

Furan–Na<sup>+</sup> (**F**)

Thiophene–Na<sup>+</sup> (**G**)

Pyridine–Na<sup>+</sup> (**H**)

**Figure 12.2.4** Optimized geometries of Heterocyclic–Na<sup>+</sup> complexes at low-lying triplet state.



## 12.5 References

- (1) Ma, J. C.; Dongherty, D. A. *Chem. Rev.* **1997**, *97*, 1303.
- (2) Karlin, S.; Zuker, M.; Brocchieri, L. *J. Mol. Biol.* **1994**, *239*, 227.
- (3) Livnah, O.; Stura, E. A.; Johnson, D. L.; Middleton, S. A.; Mulchany, L. S.; Wrighton, N. C.; Dower, W. J.; Jolliffe, L. K.; Wilson, I. A. *Science* **1996**, *255*, 306.
- (4) Cervenansky, C.; Engstorm, A.; Karlsoon, E. *Eur. J. Biochem.* **1995**, *229*, 270.
- (5) Novotny, J.; Bruccoleri, R. E.; Saul, F.A. *Biochemistry* **1989**, *28*, 4735.
- (6) Lippard, S. J.; Berg, J. M. *Principles of Bioinorganic chemistry*, University Science Books, Mill Valley, CA, 1994.
- (7) Kaim, W.; Schwederski, B. *Bioinorganic Chemistry: Inorganic Elements in the chemistry of life*, Wiley, Chichester, 1994.
- (8) Rodgers, M. T. *J. Phys. Chem. A* **2001**, *105*, 2374.
- (9) Rodgers, M. T.; Armentrout, P. B. *J. Phys. Chem. A* **1997**, *101*, 1238.
- (10) Rodgers, M. T.; Armentrout, P. B. *J. Phys. Chem. A* **1997**, *101*, 2614.
- (11) Amunugama, R.; Rodgers, M. T. *Int. J. Mass Spectrom.* **2000**, *195/196*, 439.
- (12) Vitale, G.; Valina, A. B.; Huang, H.; Amunugama, R.; Rodgers, M. T. *J. Phys. Chem. A* **2001**, *105*, 11351.
- (13) Yang, Y.; Zhang, W. J. *J. Mol. Struct. (Theochem)* **2007**, *814(1-3)*, 113-117.
- (14) Dunbar, R. C. *J. Phys. Chem. A* **2000**, *104(34)*, 8067-8074.
- (15) Feng, Y.; Liu, L.; Wang, J. T.; Li, X.-S.; Guo, Q.-X. *Chem. Commun.* **2004**, *11(1)*, 88-89.
- (16) Burk, P.; Koppel, I. A.; Koppel, I.; Kurg, R.; Gal, J.-F.; Maria, P.-C.; Herreros, M.; Notario, R.; Abboud, J.-L. M.; Anvia, F.; Taft, R. W. *J. Phys. Chem. A* **2000**, *104*, 2824.
- (17) Del Bene, J. E. *Chem. Phys.* **1979**, *40*, 329.

## Chapter 12

- (18) Del Bene, J. E. *J. Phys. Chem.* **1996**, *100*, 6284.
- (19) Gal, J. F.; Maria, P. C.; Decouzon, M.; Mo, O.; Yancz, M. *Int. J. Mass spectrom.* **2002**, *219*, 445.
- (20) Amunugama, R.; Rodgers, M. T. *Int. J. Mass spectrom.* **2003**, *227*, 339.
- (21) Lee, C.; Yang, W.; Parr, R. G. *Phys. Rev.* **1988**, *B37*, 785.
- (22) Becke, A. D. *J. Chem. Phys.* **1993**, *98*, 5648.
- (23) Frisch, M. J.; Trucks, G. W.; Schlegel, H. B.; Scuseria, G. E.; Robb, M. A.; Cheeseman, J. R.; Montgomery, J. A. Jr.; Vreven, T.; Kudin, K. N.; Burant, J. C.; Millam, J. M.; Iyengar, S. S.; Tomasi, J.; Barone, V.; Mennucci, B.; Cossi, M.; Scalmani, G.; Rega, N.; Petersson, G. A.; Nakatsuji, H.; Hada, M.; Ehara, M.; Toyota, K.; Fukuda, R.; Hasegawa, J.; Ishida, M.; Nakajima, T.; Honda, Y.; Kitao, O.; Nakai, H.; Klene, M.; Li, X.; Knox, J. E.; Hratchian, H. P.; Cross, J. B.; Adamo, C.; Jaramillo, J.; Gomperts, R.; Stratmann, R. E.; Yazyev, O.; Austin, A. J.; Cammi, R.; Pomelli, C.; Ochterski, J. W.; Ayala, P. Y.; Morokuma, K.; Voth, G. A.; Salvador, P.; Dannenberg, J. J.; Zakrzewski, V. G.; Dapprich, S.; Daniels, A. D.; Strain, M. C.; Farkas, O.; Malick, D. K.; Rabuck, A. D.; Raghavachari, K.; Foresman, J. B.; Ortiz, J. V.; Cui, Q.; Baboul, A. G.; Clifford, S.; Cioslowski, J.; Stefanov, B. B.; Liu, G.; Liashenko, A.; Piskorz, P.; Komaromi, I.; Martin, R. L.; Fox, D. J.; Keith, T.; Al-Laham, M. A.; Peng, C. Y.; Nanayakkara, A.; Challacombe, M.; Gill, P. M. W.; Johnson, B.; Chen, W.; Wong, M. W.; Gonzalez, C.; Pople, J. A.; Gaussian, Inc., Wallingford, CT, 2004.
- (24) Senapati, U.; De, D.; De, B. R. *J. Mol. Struct. (Theochem)* **2007**, *808*, 157-159.
- (25) Senapati, U.; De, D.; De, B. R. *J. Mol. Struct. (Theochem)* **2009**, *894*, 71-74.
- (26) Mandal, B.; Panda, B. K.; Sengupta, S. *Indian J. Sci.* **2014**, *8*, 16-20.
- (27) Mandal, B.; Senapati, U.; Panda, B. K.; Sengupta, S. *Indian J. Sci.* **2014**, *11*, 49-53.

- (28) Yuan, K.; Lü, L.; Liu, Y. *Chin. Sci. Bull.* **2008**, *53*(9), 1315-1323.
- (29) Su, M. D.; Chu, S. Y. *J. Am. Chem. Soc.* **1999**, *121*(17), 4229.
- (30) Glendening, E. E.; Reed, A. E.; Carpenter, J. E.; Weinhold, F. NBO(Natural Bond Orbital), vol. 5.
- (31) Pearson, R. G. *J. Chem. Sci.* **2005**, *117*(5), 369.
- (32) De Proft, F.; Geerlings, P. *Phys. Chem. Chem. Phys.* **2004**, *6*, 242.



## LIST OF PUBLICATIONS

1. The Ground state Comparative Study of Proton affinities and Associated Parameters of Conjugated  $\alpha,\beta$ -Unsaturated Carbonyl Compounds in Gas and Aqueous phases by Density functional Theory Method.  
B. Mandal, U. Senapati, B. R. De. Indian Journal of Advances in Chemical Science. Vol. 4(4), (2016), 401-408.
2. Proton Affinities of a Series of  $\alpha, \beta$  Unsaturated Carbonyl Compounds of Type-2-alkene (Acrolein, 4-hydroxy-2-nonenal, Methyl Vinyl Ketone, Acrylamide, Methyl Acrylate, and Ethylmethacrylate), in the Gas and Aqueous Phase in their Low-lying Excited Triplet State: A Density Functional Theory/Polarizable Continuum Model and Self-Consistent Reaction Field Approach  
B. Mandal, U. Senapati, B. R. De. Indian Journal of Advances in Chemical Science. Vol. 5(1), (2017) 2017, 65-75.
3. The proton affinities of a series of  $\beta$ - substituted Acrylamide in the ground state: A DFT based computational study.  
B. Mandal, U. Senapati, B. R. De. Discovery Chemistry, 2015, 1(3) 64-71.
4. The lithium affinities of a series of heterocyclic compounds pyrrole, furan, thiophene and pyridine in their low lying excited triplet state: A DFT based comparative study.  
B. Mandal, U. Senapati, B. Panda, S. Sengupta. Indian Journal of Science, 2015, 15(44), 20-24.
5. The proton affinities of a series of heterocyclic compounds pyrrole, furan, thiophene and pyridine in their low lying excited triplet state: A DFT based comparative study.  
B. Mandal, U. Senapati, B. Panda, S. Sengupta. Indian Journal of Science, 2014, 11(28), 49-53.
6. The Comparative study of basicities,  $\text{Li}^+$ ,  $\text{Na}^+$  ion affinities of a series of heterocyclic molecules (pyrrole, furan, thiophene and pyridine) in the ground state, A DFT study.  
B. Mandal<sup>\*</sup>, B. Panda, S. Sengupta, Indian Journal of science, 2014, 8(19), 16-20.
7. Ground state lithium cation affinities (LCA) and associate parameter of a series of  $\alpha,\beta$ -unsaturated carbonyl compounds of type-2-alkene chemical class (ACL, HNE, MVK, ACR, MA and EMA ): A Comparative DFT based computational study in both gas and aqueous phase.  
B. Mandal, U. Senapati, B. R. De. Communicated.





## The Ground State Comparative Study of Proton Affinities and Associated Parameters of Conjugated $\alpha,\beta$ -unsaturated Carbonyl Compounds in Gas and Aqueous Phases by Density Functional Theory Method

Biswarup Mandal<sup>1</sup>, Umasankar Senapati<sup>2</sup>, Bhudeb Ranjan De<sup>1\*</sup>

<sup>1</sup>Department of Chemistry and Chemical Technology, Vidyasagar University, Midnapore - 721 102, West Bengal, India. <sup>2</sup>Department of Chemistry, Belda College, Belda, Paschim Medinipur - 721 424, West Bengal, India.

Received 18<sup>th</sup> August 2016; Revised 25<sup>th</sup> August 2016; Accepted 18<sup>th</sup> September 2016

### ABSTRACT

The proton affinities (PA) of a series of  $\alpha,\beta$ -unsaturated carbonyl compounds (acrolein [ACL], 4-hydroxy-2-nonenal, methyl vinyl ketone, acrylamide [ACR], methyl acrylate, and ethyl methacrylate, and their O-protonated counterparts have been computed using density functional theory [Becke, Lee, Yang and Parr] method using 6-311G(d,p) basis sets with complete geometry optimizations in both gaseous and aqueous phases. The O-protonation in both phases is observed to be exothermic, and the stereochemical disposition of proton is observed to be almost equal in each case. PA values are affected due to the presence of different length of alkyl chain and the different substituent at carbonyl carbon. In gas phase, PA of ACR is maximum, whereas it is minimum in ACL. In aqueous phase, the PA of the carbonyl compounds decrease in the order as  $-H > -NH_2 > -CH_3 > -OC_2H_5 > -OCH_3$  substituent at carbonyl carbon. Atom electron density is recorded by natural population analysis along with Mulliken net charge. A proper correlation of PA with a number of computed system parameters like net charge on the carbonyl oxygen of unprotonated and protonated bases, charge on proton of protonated bases, and also the computed hardness ( $\eta$ ) of the unprotonated bases in both phases have been explained thoroughly. The overall basicities are explicated considering the contribution from carbonyl group and distant atom.

**Key words:** Unsaturated, Natural population analysis, Aqueous, Becke; Lee; Yang and Parr, Density functional theory.

### 1. INTRODUCTION

The  $\alpha,\beta$ -unsaturated carbonyl compounds of type-2-alkene series (acrolein [ACL], 4-hydroxy-2-nonenal [HNE], methyl vinyl ketone [MVK], acrylamide [ACR], methyl acrylate [MA], and ethyl methacrylate [EMA]) are considered as soft electrophiles due to their corresponding pi-electron mobility. Members of this type-2-alkene series are treated as deadly environmental pollutants as they produce toxicity via common molecular mechanism [1]. Interaction of proton (Lewis acid) with carbonyl compounds (base) is an important part of biological science and chemistry. Proton affinity (PA) is the negative of the enthalpy change of proton-base interaction implying that higher the PA, higher the basicity. Gas phase basicity and PA are generally characterized by  $B[g] + H^+[g] \rightarrow BH^+[g]$  and  $B^-[g] + H^+[g] = BH$ . Ground state basicities of carbonyl compounds are well recognized [2-4]. In recent study, the binding nature of ion with ligand (donor site) has

been a research direction of physical organic chemistry and computational chemistry [5]. There are many instances of proton attack on carbonyl oxygen in the primary step of a carbonyl system [6-9]. Experimental data of PA are scarcely available [10] in ground state, and it is not an easy task to determine experimental PA values in a protonation reaction [11]. Ground state gas phase basicities of a series of aliphatic and aromatic conjugated carbonyl systems have been reported [12,13]. There are no such comparative theoretical results on PA which have still been found for several conjugated  $\alpha,\beta$ -unsaturated carbonyl compounds of the type-2 alkene chemical class in both phases together. Therefore, we are compelled to turn to theory to investigate some quantitative thought on PA of a structurally related and biologically important carbonyl compounds in gas phase and in aqueous phases with the help of density functional theory Becke, Lee, Yang and Parr (B3LYP[DFT]) method at the 6-311G(d,p) basis set level [14]. We examine here

\*Corresponding Author:  
E-mail: biswarupmandal75@gmail.com

theoretically, the PA of various carbonyl compounds toward Lewis acid  $H^+$ , and draw the comparison to the equivalent reaction with proton in gas phase as well as in aqueous phase. We are especially interested in the effect of solvation, geometric features, conjugation, and some other chemical properties. It is seen that computed chemical properties, geometrical features provided with this level of theoretical calculations are more accurate compared to other quantum mechanical methods such as *ab-initio* (Hartree-Fock [HF]) calculations, therefore, results obtained from HF calculation are not taken into account. Basis set superposition error corrections are not taken into account for this theoretical study. We have studied the interaction of  $H^+$  ion with different electron rich sites present in the compound that is carbonyl oxygen- $H^+$  interaction, carbonyl  $\pi$ - $H^+$  interaction, and also the other electronegative atom- $H^+$  interaction. We observed that carbonyl oxygen- $H^+$  interaction energy is much lower in the series and this gives the most stable complexes. Gas phase PA determination reflects the thermodynamic and electronic properties of the compound are avoiding more complicated solvent effect [15], but in this study, we search the solvation effect on different molecular properties in the ground state. Charge on proton ( $q_H^+$ ) in the protonated complexes in both gas and aqueous phases are noticed carefully, and it is seen that migration of charge density to the added proton has taken place. Computed PA values indicate that both preprotonation charge distribution local to chromophore and protonated complex relaxation charge density are involved to develop the overall basicity of the compounds. Since the selected carbonyl compounds are known as toxic pollutants, we have studied their comparative electrophilic nature by calculating some quantum mechanical parameters from their HOMO-LUMO energy gap. Compounds studied in this theoretical calculation are given below in Figure 1 with their respective abbreviated names.

## 2. METHODOLOGY

These quantum mechanical studies have been carried out using Gaussian "09" software (Gauss-view) [16]. The optimization has been done in B3LYP(DFT) method. Since the accuracy of the computed properties is sensitive to the quality of the basis set, we employ triplet split-valence basis set with polarization function 6-311G(d,p). Water was selected as a solvent from the solvent list for structural optimization of the free bases and their O- $H^+$  complexes using polarizable continuum model [17] at the same basis set. Mulliken population analysis [18] and NBO analysis (natural population analysis only) are used to determine equivalent charges on all atoms from the free bases and their protonated complexes.

## 3. RESULT AND DISCUSSION

The  $\alpha,\beta$ -unsaturated carbonyl compounds given in Figure 1 and their O- $H^+$  complexes computed in B3LYP(DFT) method at 6-311G(d,p) basis set level in both gaseous and aqueous phases are observed to be exothermic, so reactions are thermodynamically favorable. The calculated PA values of the free bases with their respective names and proper abbreviation are listed in Table 1. Generated atomic charge is not important in this quantum mechanical calculation. Mulliken net charge density among the atoms has been observed. Charge among the atoms computes by separating orbital overlap equally between two shared atoms. Table 2 reports the net charge on carbonyl oxygen ( $q_O^-$ ) of the compounds before protonation and of the protonated complexes and charge on proton ( $q_H^+$ ) in protonated complexes. Data in Table 2 reflect that charge on O-atom decreases in the protonated species in both gaseous and aqueous phases and clear the high protonation tendency of the compounds. Charge on proton in the O- $H^+$  complexes decreases from actual value establish the fact of charge transfer from ligand to the added proton has taken place. Table 1 shows that PA is maximum for ACL ( $-218.56$  kcal/mole) in gas phase where ACL exhibits the highest affinity

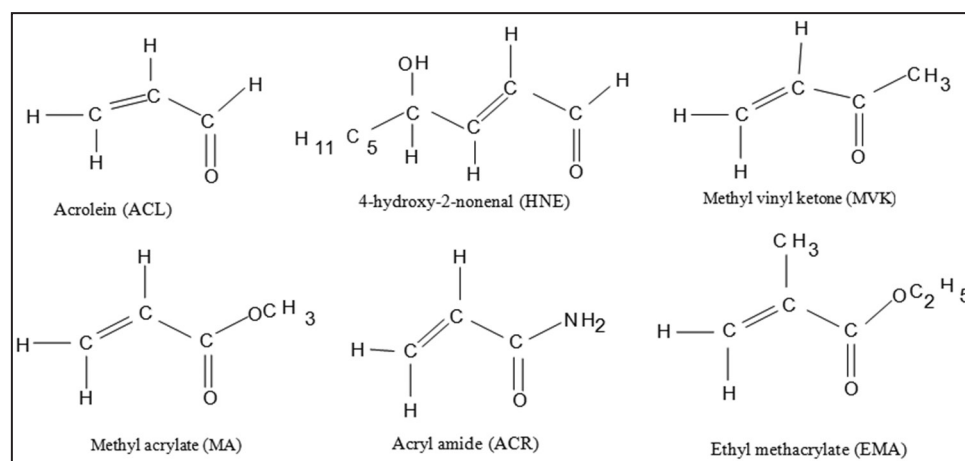


Figure 1:  $\alpha,\beta$ -unsaturated carbonyl compounds.



**Table 1:** Computed PA= $\Delta E$  of six  $\alpha,\beta$ -unsaturated carbonyl compounds for both gas and aqueous phases at the equilibrium geometry of the ground state. All data of PAs are in Hartree and kcal/mole unit.

Molecule	Gas phase PA		Aqueous phase PA	
	$\Delta E$ (Hartree)	$\Delta E$ (kcal/mol)	$\Delta E$ (Hartree)	$\Delta E$ (kcal/mole)
ACL	-0.3207	-201.24 (-194.019)*	-0.4526	-284.01
HNE	-0.3427	-215.04 (-)	-0.414	-259.78
MVK	-0.3336	-209.33 (-200.478)*	-0.4137	-259.60
ACR	-0.3483	-218.56 (-208.30)*	-0.4269	-267.88
MA	-0.3342	-209.71 (-199.28)*	-0.4104	-257.52
EMA	-0.3361	-210.90 (-203.11)*	-0.4114	-258.15

\*Experimental PA values of the respective compounds are noted in the parenthesis. Ref: Grutzmacher *et al.* 1989.  
PA: Proton affinities, ACL: Acrolein, HNE: 4-hydroxy-2-nonenal, MVK: Methyl vinyl ketone, ACR: Acrylamide, MA: Methyl acrylate, EMA: Ethyl methacrylate

**Table 2:** Computed Mulliken net charge on carbonyl oxygen atom ( $q_{O^-}$ ) of free base ( $B_1$ ) and O-protonated complexes ( $B_1H^+$ ) and net charge on proton ( $q_{H^+}$ ) of the O-protonated complexes at the equilibrium ground state and dipole moment ( $p$ ) in debye of the free bases in both phases.

Molecule	Gas phase				Aqueous phase			
	$(q_{O^-})$		$q_{H^+}$	$p$	$(q_{O^-})$		$q_{H^+}$	$p$
	$B_1$	$B_1H^+$	$B_1H^+$		$B_1$	$B_1H^+$	$B_1H^+$	
ACL	-0.2864 (-0.5056)	-0.1465 (-0.5002)	0.3200 (0.5181)	3.15	-0.4675 (-0.5673)	-0.1742 (-0.5162)	0.3389 (0.5299)	4.04
HNE	-0.2944 (-0.5214)	-0.2101 (-0.5187)	0.3206 (0.5169)	2.12	-0.3490 (-0.5530)	-0.2090 (-0.5234)	0.3437 (0.5312)	2.83
MVK	-0.3022 (-0.5494)	-0.1995 (-0.5425)	0.3162 (0.517)	2.7	-0.3574 (-0.5979)	-0.2090 (-0.5538)	0.3354 (0.5298)	3.51
ACR	-0.3594 (-0.6048)	-0.2505 (-0.5837)	0.3171 (0.5152)	3.88	-0.4316 (-0.6714)	-0.2750 (-0.5979)	0.3307 (0.5230)	5.14
MA	-0.3157 (-0.5670)	-0.1889 (-0.5567)	0.2991 (0.5085)	4.32	-0.3778 (-0.6265)	-0.222 (-0.5757)	0.323 (0.5238)	5.56
EMA	-0.3553 (-0.5587)	-0.2192 (-0.5772)	0.3106 (0.5187)	1.78	-0.3701 (-0.6180)	-0.2374 (-0.5854)	0.3278 (0.5304)	5.51

Data written in parenthesis are obtained from NPA analysis. NPA: Natural population analysis, ACL: Acrolein, HNE: 4-hydroxy-2-nonenal, MVK: Methyl vinyl ketone, ACR: Acrylamide, MA: Methyl acrylate, EMA: Ethyl methacrylate

(-284.01 kcal/mole) toward proton in aqueous media. The different PA values of the  $\alpha,\beta$ -unsaturated carbonyl compounds clear the nonunique effect of conjugated double bond and influenced by the different substituent at carbonyl carbon. In gas phase, the highest PA value in ACR is due to the presence of  $-NH_2$  group at the carbonyl carbon. Along with C-C double bond effect, lone-pair electron on nitrogen atom also move toward binding oxygen makes it more electron rich and enhanced the PA. Gas phase PA increases in the order  $ACL < MVK < MA \leq EMA < HNE < ACR$ , where it follows the decreasing order  $ACL > ACR > HNE > MVK > EMA > MA$  in the aqueous phase. In the presence of solvation effect, this order appeared by almost reversed due to the electronic relaxation effect. ACL shows the highest affinity to proton because there is no possibility of hydrogen bond formation at any center of the compound which

can restrict the shifting of  $\pi$  electron at the binding site, so the resonance effect (+R) increases the electronegativity of binding oxygen and accelerate the proton-oxygen interaction. PA value of HNE (-259.78 kcal/mole) becomes less compared to ACL in aqueous phase because of the possibility of hydrogen bond formation with hydroxyl oxygen, but it has higher PA value than MVK, MA, and EMA, this is due to the positive inductive effect (+I) exhibited by the long alkyl chain attached to the carbonyl group shifting partial negative charge at oxygen binding site [19]. PA value varies due to the presence of different substituents at the carbonyl carbon, and it also affected slightly by the substituent ( $-H$  or  $-CH_3$ ) present at the  $\alpha$ -carbon of the molecule.

PA increases in gas phase following the order as  $B = -H < -CH_3 < -OCH_3 < -OC_2H_5 < -NH_2$ . Effect of

B ( $-\text{CH}_3$ ,  $-\text{OCH}_3$  and  $-\text{OC}_2\text{H}_5$ ) on PA is more or less same for these three unsaturated compounds. Positive inductive effect (+I) of methyl group at  $\alpha$  position increase PA little bit in EMA ( $\text{A}=\text{CH}_3$ ) compared to methyl acrylate ( $\text{A}=\text{H}$ ). Lone-pair electron on the nitrogen of amide group lost their mobility toward carbonyl oxygen due to the hydrogen bond formation (N–H) in water, which is one of the causes for decreasing PA of ACR compared to ACL. +I character of methyl group enhance the PA of MVK ( $-259.6$  kcal/mole). Effect of  $-\text{OCH}_3$  at B is less on PA compare to  $-\text{OC}_2\text{H}_5$  because both substituents have a negative inductive effect (–I) and resonance (+R) effect, but due to more resonance character ( $-\text{OCH}_3 \leftarrow -\text{OC}_2\text{H}_5$ ) PA value of EMA ( $-258.15$  kcal/mole) is little more compared to MA ( $-257.52$  kcal/mole) in aqueous phase. For  $\alpha,\beta$ -unsaturated carbonyl compounds, PA increases in the order  $\text{B}=\text{OCH}_3 \leftarrow -\text{OC}_2\text{H}_5 \leftarrow -\text{CH}_3 \leftarrow -\text{NH}_2 \leftarrow -\text{H}$  (in ACL) in aqueous phase. From Table 2, it is obvious that net charge on  $\text{O}^-$  atom is higher in free bases in each compound compared to their protonated complex indicate their high protonation tendency. Charge on proton of the protonated complexes revealed the fact of extensive charge transfer during protonation, proton added to the carbonyl oxygen form a strong covalent  $\sigma$  bond. Charge density on O-atom increases markedly in aqueous phase compared to the gas phase indicating the higher charge separation in water. It is well supported by increased dipole moment in aqueous phase than that in the gas phase. Charge on proton and oxygen atom in the complexes clearly shows that shifting of charge is not local; it comes from all over the molecules. Computed net charge on oxygen atom in free compound and protonated complexes are within the range  $-0.2864$  to  $-0.3594$  and  $-0.1465$  to  $-0.2505$  in gas phase. It is  $-0.3701$  to  $-0.4635$  and  $-0.1742$  to  $-0.2750$  for free base and their  $\text{O}-\text{H}^+$  complexes in aqueous phase, respectively. Charge on adjunct proton lies within  $0.2991$ - $0.3206$  in gas phase, a little increases in the aqueous phase (from  $0.323$  to  $0.3437$ ). Some selected optimized geometrical features such as bond distance (C–O and O–H),  $\angle \text{C}-\text{O}-\text{H}^+$  bond angle surrounding carbonyl group of the computed compounds are reported in Tables 3 and 4.  $r(\text{C}-\text{O})$  bond length effected with the protonation, it increases in protonated complexes by  $0.069\text{\AA}$ - $0.092\text{\AA}$  in gas phase and  $0.067\text{\AA}$ - $0.097\text{\AA}$  in aqueous phase. In complex  $r(\text{O}-\text{H}^+)$ , bond distance remains almost equal for all compounds both in gas and aqueous phase; it varies iota ( $0.0062\text{\AA}$  in gas phase and  $0.0087\text{\AA}$  in aqueous phase). The  $\angle \text{C}-\text{O}-\text{H}^+$  bond angle for computed complexes lies within  $111.59^\circ$ - $117.57^\circ$  and  $111.397^\circ$ - $113.97^\circ$  in gas and aqueous phases, respectively. The local stereochemical and other quantum mechanical parameters obtained from DFT[B3LYP] theoretical study at 6-311G(d,p)

**Table 3:** Geometrical features of the free base and O-protonated base (length in  $\text{\AA}$  and angle in degree) at the equilibrium ground state in the gas phase.

Molecule	Free Base	O-protonated complexes		
	$r(\text{C}-\text{O})$	$r(\text{C}-\text{O})$	$r(\text{O}-\text{H}^+)$	$\angle \text{C}-\text{O}-\text{H}^+$
ACL	1.208	1.277	0.9761	114.720
HNE	1.21	1.298	0.9771	113.560
MVK	1.213	1.291	0.9721	117.570
ACR	1.22	1.30	0.9686	113.275
MA	1.203	1.296	0.9684	113.577
EMA	1.208	1.298	0.9743	111.597

ACL: Acrolein, HNE: 4-hydroxy-2-nonenal, MVK: Methyl vinyl ketone, ACR: Acrylamide, MA: Methyl acrylate, EMA: Ethyl methacrylate

**Table 4:** Geometrical features of the free base and O-protonated base (length in  $\text{\AA}$  and angle in degree) at the equilibrium ground state in aqueous phase.

Molecule	Freebase	O-protonated complexes		
	$r(\text{C}-\text{O})$	$r(\text{C}-\text{O})$	$r(\text{O}-\text{H}^+)$	$\angle \text{C}-\text{O}-\text{H}^+$
ACL	1.221	1.277	0.9762	113.970
HNE	1.21	1.288	0.9715	112.712
MVK	1.219	1.286	0.9728	113.1269
ACR	1.230	1.307	0.9687	112.432
MA	1.212	1.295	0.9694	113.4703
EMA	1.212	1.295	0.9749	111.397

ACL: Acrolein, HNE: 4-hydroxy-2-nonenal, MVK: Methyl vinyl ketone, ACR: Acrylamide, MA: Methyl acrylate, EMA: Ethyl methacrylate

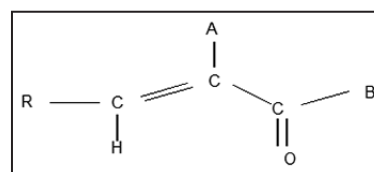


**Figure 2:** Structures for conjugated  $\alpha,\beta$ -unsaturated carbonyl compounds of type-2-alkene chemical class ( $\text{R}=\text{H}$  or alkyl group,  $\text{A}=\text{H}$  or  $-\text{CH}_3$  and  $\text{B}=\text{H}, -\text{CH}_3, -\text{OCH}_3, -\text{NH}_2, -\text{OC}_2\text{H}_5$ ).

basis set level suggest to conclude that the PA of the selected carbonyl compounds cannot be explained correctly by local carbonyl site properties only, it must consider the entire molecular contribution. We have also analyzed some other global quantum mechanical parameters to observe the comparative electrophilic nature by calculating electrophilic index ( $\omega$ ), hardness ( $\eta$ ), and softness ( $\sigma$ ) from HOMO–LUMO energy gap of the free carbonyl compounds in both gas and aqueous phases. It is observed from the data reported in Table 5 and

**Table 5:** Computed hardness, softness, chemical potential, and electrophilic index of the free base ( $B_1$ ) in the gas phase ground state by DFT method.

Molecule	{Hardness( $\eta$ )= $[\epsilon_{LUMO}-\epsilon_{HOMO}]/2$ , Softness( $\sigma$ )= $1/\eta$ , Chemical potential( $\mu$ )= $[\epsilon_{LUMO}+\epsilon_{HOMO}]/2$ , Electrophilic index ( $\omega$ )= $\mu^2/2\eta$ }					
	$\epsilon_{HOMO}$	$\epsilon_{LUMO}$	$\eta$	$\sigma$	$\mu$	$\omega$
ACL	-0.2649	-0.0735	0.0957	10.44	-0.1692	0.1495
HNE	-0.2603	-0.0717	0.0943	10.60	-0.166	0.1461
MVK	-0.2565	-0.0639	0.0963	10.38	-0.1602	0.1332
ACR	-0.2593	-0.0477	0.1058	9.45	-0.1535	0.1113
MA	-0.2781	-0.0614	0.1083	9.23	-0.1697	0.1329
EMA	-0.2725	-0.0451	0.1137	8.79	-0.1588	0.1108

ACL: Acrolein, HNE: 4-hydroxy-2-nonenal, MVK: Methyl vinyl ketone, ACR: Acrylamide, MA: Methyl acrylate, EMA: Ethyl methacrylate, DFT: Density functional theory

**Table 6:** Computed hardness (Hartree), softness, chemical potential, and electrophilic index of the free base ( $B_1$ ) in the aqueous phase ground state by DFT method.

Molecule	{Hardness ( $\eta$ )= $[\epsilon_{LUMO}-\epsilon_{HOMO}]/2$ , Softness( $\sigma$ )= $1/\eta$ , Chemical potential ( $\mu$ )= $[\epsilon_{LUMO}+\epsilon_{HOMO}]/2$ , Electrophilic index ( $\omega$ )= $\mu^2/2\eta$ }					
	$\epsilon_{HOMO}$	$\epsilon_{LUMO}$	$\eta$	$\sigma$	$\mu$	$\omega$
ACL	-0.26124	-0.06480	0.0982	10.18	-0.1630	0.1352
HNE	-0.26641	-0.07356	0.0964	10.37	-0.1699	0.1496
MVK	-0.26312	-0.06646	0.0983	10.16	-0.1647	0.1379
ACR	-0.26802	-0.04818	0.1099	9.09	-0.1581	0.1136
MA	-0.2887	-0.06312	0.1127	8.36	-0.1759	0.1371
EMA	-0.27515	-0.04065	0.1172	8.52	-0.1579	0.1063

ACL: Acrolein, HNE: 4-hydroxy-2-nonenal, MVK: Methyl vinyl ketone, ACR: Acrylamide, MA: Methyl acrylate, EMA: Ethyl methacrylate, DFT: Density functional theory

Table 6 that ACL ( $\omega=0.1495$  and  $0.1352$  in gas and aqueous phases, respectively) and HNE ( $\omega=0.1461$  and  $0.1496$  in gas and aqueous phases, respectively) are two most strong electrophiles compared to rest four compounds and EMA ( $\omega=0.1108$  and  $0.1063$  in gas and aqueous phases) have the weakest electrophilic reactivity. Based on their corresponding quantum mechanical parameter, the selected carbonyl compounds follow the electrophilicity order as  $HNE \geq ACL \gg MVK \geq MA > ACR > EMA$  in aqueous, albeit controversial in gaseous phase where ACL exhibit highest electrophilicity compared to HNE. The global parameter hardness ( $\eta$ ) obtained from  $E_{LUMO}-E_{HOMO}$  energy gap is the scale of ground state stability of the relative compounds. Calculated quantum mechanical data tabulated in Tables 5 and 6 clear that EMA ( $\eta=0.1137$  and  $0.1172$  in gas and aqueous phases) is most stable among the six compounds (Figures 2 and 3).

#### 4. CONCLUSION

Investigated PA values of six  $\alpha,\beta$ -unsaturated conjugated carbonyl compounds in both gas phase

and aqueous phases using DFT(B3LYP) method employing triple valence basis set 6-311G(d,p) cannot be explained exactly considering only electronic and stereochemical optimized parameter at or around the carbonyl moiety, proton affinities are strongly affected by the different substituents ( $B=H, -CH_3, -OCH_3, -OC_2H_5,$  and  $-NH_2$ ) attached to the carbonyl carbon. Proton affinities of the bases markedly change due to solvation. Interaction enthalpies are more negative in water. +I effect of  $\alpha$ -methyl group, +R (resonance) and -I effect of the  $-OCH_3,$  and  $-OC_2H_5$  group are responsible for the small increase of PA in EMA. So, it can be concluded that PA of the  $\alpha,\beta$ -unsaturated carbonyl compounds are obtained considering the different electronic properties strongly. It has been found that selected carbonyl derivatives are harder in aqueous phase. The electrochemical properties of the protonated complexes clear the fact that the interaction between binding oxygen site and proton is preferably an ion-induced dipole interaction and ion-dipole attraction as well rather than a covalent interaction. Overall protonation reactions are spontaneous.

**Figure 3:** Optimized structure of selected conjugated  $\alpha,\beta$ -unsaturated carbonyl compounds and their carbonyl oxygen- $H^+$  complexes in gas and aqueous phases.

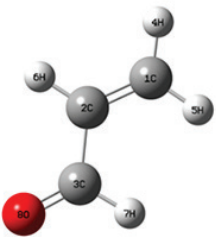
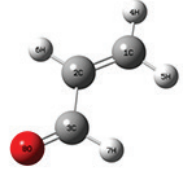
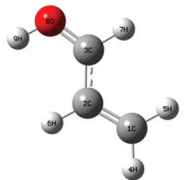
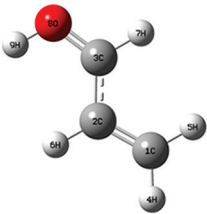
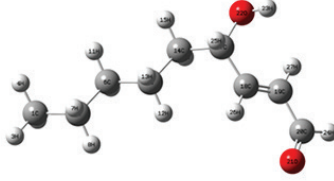
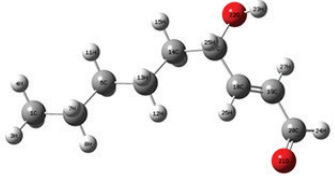
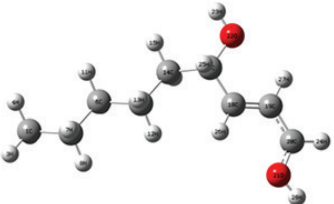
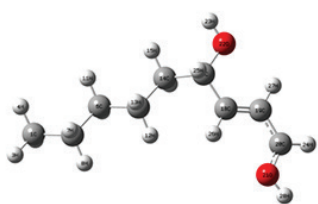
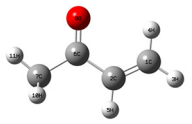
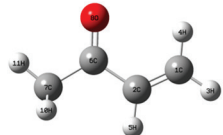
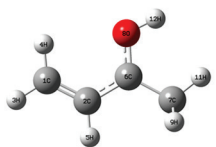
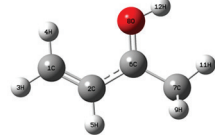
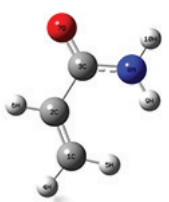
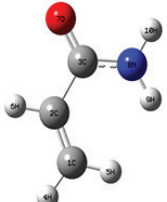
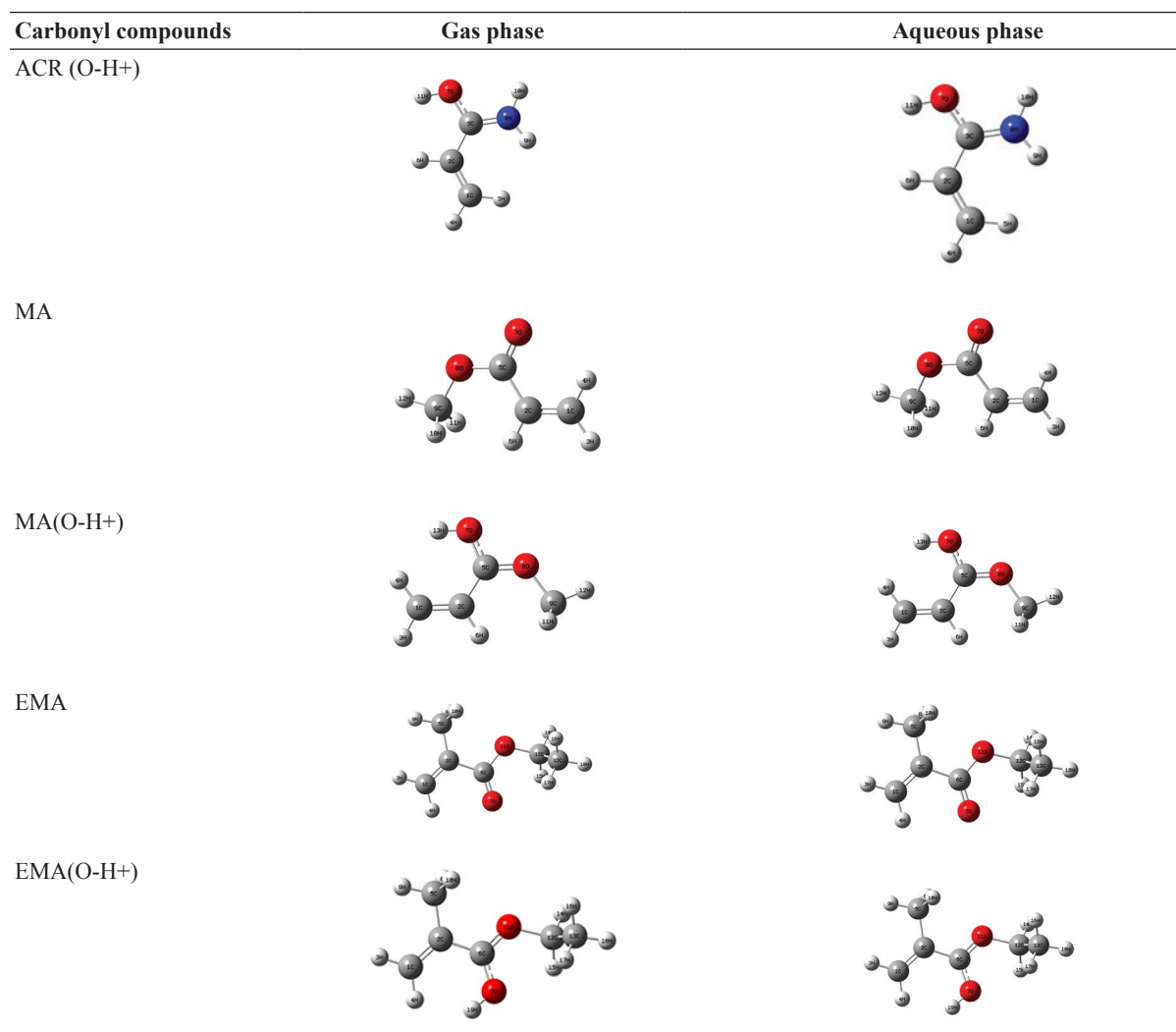
Carbonyl compounds	Gas phase	Aqueous phase
ACL		
ACL (O-H <sup>+</sup> )		
HNE		
HNE (O-H <sup>+</sup> )		
MVK		
MVK (O-H <sup>+</sup> )		
ACR		

Figure 3: (Continued)



## 5. REFERENCES

1. R. M. LoPachin, T. Gavin, (2012) Molecular mechanism of acrylamide neurotoxicity: Lessons learned from organic chemistry, *Environmental Health Perspectives*, **12**: 120.
2. L. Beauchamp, (1974) *Interaction between Ions and Molecules*, New York: Plenum. p 413, 459, 489.
3. D. K. Bohme, G. I. Mackay, H. I. Schiff, R. S. Hemsworth, (1974), Equilibrium OH<sup>-</sup> + C<sub>2</sub>H<sub>2</sub> = C<sub>2</sub>H<sup>-</sup> + H<sub>2</sub>O and the determination of Hf<sub>298</sub>(C<sub>2</sub>H<sup>-</sup>), *The Journal of Chemical Physics*, **61**: 2175.
4. J. I. Brauman, L. K. Blair, (1970), Geminal poly(1-pyrazolyl)alkanes and their coordination chemistry, *Journal of the American Chemical Society*, **92**: 5986.
5. E. A. Meyer, R. K. Castellano, F. Diederich, (2003) Interactions with aromatic rings in chemical biological recognition, *Angewandte Chemie International Edition*, **42**: 1210-1250.
6. S. P. Bhattacharya, S. C. Rakshit, M. Banerjee, (1983) The INDO/2-AHP Method for excited states, The adiabatic proton affinities of formaldehyde in 1, 3 nπ\* and 1, 3 ππ\* states, *Journal of Molecular Structure, (Theochem)*, **91**: 253.
7. J. R. L. Dekock, M. S. Kohin, (1983) MNDO study of the proton affinity of fluorinated formaldehydes and acetones, *Journal of Molecular Structure, (Theochem)*, **94**: 343.
8. O. P. Strusz, E. Kapny, C. Kosmntza, M. A. Robb, G. Theodorakopoulos, I. G. Ciszmadia, (1978), Vertical proton addinities of CH<sub>2</sub>O and CH<sub>2</sub>OH<sup>+</sup> in their ground singlet, excited triplet and ionized doubled states, *Theoretica Chimica Acta*, **48**: 215.
9. R. Yamadagni, P. J. Kebarle, (1973) Advantage of determining the ground state acid-base properties by gas phase High Pressure Mass Spectrometry method in absence of complicating effects of solvation, *Journal of the American Chemical*



- Society*, **96**: 3727.
- P. Burk, I. A. Koppel, I. Koppel, R. Kurg, J. F. Gal, P. C. Maria, M. Herreros, R. Notario, J. L. M. Abboud, F. Anvia, R. W. Taft, (2000), Revised and expanded scale of gas-phase lithium cation basicities. An experimental and theoretical study, *The Journal of Physical Chemistry*, **104A**: 2824-2833.
  - D. A. Dixon, S. G. Lias, (1987) Molecular structure and energetics. In: J. F. Liebman, A. Greenberg, (Eds.), *Physical Measurements*, Vol. 2. Deereld Beach, FL: VCH.
  - S. Pandit, D. De, B. R. De, (2006) The ground state basicities of a series of chrotonaldehyde, *Journal of Molecular Structure, (Theochem)*, **760**: 245.
  - U. Senapati, D. De, B. R. De, (2008), The basicities of a series of substituted acetophenones in the ground state: A DFT study, *Indian Journal of Chemistry*, **47A**: 548-550.
  - C. Lee, W. Yang, R. G. Parr, (1988), Development of the Colle-Salvetti correlation-energy formula into a functional of the electron density, *Physical Review*, **37B**: 785.
  - R. Wolf, H. F. Grutzmacher, (1990), The proton affinities of some  $\alpha,\beta$ -unsaturated esters and amides, *New Journal of Chemistry*, **14**: 379-382.
  - M. J. Frisch, G. W. Trucks, H. B. Schlegel, G. E. Scuseria, M. A. Robb, J. R. Cheeseman, G. Scalmani, V. Barone, B. Mennucci, G. A. Petersson, H. Nakatsuji, M. Caricato, X. Li, H. P. Hratchian, A. F. Izmaylov, J. Bloino, G. Zheng, J. L. Sonnenberg, M. Hada, M. Ehara, K. Toyota, R. Fukuda, J. Hasegawa, M. Ishida, T. Nakajima, Y. Honda, O. Kitao, H. Nakai, T. Vreven, J. A. Montgomery, Jr., J. E. Peralta, F. Ogliaro, M. Bearpark, J. J. Heyd, E. Brothers, K. N. Kudin, V. N. Staroverov, R. Kobayashi, J. Normand, K. Raghavachari, A. Rendell, J. C. Burant, S. S. Iyengar, J. Tomasi, M. Cossi, N. Rega, J. M. Millam, M. Klene, J. E. Knox, J. B. Cross, V. Bakken, C. Adamo, J. Jaramillo, R. Gomperts, R. E. Stratmann, O. Yazyev, A. J. Austin, R. Cammi, C. Pomelli, J. W. Ochterski, R. L. Martin, K. Morokuma, V. G. Zakrzewski, G. A. Voth, P. Salvador, J. J. Dannenberg, S. Dapprich, A. D. Daniels, O. Farkas, J. B. Foresman, J. V. Ortiz, J. Cioslowski, D. J. Fox, (2009), *Gaussian 09, Revision A.02*, Wallingford, CT: Gaussian Inc.
  - J. Tomasi, B. Mennucci, E. Cancès, (1999) The IEF version of the PCM solvation method: An overview of a new method addressed to study molecular solutes at the QM AB initio level, *Journal of Molecular Structure, (Theochem)*, **464(1-3)**: 211-226.
  - R. S. Mulliken, (1955) Electronic population analysis on LCAO-MO molecular wave functions. I, *The Journal of Chemical Physics*, **23(10)**: 1833-1840.
  - A. M. Striegel, P. Piotrowiak, M. B. Stephen, R. B. Cole, (1999), Polarizability and inductive effect contributions to solvent-cation binding observed in electrospray ionization mass spectrometry, *Journal of the American Society for Mass Spectrometry*, **10**: 254-260.



## Proton Affinities of a Series of $\alpha$ , $\beta$ Unsaturated Carbonyl Compounds of Type-2-alkene (Acrolein, 4-hydroxy-2-nonenal, Methyl Vinyl Ketone, Acrylamide, Methyl Acrylate, and Ethylmethacrylate), in the Gas and Aqueous Phase in their Low-lying Excited Triplet State: A Density Functional Theory/Polarizable Continuum Model and Self-Consistent Reaction Field Approach

Biswarup Mandal<sup>1</sup>, Umasankar Senapati<sup>2</sup>, Bhudeb Ranjan De<sup>1\*</sup>

<sup>1</sup>Department of Chemistry and Chemical Technology, Vidyasagar University, Midnapore - 721 102, West Bengal, India. <sup>2</sup>Department of Chemistry, Belda College, Belda, Paschim Medinipur - 721 424, West Bengal, India.

Received 15<sup>th</sup> December 2016; Revised 30<sup>th</sup> December 2016; Accepted 05<sup>th</sup> January 2017

### ABSTRACT

Density functional theory Becke 3-term functional; Lee, Yang, Parr/6-311G(d,p) calculations were performed to quantify triplet state proton affinities (PA) and transition energies of a series of  $\alpha,\beta$ -unsaturated carbonyl compounds and their O-protonated counterparts in gas phase as well as in aqueous phase. To evaluate structural behavior and different quantum mechanical properties in water, we studied our optimization process using polarizable continuum model and Self-consistent reaction field method at the same level of theory of the relevant low-lying excited state. The gas phase O-protonation turns out to be exothermic in each case and the local stereochemical disposition of the proton is found to be almost the same in each case. PA values of the different compounds are affected by substituent present at the carbonyl carbon. Different electrochemical properties (+R, +I, and effect) originate from carbonyl chain are seen to cause change of the PAs. Acrylamide (ACR) shows the highest PA in both phases. In each case, protonation at carbonyl oxygen is observed to be more energetically favorable compared to protonation at other probable binding sites present. Computed PAs of the compounds in gas phase are in the following order  $ACR \geq$  ethylmethacrylate > 4-hydroxy-2-nonenal > methyl vinyl ketone > methyl acrylate > acrolein, while in aqueous phase the PA order is ranked differently. Charge density on binding oxygen and on added proton is recorded from both Mulliken population analysis and Natural population analysis. PA values are sought to be correlated with the computed hardness of the unprotonated species in the relevant excited state. The proton induced shifts are in general red shifts for the low-lying excited triplet state. The overall reactivity is explained by distant atom contribution in addition to the contribution from the carbonyl group.

**Key words:** Density functional theory, Polarizable continuum model, Proton affinity, Low-lying, Unsaturated.

### 1. INTRODUCTION

Ion-molecule interactions are now a growing interest in the field of both experimental and theoretical research in chemistry. Proton transfer reactions are of considerable importance in chemistry. Excited state proton transfer is very important in biological process [1]. By definition, an acid is an electron acceptor whereas base is an electron donor, so there may have a relationship between charge density distribution and acid-base properties. Acid-base properties of a molecule may change from one electronic state to another due to the extensive molecular charge redistribution in the different electronic state. The basic chemistry of

a carbonyl chromophore in ground state is largely independent of the nature of alkyl or aryl group present at carbonyl carbon. By changing the electronic nature of the low-lying excited state these alkyl or aryl groups markedly influence the chemical and physical nature of the carbonyl chromophore at the lowest excited state. Excited state proton transfer process on guanine and some related species has been investigated theoretically [2,3]. Basicity of some proto-typical carbonyls in the ground and low-lying excited state has been reported earlier [4]. Gas phase methods [5-13] have the advantage for determining inherent acid-base properties in ground state avoiding solvent effect. In

\*Corresponding Author:

E-mail: biswarupmandal75@gmail.com

presence of solvent, excited state acid-base properties of a molecule can be measured utilizing absorption and fluorescence spectral data in conjugation with Forster cycle [14-17]. Different computational studies [18-20] have been performed to investigate gas phase basicities of organic molecules in the excited state. Excited state proton affinities (PAs) and vertical excitation energies of 1,5, and 1,8- diaminonaphthalene were computed with the help of Becke 3-term functional; Lee, Yang, Parr (B3LYP)/6-31G(d,p), and CIS/6-31G(d,p) method of calculations [21]. In last few years the basicities, of a series of substituted aliphatic conjugated carbonyl system (chrotonaldehyde) [22,23] in ground state and their low-lying excited state and PAs of a series of aromatic conjugated carbonyl system (acetophenone) [24] in their lowest excited triplet state has been studied theoretically. In this current work, a series of conjugated  $\alpha,\beta$ -unsaturated carbonyl derivatives of type-2-alkene chemical class has been investigated using density functional theory (DFT)/B3LYP method at most reliable 6-311G(d,p) basis set at relevant low-lying excited triplet state. Compounds investigated in this study are acrolein (ACL), 4-hydroxy-2-nonenal (HNE), methyl vinyl ketone (MVK), acrylamide (ACR), methyl acrylate (MA), and ethylmethacrylate (EMA). A ground state comparative study of proton affinities of the same compounds was previously reported [25]. These unsaturated compounds selected in this work are considered as environmental pollutants. It is also recognized that electrophilic  $\alpha,\beta$ -unsaturated carbonyl derivatives of the Type-2 alkene chemical class cause broad organ system toxicity by forming covalent Michael-type adducts with amino acids [26-28]. The purpose of this work is to deliver comparative data base for PAs and basicities of the carbonyl compounds involved in biomolecular process in their low-lying excited triplet state in both gas and aqueous phase. It was observed that several energetic values obtained in DFT/B3LYP calculation are far better (more nearer to accuracy) than those obtained in *ab initio* Hartree-Fock (H-F) study; therefore, H-F results are not taken into account. Optimized geometry of the protonated complexes tends to suggest that proton ( $H^+$ ) added to the compound prefers to bind with carbonyl oxygen in all complexes with lowest optimization energy. Both Mulliken population analysis (MPA) and Natural population analysis (NPA) have been applied for evaluating the charge density on carbonyl oxygen of the unprotonated bases and of their protonated complexes and charge on added proton of the protonated complexes. We have analyzed the transition energies ( $^1S_0 \rightarrow T_1$ ) to understand whether the pre protonation charge distribution local to the chromophore or post protonation relaxation of charge density or both are important in explaining the overall basicity of each compound in a particular state. We have also analyzed the kind and extent of spectral shift caused by protonation. In a particular state, the possibility of correlating the PA values with the global

hardness of the molecules is also explored. Following are the chemical structures (drawn with Chemdraw software) (Figure 1) of investigated unsaturated carbonyl compounds with their proper name and abbreviation.

## 2. COMPUTATIONAL DETAILS

The geometry of the six  $\alpha,\beta$ -unsaturated carbonyl compounds has been fully optimized with most accurate DFT/B3LYP method [29] at 6-311G(d,p) basis set level of Gaussian "09" program package [30]. To verify geometrical behavior PAs and other computed parameters in solvent, we used self-consistent reaction field and polarizable continuum model [31] for geometry optimization at the same level of theory. Water has been selected as solvent from the solvent list given in Gaussian program. The charge density on atoms (carbonyl oxygen and added proton) of the optimized structures was calculated in both MPA [32] and NPA [33] framework. Basis set superposition error was found to be small therefore results are not included in this work. To obtain the thermodynamic parameters (enthalpies and Gibbs free energies at 298.15 K) frequency calculations were performed for all neutral, protonated complexes at the same level of theory.

## 3. RESULTS AND DISCUSSION

PA of a base is defined as negative enthalpy change ( $-\Delta H^{298.15k}$ ) of a thermodynamic equilibrium reaction:  $B_1 + H^+ \leftrightarrow [B_1H^+]$  and basicity is defined as the negative of the free energy change ( $-\Delta G^{298.15k}$ ) associated with the same reaction. So affinity and basicity can be characterized as,

$$PA (\Delta H) = H^{298.15k} [(B_1H^+) - (B_1)] \quad (1)$$

$$\text{Basicity} (\Delta G) = G^{298.15k} [(B_1H^+) - (B_1)] \quad (2)$$

PA of the compound can be obtain computationally according to Maksic and Kovačević [34,35] that is  $PA = [E_{tot} (B_1H^+) - E_{tot} (B_1)]$  (3)

Both gas and aqueous phase total energies of six  $\alpha,\beta$ -unsaturated carbonyl compounds and of their O- protonated complexes in low-lying excited triplet state are summarized in Table 1. Evaluated PA values [following equation (3)] of the studied compounds are tabulated in Table 2. It is observed that PA's of different carbonyl compounds have a variation in the range  $-223.35$ – $-199.29$  kcal/mole in the gas phase, while in aqueous phase the PA's span is increased and it is of  $-272.61$ – $-256.11$  kcal/mole. It is clear from the obtained values that conjugated double bond effect on PA's are not uniform. The presence of different substituent (B) at the carbonyl carbon and at any other positions (A at  $\alpha$ -carbon) of the alkyl chain of the compounds is markedly influence the PAs. It is seen that in both phases ACR exhibits the highest PA values



**Table 1:** Computed total energies (hartree) of the free bases ( $B_1$ ) and their protonated complexes ( $B_1h^+$ ) at the equilibrium geometry of the low-lying excited triplet state.

Compounds	Total energy (hartree)		Total energy (hartree)	
	Gas phase		Aqueous phase	
	$B_1$	$B_1h^+$	$B_1$	$B_1h^+$
ACL	-191.8663	-192.1839	-191.8695	-192.2786
4HNE	-503.0539	-503.40	-503.0843	-503.4869
MVK	-231.1978	-231.5358	-231.2015	-231.6218
ACR	-247.2466	-247.6035	-247.2580	-247.6934
MA	-306.4280	-306.7630	-306.4378	-306.8725
EMA	-385.1056	-385.4615	-385.1150	-385.5385

ACL=Acrolien, HNE=4-hydroxy-2-nonenal, MVK=Methyl vinyl ketone, ACR=Acrylamide, MA=Methyl acrylate, and EMA=Ethyl methacrylate

**Table 2:** Evaluated PAs [ $\Delta E_g$  or  $\Delta E_s=(E_{B_1H^+}-E_{B_1})$ ] for both gas and solvent phase at the equilibrium geometry of the lowest excited triplet state (1 hartree=627.5095 kcal/mole).

Compounds	Gas phase		Aqueous phase	
	PA		PA	
	$\Delta E_g$ (in hartree)	$\Delta E_g$ (in kcal/mole)	$\Delta E_g$ (in hartree)	$\Delta E_g$ (in kcal/mole)
ACL	-0.3176	-199.29	-0.4091	-256.11
HNE	-0.3461	-217.18	-0.4026	-252.63
MVK	-0.338	-211.49	-0.4203	-263.14
ACR	-0.3569	-223.35	-0.4354	-272.61
MA	-0.335	-209.61	-0.4347	-272.17
EMA	-0.3559	-222.73	-0.4235	-265.15

ACL=Acrolien, HNE=4-hydroxy-2-nonenal, MVK=Methyl vinyl ketone, ACR=Acrylamide, MA=Methyl acrylate, and EMA=Ethyl methacrylate

(-223.35 and -272.61 kcal/mole in gas and aqueous phase, respectively). The PA value of ACL is predicted to be lowest (-199.29 kcal/mole) in the gas phase. In aqueous phase, HNE exhibits the lowest PA value (-252.563 kcal/mole.) in the series in this particular electronic state. Lone pair electron of nitrogen of  $-NH_2$  may increase the electron density on binding oxygen thus the  $O-H^+$  interaction in ACR enhanced.

Effect of B (Figure 2) on PA in the low-lying triplet state are in the following increasing order  $-H$  (in ACL) <  $-CH_3$  <  $-OCH_3$  <  $-H$  (in HNE) <  $-OC_2H_5$  <  $-NH_2$ . On salvation, this effect on PA's ranked slightly different and it is  $-H$  (in HNE) <  $-H$  (in ACL) <  $-CH_3$  <  $-OC_2H_5$  <  $-OCH_3$  <  $-NH_2$ . We observed that gas phase PA value of EMA is comparatively higher than that of MA and MVK. This is may be the cause of double substituent effect ( $B=-OC_2H_5$  and  $A=-CH_3$ ). Both +I and +R effects (B) originate from A and B of EMA makes the  $O-H^+$  interaction more strong compared to MA and MVK. The enhancement of  $-OCH_3$  and  $-CH_3$  attached at carbonyl carbon of the unsaturated compounds are less than  $-OC_2H_5$  resulted less PA for MVK (-211.49 kcal/mole) and MA (-209.61 kcal/mole). Excited state (low-lying)

PA of HNE compound (-217.18 kcal/mole) obtained little more (approximately 6-8 kcal/mole) compared to MVK and MA. This trend may be explained by the inductive effect (+I) exhibited by the long alkyl group ( $C_5H_{11}$ ) linked to the carbonyl carbon, contributes by means of bond electron donation to enhance the  $O-H^+$  interaction. Computed PA values of the unsaturated compounds are predicted little more in water. PA values in aqueous phase increases in the following order HNE < ACL < MVK < EMA < MA  $\leq$  ACR. Different PA order appeared in this phase may be due to electronic relaxation effect in presence of solvation. The change of PA order (with higher values) of the same bases in solution phase is expected, because ions can become modified with the change of phase since the gas phase environment differs from that of the solvent phase. It was already revealed from a previous investigation [36] that, the order of basicity in solution differs from that in the gas phase. Table 2 also clear the fact that, excited (low-lying) state PAs are comparatively higher in gas as well as in the solvent phase compared to that obtained in the ground state. Exceptionally, PA of ACL and HNE in this state is observed little smaller relative to the ground state. This tendency has been

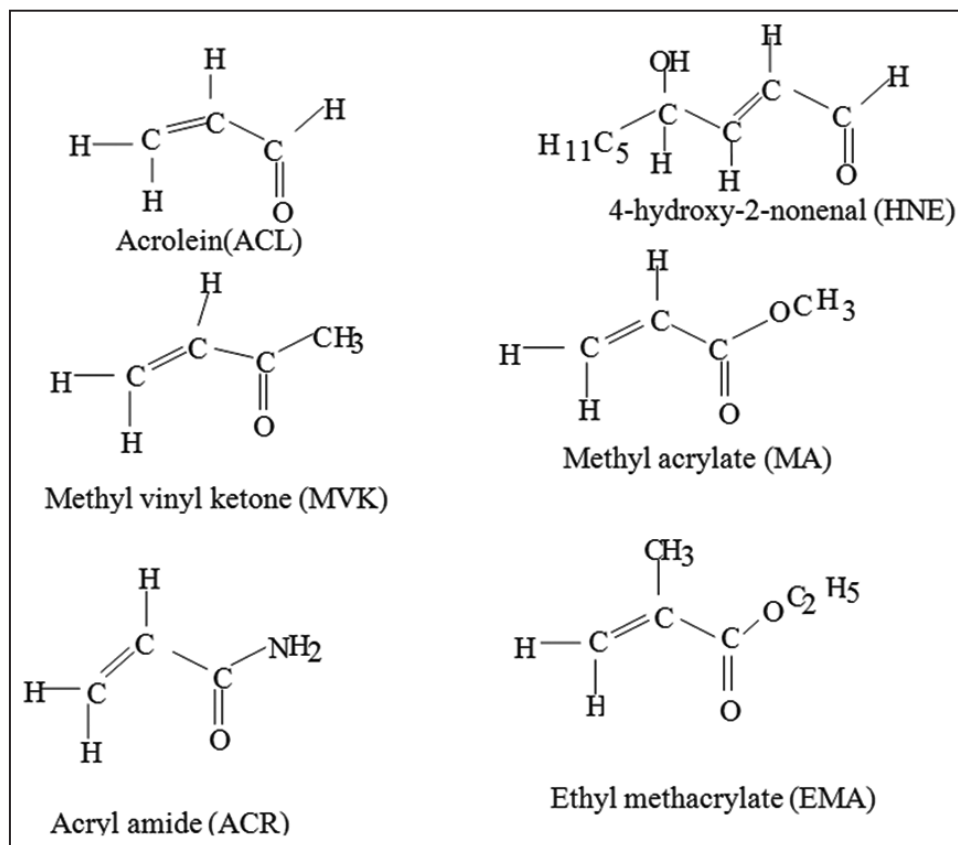


**Figure 1:** Structure of several conjugated  $\alpha,\beta$ -unsaturated carbonyl compounds.

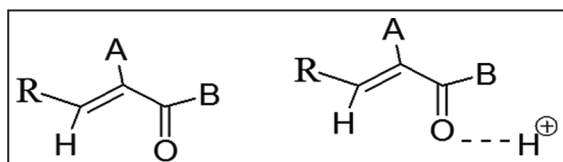


**Figure 2:** General neutral and protonated structures for conjugated  $\alpha$  and  $\beta$ -unsaturated carbonyl compounds of type-2-alkene chemical class ( $R=H$  or alkyl group,  $A=H$  or  $-CH_3$  and  $B=H, -CH_3$ , and  $-OCH_3, -NH_2, -OC_2H_5$ ).

investigated in an earlier study [37,38] which can be attributed to the phenomenon of redistribution of charges in the excited state in comparison to ground state [38]. Gas phase basicities were evaluated from calculated free energies ( $G$ ) following above equation (2). The total Gibbs free energies and evaluated basicities of the unsaturated carbonyl compounds in both gas and aqueous phases are collected in Table 3. It was observed that basicity values are closer to corresponding PA in each case, they differs only by  $\pm 4.48$  to  $\pm 8.81$  kcal/mole in gas phase and  $\pm 4.77$  to  $\pm 9.12$  kcal/mole in aqueous. The order of the basicities of the compounds is not parallel to their PA's data. Little discrepancy has been found between ACR and EMA in gas phase and between MA and ACR in aqueous phase. Table 4 reports the computed Mulliken net charge on carbonyl oxygen atom of

the free and protonated complexes and also the net charge on added proton of the protonated complexes in both phases in this particular state. Since, MPA is more method sensitive, we have tested another procedure (NPA) for evaluating partial charge on atoms. Table 5 summarized the partial charges on the same atoms obtained in the frame of NPA. From the  $Q_{CT}$  and  $q_{CT}$  values of Tables 4 and 5 clears that, in both phases, a significant charge transfer from ligand to proton has taken place. One might have expected that transferred charge will be parallel to the PA of the complexes. However this is not the case; both  $Q_{CT}$  and  $q_{CT}$  gave unexpected order in gas and aqueous phase. Charges obtained from NPA are comparatively higher compared to MPA. MPA charge on proton of the protonated complexes varies in the range of  $+0.2961$ - $0.3145$  and  $+0.3179$ - $+0.3335$  in gas and aqueous phase, respectively, while NPA results shows  $0.50$ - $0.51e$  natural charges on added proton in the gas phase and it is little bit higher in water ( $0.51e$ - $0.52e$ ). This charge migration is not local and originates from all over the compound. It is observed that there is no direct correlation between NPA or MPA results and complex stability. The  $Q_{CT}$  results are given in Table 4. According to the calculated results ( $Q_{CT}$ ), stability order of the complexes can be written as  $HNE \geq MA > ACR > EMA > ACL > MVK$  and  $MA \geq ACR > MVK \geq EMA > ACL > HNE$  in the gas and aqueous phaser, respectively.

**Table 3:** Obtained Gibbs free energies of six  $\alpha$  and  $\beta$ -unsaturated carbonyl compounds and basicities ( $\Delta G$ ) in kcal/mol) and entropies ( $\Delta S$ ) in cal/mole by B3LYP/DFT method at 6-311G (d, p) level in gas and aqueous phase at the equilibrium geometry of low-lying excited triplet state.

Compounds	Basicity calculated as: $G(B_1H^+) - G(B_1)$ in kcal/mole			
	Gas phase		Aqueous phase	
	Free energy [G] (in hartree)	$\Delta G$ (in kcal/mole)	Free energy [G] (in hartree)	$\Delta G$ (in kcal/mole)
ACL	-191.8364	-191.7	-191.8397	-248.74
ACL-H <sup>+</sup>	-192.1419		-192.2361	
HNE	-502.869	-212.6	-502.89	-247.86
HNE-H <sup>+</sup>	-503.2078		-503.285	
MVK	-231.1418	-204.37	-231.1456	-255.77
MVK-H <sup>+</sup>	-231.4675		-231.5532	
ACR	-247.2044	-214.54	-247.2163	-263.49
ACR-H <sup>+</sup>	-247.5463		-247.6362	
MA	-306.3724	-201.11	-306.3809	-263.8
MA-H <sup>+</sup>	-306.6929		-306.8013	
EMA	-384.9959	-216.23	-385.0054	-257.52
EMA-H <sup>+</sup>	-385.3405		-385.4158	

ACL=Acrolien, HNE=4-hydroxy-2-nonenal, MVK=Methyl vinyl ketone, ACR=Acrylamide, MA=Methyl acrylate, and EMA=Ethyl methacrylate

**Table 4:** Computed mulliken net charge on o-atom ( $q_o^-$ ) of free bases ( $B_1$ ) and o-protonated complexes ( $B_1H^+$ ) and computed mulliken net charge on added proton ( $q_{H^+}$ ) of the protonated complexes ( $B_1H^+$ ) and ligand to proton charge transfer ( $q_{CT}$ ) at the equilibrium geometry of low-lying excited state.

Molecule	$(q_o^-)$			$Q_{CT}$	$(q_o^-)$			$Q_{CT}$
	Gas phase				Aqueous phase			
	$B_1$	$B_1H^+$	$q_{H^+}$		$B_1$	$B_1H^+$	$q_{H^+}$	
ACL	-0.1335	-0.1438	0.3117	0.6883	-0.1481	-0.1811	0.3316	0.6684
HNE	-0.1986	-0.2556	0.2999	0.7001	-0.2989	-0.3423	0.3335	0.6665
MVK	-0.1581	-0.2148	0.3145	0.6855	-0.1737	-0.2314	0.33	0.670
ACR	-0.3684	-0.2763	0.3082	0.6918	-0.4503	-0.3075	0.3212	0.6788
MA	-0.3044	-0.2023	0.2961	0.7039	-0.3726	-0.2226	0.3179	0.6821
EMA	-0.3157	-0.2539	0.3098	0.6902	-0.3802	-0.2709	0.3232	0.6768

\*Charge transfer calculated as  $\{[\text{formal charge on proton (+1)}] - [\text{Charge obtained on proton}]\}$  in the complex.

ACL=Acrolien, HNE=4-hydroxy-2-nonenal, MVK=Methyl vinyl ketone, ACR=Acrylamide, MA=Methyl acrylate, and EMA=Ethyl methacrylate

NPA results shows different trend in gas as well as in water, it is  $HNE > MA \geq ACL > MVK > EMA$  and  $ACR \geq ACL > MA > MVK = HNE > EMA$ . This is tending to suggest that NPA results are also method sensitive. Functional sensitivity of NPA results was observed previously [39]. Hence, further exploration

in need to resolve such a major discrepancy. Tables 6 and 7 expose some important geometrical features around the functional carbon in the low-lying excited state. It is obvious from the results tabulated in Tables 6 and 7 that, optimized geometry of the compounds not changed markedly from gas

**Table 5:** Partial atomic charges on carbonyl oxygen ( $q_{O^-}$ ) of the free bases ( $B_1$ ) and their o-protonated complexes ( $B_1H^+$ ), partial charges on added proton ( $q_{H^+}$ ) of the protonated complexes ( $B_1H^+$ ) obtained from NPA and ligand to proton charge transfer ( $q_{CT}$ ) at the equilibrium geometry of low-lying excited state.

Molecule	$(q_{O^-})$			$q_{CT}$	$(q_{O^-})$			$q_{CT}$
	Gas phase				Aqueous phase			
	$B_1$	$B_1H^+$	$q_{H^+}$		$B_1$	$B_1H^+$	$q_{H^+}$	
ACL	-0.1770	-0.4692	0.5080	0.492	-0.1912	-0.4961	0.520	0.48
HNE	-0.1870	-0.5774	0.5030	0.497	-0.2050	-0.5529	0.524	0.476
MVK	-0.2004	-0.5428	0.5112	0.4888	-0.2174	-0.5503	0.524	0.476
ACR	-0.595	-0.6032	0.5089	0.4911	-0.6774	-0.6226	0.516	0.484
MA	-0.5109	-0.5573	0.5050	0.495	-0.5856	-0.5726	0.522	0.478
EMA	-0.5546	-0.5905	0.5178	0.4822	-0.6181	-0.5985	0.5268	0.4732

\*Charge transfer calculated as a formal charge on proton (+1) – Charge obtained on proton in the complex.

ACL = Acrolin, HNE = 4-hydroxy-2-nonenal, MVK = Methyl vinyl ketone, ACR = Acrylamide, MA = Methyl acrylate, EMA = Ethyl methacrylate, and NPA = Natural population analysis

**Table 6:** Geometrical features of the free base and O-protonated base (length in Å and angle in degree) in gas phase at equilibrium geometry of the low-lying excited state.

Molecules	Free base		O-protonated base		
	r(C-O)	r(C-O)	R(O-H+)	<C-O-H+	<C-C-O-H+
ACL	1.3106	1.3086	0.9743	114.8519	0.00
HNE	1.33	1.33	0.9766	118.76	-18.761
MVK	1.315	1.319	0.9717	113.0363	179.999
ACR	1.23	1.32	0.9670	113.332	0.00
MA	1.236	1.310	0.9675	113.4913	-13.491
EMA	1.214	1.30	0.9728	110.869	-10.8693

ACL=Acrolin, HNE=4-hydroxy-2-nonenal, MVK=Methyl vinyl ketone, ACR=Acrylamide, MA=Methyl acrylate, and EMA=Ethyl methacrylate

**Table 7:** Geometrical features of the free base and O-protonated base (length in Å and angle in degree) in aqueous phase

Molecules	Free base		O-protonated base		
	r(C-O)	r(C-O)	R(O-H+)	<C-O-H+	<C-C-O-H+
ACL	1.310	1.308	0.9743	113.77	0.00
HNE	1.296	1.31	0.9706	111.75	178.28
MVK	1.315	1.31	0.9719	112.57	-12.57-
ACR	1.245	1.32	0.9672	111.94	0.00
MA	1.238	1.30	0.9742	111.24	-11.24-
EMA	1.223	1.308	0.9731	110.59	-10.59-

ACL=Acrolin, HNE=4-hydroxy-2-nonenal, MVK=Methyl vinyl ketone, ACR=Acrylamide, MA=Methyl acrylate, and EMA=Ethyl methacrylate

to aqueous phase. C=O bond distance elongated slightly from unprotonated bases to protonated complexes. It is 0.004-0.09 Å in gas and quite similar 0.004-0.085 Å in aqueous phase. The O-H<sup>+</sup> bond distance has a variation in the range of 0.967-0.9766 Å and 0.9672-0.9743 Å in gas and aqueous phase, respectively. In both phases < C-O H<sup>+</sup> bond angle of all protonated complexes remain in between 110.869°

and 118.76° in gas phase. The range is reduced on aqueous environment (110.59-113.77°). Among six unsaturated compounds HNE, MVK, and EMA shows planarity in both phases with  $\tau$  (C-C-O-H<sup>+</sup>) dihedral angle -179.98°, 179.99°, and -179.51° in gas phase, 178.28°, -179.99°, and -179.60° in aqueous. In both phases, optimized geometries of ACL, ACR, and MA provide non-planar structure. The almost invariant

**Table 8:** Computed adiabatic transition energies ( $^1S_0 \rightarrow T_1$ ) (hartree) and proton-induced shifts (PIS, Hartree) in the low-lying excited triplet state.

Molecule	Gas phase			Aqueous phase		
	Transition energy		PIS	Transition energy		PIS
	B	BH+		B	BH+	
ACL	0.1019	0.105	0.0031	0.1046	0.1481	0.0435
HNE	0.1012	0.0979	-0.0033	0.0801	0.0915	0.0114
MVK	0.1042	0.0998	-0.0044	0.1065	0.0999	-0.0066
ACR	0.1192	0.1106	-0.0086	0.1186	0.1101	-0.0085
MA	0.1134	0.1126	-0.0008	0.1137	0.0894	-0.0243
EMA	0.1083	0.0885	-0.0198	0.1047	0.0838	-0.0209

ACL=Acrolien, HNE=4-hydroxy-2-nonenal, MVK=Methyl vinyl ketone, ACR=Acrylamide, MA=Methyl acrylate, EMA=Ethyl methacrylate, and PIS=Proton induced shifts

**Table 9:** Estimated dipole moment ( $\mu$ ) of six  $\alpha$  and  $\beta$ -unsaturated carbonyl compounds in gas phase as well as in aqueous phase at low-lying excited state ( $T_1$ ) and ground state.

Compounds	Gas phase		Aqueous phase	
	Dipole moment ( $\mu$ )		Dipole moment ( $\mu$ )	
	Ground state	Low-lying excited state	Ground state	Low-lying excited state
ACL	3.15	0.833	4.04	0.991
HNE	2.12	1.68	2.83	1.79
MVK	2.7	2.01	3.51	2.60
ACR	3.88	3.97	5.14	5.21
MA	4.32	4.35	5.56	5.71
EMA	1.78	4.22	5.51	5.76

ACL=Acrolien, HNE=4-hydroxy-2-nonenal, MVK=Methyl vinyl ketone, ACR=Acrylamide, MA=Methyl acrylate, and EMA=Ethyl methacrylate

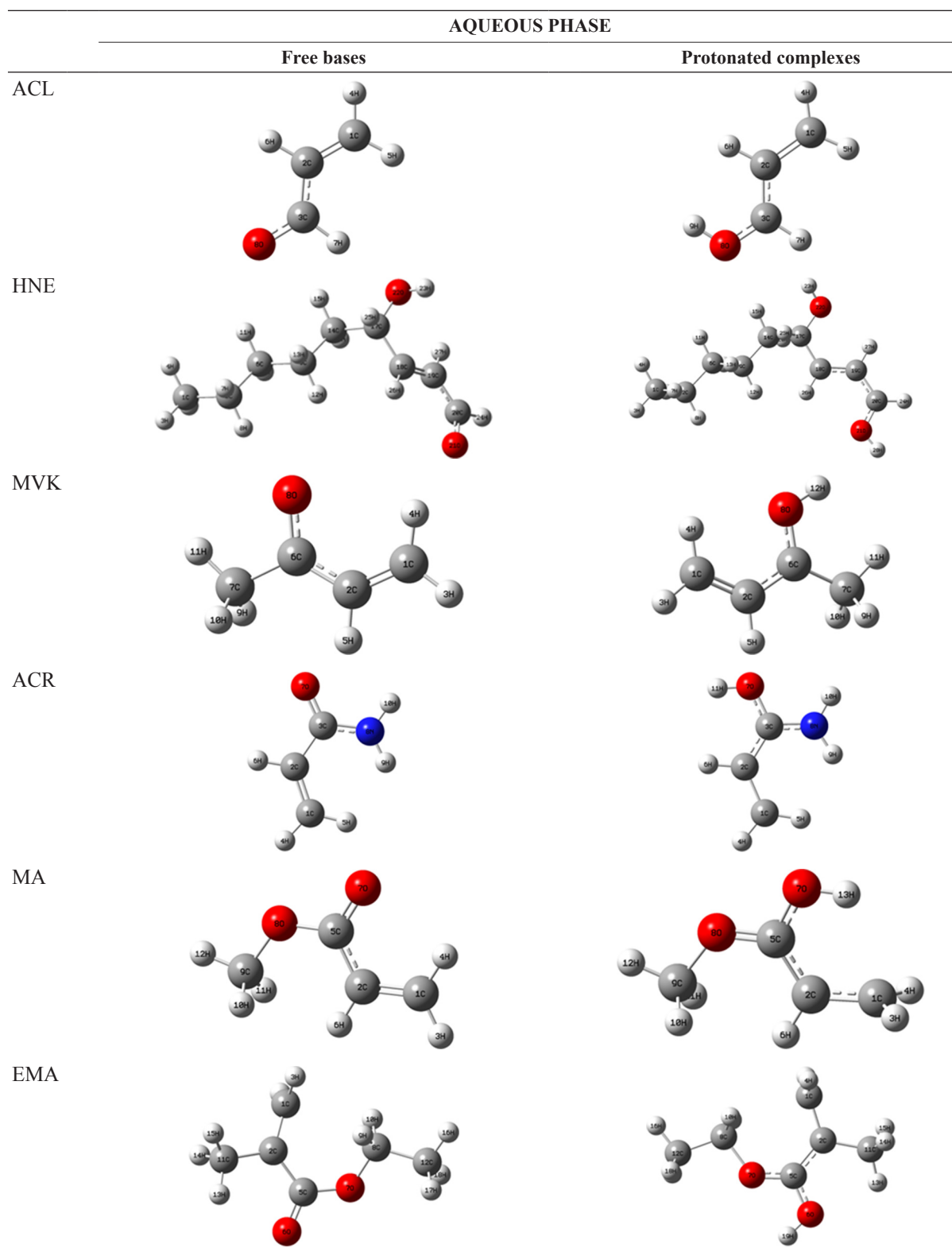
stereochemistry around the binding oxygen site tends to suggest that, PA's of the studied compounds cannot be predicted properly unless considering the contributions from distant atom. Table 8 reports the computed transition energies ( $^1S_0 \rightarrow T_1$ ) as state energies differences and shifts due to protonation. The proton induced shifts (PIS) are red shift in all cases with an exception of ACL, in which it is a blue shift. On aqueous environment, the PIS for ACL and HNE show blue shift whereas other unsaturated carbonyl bases of the series show red shifts. These trends of PIS refer to gas phase protonation of the isolated compounds without any additional effects due to solvation. It is seen from the data recorded in Table 9, low-lying excited state ( $T_1$ ) dipole moment ( $\mu$ ) of the ACL, HNE, and MVK are reduced relative to that of the ground state in both gas and aqueous phase whereas, it ( $\mu$ ) has been estimated to be higher in ACR, MA, and EMA than that in the ground state. This increase of dipole moment in these three carbonyl compounds may cause by the shifting of electron density from different substituent ( $-\text{NH}_2$ ,  $-\text{OCH}_3$  and  $-\text{OC}_2\text{H}_5$ ) to carbonyl chromophore.

#### 4. CONCLUSION

From this theoretical study, it can be concluded that both gas and aqueous phase protonation of the studied  $\alpha,\beta$ -unsaturated carbonyl compounds in low-lying excited state is spontaneous. ACR exhibits the highest PA values ( $-223.35$  kcal/mole and  $-272.61$  kcal/mole in gas and an aqueous phase, respectively). The PA values are little higher in this particular electronic state relative to their ground state in both gas and aqueous phase. The reverse trend also found due to the redistribution of electron density on atoms from one electronic state to another ( $S_0 \rightarrow T_1$ ). Effects of conjugated double on PA's are not uniform. The presence of different substituent (B) at the carbonyl carbon and at any other positions (A at  $\alpha$ -carbon) of the alkyl chain of the compounds are influenced the PAs markedly. Dipole moment of several unsaturated compounds is reduced in low-lying excited state compared to their ground state values. PIS are red shifts in general with the exception of ACL in gas phase and both ACL and HNE in aqueous phase. Overall, PA values of the investigated bases cannot be predicted properly without considering the contribution from distant atom along with the contribution from carbonyl moiety.







## 5. REFERENCES

1. J. Rucker, Y. Cha, T. Jonsson, K. L. Grant, J. P. Klinman, (1992) Role of internal thermodynamics in determining hydrogen tunnelling in enzyme-catalyzed hydrogen transfer reactions, *Biochemistry*, **31**: 11489.

- A. J. Beveridge, G. C. Heywood, (1993), A quantum mechanical study of the active site of aspartic proteinases, *Biochemistry*. **32**: 3325.
- I. A. Rose, D. J. Kuo, (1992), *ibid.* **31**: 5887.
- D. N. Silverman, S. Lindskog, (1988) The catalytic mechanism of carbonic anhydrase:

- Implications of a rate-limiting protolysis of water, *Accounts of Chemical Research*, **21**: 30.
- M. K. Shukla, J. Leszozynsky, (2005) Excited state proton transfer in guanine in the gas phase and in water solution: A theoretical study, *Journal of Physical Chemistry A*, **109**: 7775-7780.
  - A. J. A. Aquino, H. Lisohka, C. Haettig, (2005) Excited-State intramolecular proton transfer: A survey of TDDFT and RI-CC2 excited-state potential energy surfaces, *Journal of Physical Chemistry A*, **109**: 3201-3208.
  - S. P. Bhattacharya, C. Medhi, (1993) Basicity of some proto-typical carbonyls in the ground and some low lying excited states: Application of the orthogonal gradient method of orbital optimization in an INDO-MC-SCF framework-I, *Proceedings of the Indian Academy of Sciences – Chemical Sciences*, **105(3)**: 195-208.
  - D. K. Bohme, G. I. Mackay, H. I. Shiff, R. S. Hemsworth, (1973) Determination of proton affinity from the kinetics of proton transfer reactions. II. Kinetic analysis of the approach to the attainment of equilibrium, *The Journal of Chemical Physics*, **58**: 3504.
  - L. Beauchamp, (1974) *Interaction between Ions and Molecules*, New York: Plenum. p413, 459, 489.
  - R. Yamadagni, P. J. Kebarle, (1973) Advantage of determining the ground state acid-base properties by gas phase high pressure mass spectrometry method in absence of complicating effects of solvation, *Journal of the American Chemical Society*, **96**: 3727.
  - D. K. Bohme, G. I. Mackay, H. I. Shiff, R. S. Hemsworth, (1974) Equilibrium  $\text{OH}^- + \text{C}_2\text{H}_2 = \text{C}_2\text{H}^- + \text{H}_2\text{O}$  and the determination of  $\text{Hf}298(\text{C}_2\text{H}^-)$ , *The Journal of Chemical Physics*, **61**: 2175.
  - J. J. Solomon, M. N. Meot, F. M. Field, (1974) Kinetic equilibrium and negative temperature dependence in the bimolecular reaction  $\text{tert-C}_4\text{H}_9^+ + (\text{iso-C}_5\text{H}_{12}, \text{iso-C}_4\text{H}_{10}) \text{tert-C}_5\text{H}_{11}^+$  between 190 and 5700K, *Journal of the American Chemical Society*, **96**: 3727.
  - J. W. Long, J. L. Franklin, (1974) Ion-solvation reactions of phosphine, *Journal of the American Chemical Society*, **96**: 2320-2327.
  - J. I. Brauman, L. K. Blair, (1970) Geminal poly(1-pyrazolyl)alkanes and their coordination chemistry, *Journal of the American Chemical Society*, **92**: 5986.
  - R. D. Wieting, R. H. Staley, J. L. Beauchamp, (1974) Relative stability of carbonium ion in the gas phase and solution, comparison of cyclic and acyclic alkyl carbonium ions, acyl cations and cyclic halonium ions, *Journal of the American Chemical Society*, **96**: 7552.
  - R. H. Staley, J. L. Beauchamp (1975) Intrinsic acid base properties of molecules, Binding energies of  $\text{Li}^+$  to  $\pi$  and  $n$  – Donor Bases, *Journal of the American Chemical Society*, **97**: 5920.
  - T. Forster, (1950) Electrolytische dissoziation angeregter Molekule, *Electrochemistry*, **42(54)**: 1929.
  - M. Ottolenghi, (1973) Charge transfer complexes in the excited state. Lasser photolysis Studies, *Accounts of Chemical Research*, **6**: 153.
  - F. D. Saeva, G. R. Olin, (1975) Utilization of excited state PK's to initiate a ground state chemical reaction, *Journal of the American Chemical Society*, **97(19)**: 5631.
  - J. F. Ireland, P. A. H. Wyatt, (1976) Acid-base properties of electronically excited states of organic molecules. In: V. Gold, D. Bethell, (Eds.), *Advances in Physical Organic Chemistry*, Vol. 12. London: Academic Press. p138.
  - I. Antol, M. Eckert-Maksić, H. Lischka, (2004) Abinitio MR-CISD study of gas-phase basicity of formamide in the first excited singlet state, *Journal of Physical Chemistry A*, **108(46)**: 10317-10325.
  - H. Mishra, S. Maheshwary, H. B. Tripathi, N. Sathyamurthy, (2005) An experimental and theoretical investigation of photophysics of 1-hydroxy-2-naphthoic acid, *Journal of Physical Chemistry A*, **109(12)**: 2746-2754.
  - G. A. Ibanez, G. Labadie, G. M. Escandar, A. C. Olivieri, (2003) Ground and excited state intramolecular proton transfer of 3, 5- dibromosalicylic acid, *Journal of Molecular Structure (Theochem)*, **645**: 61-68.
  - K. Takehira, Y. Sugawara, S. Kowase, S. Tobita, (2005) A picosecond time-resolved study of prototropic reactions of electronically excited 1,5- and 1,8- diamino naphthalenes in aqueous solution, *Photochemical and Photobiological Sciences*, **4**: 287-293.
  - S. Pandit, D. De, B. R. De, (2006) The ground state basicities of a series of crotonaldehyde, *Journal of Molecular Structure (Theochem)*, **760(1)**: 245-246.
  - S. Pandit, D. De, B. R. De, (2006) The basicities of a series of substituted crotonaldehyde in their low-lying excited triplet state, *Journal of Molecular Structure (Theochem)*, **778**: 1-3.
  - U. Senapati, D. De, B. R. De, (2007) The proton affinity of a series of substituted acetophenones in their low-lying excited triplet state: A DFT study, *Journal of Molecular Structure (Theochem)*, **808(1)**: 153-155.
  - B. Mandal, U. Senapati, B. R. De, (2016) The ground state comparative study of proton affinities and associated parameters of conjugated  $\alpha,\beta$ -unsaturated carbonyl compounds in gas and aqueous phases by density functional theory method, *Indian Journal of Advances in Chemical Science*, **4(4)**: 401-408.
  - D. S. Barber, R. M. LoPachin, (2004) Proteomic



- analysis of acrylamide-protein adduct formation in rat brain synaptosomes, *Toxicology Applied Pharmacology*, **201(2)**: 120-136.
27. D. S. Barber, S. Stevens, R. M. LoPachin, (2007) Proteomic analysis of rat striatal synaptosomes during acrylamide intoxication at a low dose-rate, *Toxicological Sciences*, **100**: 156-167.
  28. R. M. LoPachin, A. I. Schwarcz, C. L. Gaughan, S. Mansukhani, S. Das, (2004) *In vivo* and *in vitro* effects of acrylamide on synaptosomal neurotransmitter uptake and release, *Neuro Toxicology*, **25**: 349-363.
  29. C. Lee, W. Yang, R. G. Parr, (1988) Development of the Colle-Salvetti correlation-energy formula into a functional of the electron density, *Physical Review*, **37B**: 785.
  30. M. J. Frisch, G. W. Trucks, H. B. Schlegel, G. E. Scuseria, M. A. Robb, J. R. Cheeseman, G. Scalmani, V. Barone, B. Mennucci, G. A. Petersson, H. Nakatsuji, M. Caricato, X. Li, H. P. Hratchian, A. F. Izmaylov, J. Bloino, G. Zheng, J. L. Sonnenberg, M. Hada, M. Ehara, K. Toyota, R. Fukuda, J. Hasegawa, M. Ishida, T. Nakajima, Y. Honda, O. Kitao, H. Nakai, T. Vreven, J. A. Montgomery, Jr., J. E. Peralta, F. Ogliaro, M. Bearpark, J. J. Heyd, E. Brothers, K. N. Kudin, V. N. Staroverov, R. Kobayashi, J. Normand, K. Raghavachari, A. Rendell, J. C. Burant, S. S. Iyengar, J. Tomasi, M. Cossi, N. Rega, J. M. Millam, M. Klene, J. E. Knox, J. B. Cross, V. Bakken, C. Adamo, J. Jaramillo, R. Gomperts, R. E. Stratmann, O. Yazyev, A. J. Austin, R. Cammi, C. Pomelli, J. W. Ochterski, R. L. Martin, K. Morokuma, V. G. Zakrzewski, G. A. Voth, P. Salvador, J. J. Dannenberg, S. Dapprich, A. D. Daniels, O. Farkas, J. B. Foresman, J. V. Ortiz, J. Cioslowski, D. J. Fox, (2009) *Gaussian 09, Revision A.02*, Wallingford, CT: Gaussian Inc.
  31. J. Tomasi, B. Mennucci, E. Cancès, (1999) The IEF version of the PCM solvation method: An overview of a new method addressed to study molecular solutes at the QM AB initio level, *Journal of Molecular Structure (Theochem)*, **464(1-3)**: 211-226.
  32. R. S. Mulliken, (1955) Electronic population analysis on LCAO-MO molecular wave functions. I, *The Journal of Chemical Physics*, **23(10)**: 1833-1840.
  33. E. E. Glendening, A. E. Reed, J. E. Carpenter, F. Weinhold, (1999) *NBO (Natural Bond Orbital)*, Vol. 5. Chichester, UK: Wiley & Sons.
  34. Z. B. Maksić, B. Kovačević, (1998) Toward organic superbases: The electronic structures and absolute proton affinity of quinodiimines and some related compounds, *Journal of Physical Chemistry A*, **102**: 7324-7328.
  35. Z. B. Maksić, B. Kovačević, D. Kovaček, (1997) Simple ab initio model for calculating the absolute proton affinity of aromatics, *Journal of Physical Chemistry A*, **101**: 7446-7453.
  36. A. Ma'an H, B. C. Nadja, S. J. George, G. E. Christie, (2000) Importance of gas-phase proton affinities in determining the electrospray ionization response for analytes and solvents, *Journal of Mass Spectrometry*, **35**: 784-789.
  37. A. H. Goeller, D. Strehlow, G. Hermann, (2005) The excited-state chemistry of phycocyanobilin: A semiempirical study, *European Journal of chemical Physics and Physical Chemistry*, **6(7)**: 1259-1268.
  38. I. Antol, M. Eckert-Maksić, M. Klessinger, (2003) Abinitio study of excited state protonation of monosubstituted benzenes, *Journal of Molecular Structure (Theochem)*, **664-665**: 309-317.
  39. A. B. Sannigrahi, P. K. Nandi, (1993) Ab initio theoretical study of the electronic structure, stability and bonding of dialkali halide cations, *Chemical Physics Letter*, **204**: 73-79.





## The proton affinities of a series of $\beta$ -substituted Acrylamide in the ground state: A DFT based computational study

Biswarup Mandal<sup>1</sup>, Umasankar Senapati<sup>2</sup>, Bhudeb Ranjan De<sup>1\*</sup>

1. Department of Chemistry and Chemical Technology, Vidyasagar University, Midnapore, W.B., India, Pin – 721102, *E-mail*: biswarupmandal75@gmail.com
2. Department of Chemistry, Belda College, Belda, Paschim Medinipur, Pin- 721424, W.B., India, *E-mail*: Senapatiumasankar@gmail.com

\* **Corresponding author**: Prof. Bhudeb Ranjan De, E-mail: biswarupmandal75@gmail.com

### Publication History

Received: 26 September 2015

Accepted: 19 October 2015

Published: 30 October 2015

### Citation

Biswarup Mandal, Umasankar Senapati, Bhudeb Ranjan De. The proton affinities of a series of  $\beta$ -substituted Acrylamide in the ground state: A DFT based computational study. *Discovery Chemistry*, 2015, 1(3), 64-71

### Publication License



This work is licensed under a Creative Commons Attribution 4.0 International License.

### General Note



Article is recommended to print in recycled paper.

## ABSTRACT

A detailed study of the proton affinities of a series of  $\beta$ -substituted acrylamides and their O-protonated counterparts has been performed by B3LYP (DFT) method using 6-311G(d,p) basis sets with complete geometry optimization both before and after protonation. The gas phase O-protonation is observed to be exothermic and the local stereochemical disposition of the proton is found to be almost the same in each case. The presence of  $\beta$ -substituent is seen to cause very little change of the proton affinities, relative to the unsubstituted acrylamides. Computed proton affinities are sought to be correlated with a number of computed system parameters such as the Mulliken net charge on the carbonyl oxygen of the unprotonated bases, Mulliken net charge on the carbonyl oxygen and Mulliken net charge on the proton of the protonated bases. The overall

Biswarup Mandal et al.

The proton affinities of a series of  $\beta$ -substituted Acrylamide in the ground state: A DFT based computational study, *Discovery Chemistry*, 2015, 1(3), 64-71,

[www.discoveryjournals.com](http://www.discoveryjournals.com)

© 2015 Discovery Publication. All Rights Reserved

basicity is explained by the distant atom contribution in addition to the contribution from the carbonyl group. The electron-releasing substituents are seen to increase the computed proton affinities (PAs) while the electron-withdrawing groups have an opposite effect as expected.

**Keywords:** B3LYP DFT; GAUSSIAN; Acrylamides; Charge distribution; Gas phase

## 1. INTRODUCTION

The acid base interactions are of great importance in chemistry. These quantitative studies in the gas phase methods (Bhome et al., 1973; Beauchamp et al., 1974; Yamadagni et al., 1973; Bhome et al., 1974; Solomon et al., 1974; Long et al., 1974; Brauman et al., 1970; Wieting et al., 1974; Staley et al., 1975) have the advantage of determining the intrinsic ground state acid base properties in the absence of complicating effects of solvation. For molecules containing carbonyl chromophores, protonation and hydrogen bonding are very much important. Recently the basicities of a series of substituted crotonaldehyde and acetophenone in their ground states have been theoretically calculated (Pandit et al., 2006; Senapati et al., 2008). The systems were aliphatic and aromatic conjugated carbonyl systems. In an effort to understand the nature and origin of variation in the relative magnitude of the proton affinities to be expected in a series of aliphatic carbonyls, namely, acrylamides, producing neurotoxicity in exposed humans and laboratory animals, we have calculated the gas phase ground state proton affinities of a number of  $\beta$ -substituted acrylamides by B3LYP(DFT) method using 6-311G(d,p) basis sets (Frisch et al., 2004; Lee et al., 1988; Becke et al., 1993). We have analysed the computed proton affinity values (PAs) to understand whether the pre-protonation charge distribution local to the chromophore or post-protonation relaxation of charge density or both are important in shaping the overall basicity of the acrylamides. We have also looked into the possible origin of the small shift in the proton affinities as one goes from the unsubstituted to the  $\beta$ -substituted acrylamides. In a particular state the possibility of correlating the proton affinity with the global hardness of the molecules is also explored. We have also calculated an important parameter softness to account for the stability of a molecule and the direction of acid-base reactions.

## 2. COMPUTATIONAL DETAILS

Calculations were performed using Gaussian 03W software and B3LYP(DFT) method with 6-311G(d,p) basis sets. In all calculations complete geometry optimizations has been carried out on the molecules both before and after protonation.

## 3. RESULT AND DISCUSSION

The molecules studied theoretically are  $\beta$ -substituted acrylamides and its protonated species. The molecules studied are listed in table 1 along with their respective abbreviated names and computed total energies and proton affinities in DFT method using 6-311G(d,p) basis set. Table 2 reports the computed Mulliken net charge on the carbonyl oxygen atoms at the equilibrium ground state of the unprotonated free base molecules as well as the computed Mulliken net charge carried out by proton and the Mulliken net charge on the carbonyl oxygen at the equilibrium ground state of the protonated bases. Atomic charge is not an observable quantum mechanical property. All methods for computing the atomic charges are necessarily arbitrary. Electron density among the atoms in a molecular system is being partitioned. Mulliken population analysis computes charges by dividing orbital overlap equally between the two atoms involved. Therefore the values are non-unique. Still, it is widely used. From table 1 it is seen that the proton affinities (PAs) of all the  $\beta$ -substituted acrylamides are in the range -0.2664 to -0.3654 hartree. Proton affinities (PAs) of all the  $\beta$ -substituted acrylamides indicate that the gas phase O-protonation is exothermic in each case. The electron-releasing substituents are seen to increase the computed PAs while electron-withdrawing groups have an opposite effect as expected. Table 1 reveals that proton affinity is highest for  $\beta$ AACR, X = -NH<sub>2</sub>. From table 4 it is clear that lower softness value of  $\beta$ AACR, X = -NH<sub>2</sub> and highest softness value of  $\beta$ NACR, X = -NO<sub>2</sub> indicates  $\beta$ AACR is a hard base and favours protonation (since H<sup>+</sup> is a hard acid). This is one of the reasons of highest PA of  $\beta$ AACR. A perusal of table 2 reveals that the computed net charge on the proton is small in each case and is in the range 0.2864 to 0.3651 showing that a rather large migration of electron density to the added proton has taken place. The proton adds to the base, giving polar covalent sigma bond with a very extensive charge transfer. The base molecule carries the rest of the positive charge. The large degree of charge transfer results from the fact that H<sup>+</sup> is a bare nucleus, with a very low energy unfilled 1S orbital. That these migrations is not local and originates from all over the molecule is clearly reflected in the computed net charges on the carbonyl oxygen atom of the protonated bases as shown in table 2. The oxygen atom still carries a net negative charge, albeit depleted, relative to the unprotonated base. It is also seen that the charge density of O-atom before protonation is higher when X is an electron-releasing group. This favours protonation. The reverse is the case with electron-attracting group. This may be one of the reasons for the slight increase and decrease of PA values relative to unsubstituted acrylamides. It can therefore, be anticipated that the proton affinities of these carbonyl bases cannot be modelled or described by local properties of the carbonyl moiety only. It must be shaped strongly by distant atom contribution in addition to the contribution from the carbonyl group.

The local characteristics at or around the carbonyl moiety cannot model the substituent effects. This is again revealed from the data reported in table 3 where some of the selected computed geometrical parameters around the carbonyl group are listed. The O-H<sup>+</sup> bond length has a variation in the range 0.9669 to 1.4448 Å for all the protonated bases. The C-O-H<sup>+</sup> bond angle is virtually within 102.8165 –116.1180° in all the cases. Similarly, the torsion angle  $\tau$  (C-C-O-H<sup>+</sup>) shows only a small variation in all the cases. The C-O length of all the protonated bases increase except for  $\beta$ MyACR where it is same after protonation. The carbonyl ring near invariant stereochemistry around the protonation site of each base tends to suggest that

the entire contribution from substituent effects to PA cannot be modelled properly unless contribution from far away centers are taken into account. It also points to the fact that "local" effects of the group must be very nearly identical in each case.

As the local parameter we have chosen the computed net charge density on the carbonyl oxygen atom of the unprotonated bases ( $q_{O^-}$ ) and the net charge density on the proton ( $q_{H^+}$ ) of the fully relaxed  $BH^+$ . It is seen that the plot of the computed gas phase proton affinities (PAs) against the computed net charge density on the carbonyl oxygen atom of the unprotonated bases ( $q_{O^-}$ ) (figure 1) is not linear. It is also seen that the plot of the computed gas phase proton affinities (PAs) versus  $q_{H^+}$  of the fully relaxed  $BH^+$  (figure 2) is not linear. We have also searched for the possibility of existence of correlation with a single global parameter of the entire molecule. As the global parameter we have chosen the hardness,  $\eta = (I - A)/2 = (\epsilon_{LUMO} \sim \epsilon_{HOMO})/2$  listed in tables 4. It is seen that no perfect correlation between the hardness and proton affinity in the series could be made. This is further revealed from figure 3 where the gas phase proton affinity versus computed hardness is plotted which shows no linearity. Thus all these reveal marginal linearity of the computed PA's with respect to local and global parameters. This indicates that both pre- and post-protonation correlations with local charge densities in the immediate neighbourhood of the protonation site are weak.

#### 4. CONCLUSION

The above computational study shows that gas phase O-protonation of  $\beta$ -substituted acrylamides and their O-protonated counterparts is spontaneous irrespective of their electron releasing or withdrawing nature. The overall proton affinity is explained by distant atom contribution in addition to the contribution from the carbonyl group. The carbonyl ring near invariant stereochemistry around the protonation site of each base tends to suggest that the entire contribution from substituent effects to PA cannot be modelled properly unless contributions from far away centres are taken into account.

#### ACKNOWLEDGMENT

Authors expressed big gratitude to the Prof. B.R. DE for his kind co-operation to complete this work and also grateful to the Department of Chemistry and Chemical technology, Vidyasagar University, Medinipur, West Bengal, India, for providing all the facilities for doing research works in this area. A lot of thanks to other researchers for their important comment in various circumstances for this work.

#### REFERENCES

- Bhome DK, Hemsworth RS, Rundle HI, Schiff, HI. *J. Chem. Phys.* 1973, 58, 3504.
- Beauchamp JL, "Interaction between Ions and Molecules", (Plenum, New York) 1974, 413, 459, 489.
- Yamadagni R, Kebarle PJ. *J. Am. Chem. Soc.* 1973, 96, 727.
- Bhome DK, Mackay GI, Schiff HI, Hemsworth RS. *J. Chem. Phys.* 1974, 61, 2175.
- Solomon JJ, Meot MN, Field FM. *J. Am. Chem. Soc.* 1974, 96, 3727.
- Long JI, Franklin JL. *J. Am. Chem. Soc.* 1974, 96, 2320.
- Brauman JI, Blair LK. *J. Am. Chem. Soc.* 1970, 92, 5986.
- Wieting RD, Staley RH, Beauchamp JL. *J. Am. Chem. Soc.* 1974, 96, 7552.
- Staley RH, Beauchamp JL. *J. Am. Chem. Soc.* 1975, 96, 3727.
- Pandit S, De D, De BR. *J. Mol. Struct. (Theochem)*. 2006, 760, 245-246.
- Senapati U, De D, De BR. *Indian J. Chem.* 2008, 47A, 548-550.
- Frisch MJ, Trucks GW, Schlegel HB, Scuseria GE, Robb MA, Cheeseman JR, Montgomery JA, Jr, Vreven T, Kudin KN, Burant JC, Millam JM, Iyengar SS, Tomasi J, Barone V, Mennucci B, Cossi M, Scalmani G, Rega N, Petersson GA, Nakatsuji H, Hada M, Ehara M, Toyota K, Fukuda R, Hasegawa J, Ishida M, Nakajima T, Honda Y, Kitao O, Nakai H, Klene M, Li X, Knox JE, Hratchia HP, Cross JB, Adamo C, Jaramillo J, Gomperts R, Stratmann RE, Yazyev O, Austin AJ, Cammi R, Pomelli C, Ochterski JW, Ayala PY, Morokuma K, Voth GA, Salvador P, Dannenberg JJ, Zakrzewski VG, Dapprich S, Daniels AD, Strain MC, Farkas O, Malick DK, Rabuck AD, Raghavachari K, Foresman JB, Ortiz JV, Cui Q, Baboul AG, Clifford S, Cioslowski J, Stefanov BB, Liu G, Liashenko A, Piskorz P, Komaromi I, Martin RL, Fox DJ, Keith T, Al-Laham MA, Peng CY, Nanayakkara A, Challacombe M, Gill PMW, Johnson B, Chen W, Wong MW, Gonzalez C, Pople JA, Gaussian, Inc, Wallingford, CT, 2004.
- Lee C, Yang W, Parr RG. *Phys. Rev.* 1988, B37, 785; Becke AD. *J. Chem. Phys.* 1993, 98, 5648.

Table 1

Computed total energy (hartree) of free base (B) and O- protonated base (BH<sup>+</sup>) and proton affinities [ PA=(EBH<sup>+</sup>-EB), hartree] at the equilibrium geometry of the ground state.

Molecule	Total Energy(hartree)		Proton Affinity(hartree)
	B	BH <sup>+</sup>	
ACR, X = -H	-247.3692	-247.7160	-0.3468
βMACR, X = -CH <sub>3</sub>	-286.6979	-287.0491	-0.3512
βMyACR, X = -OCH <sub>3</sub>	-361.7297	-361.9961	-0.2664
βAACR, X = -NH <sub>2</sub>	-302.7594	-303.1248	-0.3654
βCIACR, X = -Cl	-706.9850	-707.3301	-0.3451
βCnACR, X = -CN	-339.6279	-339.9596	-0.3317
βNACR, X = -NO <sub>2</sub>	-451.9159	-452.2472	-0.3313

Table 2

Computed net charge on O-atom (q<sub>O</sub><sup>-</sup>) of free base (B) and O-protonated base (BH<sup>+</sup>) and computed net charge on proton (q<sub>H<sup>+</sup></sub>) at the equilibrium ground state of protonated base (BH<sup>+</sup>) and free base (B)

Molecule	Charge on Carbonyl Oxygen atom(q <sub>O</sub> <sup>-</sup> )		Charge on Proton(q <sub>H<sup>+</sup></sub> )
	B	BH <sup>+</sup>	
ACR, X = -H	-0.3637	-0.2457	0.3059
βMACR, X = -CH <sub>3</sub>	-0.3757	-0.2710	0.2951
βMyACR, X = -OCH <sub>3</sub>	-0.3897	-0.2817	0.3651
βAACR, X = -NH <sub>2</sub>	-0.4432	-0.3436	0.2963
βCIACR, X = -Cl	-0.3429	-0.2316	0.2864
βCnACR, X = -CN	-0.3319	-0.2471	0.3091
βNACR, X = -NO <sub>2</sub>	-0.3449	-0.2386	0.3070

Table 3

Geometrical features of the free base and O-protonated base (length in Å and angle in degree).

Molecule	Free base	O-protonated base			
	r(C-O)	r(C-O)	r(O-H <sup>+</sup> )	<C-O-H <sup>+</sup>	<C-C-O-H <sup>+</sup>
ACR, X = -H	1.2183	1.3057	0.9679	113.2913	-5.4293
βMACR, X = -CH <sub>3</sub>	1.2219	1.3105	0.9690	114.6336	180.0044
βMyACR, X = -OCH <sub>3</sub>	1.2232	1.2232	1.4448	102.8165	-174.3517
βAACR, X = -NH <sub>2</sub>	1.2375	1.3328	0.9669	114.1474	-179.4498
βCIACR, X = -Cl	1.2155	1.3017	0.9770	112.3551	-0.0481
βCnACR, X = -CN	1.2152	1.3008	0.9703	116.1180	179.9410
βNACR, X = -NO <sub>2</sub>	1.2188	1.3071	0.9708	115.1478	-179.9838

Table 4

Computed hardness (hartree) and softness (hartree) of the free base (B) in the ground state by B3LYP(DFT) method using 6-311G(d,p) basis set.

Molecule	$\epsilon_{\text{HOMO}}$	$\epsilon_{\text{LUMO}}$	$\eta$ (Hardness)	$S = 1/2\eta$ (Softness)
ACR, X = -H	-0.2585	-0.0410	0.1087	4.5998
$\beta$ MACR, X = -CH <sub>3</sub>	-0.2509	-0.0341	0.1084	4.6125
$\beta$ MyACR, X = -OCH <sub>3</sub>	-0.2205	-0.0533	0.0836	5.9808
$\beta$ AACR, X = -NH <sub>2</sub>	-0.2118	-0.0079	0.1019	4.9067
$\beta$ CIACR, X = -Cl	-0.2587	-0.0537	0.1025	4.8780
$\beta$ CnACR, X = -CN	-0.2756	-0.0910	0.0923	5.4171
$\beta$ NACR, X = -NO <sub>2</sub>	-0.2829	-0.1244	0.0792	6.3131

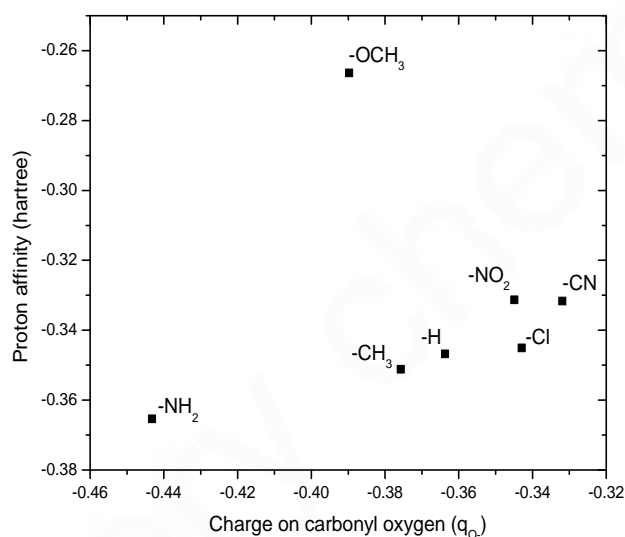


Figure 1

lot of gas phase ground state proton affinity vs. charge on the carbonyl oxygen atom of the free bases.

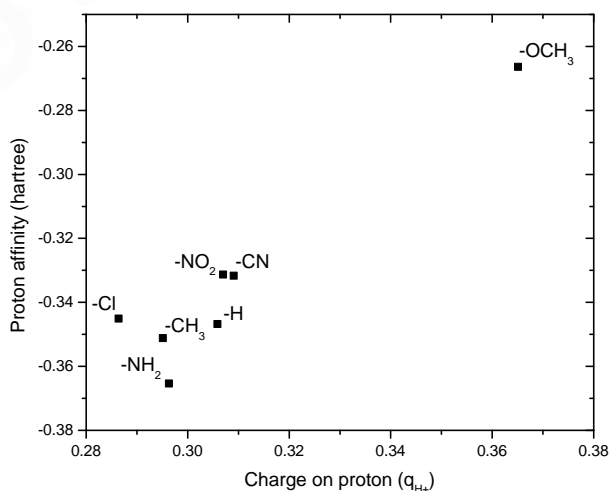


Figure 2

Plot of gas phase ground state proton affinity vs. charge on the proton of the complex BH<sup>+</sup>

Biswarup Mandal et al.

The proton affinities of a series of  $\beta$ -substituted Acrylamide in the ground state: A DFT based computational study, Discovery Chemistry, 2015, 1(3), 64-71,

[www.discoveryjournals.com](http://www.discoveryjournals.com)

© 2015 Discovery Publication. All Rights Reserved

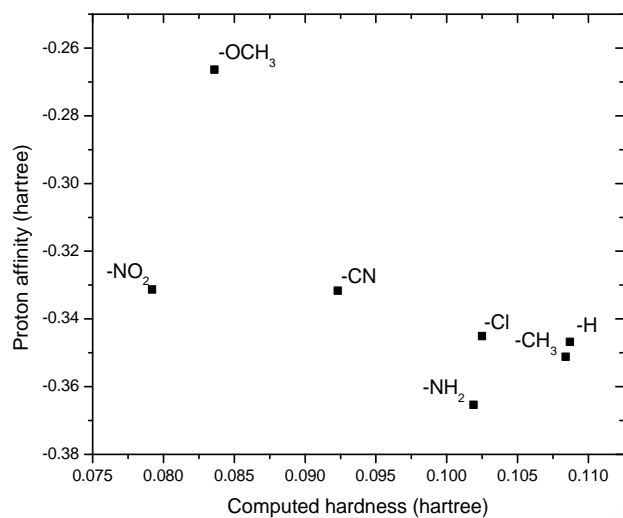
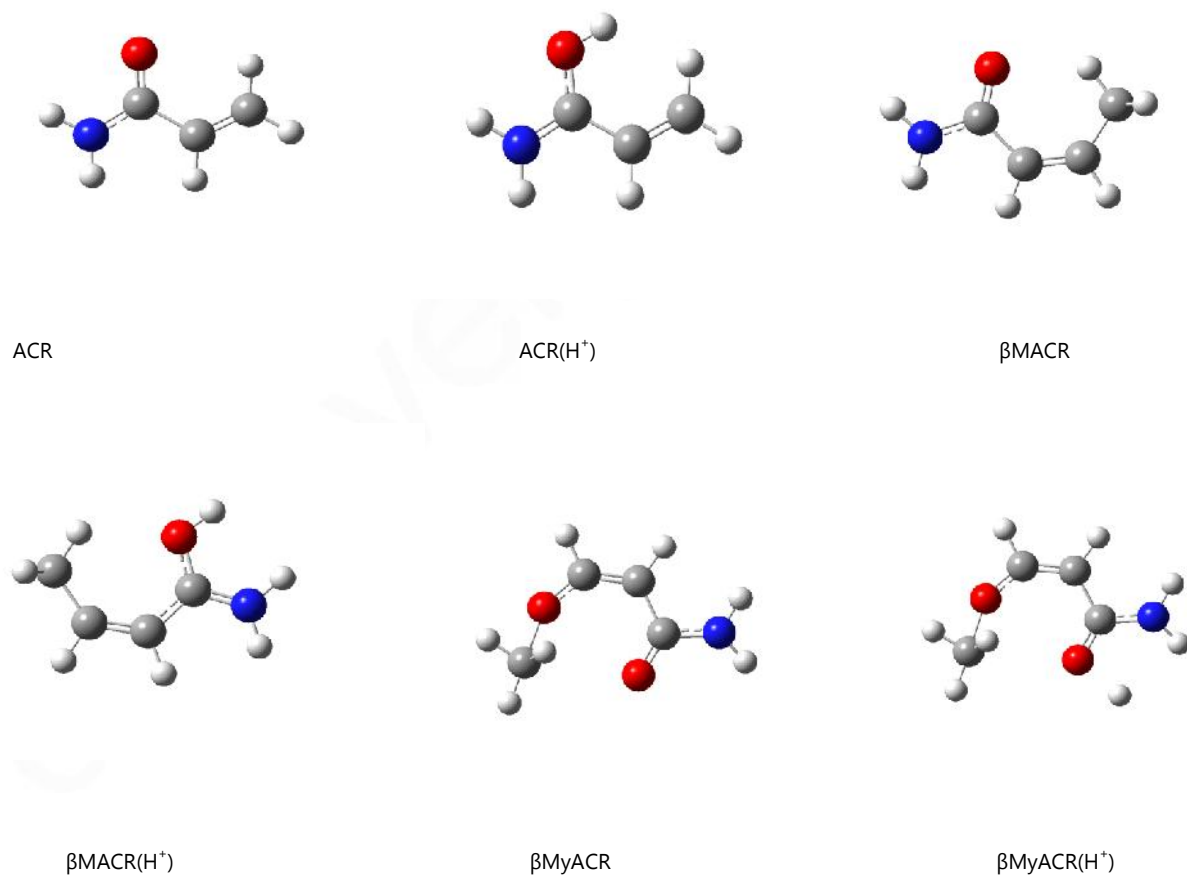
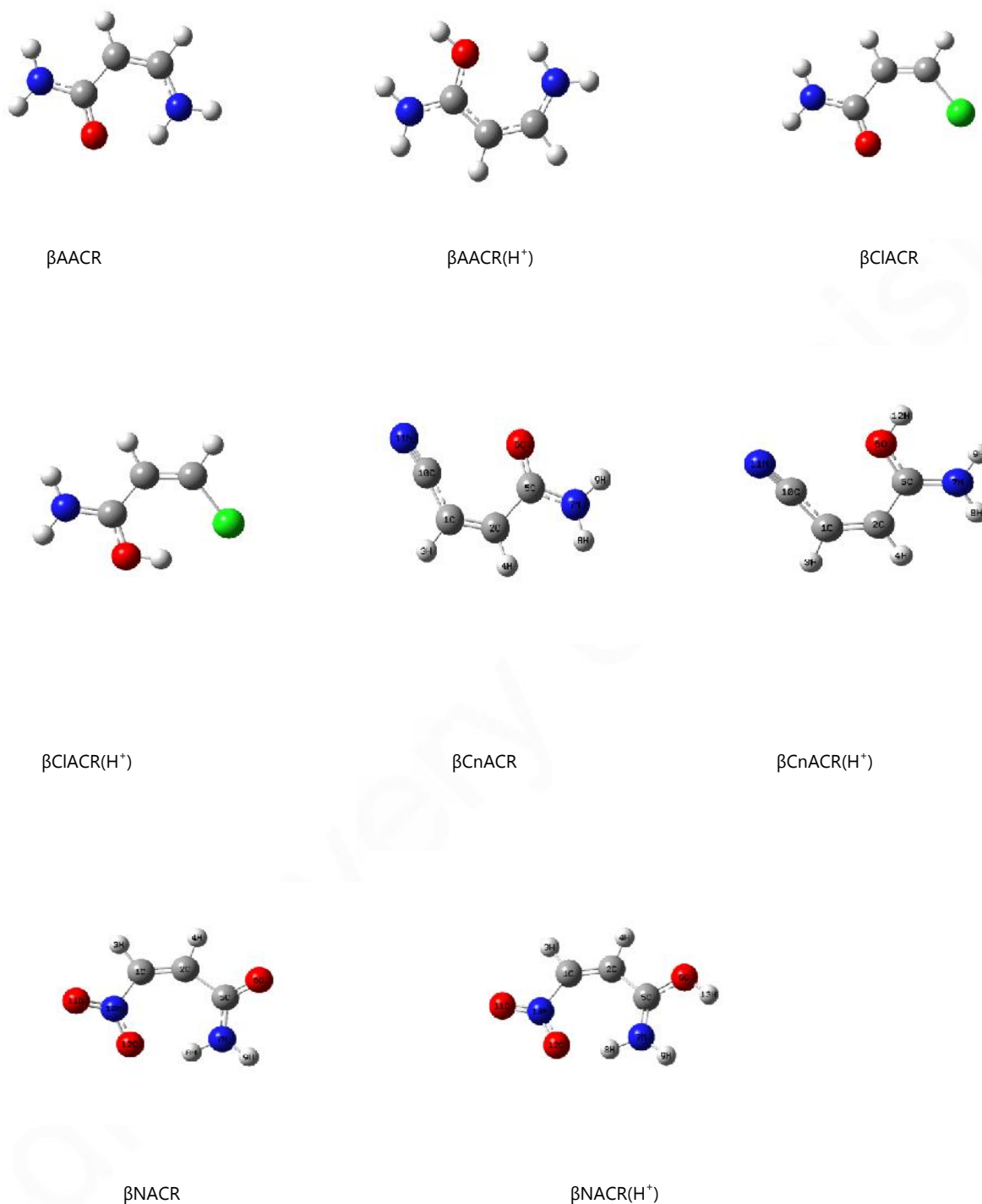


Figure 3  
Plot of gas phase ground state proton affinity vs. computed hardness.







**Figure 4**  
Optimized structure of  $\beta$ -substituted acrylamides and their O-protonated counterparts in the ground state.

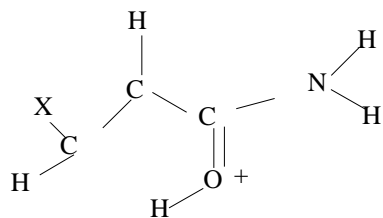
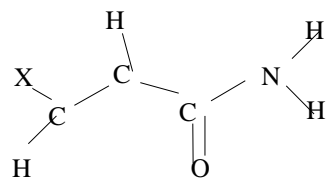
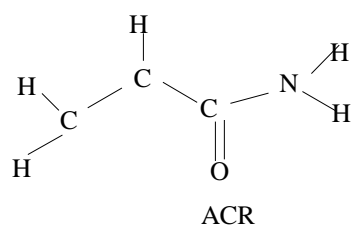


Figure 5

Structure of ACR, Beta Substituted ACR and their Protonated Counterparts

## The lithium affinities of a series of heterocyclic compounds pyrrole, furan, thiophene and pyridine in their low-lying excited triplet state: A DFT based comparative study

Umasankar Senapati<sup>1</sup>, Bikash Kumar Panda<sup>2</sup>, Suman Sengupta<sup>3</sup>, Biswarup Mandal<sup>4</sup>\*

1. Assistant Professor, Dept. of Chemistry, Santipur College, Santipur, Nadia, Pin- 741404, W.B., India; E-mail: senapatiumasankar@gmail.com
2. Assistant Professor, Dept. of Chemistry, Jangipur College, Murshidabad, Pin- 742213, W.B., India.
3. Assistant Professor, Dept. of Chemistry, Ananda Chandra College, Jalpaiguri, Pin- 735101, W.B., India.
4. Assistant Professor, Dept. of Chemistry, Sitananda College, Nandigram, Purba Medinipur Pin- 721631, W.B., India.

\*Corresponding author: Assistant Professor, Dept. of Chemistry, Sitananda College, Nandigram, Purba Medinipur Pin- 721631, W.B., India; E-mail: biswarupmandal75@gmail.com (Biswarup Mandal)

### Publication History

Received: 09 February 2015

Accepted: 16 March 2015

Published: 1 April 2015

### Citation

Umasankar Senapati, Bikash Kumar Panda, Suman Sengupta, Biswarup Mandal. The lithium affinities of a series of heterocyclic compounds pyrrole, furan, thiophene and pyridine in their low-lying excited triplet state: A DFT based comparative study. *Indian Journal of Science*, 2015, 15(44), 20-24

### ABSTRACT

Gas phase lithium affinities ( $\Delta E_s$ ) and transition energies of a series of heterocyclic compounds (pyrrole, furan, thiophene and pyridine) and their  $\text{Li}^+$  complexes have been performed using density functional theory (Becke, Lee, Yang and Parr [B3LYP]) method using 6-311G(d,p) basis set with complete geometry optimization in their low-lying excited triplet state. As in the case of ground states, the gas phase  $\text{Li}^+$  complex formation turns out to be exothermic case and the local stereochemical disposition of the  $\text{Li}^+$  is found to be almost the same in each case. It is seen that lithium affinity is highest for pyridine (-0.08 hartree) and lowest for pyrrole (-0.0178 hartree). Computed lithium affinities are also sought to be correlated with the number of computed system parameters such as the net computed charge on the hetero atoms of the free bases and  $\text{Li}^+$  complexes, charge on the  $\text{Li}^+$  of the  $\text{Li}^+$  complexes and the computed hardness of the free bases in their relevant excited states. The lithium induced shifts (LIS) are in general red shifts for the lowest excited triplet states.

**Key words:** B3LYP DFT; GAUSSIAN; Pyrrole; Furan; Thiophene; Pyridine; Charge distribution; Gas phase.

Umasankar Senapati et al.

The lithium affinities of a series of heterocyclic compounds pyrrole, furan, thiophene and pyridine in their low-lying excited triplet state: A DFT based comparative study, *Indian Journal of Science*, 2015, 15(44), 20-24, <http://www.discovery.org.in/ijs.htm>

[www.discovery.org.in](http://www.discovery.org.in)

© 2015 Discovery Publication. All Rights Reserved

## 1. INTRODUCTION

Ion-molecule complexes are frequently involved in molecular recognition processes (Ma et al., 1997) and these interactions are also expected to be involved in many important biological processes (Karlín et al., 1994; Livnah et al., 1996; Cervenansky et al., 1995; Novotny et al., 1989), electron transfer processes (Lippard et al., 1994; Kaim et al., 1994) and more complicated biological systems. Some  $\text{Li}^+$  complexes were already studied theoretically and experimentally (Burk et al., 2000; Del Bene et al., 1979; Del Bene et al., 1996; Gal et al., 2002; Amunugama et al., 2003). The  $\text{Li}^+$  ion affinity introduces the idea that there must be some relation between the molecular electron density distribution and the affinity. This also implies that this property may vary from state to state of the same molecule due to some electronic transitions which are accompanied by extensive reorganization of molecular electronic charge distribution. The purpose of the present work is to examine the relative lithium ion affinities ( $\Delta E$ ) of a series of heterocyclic compounds (pyrrole, furan, thiophene and pyridine) in their low-lying excited triplet state using Gaussian 03W software (Frisch et al., 2004; Lee et al., 1988; Becke et al., 1993) and B3LYP (DFT) method with 6-311G (d, p) basis sets. Recently the  $\text{Li}^+$  affinities of a series of substituted acetophenone in their ground (Senapati et al., 2007) and excited triplet state Senapati et al., 2009) were reported in the literature. Proton affinities of a series of heterocyclic compounds (pyrrole, furan, thiophene and pyridine) in the ground and excited triplet state (Mandal et al., 2014) has been studied already. We have analysed the computed  $\text{Li}^+$  affinity values, transition energies to understand whether the pre-complex formation charge distribution local to the heteroatom or post-complex relaxation of charge density or both are important in shaping the overall reactivities in a particular state. We have also analysed the kind and extent of spectral shift caused by complex formation in the relevant state. In a particular state the possibility of correlating the  $\text{Li}^+$  affinity with the global hardness of the molecules is also explored.

## 2. COMPUTATIONAL DETAILS

Calculations were performed using Gaussian 03W software and B3LYP (DFT) method with 6-311G (d, p) basis sets. In all calculations complete geometry optimization has been carried out on the molecules both before and after  $\text{Li}^+$  complex formation.  $\text{Li}^+$  affinities ( $\Delta E$ s), were computed as  $(E_{\text{BLi}^+} - E_{\text{B}} - E_{\text{Li}^+})$ .

## 3. RESULT AND DISCUSSION

The molecules studied are listed in Table 1 along with their respective abbreviated names and computed total energy (hartree) of the free base (B) and their  $\text{Li}^+$  complexes and also the computed  $\text{Li}^+$  affinities ( $\Delta E$ s).

Table 1 reports the computed total energies (hartree) of the free base (B) = { $B_1, B_2, B_3, B_4$ } and  $\text{Li}^+$  complexes ( $\text{BLi}^+$ ) = ( $B_1 \text{Li}^+, B_2 \text{Li}^+, B_3 \text{Li}^+, B_4 \text{Li}^+$ ). It also reports the computed  $\text{Li}^+$  affinities ( $\Delta E$ s) of the lowest excited triplet state.

In this method B3LYP(DFT) with 6-311G (d, p) basis set, it is seen that the lithium affinity values is highest for Pyridine -0.08(hartree) where it is -0.0178, -0.0611 and -0.0425 hartree for pyrrole, furan and thiophene respectively. The  $\Delta E$  values indicate that the gas phase  $\text{Li}^+$  complex formation turns out to be exothermic. Table 2 summarizes the computed net charge on the hetero atom(X) (where X= N, O, S, N for pyrrole, furan, thiophene and pyridine respectively) both before and after  $\text{Li}^+$  complex formation of the base molecules in their optimized lowest excited triplet state. This also includes the computed net charge carried out by  $\text{Li}^+$  of the complexes in the same optimized state. The computed net charge on  $\text{Li}^+$  vary within the range 0.7127 to 0.8421. The magnitude of charges of the complexes indicate that the interaction between  $\text{Li}^+$ -free base is predominantly an ion-dipole attraction and ion-induced dipole interaction as well rather than a covalent interaction. This also reveals that both pre- and post-complex correlation with local charge densities in the immediate neighbourhood of the complex formation site are weak. Although it seems that there is a good but non perfect linear correlation between the charge on hetero atom in the free base (B) and it must be shaped strongly by distant atom contribution in addition to the contribution from hetero atom. It is also seen that the computed net charge on the  $\text{Li}^+$  is small in each case showing that a rather large migration of electron density to the added  $\text{Li}^+$  has taken place. The hetero atom still carries a net negative charge(excepting thiophene where the charge on S atom is positive). Compared to the ground state values in all cases charge on hetero atom is increased(with the exception of thiophene where it is decreased) relative to the  $\text{Li}^+$  complexes. We have searched for the possibility of existence of correlation with a single global parameter of the entire molecule in the relevant state. As the global parameter we have chosen the hardness,  $\eta = (I \sim A)/2 = (\epsilon_{\text{LUMO}} \sim \epsilon_{\text{HOMO}})/2$  listed in Table 5 along with their respective ground state values. From Table 5 it is seen that in the triplet state lower  $\epsilon_{\text{LUMO}}$  and lower  $\eta$  values, compared to the respective ground state, favour  $\text{Li}^+$  complex formation, in general. This indicates that both pre-and post- $\text{Li}^+$  complex formation correlations with local charge densities in the immediate neighbourhood of the  $\text{Li}^+$  complex formation site are weak. Table 3 reveals some interesting features around the hetero atom in the lowest excited triplet state. The X- $\text{Li}^+$  bond length has a variation in the range 0.9705 to 3.2736 Å for all the  $\text{Li}^+$  complexes. The C-X- $\text{Li}^+$  bond angle is in the range 105.3029 to 134.5156 degree in all the cases. Similarly the torsion angle(C-C-X- $\text{Li}^+$ ) shows a small variation within the range -92.1195 to 179.9985 degree. All the heterocyclic compounds studied are planar(from literature). After  $\text{Li}^+$  complex formation here we have seen the torsion angle for furan, thiophene and pyridine are 179.9890, 179.7048 and 179.9985<sup>0</sup> respectively i.e., planarity retained but for pyrrole this value is effected by global density and planarity is destroyed. The C-X bond length has been decreased slightly after  $\text{Li}^+$  complex formation for  $B_2$  and  $B_4$  where it is increased for  $B_1$  and  $B_3$ . Table 4 shows the computed transition energies [ $S_0 \rightarrow T_1$  (lowest excited triplet state)] and shifts caused by  $\text{Li}^+$  complex formation. It is clear from the data that in case of furan and pyridine the lithium induced shifts (LIS) are red shifts where in case of pyrrole and thiophene lithium induced shifts are blue shifts. These data refer to the gas phase  $\text{Li}^+$  complex formation of the isolated base molecules without any additional effects caused by solvation.

Umasankar Senapati et al.

The lithium affinities of a series of heterocyclic compounds pyrrole, furan, thiophene and pyridine in their low-lying excited triplet state: A DFT based comparative study,

Indian Journal of Science, 2015, 15(44), 20-24,

<http://www.discovery.org.in/ijs.htm>

[www.discovery.org.in](http://www.discovery.org.in)

© 2015 Discovery Publication. All Rights Reserved

## 4. CONCLUSION

From the present theoretical study it can be well concluded that the gas phase lithium affinities of the pyrrole, furan, thiophene and pyridine are spontaneous. The overall reactivity is fully explained by distant atom contribution in addition to the contribution from the hetero atoms of the free bases.

## ACKNOWLEDGEMENTS

The authors gratefully acknowledge the financial support of CSIR, UGC and DST, New Delhi. We are thankful to Prof. Bhudeb Ranjan De, Vidyasagar University, Midnapore, West Bengal, for his valuable suggestions through out the work.

## REFERENCES

1. Ma JC, Dongherty DA. *Chem. Rev.* 1997, 97, 1303.
2. Karlin S, Zuker M, Brocchieri L. *J. Mol. Biol.* 1994, 239, 227.
3. Livnah O, Stura EA, Johnson DL, Middleton SA, Mulchany LS, Wrighton NC, Dower WJ, Jolliffe LK, Wilson I A. *Science* 1996, 255, 306.
4. Cervenansky C, Engstorm A, Karlsoon E. *Eur. J. Biochem.* 1995, 229, 270.
5. Novotny J, Bruccoleri RE, Saul FA. *Biochemistry* 1989, 28, 4735.
6. Lippard SJ, Berg JM. *Principles of Bioinorganic chemistry*, University Science Books, Mill Valley, CA, 1994.
7. Kaim W, Schwederski B. *Bioinorganic Chemistry: Inorganic Elements in the chemistry of life*, Wiley, Chichester, 1994.
8. Burk P, Koppel IA, Koppel I, Kurg R, Gal J-F, Maria P-C, Herreros M, Notario R, Abboud J-L M, Anvia F, Taft RW. *J. Phys. Chem. A* 2000, 104, 2824.
9. Del Bene JE. *Chem. Phys.* 1979, 40, 329.
10. Del Bene JE. *J. Phys. Chem.* 1996, 100, 6284.
11. Gal JF, Maria PC, Decouzon M, Mo O, Yancz M. *Int. J. Mass spectrom.* 2002, 219, 445.
12. Amunugama R, Rodgers MT. *Int. J. Mass spectrom.* 2003, 227, 339.
13. Frisch MJ, Trucks GW, Schlegel HB, Scuseria GE, Robb MA, Cheeseman JR, Montgomery JA. Jr, Vreven T, Kudin KN, Burant JC, Millam JM, Iyengar SS, Tomasi J, Barone V, Mennucci B, Cossi M, Scalmani G, Rega N, Petersson GA, Nakatsuji H, Hada M, Ehara M, Toyota K, Fukuda R, Hasegawa J, Ishida M, Nakajima T, Honda Y, Kitao O, Nakai H, Klene M, Li X, Knox JE, Hratchia HP, Cross JB, Adamo C, Jaramillo J, Gomperts R, Stratmann RE, Yazyev O, Austin AJ, Cammi R, Pomelli C, Ochterski JW, Ayala PY, Morokuma K, Voth GA, Salvador P, Dannenberg JJ, Zakrzewski VG, Dapprich S, Daniels AD, Strain MC, Farkas O, Malick DK, Rabuck AD, Raghavachari K, Foresman JB, Ortiz JV, Cui Q, Baboul AG, Clifford S, Cioslowski J, Stefanov BB, Liu G, Liashenko A, Piskorz P, Komaromi I, Martin RL, Fox DJ, Keith T, Al-Laham MA, Peng CY, Nanayakkara A, Challacombe M, Gill PMW, Johnson B, Chen W, Wong MW, Gonzalez C, Pople JA, Gaussian, Inc, Wallingford, CT, 2004.
14. Lee C, Yang W, Parr RG. *Phys. Rev.* 1988, B37, 785; Becke AD. *J. Chem. Phys.* 1993, 98, 5648.
15. Senapati U, De D, De BR. *J. Mol. Struct. (Theochem)* 2007, 808, 157-159.
16. Senapati U, De D, De BR. *J. Mol. Struct. (Theochem)* 2009, 894, 71-74.
17. Mandal B, Panda BK, Sengupta S. The comparative study of basicities, Li<sup>+</sup> and Na<sup>+</sup> affinities of a series of heterocyclic molecules (pyrrole, furan, thiophene and pyridine) in the ground state. A DFT study, *Indian Journal of Science*, 2014, 8, 16-20.
18. Mandal B, Senapati U, Panda BK, Sengupta S. The proton affinities of a series of heterocyclic compounds (pyrrole, furan, thiophene and pyridine) in their low-lying excited triplet state. A DFT based comparative study, *Indian Journal of Science*, 2014, 11, 49-53.

**Table 1**

Computed total energies (hartree) of free base (B) and Li<sup>+</sup> complex (BLi<sup>+</sup>) and Lithium ion affinities [ $\Delta E = (E_{BLi^+} - E_B - E_{Li^+})$ , hartree] at the equilibrium geometry of the lowest excited triplet state.  $E_{Li^+} = -7.2336$  hartree.

Molecules	Total Energy of B	Total Energy of BLi <sup>+</sup>	$\Delta E = (E_{BLi^+} - E_B - E_{Li^+})$ , hartree
[B <sub>1</sub> ]	- 210.0843	- 217.3871	-0.0178
[B <sub>2</sub> ]	- 229.9546	- 237.3007	-0.0611
[B <sub>3</sub> ]	- 552.9511	- 560.2786	-0.0425
[B <sub>4</sub> ]	- 248.2048	- 255.5698	-0.0800

**Table 2**

Computed net charge on hetero atom of free base (B) and Li<sup>+</sup> complex (BLi<sup>+</sup>) and computed net charge on lithium at the equilibrium geometry of the lowest excited triplet state of complex (BLi<sup>+</sup>).

Molecules	q <sub>X</sub>		q <sub>Li<sup>+</sup></sub>
	B	BLi <sup>+</sup>	
B <sub>1</sub> (X = N)	- 0.42438	- 0.82415	0.83891
B <sub>2</sub> (X = O)	- 0.30204	- 0.48921	0.84212
B <sub>3</sub> (X = S)	0.17334	0.27187	0.71272
B <sub>4</sub> (X = N)	- 0.23582	- 0.54104	0.77516

**Table 3**

Geometrical features of the free base (B) and the complex (BLi<sup>+</sup>) (length in Å and angle in degree) at the equilibrium geometry of the lowest excited triplet state.

Molecules	r (X-Li <sup>+</sup> )	<C-X-Li <sup>+</sup>	<C-C-X-Li <sup>+</sup>
B <sub>1</sub> (X = N)	1.9287	105.3029	-92.1195
B <sub>2</sub> (X = O)	1.8164	127.9122	179.9890
B <sub>3</sub> (X = S)	2.2863	134.5156	179.7048
B <sub>4</sub> (X = N)	1.9007	121.0744	179.9985

**Table 4**

Computed adiabatic transition energies (<sup>1</sup>S<sub>0</sub> → T<sub>1</sub>) (hartree) and lithium induced shifts (LIS, hartree) in the lowest excited triplet state

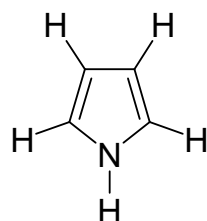
Molecules ( <sup>1</sup> S <sub>0</sub> → T <sub>1</sub> )	Transition energy		LIS
	B	BLi <sup>+</sup>	
B <sub>1</sub> (X = N)	0.1417	0.1936	0.0519
B <sub>2</sub> (X = O)	0.1288	0.1178	- 0.0110
B <sub>3</sub> (X = S)	0.1185	0.1351	0.0166
B <sub>4</sub> (X = N)	0.1420	0.1403	- 0.0017

**Table 5**

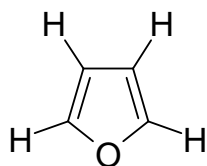
Computed hardness (hartree) of the free base (B) in the lowest excited triplet state

Molecules	$\epsilon_{\text{HOMO}}$	$\epsilon_{\text{LUMO}}$	$\eta$
B <sub>1</sub> (X = N)	- 0.0722 (- 0.2124)	- 0.1092 (0.0365)	0.0185 (0.1244)
B <sub>2</sub> (X = O)	- 0.1074 (- 0.2347)	- 0.1249 (0.0067)	0.0087 (0.1207)
B <sub>3</sub> (X = S)	- 0.1228 (- 0.2425)	- 0.1379 (- 0.0182)	0.0075 (0.1121)
B <sub>4</sub> (X = N)	- 0.1137 (- 0.2597)	- 0.1648 (- 0.0333)	0.0255 (0.1132)

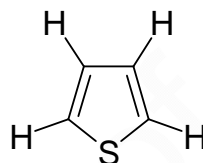
The values in the parenthesis are for the respective ground state.



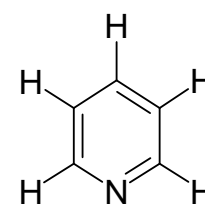
Pyrrole (B1)



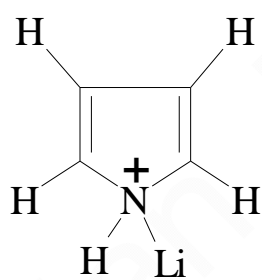
Furan (B2)



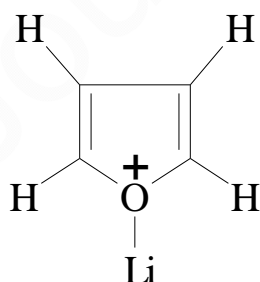
Thiophene (B3)



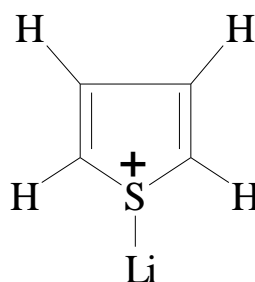
Pyridine (B4)



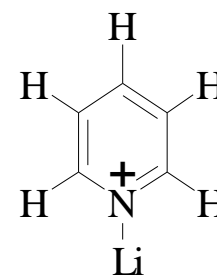
B<sub>1</sub>Li<sup>+</sup>



B<sub>2</sub>Li<sup>+</sup>



B<sub>3</sub>Li<sup>+</sup>



B<sub>4</sub>Li<sup>+</sup>

**Figure**

Structure of heterocyclic compounds and their Lithium complexes; B<sub>1</sub>= Pyrrole, B<sub>2</sub>= Furan, B<sub>3</sub>= Thiophene, B<sub>4</sub>= Pyridine.





## The proton affinities of a series of heterocyclic compounds pyrrole, furan, thiophene and pyridine in their low-lying excited triplet state: A DFT based comparative study

Biswarup Mandal<sup>1</sup>, Umasankar Senapati<sup>2</sup>, Bikash Kumar Panda<sup>3</sup>, Suman Sengupta<sup>4</sup>

1. Assistant Professor, Dept. of Chemistry, Sitananda College, PIN-721631, Nandigram, Purba medinipur, W.B., India
2. Assistant Professor, Department of Chemistry, Santipur College, Santipur, Nadia, 741404, W. B, India
3. Assistant Professor, Dept. of Chemistry, Jangipur College, PIN-742213, Murshidabad, W.B., India
4. Assistant Professor, Dept. of Chemistry, Ananda Chandra College, Jalpaiguri, PIN-735101, W.B., India

\*Corresponding author: E-mail: biswarupmandal75@gmail.com (Biswarup Mandal)

**Publication History**

Received: 18 July 2014

Accepted: 24 August 2014

Published: 10 December 2014

**Citation**Biswarup Mandal, Umasankar Senapati, Bikash Kumar Panda, Suman Sengupta. The proton affinities of a series of heterocyclic compounds pyrrole, furan, thiophene and pyridine in their low-lying excited triplet state: A DFT based comparative study. *Indian Journal of Science*, 2014, 11(28), 49-53**ABSTRACT**

Gas phase proton affinities(PAs) and transition energies of a series of heterocyclic compounds (pyrrole, furan, thiophene and pyridine) and their protonated counterparts have been performed using density functional theory (Becke, Lee, yang and parr [B3LYP]) method using 6-311G(d,p) basis set with complete geometry optimization in their low-lying excited triplet state. As in the case of ground states, the gas phase protonation turns out to be exothermic case and the local stereochemical disposition of the proton is found to be almost the same in each case. It is seen that proton affinities are highest for pyridine (-0.3741 hartree) and lowest for furan (-0.2924 hartree). Computed proton affinities are also sought to be correlated with the number of computed system parameters such as the net computed charge on the hetero atoms of the free bases and protonated species, charge on the proton of the protonated species and the computed hardness of the unprotonated species in their relevant excited states. The proton induced shifts are in general red shifts for the lowest excited triplet states.

**Key words:** B3LYP DFT; GAUSSIAN; Pyrrole; Furan; Thiophene; Pyridine; Charge distribution; Gas phase.

## 1. INTRODUCTION

The electron donor and acceptor definition of acidity and basicity introduces the idea that there must be some relation between the molecular electron density distribution and the acid-base properties. This also implies that this property may vary from state to state of the same molecule due to some electronic transitions which are accompanied by extensive reorganization of molecular electronic charge distribution. Absorption and fluorescence spectral data in conjunction with Forster cycle (Forster et al., 1950; Ottolenghi et al., 1973; Saeva et al., 1975; Ireland et al., 1976) are utilized for the experimental determination of acid-base properties of molecules in excited states in presence of solvents. Gas phase methods (Beauchamp et al., 1974; Brauman et al., 1970; Frieiser et al., 1977) which ignore the complicating effects of solvation, have been successfully applied to determine the gas phase acid-base properties of molecules in excited states. Systematic experimental data on the proton affinities of a series of heterocyclic compounds (pyrrole, furan, thiophene and pyridine, (Figure 1) in the excited states are scarcely available. We are therefore compelled to turn to theory to obtain some quantitative idea about the relative proton affinities of a series of heterocyclic compounds in their low-lying excited triplet state using Gaussian O3W software (Frisch et al., 2004; Lee et al., 1988; Becke et al. 1993) and B3LYP(DFT) method with 6-311G(d,p) basis sets. Recently the basicities of a series of substituted crotonaldehyde and acetophenone in their ground states and lowest excited triplet state have been theoretically calculated (Pandit et al., 2006; Pandit et al., 2006; Senapati et al., 2008; Senapati et al., 2007). Ground state proton affinity of a series of hetero cyclic molecules (Pyrrole, Furan, Thiophene and Pyridine) has been studied already (Mandal et al. 2014). We have analysed the PA values, transition energies to understand whether the pre-protonation charge distribution local to the heteroatom or post-complex relaxation of charge density or both are important in shaping the overall reactivities of the free bases. We have also analysed the kind and extent of spectral shift caused by protonation. In a particular state the possibility of correlating the PA values with the global hardness of the molecules is also explored.

## 2. COMPUTATIONAL DETAILS

Calculations were performed using Gaussian O3W software and B3LYP (DFT) method with 6-311G (d, p) basis sets. In all calculations complete geometry optimization has been carried out on the molecules both before and after protonation. Proton affinities (PA), were computed as ( $E_{BH^+} - E_B$ ).

## 3. RESULT AND DISCUSSION

The molecules studied are listed in Table 1 along with their respective abbreviated names and computed total energy (hartree) of the free base (B) and their protonated complexes and also the computed PA ( $\Delta E$ ).

Table 1 reports the computed total energies (hartree) of the free base (B) = {B<sub>1</sub>, B<sub>2</sub>, B<sub>3</sub>, B<sub>4</sub>} and protonated base (BH<sup>+</sup>) = (B<sub>1</sub> H<sup>+</sup>, B<sub>2</sub> H<sup>+</sup>, B<sub>3</sub> H<sup>+</sup>, B<sub>4</sub> H<sup>+</sup>). It also reports the computed proton affinities (PAs) of the lowest excited triplet state.

In this method B3 LYP (DFT) with 6-311G (d, p) basis set, it is seen that the PA values is highest for Pyridine - 0.3741(hartree) where it is -0.3504, -0.2924 and -0.3015 for pyrrole, furan and thiophene respectively. The  $\Delta E$  values indicate that the gas phase H<sup>+</sup> complex formation turns out to be exothermic. Table 2 summarizes the computed net charge on the hetero atom(X) (where X= N, O, S, N for pyrrole, furan, thiophene and pyridine respectively) both before and after protonation of the base molecules in their optimized lowest excited triplet state. This also includes the computed net charge carried out by proton of the protonated bases in the same optimized state. The computed net charge on proton varies within the range 0.02174 to 0.392106. The magnitude of charges of the complexes indicates that the interaction between proton-free bases is predominantly an ion-dipole attraction and ion-induced dipole interaction as well rather than a covalent interaction. This also reveals that both pre and post complex correlation with local charge densities in the immediate neighbourhood of the complex formation site are weak. Although it seems that there is a good but not perfect linear correlation between the charges on hetero atom in the free base (B) and it must be shaped strongly by distant atom contribution in addition to the contribution from hetero atom. It is also seen that the computed net charge on the proton is small in each case showing that a rather large migration of electron density to the added proton has taken place. The hetero atom still carries a net negative charge (excepting thiophene where the charge on S atom is positive). Compared to the ground state values in case of B<sub>2</sub> and B<sub>4</sub> though the charge on hetero atom is little bit increased relative to the unprotonated bases while in case of B<sub>1</sub> it decreases slightly. We have searched for the possibility of existence of correlation with a single global parameter of the entire molecule in the relevant state. As the global parameter we have chosen the hardness,  $\eta = (I \sim A)/2 = (\epsilon_{LUMO} \sim \epsilon_{HOMO})/2$  listed in Table 5 along with the respective ground state values. From Table 5 it is seen that in the triplet state lower  $\epsilon_{LUMO}$  and lower  $\eta$  values, compared to the respective ground state, favour protonation, in general. This indicates that both pre-and post-protonation correlations with local charge densities in the immediate

neighbourhood of the protonation site are weak. Table 3 reveals some interesting features around the hetero atom in the lowest excited triplet state. The X–H<sup>+</sup> bond length has a variation in the range 0.97 to 3.27 Å for all the protonated bases. The C–X–H<sup>+</sup> bond angle is in the range 120.5 to 178.7 degree in all the cases. Similarly the torsion angle(C–C–X–H<sup>+</sup>) shows a small variation within the range -53.67 to 180.0 degree. All the heterocyclic compounds studied are planer (from literature). After protonation here we have seen the torsion angle for pyrrole, furan and pyridine is 179.94, 179.9, 180.0<sup>o</sup> respectively i.e., planarity retained but for thiophene this value is effected by global density and planarity is destroyed. The C–X bond length has been decreased slightly after protonation for B<sub>2</sub> and B<sub>4</sub> where it is increased for B<sub>1</sub> and B<sub>3</sub>. Table 4 shows the computed transition energies [<sup>1</sup>S<sub>0</sub> → T<sub>1</sub> (lowest excited triplet state)] and shifts caused by protonation. It is clear from the data that in all cases the proton induced shifts (PIS) are red shifts. These data refer to the gas phase protonation of the isolated base molecules without any additional effects caused by solvation.

#### 4. CONCLUSION

From the present theoretical study it can be well concluded that the gas phase proton affinities of the pyrrole, furan, thiophene and pyridine are spontaneous. The overall reactivity is fully explained by distant atom contribution in addition to the contribution from the hetero atoms of the free bases.

#### ACKNOWLEDGEMENTS

The authors gratefully acknowledge the financial support of CSIR, UGC and DST, New Delhi. We are thankful to Prof. Bhudeb Ranjan De, Vidyasagar University, Midnapore, West Bengal, for his valuable scientific advice throughout the work.

#### REFERENCE

- Forster T. Die pH-Abhaengigkeit der Fluoreszenz von Naphthalinderivaten, *Z. Elektrochem.*, 1950, 54, 42-53.
- Ottolenghi M. Charge-transfer complexes in the excited state. Laser photolysis studies, *Acc. Chem. Res.*, 1973, 6, 153-160.
- Saeva F. D., Olin G. R. Utilization of excited state pK's to initiate a ground state chemical reaction, *J. Am. Chem. Soc.*, 1975, 97, 5631-5632.
- Ireland J. F., Wyatt P. A. H. Acid-Base Properties of Electronically Excited States of Organic Molecules, *Adv. Phys. Org. Chem.*, 1976, 12, 131-221.
- Beauchamp J. L. *Interaction between Ions and Molecules*, (Plenum, New York) 1974, 413, 459, 489.
- Brauman J. I., Blair L. K. Gas-phase acidities of alcohols, *J. Am. Chem. Soc.*, 1970, 92, 5986-5992.
- Frieiser B. S., Beauchamp J. L. Acid-base properties of molecules in excited electronic states utilizing ion cyclotron resonance spectroscopy, *J. Am. Chem. Soc.*, 1977, 99, 3214-3225.
- Frisch M. J., Trucks G. W., Schlegel H. B., Scuseria G. E., Robb M. A., Cheeseman J. R., Jr. Montgomery J. A., Vreven T., Kudin K. N., Burant J. C., Millam J. M., Iyengar S.S., Tomasi J., Barone V., Mennucci B., Cossi M., Scalmani G., Rega N., Petersson G. A., Nakatsuji H., Hada M., Ehara M., Toyota K., Fukuda R., Hasegawa J., Ishida M., Nakajima T., Honda Y., Kitao, O., Nakai, H., Klene, M., Li, X., Knox, J. E., Hratchian H. P., Cross, J. B., Adamo, C., Jaramillo J., Gomperts R., Stratmann R. E., Yazyev O., Austin A. J., Cammi R., Pomelli C., Ochterski J. W., Ayala P. Y., Morokuma K., Voth, G. A., Salvador P., Dannenberg J. J., Zakrzewski V. G., Dapprich S., Daniels A. D., Strain M. C., Farkas O., Malick D. K., Rabuck A. D., Raghavachari K., Foresman J. B., Ortiz, J. V., Cui Q., Baboul A. G., Clifford S., Cioslowski J., Stefanov B. B., Liu G., Liashenko A., Piskorz P., Komaromi I., Martin R. L., Fox D. J., Keith T., Al-Laham M. A., Peng C. Y., Nanayakkara A., Challacombe M., Gill P. M. W., Johnson B., Chen W., Wong M. W., Gonzalez C., Pople J. A., *Gaussian, Inc., Wallingford, CT*, 2004; Lee C., Yang W., Parr R. G. Development of the Colle-Salvetti correlation-energy formula into a functional of the electron density, *Phys. Rev.* 1988, B37, 785; Becke A. D. Density-functional thermochemistry. III. The role of exact exchange, *J. Chem. Phys.* 1993, 98, 5648-5652.
- Pandit S, De. D, De B R. The basicities of a series of substituted crotonaldehyde, *J. Mol. Struct. (Theochem)*, 2006, 760, 245-246.
- Pandit S., De D., De B. R. The basicities of a series of substituted crotonaldehyde in their low-lying excited triplet state, *J. Mol. Struct. (Theochem)* 2006, 778, 1-3.
- Senapati U., De D., and De B. R. The basicities of a series of substituted acetophenones in the ground state: A DFT study, *Indian J. Chem.*, 2008, 47A, 548-550.
- Senapati, U.; De, D.; De, B. R. The proton affinity of a series of substituted acetophenones in their low-lying excited triplet state: A DFT study, *J. Mol. Struct. (Theochem)* 2007, 808, 153-155.
- Mandal B., Panda B. K., Sengupta S. The comparative study of basicities, Li<sup>+</sup> and Na<sup>+</sup> affinities of a series of heterocyclic molecules (Pyrrole, Furan, Thiophene and Pyridine) in the ground state. A DFT Study, *Indian Journal of Science*, 2014, 8, 16-20

**Table 1**

Computed total energies (hartree) of free bases (B) = [B<sub>1</sub>, B<sub>2</sub>, B<sub>3</sub>, B<sub>4</sub>] and their Protonated complexes (BH<sup>+</sup>) and Proton affinities [PA = (E<sub>BH<sup>+</sup></sub> – E<sub>B</sub>) hartree] at the equilibrium geometry of the lowest excited triplet state

Molecules	Total Energy of B	Total Energy of BH <sup>+</sup>	PA = (E <sub>BH<sup>+</sup></sub> – E <sub>B</sub> )
[B <sub>1</sub> ]	- 210.0843	- 210.4347	- 0.3504
[B <sub>2</sub> ]	- 229.9546	- 230.2470	- 0.2924
[B <sub>3</sub> ]	- 552.9511	- 553.2526	- 0.3015
[B <sub>4</sub> ]	- 248.2048	- 248.5789	- 0.3741

**Table 2**

Computed net charge on 'X' atom (q<sub>X<sup>-</sup></sub>) of free bases (B)=[B<sub>1</sub>, B<sub>2</sub>, B<sub>3</sub>, B<sub>4</sub>], and their Protonated complexes (BH<sup>+</sup> = B<sub>1</sub>H<sup>+</sup>, B<sub>2</sub>H<sup>+</sup>, B<sub>3</sub>H<sup>+</sup>, B<sub>4</sub>H<sup>+</sup>) in the equilibrium lowest excited triplet state of free bases and (BH<sup>+</sup>) complexes

Molecules	q <sub>X<sup>-</sup></sub>		q <sub>H<sup>+</sup></sub>
	B	BH <sup>+</sup>	
B <sub>1</sub> (X = N)	- 0.424383	- 0.294161	0.047893
B <sub>2</sub> (X = O)	- 0.302042	- 0.324148	0.392106
B <sub>3</sub> (X = S)	0.173342	0.492688	0.021174
B <sub>4</sub> (X = N)	- 0.235821	- 0.366604	0.293592

**Table 3**

Geometrical features of the complexes [BH<sup>+</sup>] (length in Å and angle in degree) at the equilibrium geometry of lowest excited triplet state

Molecules	r (X-H <sup>+</sup> )	<C-X-H <sup>+</sup>	<C-C-X-H <sup>+</sup>
B <sub>1</sub> (X = N)	3.0652	125.4901	179.9485
B <sub>2</sub> (X = O)	0.9705	125.7486	179.9098
B <sub>3</sub> (X = S)	3.2736	178.7846	- 53.6718
B <sub>4</sub> (X = N)	1.0124	120.5278	180.0000

**Table 4**

Computed adiabatic transition energies (<sup>1</sup>S<sub>0</sub> → T<sub>1</sub>) (hartree) and proton induced shifts (PIS, hartree) in the lowest excited triplet state

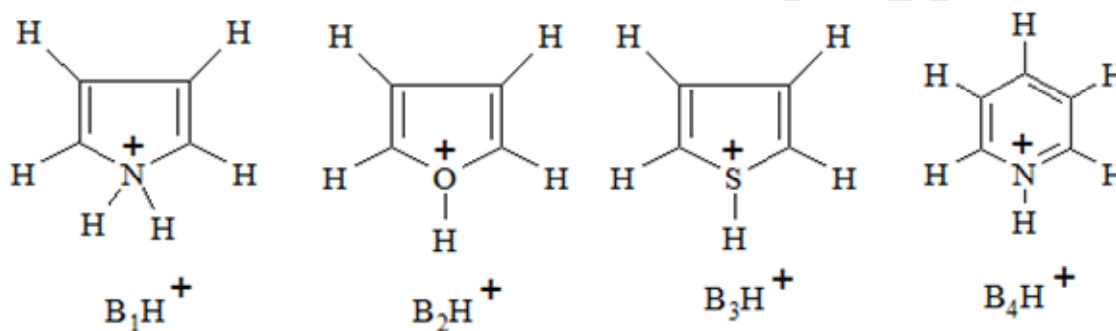
Molecules ( <sup>1</sup> S <sub>0</sub> → T <sub>1</sub> )	Transition energy		PIS
	B	BH <sup>+</sup>	
B <sub>1</sub> (X = N)	0.1417	0.1061	- 0.0356
B <sub>2</sub> (X = O)	0.1288	0.1135	- 0.0153
B <sub>3</sub> (X = S)	0.1185	0.1038	- 0.0147
B <sub>4</sub> (X = N)	0.1420	0.1389	- 0.0031

**Table 5**

Computed hardness (hartree) of the free base (B) in the lowest excited triplet state

Molecules	$\epsilon_{\text{HOMO}}$	$\epsilon_{\text{LUMO}}$	H
B <sub>1</sub> (X = N)	-0.0722 (-0.2124)	-0.1092 (0.0365)	0.0185 (0.1244)
B <sub>2</sub> (X = O)	-0.1074 (-0.2347)	-0.1249 (0.0067)	0.0087 (0.1207)
B <sub>3</sub> (X = S)	-0.1228 (-0.2425)	-0.1379 (-0.0182)	0.0075 (0.1121)
B <sub>4</sub> (X = N)	-0.1137 (-0.2597)	-0.1648 (-0.0333)	0.0255 (0.1132)

The values in the parenthesis are for the respective ground state

**Figure 1**

Structure of the proton Complexes of (Pyrrole, Furan, Thiophene and Pyridine)



The comparative study of basicities,  $\text{Li}^+$  and  $\text{Na}^+$  affinities of a series of heterocyclic molecules (Pyrrole, Furan, Thiophene and Pyridine) in the ground state. A DFT Study

**Biswarup Mandal<sup>1\*</sup>, Bikash Kumar Panda<sup>2</sup>, Suman Sengupta<sup>3</sup>**

1. Assistant Professor, Dept. of Chemistry, Sitananda College, Pin-721631, Nandigram, Purba medinipur, W.B., India
2. Assistant Professor, Dept. of Chemistry, Jangipur College, Pin-742213, Murshidabad, W.B., India
3. Assistant Professor, Dept. of Chemistry, Ananda Chandra College, Jalpaiguri, PIN-735101, W.B., India

\***Corresponding Author:** Assistant Professor, Dept. of Chemistry, Sitananda College, PIN-721631, Nandigram, Purba medinipur, W.B., India; Email: biswarupmandal75@gmail.com (Biswarup Mandal).

#### Publication History

Received: 27 November 2013

Accepted: 20 January 2014

Published: 5 February 2014

#### Citation

Biswarup Mandal, Bikash Kumar Panda, Suman Sengupta. The comparative study of basicities,  $\text{Li}^+$  and  $\text{Na}^+$  affinities of a series of heterocyclic molecules (Pyrrole, Furan, Thiophene and Pyridine) in the ground state. A DFT Study. *Indian Journal of Science*, 2014, 8(19), 16-20

---

### ABSTRACT

A comparative study of the proton affinities (PA),  $\text{Li}^+$  affinities and  $\text{Na}^+$  affinities of a series of heterocyclic molecules Pyrrole, Furan, Thiophene and pyridine and their protonated, lithium and sodium complexes in the gas phase have been performed theoretically by B3LYP(DFT) method using 6-311G(d,p) basis set with complete geometry optimization both before and after protonation,  $\text{Li}^+$  complex formation and  $\text{Na}^+$  complex formation. The gas phase protonation,  $\text{Li}^+$  complex formation and  $\text{Na}^+$  complex formation turns out to be exothermic and the local stereochemical disposition of proton,  $\text{Li}^+$ , and  $\text{Na}^+$  is found almost same in each case. Computed proton, lithium and sodium affinities are sought to be correlated with a number of computed system parameters like the net computed charge on the hetero atom (X) of the free molecules and the net charge on the hetero atom (X) and on proton,  $\text{Li}^+$ , and  $\text{Na}^+$  of the protonated, lithium and sodium complexes. The energetics structural and electronic properties of the complexes indicate that the interaction between proton-free molecule, lithium-free molecule and sodium-free molecule is predominantly an ion-dipole attraction and the ion-induced dipole interaction as well rather than a covalent interaction. The overall reactivity is explained by distant atom contribution in addition to the contribution from free base.

**Key words:** B3LYP, DFT, Gaussian, Gas phase, PA, Li-A, Na-A

---



## 1. INTRODUCTION

The interactions of acid and base are of great importance in chemistry. Quantitative studies in the gas phase provide the intrinsic acidities and basicities free from interference from solvent molecules and counterions. The most widespread study concerns different gas phase proton transfer equilibria (Hunter et al., 1998). The heterocyclic molecules have lately attracted attention due to their "shifted PKa values" upon complexation to metal ions, because it can rationalize the existence of nucleobases of differing protonation state at physiological P<sup>H</sup> (Roitzsah et al., 2004). In an effort to understand the nature and origin of variation in the relative magnitude of the basicities to be expected in a series of above said heterocyclic molecules, the most deadly poisons. Alkali metal ions were the first metal cations to be studied in the gas phase for their coordination properties. This is due to their relatively easy production under vacuum. In contrast with transition metal ions, their reactivity towards ligands is quite simple: in general, they form adducts, or clusters that can be considered as ions "solvated" by one or several ligands (Burk et al., 2000). A comparative study of proton affinity, Li<sup>+</sup> affinity and Na<sup>+</sup> affinity of a series of heterocyclic compounds in the ground state have been calculated theoretically by B3LYP(DFT) method using 6-311G(d,p) basis sets. Recently the ground state basicities of a series of substituted crotonaldehyde and acetophenone in their ground state were reported in the literature (Pandit et al., 2006; Senapati et al., 2008). The ground state Li<sup>+</sup> and Na<sup>+</sup> affinities of a series of substituted crotonaldehyde and acetophenone were also reported in the literature (Pandit et al., 2007; Senapati et al., 2007; Senapati et al., 2010). The purpose of the present work is not only to study the basicities, Li<sup>+</sup> and Na<sup>+</sup> affinities of the above said heterocyclic molecules but also to study on geometrical features of their protonated, lithium, and sodium complexes.

Gas phase methods (Beauchamp et al., 1974; Solomon et al., 1974; Long et al., 1974; Wieting et al., 1974) have the advantage for determining the intrinsic ground state, acid base properties in the absence of complicating effect of solvation. To determine the basicities, geometrical features also in the ground state by B3LYP(DFT) method by using Gaussian O3W program (Lee et al., 1988). Here we analyzed the PA, Li-A and Na-A values ( $\Delta E$ ) to understand whether the pre-complex charge distribution local to the molecules or post-complex relaxation of charge density or both are important for explaining the overall basicity of the molecules in a particular state.

These ion-molecule complexes are involved in molecular recognition process (Ma et al., 1997) and help in removing metal cations from contaminated media. These studied may be used to gain insight into many important biological processes (Karlin et al., 1994; Cervenansky et al., 1995; Novotny et al., 1989), electron transfer process (Lippard et al., 1994; Kallim et al., 1994) and more complicated biological system. We have also looked into the possible origin of the small shift in the Li<sup>+</sup> and Na<sup>+</sup> affinities on the heterocyclic molecules. We have looked that the bond formed by Li<sup>+</sup> and Na<sup>+</sup> is largely ionic, and the alkali metal cation retains 0.8-0.9 units of the positive charge in the complex (Alcami et al., 1989; Alcamí et al., 1990; Speers et al., 1994; Alcamí et al., 1990; Anvia et al., 1990; Alcamí et al., 1996).

## 2. COMPUTATIONAL DETAILS

Calculations were performed using Gaussian O3W software and B3LYP(DFT) method with 6-311G(d,p) basis sets. In all calculations complete geometry optimization has been carried out on the molecules both before and after protonation, Li<sup>+</sup> complex and Na<sup>+</sup> complex formation. Proton affinities (PA), Li<sup>+</sup> affinities and Na<sup>+</sup> affinities were computed as ( $E_{BH^+} - E_B$ ), ( $E_{BLi^+} - E_B - E_{Li^+}$ ), ( $E_{BNa^+} - E_B - E_{Na^+}$ ) respectively.

## 3. RESULT AND DISCUSSION

The molecules studied are listed in table 1 along with their respective abbreviated names and computed total energy (hartree) of the free base(B) and their protonated, Li<sup>+</sup> and Na<sup>+</sup> complexes and also the PA, computed Li<sup>+</sup> affinities and computed Na<sup>+</sup> affinities( $\Delta E$ ). Table 1 reports the computed total energies (hartree) of the free base (B)=(B<sub>1</sub>, B<sub>2</sub>, B<sub>3</sub>, B<sub>4</sub>), BH<sup>+</sup>=(B<sub>1</sub>H<sup>+</sup>, B<sub>2</sub>H<sup>+</sup>, B<sub>3</sub>H<sup>+</sup>, B<sub>4</sub>H<sup>+</sup>), BLi<sup>+</sup>=(B<sub>1</sub>Li<sup>+</sup>, B<sub>2</sub>Li<sup>+</sup>, B<sub>3</sub>Li<sup>+</sup>, B<sub>4</sub>Li<sup>+</sup>), BNa<sup>+</sup>=(B<sub>1</sub>Na<sup>+</sup>, B<sub>2</sub>Na<sup>+</sup>, B<sub>3</sub>Na<sup>+</sup>, B<sub>4</sub>Na<sup>+</sup>). It also reports the proton affinities(P.A)=[ $E_{BH^+} - E_B$ ], Li<sup>+</sup> affinities( $\Delta E$ )= [ $E_{BLi^+} - E_B - E_{Li^+}$ ] and Na<sup>+</sup> affinities( $\Delta E$ )= [ $E_{BNa^+} - E_B - E_{Na^+}$ ] of the above said molecules at the equilibrium geometry of the G.S. In this method B3LYP (DFT) with 6-311G (d, p) basis set, it is seen that the P.A values is highest for Pyridine -0.371(hartree) where it is -0.314, -0.2771 and -0.2868 for Pyrrole, Furan and Thiophene respectively. Here we observed that Li<sup>+</sup>affinities of the complex varies in the range -0.0502 to -0.0784(hartree) where as Na<sup>+</sup>affinities of the same complex are in the range -0.0389 to -0.0615(hartree). The  $\Delta E$  values indicating that the gas phase Li<sup>+</sup> and Na<sup>+</sup> complex formation turns out to be exothermic in each case.

Table 2 reports the net charge on X atom (X=N,O,S,N for Pyrrole, Furan, Thiophene and pyridine respectively) at the equilibrium G.S of the free base molecule as well as the computed net charge carried out by proton, lithium, sodium at the equilibrium G.S of protonated, Li<sup>+</sup> substituted and Na<sup>+</sup> substituted complexes. The computed net charge on proton, Li<sup>+</sup> and Na<sup>+</sup> vary within the range 0.18 to 0.38, 0.574 to 0.853 and 0.794 to 0.906 respectively. The



**Table 1**

Computed total energies (hartree) of free bases (B)=[B<sub>1</sub>,B<sub>2</sub>,B<sub>3</sub>,B<sub>4</sub>] and their Protonated(BH<sup>+</sup>), Li<sup>+</sup> complex (BLi<sup>+</sup>) and Na<sup>+</sup> complex (BNa<sup>+</sup>) and Proton affinities [PA = (E<sub>BH<sup>+</sup></sub> - E<sub>B</sub>) hartree], Lithium ion affinities[ΔE= (E<sub>BLi<sup>+</sup></sub> - E<sub>B</sub> - E<sub>Li<sup>+</sup></sub>), hartree] and Sodium ion affinities [ΔE = (E<sub>BNa<sup>+</sup></sub> - E<sub>B</sub> - E<sub>Na<sup>+</sup></sub>), hartree] at the equilibrium geometry of the ground state

Molecules	Total Energy of B	Total Energy of BH <sup>+</sup>	Total Energy of BLi <sup>+</sup>	Total Energy of BNa <sup>+</sup>	PA = (E <sub>BH<sup>+</sup></sub> - E <sub>B</sub> )	Lithium Ion Affinity = (E <sub>BLi<sup>+</sup></sub> - E <sub>B</sub> - E <sub>Li<sup>+</sup></sub> )	Sodium Ion Affinity = (E <sub>BNa<sup>+</sup></sub> - E <sub>B</sub> - E <sub>Na<sup>+</sup></sub> )
[B <sub>1</sub> ]	-210.2260	-210.5408	-217.5807	-372.3588	-0.3148	-0.0698	-0.0514
[B <sub>2</sub> ]	-230.0834	-230.3605	-237.4185	-392.2037	-0.2771	-0.0502	-0.0389
[B <sub>3</sub> ]	-553.0696	-553.3564	-560.4137	-715.1938	-0.2868	-0.0592	-0.0428
[B <sub>4</sub> ]	-248.3468	-248.7178	-255.7101	-410.4897	-0.371	-0.0784	-0.0615

**Table 2**

Computed net charge on 'X' atom (q<sub>X</sub><sup>-</sup>) of free bases (B)=[B<sub>1</sub>,B<sub>2</sub>,B<sub>3</sub>,B<sub>4</sub>], and their Protonated (BH<sup>+</sup>), Li<sup>+</sup> complex (BLi<sup>+</sup>) and Na<sup>+</sup> complex (BNa<sup>+</sup>) and also the Computed net charge on Proton (q<sub>H<sup>+</sup></sub>), Lithium ion (q<sub>Li<sup>+</sup></sub>), Sodium ion (q<sub>Na<sup>+</sup></sub>) in the equilibrium ground state of free bases and (BH<sup>+</sup>), (BLi<sup>+</sup>) and (BNa<sup>+</sup>) complexes

Molecules	q <sub>X</sub> <sup>-</sup>				q <sub>H<sup>+</sup></sub>	q <sub>Li<sup>+</sup></sub>	q <sub>Na<sup>+</sup></sub>
	B	BH <sup>+</sup>	BLi <sup>+</sup>	BNa <sup>+</sup>			
B <sub>1</sub> (X=N)	-0.327407	-0.331879	-0.335869	-0.313345	0.320275	0.596757	0.801689
B <sub>2</sub> (X=O)	-0.229623	-0.251790	-0.434773	-0.404675	0.381043	0.853002	0.906794
B <sub>3</sub> (X=S)	0.263189	0.552293	0.429777	.368277	0.183935	0.574659	0.794346
B <sub>4</sub> (X=N)	-288795	-0.316448	-.523101	-.516291	0.294105	0.784705	0.864955

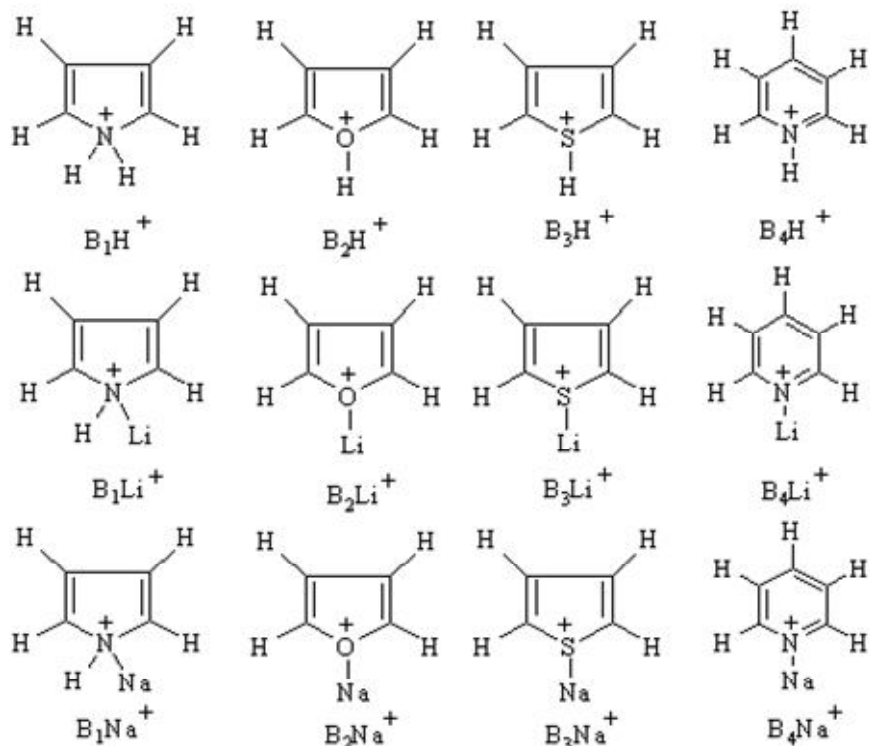
**Table 3**

Geometrical features of the complexes (BH<sup>+</sup>, BLi<sup>+</sup>, BNa<sup>+</sup>) (length in Å and angle in degree) at the equilibrium geometry of G.S.

Molecules	r (X-H <sup>+</sup> )	r (X-Li <sup>+</sup> )	r (X-Na <sup>+</sup> )	<C-X-H <sup>+</sup>	<C-X-Li <sup>+</sup>	<C-X-Na <sup>+</sup>	<C-C-X-H <sup>+</sup>	<C-C-X-Li <sup>+</sup>	<C-C-X-Na <sup>+</sup>
B <sub>1</sub> (X=N)	1.0289	2.1885	2.8535	111.1908	74.7736	73.1617	120.5375	-63.691	-63.1498
B <sub>2</sub> (X=O)	0.9767	1.8461	2.2387	119.9221	126.8766	126.904	-146.3458	179.9526	179.9928
B <sub>3</sub> (X=S)	1.3622	2.4651	2.9288	99.7029	64.1053	67.7677	105.8556	61.7878	66.8054
B <sub>4</sub> (X=N)	1.1016	1.918	2.3000	118.3758	121.1630	121.2712	-180.0163	179.9663	-180.0035

magnitude of charges of the complexes indicate that the interaction between proton-free base, Li<sup>+</sup>-free base and Na<sup>+</sup>-free base is predominantly an ion-dipole attraction and ion-induced dipole interaction as well rather than a covalent interaction. This also showed that both pre and post complex correlation with local charge densities in the immediate neighborhood of the complex formation site are weak. It can therefore be anticipated that the Li<sup>+</sup> and Na<sup>+</sup> affinities of these bases cannot be modeled or described by local properties of the hetero atom moiety only. Although it seems that there is a good but non perfect linear correlation between the charge on X atom in the free base (B), and the both Li<sup>+</sup> and Na<sup>+</sup> affinities still it must be shaped strongly by distant atom contribution in addition to the contribution from free base.

The local characteristics at or around the molecules are very nearly identical in each case. This is revealed from the data reported in Table 3. Where some of the selected computed geometrical parameters of BH<sup>+</sup>, BLi<sup>+</sup>, BNa<sup>+</sup> complexes in the G.S are listed. It is seen that X-H<sup>+</sup> bond length varies in the range of 0.97Å<sup>0</sup>-1.36Å<sup>0</sup>. For Li<sup>+</sup> and Na<sup>+</sup>



Structure of the proton, Li<sup>+</sup> and Na<sup>+</sup> Complexes of (Pyrrole, Furan, Thiophene and Pyridine)

affinities, lithium ion affinities and sodium ion affinities of the Pyrrole, Furan, Thiophene and Pyridine are spontaneous. The overall reactivity is fully explained by distant atom contribution in addition to the contribution from the free base.

## ACKNOWLEDGEMENTS

The authors gratefully acknowledge the financial support of CSIR, UGC and DST, New Delhi. We are thankful to Prof: Bhudeb Ranjan De, VU, for his valuable scientific advice throughout the work.

## REFERENCE

- Hunter E P L., Lias S G. Evaluated gas phase basicities and proton affinities of molecules: an update, *J. Phys. Chem. Ref. Data*, 1998, 27, 413-656
- Roitzsah M R, Lippert B. Metal Coordination and Imine–Amine Hydrogen Bonding as the Source of Strongly Shifted Adenine pK<sub>a</sub> Values, *J. Am. Chem. Soc.*, 2004, 126, 2421-2424
- Burk P, Koppel I A, Koppel I, Kurg R, Gal J F, Maria P C, Herreros M, Notario R, Abboud J L. M., Anvia F, Taft R. W. Revised and Expanded Scale of Gas-Phase Lithium Cation Basicities. An Experimental and Theoretical Study, *J. Phys. Chem. A*, 2000, 104, 2824-2833
- Pandit S, De D, De B R. The basicities of a series of substituted crotonaldehyde, *J. Mol. Struct. (Theochem)*, 2006, 760, 245-246
- Senapati U, De D, and De B R. The basicities of a series of substituted acetophenones in the ground state: A DFT study, *Indian J. Chem.*, 2008, 47A, 548-550
- Pandit S, De D, De B R. The Li<sup>+</sup> affinities of a series of a substituted crotonaldehyde in the ground state: A DFT study, *J. Mol. Struct. (Theochem)*, 2007, 819, 160-162
- Senapati U, De D, and De B R. The ground state Li<sup>+</sup> affinities of a series of a substituted acetophenone: A DFT study, *J. Mol. Struct. (Theochem)*, 2007, 808, 157-159
- Senapati U, De D, and De B R. The ground state Na<sup>+</sup> affinities of a series of a substituted acetophenone: A DFT study, *Molecular Simulation*, 2010, 36, 448-453
- Beauchamp J L. Interactions between ions and molecules, New York, *Plenum*, 1974, 413, 459-489
- Solomon J J, Meot M N, Field F H. Kinetics, equilibrium, and negative temperature dependence in the bimolecular reaction tert-C<sub>4</sub>H<sub>9</sub><sup>+</sup>(iso-C<sub>5</sub>H<sub>12</sub>, iso-C<sub>4</sub>H<sub>10</sub>) tert-C<sub>5</sub>H<sub>11</sub><sup>+</sup> between 190 and 5700K, *J. Am. Chem. Soc.*, 1974, 96, 3727-3732
- Long J W, Franklin J L. Ion-solvation reactions of phosphine, *J. Am. Chem. Soc.*, 1974, 96, 2320-2327
- Wieting R D, Staley R H, Beauchamp J L. Relative stabilities of carbonium ions in the gas phase and solution. Comparison of cyclic and acyclic alkylcarbonium ions, acyl cations and cyclic halonium ions, *J. Am. Chem. Soc.*, 1974, 96, 7552-7554

Biswarup Mandal et al.

The comparative study of basicities, Li<sup>+</sup> and Na<sup>+</sup> affinities of a series of heterocyclic molecules (Pyrrole, Furan, Thiophene and Pyridine) in the ground state. A DFT Study, *Indian Journal of Science*, 2014, 8(19), 16-20, <http://www.discovery.org.in/ijs.htm>

complexes X-Li<sup>+</sup> and X-Na<sup>+</sup> bond length varies between 1.8 Å<sup>0</sup> to 2.46 Å<sup>0</sup> and 2.23 Å<sup>0</sup> to 2.92 Å<sup>0</sup> respectively for said four heterocyclic molecules. The <C-X-H<sup>+</sup>, <C-X-Li<sup>+</sup> and <C-X-Na<sup>+</sup>, bond angles are varies in the range 99<sup>0</sup>-119<sup>0</sup>, 64<sup>0</sup>-126<sup>0</sup> and 67<sup>0</sup>-126<sup>0</sup> respectively. Similarly torsion angle <C-C-X-H<sup>+</sup>, <C-C-X-Li<sup>+</sup> and <C-C-X-Na<sup>+</sup> for heterocyclic complexes shows a variation in the range -180.01<sup>0</sup> to 120.53<sup>0</sup>, -63.69<sup>0</sup> to 179.96<sup>0</sup> and -180.00<sup>0</sup> to 179.99<sup>0</sup> respectively in the B3LYP (DFT) calculation using 6-311G(d,p) basis set. The torsion angle shows a wide variation. All the molecules in this theoretical study are planer in geometrical structure (from literature). After protonation here we have seen the torsion angle for pyridine is -180.01<sup>0</sup> but for pyrrole, furan and thiophene this values are effected by global density and planarity are destroyed. In case of Li<sup>+</sup> and Na<sup>+</sup> complexes planarity are destroyed for thiophene and for furan, pyridine planarity retained which is established by the value of torsion angle.

## 4. CONCLUSION

From the present theoretical study it can be well concluded that the gas phase proton

affinities of a series of a substituted acetophenone: A DFT study, *J. Mol. Struct. (Theochem)*, 2007, 808, 157-159

The ground state Na<sup>+</sup> affinities of a series of a substituted acetophenone: A DFT study, *Molecular Simulation*, 2010, 36, 448-453

Interactions between ions and molecules, New York, *Plenum*, 1974, 413, 459-489

Kinetics, equilibrium, and negative temperature dependence in the bimolecular reaction tert-C<sub>4</sub>H<sub>9</sub><sup>+</sup>(iso-C<sub>5</sub>H<sub>12</sub>, iso-C<sub>4</sub>H<sub>10</sub>) tert-C<sub>5</sub>H<sub>11</sub><sup>+</sup> between 190 and 5700K, *J. Am. Chem. Soc.*, 1974, 96, 3727-3732

Ion-solvation reactions of phosphine, *J. Am. Chem. Soc.*, 1974, 96, 2320-2327

Relative stabilities of carbonium ions in the gas phase and solution. Comparison of cyclic and acyclic alkylcarbonium ions, acyl cations and cyclic halonium ions, *J. Am. Chem. Soc.*, 1974, 96, 7552-7554

The ground state Li<sup>+</sup> affinities of a series of a substituted acetophenone: A DFT study, *J. Mol. Struct. (Theochem)*, 2007, 808, 157-159

The ground state Na<sup>+</sup> affinities of a series of a substituted acetophenone: A DFT study, *Molecular Simulation*, 2010, 36, 448-453

Interactions between ions and molecules, New York, *Plenum*, 1974, 413, 459-489

Kinetics, equilibrium, and negative temperature dependence in the bimolecular reaction tert-C<sub>4</sub>H<sub>9</sub><sup>+</sup>(iso-C<sub>5</sub>H<sub>12</sub>, iso-C<sub>4</sub>H<sub>10</sub>) tert-C<sub>5</sub>H<sub>11</sub><sup>+</sup> between 190 and 5700K, *J. Am. Chem. Soc.*, 1974, 96, 3727-3732

Ion-solvation reactions of phosphine, *J. Am. Chem. Soc.*, 1974, 96, 2320-2327

Relative stabilities of carbonium ions in the gas phase and solution. Comparison of cyclic and acyclic alkylcarbonium ions, acyl cations and cyclic halonium ions, *J. Am. Chem. Soc.*, 1974, 96, 7552-7554

The ground state Li<sup>+</sup> affinities of a series of a substituted acetophenone: A DFT study, *J. Mol. Struct. (Theochem)*, 2007, 819, 160-162

The ground state Na<sup>+</sup> affinities of a series of a substituted acetophenone: A DFT study, *Molecular Simulation*, 2010, 36, 448-453

Interactions between ions and molecules, New York, *Plenum*, 1974, 413, 459-489

Kinetics, equilibrium, and negative temperature dependence in the bimolecular reaction tert-C<sub>4</sub>H<sub>9</sub><sup>+</sup>(iso-C<sub>5</sub>H<sub>12</sub>, iso-C<sub>4</sub>H<sub>10</sub>) tert-C<sub>5</sub>H<sub>11</sub><sup>+</sup> between 190 and 5700K, *J. Am. Chem. Soc.*, 1974, 96, 3727-3732

Ion-solvation reactions of phosphine, *J. Am. Chem. Soc.*, 1974, 96, 2320-2327

Relative stabilities of carbonium ions in the gas phase and solution. Comparison of cyclic and acyclic alkylcarbonium ions, acyl cations and cyclic halonium ions, *J. Am. Chem. Soc.*, 1974, 96, 7552-7554

13. Lee C, Yang W, Parr R G. Development of the Colle-Salvetti correlation-energy formula into a functional of the electron density, *Phys. Rev.*, 1988, B-37, 785-789
14. Ma JC, Dongherty DA. The Cation- $\pi$  Interaction, *Chem. Rev.*, 1997, 97, 1303-1324
15. Karlin S, Zuker M, Brocchieri L. Measuring Residue Association in Protein Structures Possible Implications for Protein Folding, *J. Mol. Biol.*, 1994, 239, 227-248
16. Cerveansky C, Engstorm A, Karlsson E. Role of Arginine Residues for the Activity of Fasciculin, *Eur. J. Biochem.* 1995, 229, 270-275
17. Novotny J, Bruccoleri R E, Saul F A. On the attribution of binding energy in antigen-antibody complexes McPC 603, D1.3, and HyHEL-5, *Biochemistry*, 1989, 28, 4735-4749
18. Lippard S J, Berg J M. *Principles of Bioinorganic Chemistry*, University Science Books, Mill Valley, CA, 1994
19. Kallim W, Schwderski B, Bioinorganic Chemistry, Inorganic Elements In the Chemistry of Life, Wiley, Chichester, 1994
20. Alcamì M, Mo O, Yanez M. A molecular orbital study of azole-lithium(1+) complexes, *J. Phys. Chem.*, 1989, 93, 3929-3936
21. Alcamì M, Mo O, de Paz J J G, Yanez M. Enhanced Li<sup>+</sup> binding energies of some azines: a molecular orbital study, *Theor. Chim. Acta*, 1990, 77, 1-15
22. Speers P, Laidig K E. Theoretical studies of protonation and lithiation of first- and second-row aldehydes, *J. Chem. Soc., Perkin Trans.* 1994, 2, 799-806
23. Alcamì M, Mo O, Yanez M, Anvia F, Taft R W. Experimental and theoretical study of lithium(1+) affinities of methyldiazoles, *J. Phys. Chem.* 1990, 94, 4796-4804
24. Anvia F, Walsh S, Capon M, Koppel I A, Taft R W, de Paz J L G, Catalan J. Formation of three- and four-membered-ring structures for the lithium(1+) adducts of appropriate azines, *J. Am. Chem. Soc.*, 1990, 112, 5095-5097
25. Alcamì M, Mo O, Yanez M. Modelling Intrinsic Basicities: The use of the Electrostatic Potentials and Atoms-in-Molecules Theory. In *Molecular Electrostatic Potentials: Concepts and Applications*; Murray J S, Sen K, Eds; Elsevier: Amsterdam, 1996